

Identification of novel pathways involved in heterochromatin establishment and maintenance

A thesis submitted for the degree of
Doctor of Philosophy

By

Raquel Sales Gil

College of Health and Life Sciences
Brunel University London
December 2019



Declaration

I, **Raquel Sales Gil**, hereby declare that the data presented in this thesis is the result of my own work, unless otherwise specified, and that it has not been previously submitted for the award of any other degree.

Acknowledgements

This thesis would have not been possible without all the support and guidance of the best supervisor I could have ever had, Professor Paola Vagnarelli. Thank you for believing in me and pushing me to my limits, for sharing all your knowledge and experience, and giving me all your support and encouragement. Facing most of the time the two of us alone in the team has created an incredible bond that I will never forget. Thank you for everything you did for me and for making this journey a bit easier. Well, why should we lie? Sometimes much more complicated than I would have ever imagined, especially with those: “Oh, you know what you could do?” or “I think you should try to do this. What do you think?”, when I thought I was already done! However, I could not think of a better way of guiding and getting the best out of me than the way you did it. Thank you Paola, from my heart.

To my other half, Jordi Canals, to whom there are not enough words in the world to describe how much I appreciate him. Thank you for bearing my ups and downs almost every day, for supporting and believing in me when it was difficult for me to do so, and specially for dragging me into the triathlon world, enabling me to keep a perfect life-work balance. Thank you Jordi, only you know how special you are to me.

To Alexia Tsakaneli, my pillar in the University during these past three years. Since that first day when I started the PhD, she has been one of the most important people around and outside the lab in London. All our lunch and coffee breaks, the barbecues, the trainings, our talks about western blots that don't work, and the excitement when some finally did work, the lab meetings, the tears, and, most importantly, the laughs. You helped me countless times with my issues (many) I encountered during the PhD, and I am sure if you did the App named *AskAlexia!* it will be a total success. The best doctoral researcher I have ever met. I cannot imagine going to a work place where you are not around. Thank you Alexia, you know I could not have done it without you.

To my family, who have always guided me in life and supported every decision I took. They always know how to make me feel better and I can fully count on their wise advices.

To the other members of the team: Florentin, Dorothee, and Marta. Since they arrived, they have changed my days and have done the lab such a fun place, emphasizing my craziness and absurdity, a clear result of too many hours of tough experiments!

To the rest of my supervisory team, Professor Juliette Legler and Dr Luigi Margiotta-Casalucci, and the technician Marjo den Broeder, for all your support, guidance, training, and tips with the zebrafish. Also, to the animal facility team, Julie and Neil. Without all of them, the zebrafish work would have been impossible.

To my friends back home, especially Irene, Adriana, Esther and Cristian, with our sometimes-too-long Whatsapp audios on my way to the university. They listened and made me feel at home every single day during these 3 years. All their love and support is incredible and I am extremely grateful to have them as friends. Being far from home is difficult, but they clearly made things much easier. Cannot wait to see you all calling me Doctor!

Finally, to all the colleagues that helped me with a specific experiment at some point: Dr Makarov with DNA cloning, Dr Sisu with the RNA-sequencing analysis, Dr Karteris for the RNA samples delivery and the tissue lyser, and the technicians of the University.

Publications

Gil, R.S., De Castro, I.J., Ligammari, L., Di Giacinto, M.L. & Vagnarelli, P. 2018, "CDK1 and PLK1 coordinate the disassembly and reassembly of the nuclear envelope in vertebrate mitosis", *Oncotarget*, vol. 9, no. 8, pp. 7763

Gil, R.S., de Castro, I.J., Berihun, J. & Vagnarelli, P. 2018, "Protein phosphatases at the nuclear envelope", *Biochemical Society transactions*, vol. 46, no. 1, pp. 173-182.

Gil, R.S. & Vagnarelli, P. 2019, "Protein phosphatases in chromatin structure and function", *Biochimica et Biophysica Acta (BBA)-Molecular Cell Research*, vol. 1866, no. 1, pp. 90-101.

Gil, R.S. & Vagnarelli, P. 2019, "Ki-67: More Hidden behind a 'Classic Proliferation Marker'", *Trends in biochemical sciences*, vol. 43, no. 10, pp. 747-748.

Contents

Declaration	ii
Acknowledgements	iii
Publications	v
Contents	vi
List of figures	x
List of tables	xii
List of abbreviations	xiii
Abstract	xvi
1. INTRODUCTION	1
1.1. Chromatin structure	2
1.1.1. Euchromatin and heterochromatin	4
1.1.2. 3D genome organization	5
1.1.3. Histones.....	10
1.1.4. Chromosome segregation	11
1.2. Heterochromatin and epigenetics.....	14
1.2.1. Heterochromatin protein 1 (HP1).....	16
1.2.2. Other heterochromatin marks: H3K27me3.....	25
1.3. Histone variant H2A.Z.....	26
1.3.1. H2A.Z variants.....	27
1.3.2. Mechanisms of H2A.Z loading	30
1.3.3. H2A.Z localization in the genome	32
1.3.4. Roles of H2A.Z.....	33
1.4. Protein phosphatases	35
1.4.1. Protein kinases and phosphatases in chromatin regulation	35
1.4.2. Protein phosphatase 1	37
1.4.3. Repo-man/PP1 holoenzyme	41
1.5. Aims of the thesis	46
2. MATERIALS AND METHODS	47
Cell culture methodology	48
2.1. Tissue culture	48
2.1.1. DNA and siRNA Transfection	48
2.1.2. Transfection with Neon electroporation system.....	50
2.1.3. Generating stable cell lines.....	50

2.1.4.	Drug treatments.....	51
2.2.	Immunofluorescence.....	51
2.3.	Immuno-fiber FISH.....	52
2.3.1.	List of solutions.....	53
2.4.	Fluorescent microscopy and statistical analysis.....	53
2.4.	Fluorescence-activated cell sorting (FACS).....	53
2.5.	Statistical analyses.....	54
2.6.	RNA extraction.....	54
2.7.	Differential gene expression.....	55
2.7.1.	cDNA retro-transcription.....	55
2.7.2.	Quantitative Polymerase Chain Reaction (qPCR).....	56
2.7.3.	Statistical analysis.....	57
2.8.	Western Blotting.....	58
2.8.1.	Cell lysate preparation.....	58
2.8.2.	Mouse tissues lysate preparation.....	58
2.8.3.	SDS-PAGE gel electrophoresis, transfer and visualization.....	59
2.8.4.	List of solutions.....	60
2.9.	Molecular cloning.....	62
2.9.1.	Primer design and PCR.....	62
2.9.2.	Cloning into pGEM [®] -T Easy vector.....	64
2.9.3.	Subcloning from a vector to another plasmid.....	65
2.9.4.	Preparation of <i>E. coli</i> competent cells.....	66
2.9.5.	List of solutions.....	66
2.9.6.	Map of plasmids used for the study.....	67
2.10.	RNA sequencing.....	68
	Zebrafish methodology.....	69
2.11.	Zebrafish husbandry and egg line collection.....	69
2.11.1.	List of solutions.....	69
2.12.	Immunofluorescence.....	70
2.13.	Differential gene expression.....	70
2.13.1.	RNA extraction from zebrafish embryos.....	71
2.13.2.	cDNA retro-transcription.....	71
2.13.3.	Quantitative Polymerase Chain Reaction (qPCR).....	71
2.14.	Western Blotting.....	72
2.14.1.	List of solutions.....	73
2.15.	In Situ Hybridization of zebrafish embryos.....	73

2.15.1.	Probe synthesis.....	73
2.15.2.	In situ hybridization.....	74
2.15.3.	List of solutions	75
2.16.	Genotyping of zebrafish larvae and adults.....	76
2.17.	CDCA2 mutant line analysis.....	77
2.17.1.	Behavioural study	77
2.17.2.	Cardiovascular and growth analysis.....	78
2.17.3.	Fertility study	78
3.	ROLE OF PHOSPHATASES AS REGULATORS OF HETEROCHROMATIN MAINTENANCE.....	79
3.1.	Introduction.....	80
3.2.	Results.....	82
3.2.1.	Development of stable GFP:HP1 α cell lines	82
3.2.2.	Screening of PP1 subunits on HP1 distribution	85
3.2.3.	Differential expression analyses of Ki-67-depleted cells.....	88
3.3.	Discussion.....	91
4.	ANALYSES OF CDCA2/PP1 COMPLEX DURING ZEBRAFISH DEVELOPMENT	95
4.1.	Introduction.....	96
4.1.1.	Zebrafish.....	96
4.1.2.	Epigenetics in zebrafish development	99
4.1.3.	CDCA2 in zebrafish	100
4.2.	Results.....	102
4.2.1.	CDCA2 characterization during zebrafish development	102
4.2.2.	Mutant CDCA2 zebrafish line analysis.....	111
4.3.	Discussion.....	118
5.	ROLE OF H2A.Z VARIANTS IN HETEROCHROMATIN REGULATION.....	122
5.1.	Introduction.....	123
5.2.	Results.....	127
5.2.1.	H2A.Z.1 and H2A.Z.2 knockdown.....	127
5.2.2.	Analyses of the effect of H2A.Z.1 or H2A.Z.2 depletion on HP1 α localisation ..	129
5.2.3.	Role of H2A.Z.1 and H2A.Z.2 on chromosome segregation	133
5.2.4.	H2A.Z.2.1 regulates nuclear morphology.....	137
5.2.5.	H2A.Z depletion compromises the repressive chromatin landscape	139
5.2.1.	Distinct roles of the H2A.Z.1 and H2A.Z.2 variants on gene expression	141
5.2.2.	Is H2A.Z sufficient to drive de novo heterochromatin assembly?.....	146
5.1.	Discussion.....	150

6. DISCUSSION	154
7. APPENDIX	165
8. REFERENCES.....	166

List of figures

Figure 1.3. Hierarchical chromatin organization model.	9
Figure 1.5. HP1 α protein structure and alignment.....	18
Figure 1.6. Structure of the HP1-dinucleosome bridge complex.....	21
Figure 1.7. HP1 post-translational modifications sites.	22
Figure 1.8. Role of HP1 at the centromere.	24
Figure 1.9. Main differences between H2A and H2A.Z.....	29
Figure 1.10 Alignment of the three human H2A.Z protein sequences.....	29
Figure 1.11. Schematic representation of the yeast SWR1 complex	31
Figure 1.13. Repo-man structure and alignment of different species	42
Figure 1.14. Repo-man:PP1 and Ki-67:PP1 holoenzyme complex	43
Figure 1.15. Module of CDCA2/PP1 function during mitosis.....	45
Figure 2.1. Map of pEGFP-C1 vector.....	67
Figure 3.1. GFP:HP1 stable cell lines.....	83
Figure 3.2 HeLa and MRC5 GFP:HP1 validation.....	84
Figure 3.3. Screening of PP1 subunits on HP1 distribution.....	87
Figure 3.4. Differential expression analysis between Ki-G and Ki-5 siRNA-mediated knockdown cells.....	89
Figure 3.5. MYH9 knockdown, but not RBL2, regulates HP1 distribution.....	90
Figure 4.1. Zebrafish developmental stages.....	98
Figure 4.2. Human CDCA2 and zebrafish CDCA2 full protein alignment.....	101
Figure 4.3. CDCA2 expression analysis in zebrafish.....	104
Figure 4.4. CDCA2 RNA expression data in human tissues.....	105
Figure 4.5. Anti-human CDCA2 specificity testing against the zebrafish protein.....	108
Figure 4.6. Whole zebrafish embryo immunofluorescence.....	109
Figure 4.7. Whole zebrafish embryo immunofluorescence with antibodies specific for the CDCA2 zebrafish protein.....	110
Figure 4.8. Mutant CDCA2 zebrafish line.....	112
Figure 4.9. CDCA2 mutant lines undergo non-sense mediated mRNA decay.....	113
Figure 4.10. Central nervous system analysis on the CDCA2 mutant zebrafish line.....	115
Figure 4.11. Cardiovascular system analysis on the CDCA2 mutant zebrafish line.....	116

Figure 4.12. Fertilization analysis on the CDCA2 mutant fish line.	117
Figure 5.1. Histone variants enriched at HP1-bound chromatin regions.....	125
Figure 5.2. Validation of the H2A.Z siRNA-mediated knockdowns.....	128
Figure 5.3. H2A.Z.2, but not H2A.Z.1, is possibly involved in heterochromatin maintenance.	130
Figure 5.4. Overexpression of H2A.Z.2.1 is toxic for the cells.....	131
Figure 5.5. Cell cycle progression on H2A.Z knockdowns.....	132
Figure 5.6. H2A.Z.2 knockdown leads to chromosome segregation defects.	135
Figure 5.7. H2A.Z.2 knockdown results in cohesin impairment.	136
Figure 5.8. H2A.Z.1 knockdown results in aberrant nuclear shape.	138
Figure 5.9. H2A.Z.1 and H2A.Z.2 have different effects on repressive chromatin.	140
Figure 5.10. Biological replicates present low correlation coefficient.....	143
Figure 5.12. RNA sequencing analysis.	145
Figure 5.13. YL1 is sufficient to recruit H2A.Z.1 and H2A.Z.2.....	148
Figure 5.14. H2A.Z is not fully incorporated onto the chromatin by YL1.....	149

List of tables

Table 1-1. List of epigenetic marks for euchromatin vs heterochromatin.....	16
Table 1-2. Composition of the NuA4, SWR1, p400/tip60 and SRCAP complexes	32
Table 2-1. siRNA sequences used for the knockdown experiments.	49
Table 2-2. List of antibodies used for immunofluorescence.....	51
Table 2-3. Reverse transcription reaction	55
Table 2-4. Set of qPCR primers	56
Table 2-5. qPCR reaction mix.....	57
Table 2-6. QuantStudio 7 qPCR reaction parameters	57
Table 2-7. List of antibodies used for Western Blots.....	59
Table 2-8. PCR primer sequences for cloning	63
Table 2-9. PCR reaction components.....	63
Table 2-10. PCR reaction parameters	63
Table 2-11. Ligation into pGEM[®]-T Easy vector	64
Table 2-12. Digestion reaction.....	65
Table 2-13. Ligation reaction with T4 ligase	65
Table 2-15. KASP reaction	77
Table 2-16.KASP thermal cycling conditions	77
Table 4-1. Major epigenetic differences between mammalian and zebrafish development.....	100
Table 7-1. List of kits used in the project.....	165

List of abbreviations

ATP	Adenosine triphosphate
BCIP	5-bromo-4-chloro-3-indolyl phosphate
CAF-1	Chromatin assembly factor-1
CBX5	Chromobox homolog 5
CDCA2	Cell Division Cycle Associated 2
CENP-A	Centromere Protein A
ChIP	Chromatin Immunoprecipitation
CNS	Central Nervous system
CPC	Chromosomal Passenger Complex
CTCF	CCCTC-binding factor
DAPI	4',6-diamidino-2-phenylindole
DNA	Deoxyribonucleic acid
dpf	Days post-fertilization
DSB	Double Strand Breaks
E. coli	Escherichia coli
EZH2	Enhancer of zeste homolog 2
FACS	Fluorescence-activated cell sorting
FBS	Foetal Bovine Serum
FISH	Fluorescence In Situ Hybridization
GFP	Green Fluorescent Protein
HLB	Histone Locus Body
HP1	Heterochromatin protein 1
hpf	Hours post-fertilization

IDR	Intrinsically disordered regions
IF	Immunofluorescence
INM	Inner Nuclear Membrane
KASP	Kompetitive Allele Specific PCR
LAD	Lamina-Associated Domain
LBD	Lamin Binding Domain
LBR	Lamin Binding Receptor
Lys/K	Lysine
MBT	Midblastula transition
me	Methylation
MeOH	Methanol
MN	Micronuclei
NBT	nitro blue tetrazolium
NE	Nuclear envelope
NIPP1	Nuclear inhibitor of PP1
NLS	Nuclear Localization Signal
NP	Nuclear periphery
PBT	PBS Tween
PEV	Position-Effect Variegation
PIP	PP1 Interactive Protein
PNUTS	Phosphatase 1 Nuclear Targeting Subunit
PP1	Protein phosphatase 1
PP2A	Protein phosphatase 2A
PRC2	Polycomb Repressive Complex 2
Pro/P	Proline
PRR14	Proline Rich 14

PTEN	Phosphatase and tensin homolog
PTM	Post-translational modifications
RFP	Red Fluorescent Protein
RIPPO	Regulatory Interactor of Protein Phosphatase One
RNA	Ribonucleic acid
RT	Room temperature
<i>S. cerevisiae</i>	<i>Saccharomyces cerevisiae</i>
<i>S. pombe</i>	<i>Schizosaccharomyces pombe</i>
Ser/S	Serine
Sgo	Shugoshin
siRNA	Short interference RNA
SLiM	Short linear motifs
Su(var)	Suppressor of variegation
SWR1	Swi2/snif2-related 1
TADs	Topologically Associated Domains
TSS	Transcription start sites
WT	Wild Type
YSL	Yolk syncytial layer
ZIRC	Zebrafish International Resource Center
ZMF	Zebrafish Mutation Project

Abstract

Chromatin organization and dynamics is crucial for many aspects of cell biology. Heterochromatin, tightly packed DNA, is established in early development through controlled epigenetic processes and needs to be maintained throughout cell generations to ensure proper gene expression and cell function. Heterochromatin protein 1 (HP1) is a highly conserved protein that has been used as a marker for heterochromatin, as by binding to di- and tri-methylated histone H3K9, regulates heterochromatin structure, gene expression, DNA replication, DNA repair, cell cycle, cell differentiation and development. Beside phosphorylations of Histone H3 Ser10 that has been shown to modulate HP1 α binding to H3K9me3, several studies have also highlighted the importance of HP1 α phosphorylations and histone modifications for the modulation of HP1 chromatin binding ability and heterochromatin formation. By generating a human GFP:HP1 α cell line, I aimed to identify new regulators of heterochromatin formation, and I have analysed for the first time on a living organism one of the known HP1-chromatin binding regulators, Repo-man/PP1. As histone variants have a crucial role on chromatin organization, I have also analysed and differentiated the role of two H2A.Z variants, H2A.Z.1 and H2A.Z.2, on chromatin organization, cell cycle and gene expression.

1. INTRODUCTION

Approximately 20,000 – 25,000 genes, organized into 23 chromosome pairs, constitute the human genome. The same genetic information is present in all somatic cells even though there are more than 200 different cell types in the human body, each of them with a specific function, size, structure, and shape. This is due to the huge amount of biological mechanisms that orchestrate chromatin organization and control gene expression. Alterations on any of these mechanisms can have catastrophic consequences for the cell and might result in several diseases, thus the importance of understanding the processes that regulate chromatin organization, gene expression, and ultimately, cell function.

1.1. Chromatin structure

Four chemical bases make up our DNA: adenine (A), guanine (G), cytosine (C), and thymine (T). The combination of about 3 billion bases, paired as A with T and C with G, form the human DNA; the same base combination is found in every cell of our organism. The stretched length of the DNA is about 2m long and needs to be compacted in a controlled and specific manner in order to fit into a tiny cell nucleus.

The first level of DNA compaction is the nucleosome, where the DNA double helix wraps around histone proteins to form the basic unit of chromatin. Nucleosomes consist of 146 base pairs of DNA wrapped around an octamer of the four core histone proteins: H2A, H2B, H3 and H4 (Luger, Mäder, Richmond, Sargent, & Richmond, 1997). The central histone octamer consists of two H2A/H2B heterodimers and two H3/H4 heterodimers and it is connected to the adjacent nucleosome core through a linker DNA, which is usually associated with the linker histone protein H1. Nucleosomes are organized into 10nm chromatin fibers that has been thought to further compact into a 30nm fiber (McGhee et al., 1980) to form chromosomes, the higher degree of DNA compaction. However, the 30nm chromatin fiber was firstly reported in vitro and there is some controversy regarding whether it really exist in living cells (Eltsov et al., 2008, Fussner et al., 2012, Gan, Ladinsky & Jensen, 2013, Razin, Gavrillov, 2014) (Figure 1.1).

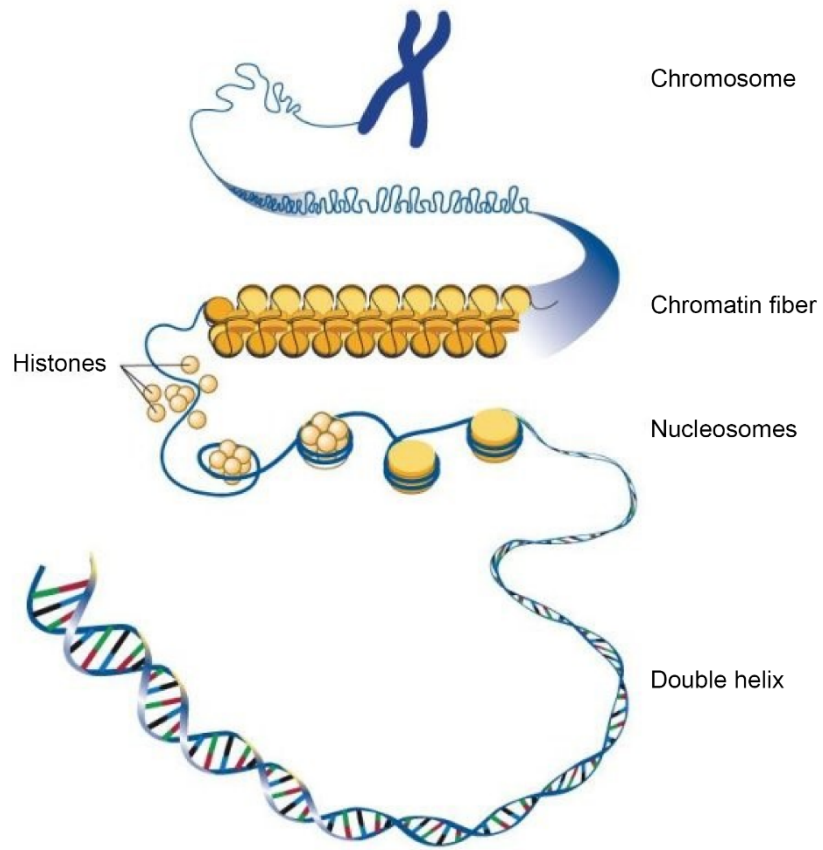


Figure 1.1. Chromatin structure. DNA is wrapped around histones to form the nucleosomes. Nucleosomes fold into a fiber-like structure of about 30nm, named chromatin fibers, which are further compacted onto chromosomes (from Creative Diagnostics Blog).

1.1.1. Euchromatin and heterochromatin

Generally, chromatin is not uniform with regards to its architecture, replication timing, gene distribution and transcriptional activity; instead it is divided into two different major domains termed heterochromatin and euchromatin. Euchromatin refers to regions in where chromatin is decondensed and contains actively transcribing genes, whereas heterochromatin is defined as tightly packed chromatin usually transcriptionally inactive and found around the nuclear periphery (Figure 1.2.A). Some heterochromatic regions are specific of each cell type, thus a DNA sequence in one cell type can be heterochromatic (and be silenced), but euchromatic (and be transcriptionally active) in another; this type of heterochromatin is known as facultative heterochromatin. However, some chromosome regions are heterochromatic in all cell types and are referred to as constitutive heterochromatin. Constitutive heterochromatin is mainly composed of repetitive elements, including satellite and telomeric DNA, and transposable elements. Hence, constitutive heterochromatin is found in pericentromeres and telomeres, where it has structural functions, and is important for the silencing of transposable elements that can lead to genome instability (Figure 1.2.B) (Woodcock, Ghosh, 2010, Nishibuchi & Dejardin, 2017).

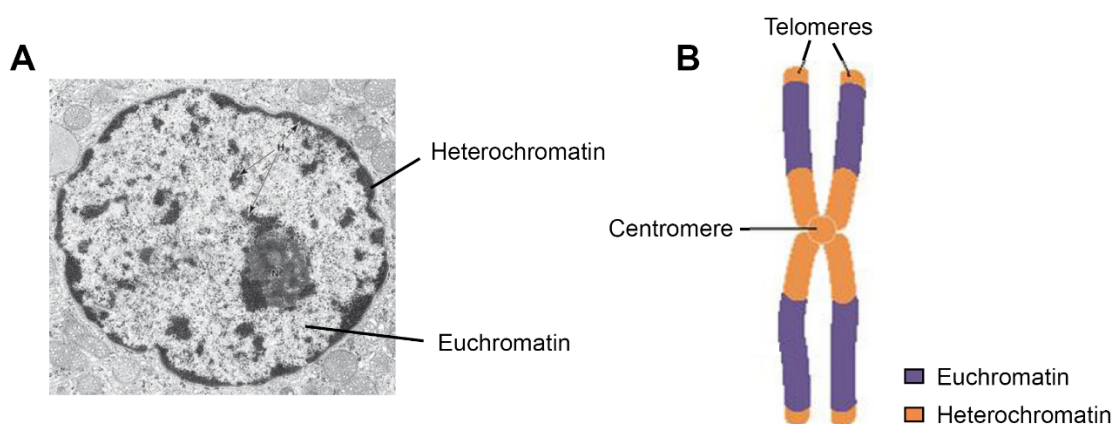


Figure 1.2. Euchromatin and heterochromatin. **A)** Heterochromatin corresponds to dark areas in the cell where chromatin is more compacted, whereas euchromatin is less compacted chromatin, transcriptionally active (from (Junqueira, Mescher, 2013)). **B)** Constitutive heterochromatin is usually found in certain areas of the chromosomes, like the telomeres and the centromeres.

1.1.2. 3D genome organization

Chromatin is not randomly distributed around the nucleus of the cell, and chromosomes have rather preferred positions within the 3D nuclear space. Although some indications that different sequences of the genome associate with specific cell structures were made earlier in the decade (Craig, Bickmore, 1997), it was not until 1999 that Croft and colleagues (Croft et al., 1999) first described this phenomenon for chromosomes 18 and 19. Using Fluorescent In Situ Hybridization (FISH) they showed that chromosomes have specific positions within the nucleus. Since then, many studies on chromosome positioning have been made, and it is now known that chromosomes organize in a specific manner respect to the centre or periphery of the nucleus, and with respect to each other, with gene-poor chromatin localized at the nuclear periphery (Craig, Bickmore, 1997, Boyle et al., 2011). The fact that low gene dense regions locate to the nuclear periphery does not mean that the genes on those regions are not transcribed (Mahy et al., 2002). Actually, it has been seen that some genes relocate outside the chromosome territory at some specific points and that this is related to transcription activation (Mahy et al., 2002, Chambeyron, Bickmore, 2004, Brown et al., 2006, Morey et al., 2007). In addition, within chromosome territories, the positioning of the genes (interior, exterior or surface of the territory) has also implications in its activity/inactivity (Kurz et al., 1996, Mahy et al., 2002).

Chromosome organization varies between cell types and has profound implications on gene expression and chromosome-chromosome interactions (Bickmore, Teague, 2002, Parada et al., 2004). Due to its importance for cell biology, several models for genome architecture have been since proposed, and as available technologies moved from individual cell microscopy, mainly by fluorescence in situ hybridization (FISH), to chromosome conformation capture (3C) and whole-genome Hi-C molecular approaches, a more detailed map of genome organization has been exposed. With FISH it was possible to visualize by fluorescent microscopy the nuclei localization of genes using a fluorescent probe that hybridizes with genomic regions or even whole chromosomes (Fraser, Bickmore, 2007). In 2002, Dekker and colleagues (Dekker et al., 2002) introduced 3C, giving the possibility to quantify the interactions between

genomic loci that are in close proximity in the nucleus. Seven years later, they introduced Hi-C (Lieberman-Aiden et al., 2009), a method that combines 3C with genome sequencing that allowed researchers to identify long-range interactions genome-wide in an unbiased way. However, this method presents some limitations, and recently other methods for 3D genome organization studies have been developed, including Genome Architecture Mapping (GAM) (Beagrie et al., 2017), split-pool recognition of interactions by tag extension (SPRITE) (Quinodoz et al., 2018), and Tyramide signal amplification (TSA)-seq (Chen et al., 2018). One of the limitations of 3C-based methods is the need of proximity ligation, meaning that only DNA regions that are in close proximity will be ligated and therefore detected. GAM and SPRITE overcome these limitations as they do not rely on proximity ligation and are able to detect interactions between genomic regions further apart. TSA-seq development introduced a “cytological ruler” to be able to study the exact distances between chromosomes and specific nuclear compartments.

As we understand it now, the genome is organized in a hierarchical way where distant genomic loci might interact with each other in so-called topologically associated domains (TADs), on the scale of 500 kilobases (kb) to 1 megabase (Mb) (Dixon et al., 2012). TADs are defined by DNA sequence regions that interact with each other more frequently than with others and can be composed of sub-TADs with even higher interaction frequency (Figure 1.3). The current model postulates that TADs are formed as a consequence of DNA looping via anchor proteins such as the CCCTC-binding factor (CTCF)–cohesin complex (Splinter et al., 2006, Hadjur et al., 2009, Rao, Suhas SP et al., 2014). Actually, deletion of cohesin either by its rapid degradation using an auxin-inducible degron (AID) (Rao et al., 2018, Vian et al., 2019) or by depleting the protein responsible for its loading to chromatin (Nipbl) (Schwarzer et al., 2017) eliminated all loop domains, although the compartment domains were preserved. Similarly, knockout of WAPL, the protein responsible for releasing cohesin from the chromatin, led to the extension of chromatin loops and increased the interaction frequency between nearby TADs (Haarhuis et al., 2017).

In the absence of CTCF, compartmental domains and individual TADs are not affected, as cohesin is still able to maintain the loop; however, in the absence of cohesin, TADs remain intact, (Zuin et al., 2014, Rao, Suhas et al., , Wutz et al., 2017).

In addition to chromosome loops being organized in TADs, there are other domains near the nuclear periphery or nuclear lamina, known as lamina-associated domains (LADs), that also influence chromosome organization. DamID together with ChIP experiments have shown that LADs are characterized by low-expression gene regions, indicating that silent chromatin concentrates at the nuclear lamina (Guelen et al., 2008). However, electron microscopy revealed zones at the nuclear periphery exempted of heterochromatin, termed heterochromatin exclusion zones (HEZs), which correlate with the presence of nuclear pore complexes (NPCs), a net of proteins that mediate all transport between the nucleus and the cytoplasm (Watson, 1959, Swift, 1959, Schermelleh et al., 2008). Generally, gene-dense regions are situated in the interior of the nucleus, whereas areas with low gene density, and thus low gene expression, like heterochromatin, locate around the nuclear periphery (Weierich et al., 2003, Gilchrist et al., 2004, Küpper et al., 2007). There is also evidence that some heterochromatin also accumulates at the nucleolar periphery (van Koningsbruggen et al., 2010, Németh et al., 2010, Pontvianne et al., 2013).

Chromatin organization inside the nucleus is critical for the correct function of the cell, and it reorganizes if needed for specific situations during the cell lifespan. For instance, heterochromatin accumulates at the centre of the nucleus in the photoreceptor cells of nocturnal mammals in order to change gene expression patterns and reduce light loss in the retina (Solovei et al., 2009). Moreover, during senescence, the nuclear pore density increases and the nucleoporin TPR is responsible for reorganizing heterochromatin to the interior of the cell (Lenain et al., 2017, Boumendil et al., 2019). Heterochromatin also reorganizes during cell differentiation to allow lineage-specific genome distribution (Guelen et al., 2008, Peric-Hupkes et al., 2010, Kohwi et al., 2013, See et al., 2019).

The molecular mechanisms by which heterochromatin is tethered to the nuclear periphery are still poorly understood. The implications of the nuclear periphery (NP) on chromosome organization were reported early in the XXI century, when Chubb and

colleagues (Chubb et al., 2002) studied the mobility of chromosomes and showed that the chromatin associated with the NP was less dynamic than the nucleoplasmic one. Since then, three proteins have been suggested to act as tethers to attach heterochromatin to the nuclear periphery. One of these proteins is the Lamin B Receptor (LBR), a nuclear membrane protein that binds to Heterochromatin Protein 1 (HP1) through its interaction with H3K9me3 (Ye, Worman, 1996, Ye et al., 1997). Another protein is the *C. elegans* CEC-4 protein, which encodes an HP1-like chromodomain, that has also been reported to interact with the nuclear membrane and H3K9me1/2/3 (Gonzalez-Sandoval et al., 2015). Finally, Proline Rich 14 (PRR14) protein has also been reported to act as a tether for heterochromatin binding to the nuclear periphery. Unlike LBR and CEC-4 proteins, PRR4 is not a membrane protein but it has a lamina binding domain (LBD) that is regulated by Protein Phosphatase 2A (PP2A) (Poleshko et al., 2013, Dunlevy et al., 2019).

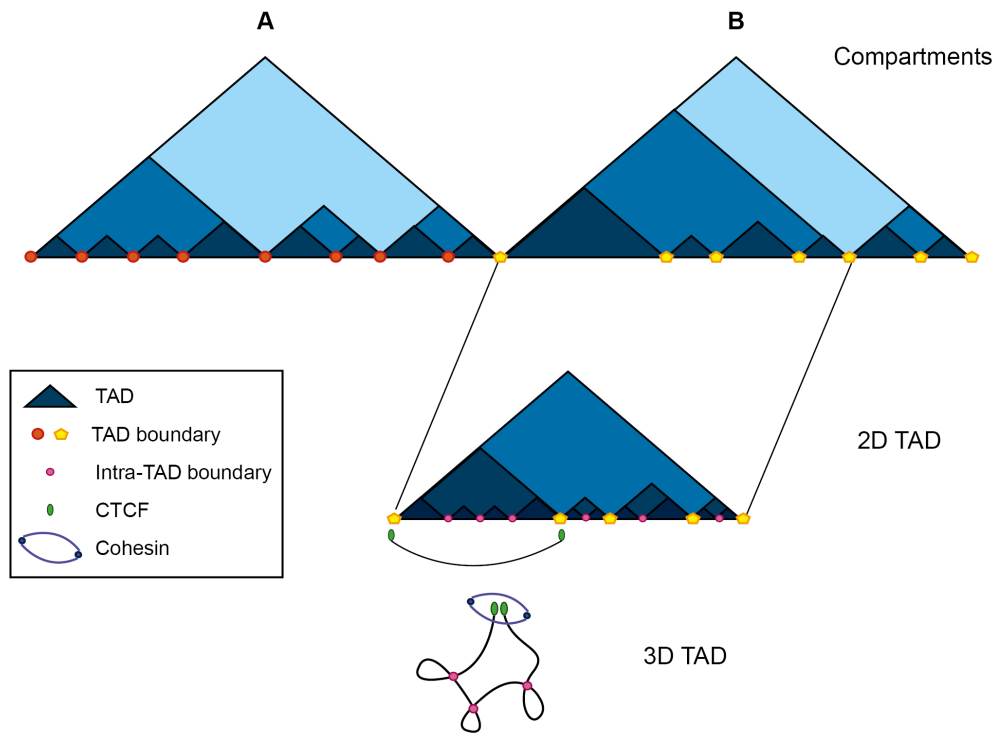


Figure 1.3. Hierarchical chromatin organization model. The figure shows a cartoon version of an actual Hi-C heat map, where the 3D genome is organized in higher-order compartments (A and B) that are composed of several topologically associated domains (TADs), smaller regions of the genome with elevated interaction intensity (tones of blue). TADs contain smaller sub-TADs with even higher interaction frequencies (dark blue) (2D TAD), which are formed from DNA loops anchored by CTCF-cohesin complexes (3D TAD). Figure adapted from (Mishra, Hawkins, 2017, Rowley, Corces, 2018).

1.1.3. Histones

Canonical histones are generally encoded by multiple genes, mainly organized into clusters throughout the genome, and their expression is carefully regulated at multiple levels (Albig, Doenecke, 1997). In metazoans, there are 10-20 functional copies of these genes for each core histone protein, clustered in two chromatin loci: HIST1 (which comprises about 80% of the histone genes and is located in chromosome 6 in humans) and HIST2 (located in human chromosome 1) (Wang, Z. et al., 1996). These histone genes are only transcribed during S-phase, and their deposition on the chromatin relies on DNA-synthesis, whereby they assemble into nucleosomes behind the replication fork and at sites of DNA repair (Buschbeck, Hake, 2017). The mRNA of canonical histones lacks introns and the polyA tail is replaced with a special stem-loop structure that binds to stem-loop binding proteins and regulates their processing and translation (Birnstiel et al., 1985). Because canonical histone genes have these unique transcription properties, the factors involved in histone mRNA biosynthesis are concentrated in a unique nuclear body called the Histone Locus Body (HLB).

There are also other histones, known as histone variants that are not cell-cycle regulated and can replace canonical histones at specific times and sites to control chromatin organization and function. These histones differ from canonical histone biosynthesis, as they contain introns and a polyA tail and transcribe as most other genes in the genome. They are also only encoded by one gene and might differ largely among species (Singh et al., 2018). There are several histone variants for each canonical histone, except for histone H4 for which no histone variant has been identified yet in higher eukaryotes. The most studied histone variants are histone H2A.X, and histone H2A.Z for the canonical histone H2A, and H3.3 and histone H3-like centromeric protein A (CENP-A) for histone H3. For the purpose of these thesis, the literature of the variant H2A.Z will be further reviewed later on.

Although nucleosomes are considered the first level of chromatin compaction, they are just a small fraction of the condensation needed to fit the genome into an interphase nucleus, revealing that there should be other levels of chromatin condensation.

Histone proteins consist of a globular C-terminal domain important for nucleosome formation and a flexible N-terminal tail that protrudes from the nucleosome. In total, ten flexible tails protrude from the nucleosome core, one N-terminal tail from each core histone, and two additional C-terminal tails from histone H2A (McGinty & Tan, 2014). These tails are targets for a variety of epigenetic post-translational modifications, including acetylation, phosphorylation and methylation (Grewal & Rice, 2004), which contribute to the higher levels of chromatin organization and that will determine chromatin structure. The study of these histone modifications and variants, together with the changes in the DNA that do not alter the DNA sequence itself, is referred to as epigenetics. The specific chromatin organization during the different stages of the cell cycle is crucial for many aspects of cell biology, including gene expression, cellular differentiation, and genome stability. Identifying the specific histone modifications and epigenetic marks that are characteristic of each cell cycle stage, as well as the components that regulate them, is important to understand chromatin dynamics and therefore, cell biology.

1.1.4. Chromosome segregation

Chromosome segregation is the process in mitosis and meiosis by which two sister chromatids (or chromosome homologues for meiosis I) separate from each other to allow proper division of chromatin into the two daughter cells.

There are four key elements to consider in chromosome segregation: the centromeres, the kinetochores, the assembly of a functional spindle, and the spindle assembly checkpoint (SAC). Centromeres are regions of the chromosome that link two sister chromatids together. They are the sites where kinetochores form and attach to the spindle microtubules, allowing chromatids to be pulled apart towards the spindle poles. In most eukaryotes, the centromeres are dictated by epigenetic changes rather than by the DNA sequence itself, and active centromeres are defined by the presence of the histone 3 variant CENP-A (Sullivan et al., 1994, Warburton et al., 1997). Shortly before mitotic entry, kinetochores assemble onto centromeres in a process that

involves the interplay of many protein complexes and remains largely unknown. For an extensive review of the kinetochore assembly and function see (Musacchio, Desai, 2017).

The chromosome passenger complex (CPC), with Aurora B kinase as the enzymatic protein of this complex, is crucial for proper chromosome segregation. CPC is composed of three other proteins: INCENP, Borealin and Survivin. INCENP acts as a bridge between Aurora B and the sub-complex formed by Borealin and Survivin, which controls the localization of CPC during mitosis (Klein et al., 2006, Jeyaprakash et al., 2007, Carmena et al., 2012). During mitosis, CPC recruitment to the centromere depends on the activity of other proteins, mainly Haspin, Shugoshin (Sgo) and Bub1. Haspin and Bub1 are kinases that phosphorylate H3T3 and H2AT120, respectively; these histone marks are recognized by the Borealin/Survivin sub-complex (the H2AT120ph is first recognized by Sgo which can then be recognized by Survivin) and they are able to recruit the CPC to the centromere (Jeyaprakash et al., 2007, Kelly et al., 2010, Wang, F. et al., 2010, Yamagishi et al., 2010). Once at the centromere, Aurora B phosphorylate different kinetochore substrates which will ultimately result in the activation of the spindle assembly checkpoint (SAC). This machinery is essential to detect and correct improper kinetochore-microtubule attachments thus safeguarding chromosome segregation.

Another important regulator of chromosome segregation is cohesin (Tanaka et al., 2000), a protein complex that holds sister chromatids together from DNA replication to anaphase, when its removal results in sister chromatids separation. Cohesin ensures that chromosomes do not separate before all the kinetochores are properly attached to the microtubules; when the SAC is inactivated, cohesin is then disassembled and chromatid segregation allowed. Thus, defects in the cohesin complex or its assembly lead to chromosome segregation defects (Michaelis et al., 1997, Vass et al., 2003, Vagnarelli et al., 2004). Cohesin is removed from chromosome arms during prophase by Wapl in a process that involves phosphorylation of several proteins by CDK1, PLK1 and Aurora B (Kueng et al., 2006, Nishiyama et al., 2013). However, cohesin is kept at the centromeres until anaphase, when the microtubules are properly attached to the kinetochores and the protease Separase cleaves cohesin from the centromeres,

enabling chromosome segregation (Waizenegger et al., 2000). Shugoshin and PP2A are responsible for counteracting CDK1 and PLK1 activity and ensure sister chromatid cohesion until all kinetochores are attached to the microtubules. A scheme of the major players in the process is presented in Figure 1.4. For an extensive review on cohesin please refer to (Makrantonis, Marston, 2018).

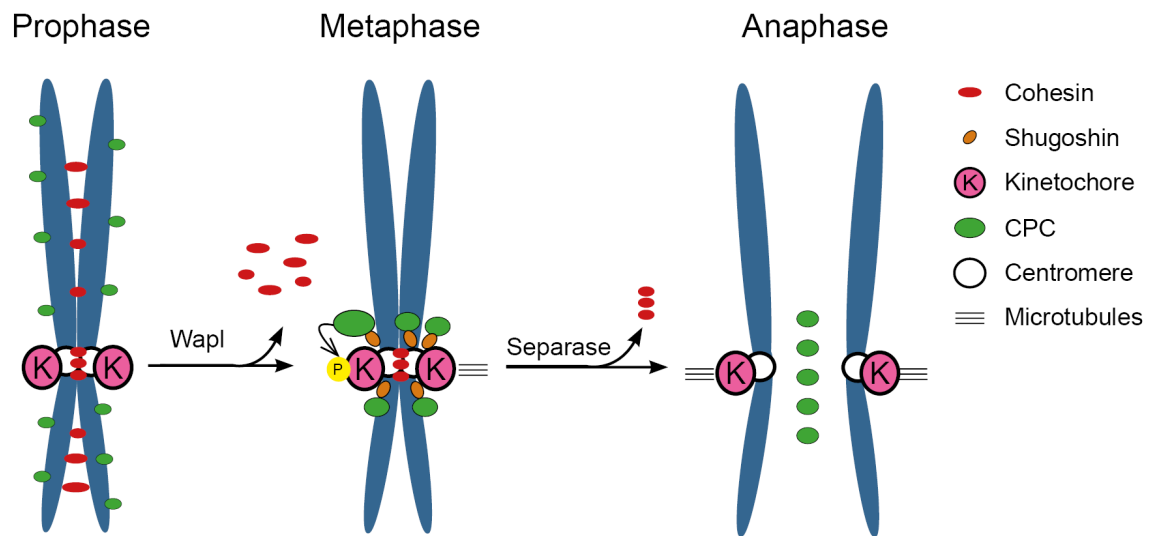


Figure 1.4. Scheme of the key players in chromosome segregation (adapted from (Meppelink et al., 2015)). During prophase, Wapl is responsible for releasing cohesin from chromosome arms, although a fraction of cohesin is kept at the centromeres during metaphase. During prometaphase/metaphase, the CPC is relocalized from the chromosome arms to the centromere by Shugoshin, where it phosphorylates kinetochore proteins and enables microtubule attachment. Once all microtubules are properly attached, separase releases cohesin from the centromeres and chromosomes are pulled apart, allowing proper chromosome segregation.

1.2. Heterochromatin and epigenetics

As described earlier, heterochromatin is tightly packed chromatin generally silent, and it is established during early development through controlled epigenetic processes. Epigenetics has been described as the study of heritable changes in genome function that do not involve changes in the DNA sequence itself, including DNA methylation, histone modifications or RNA interference (RNAi), that are crucial for correct chromatin organization and cell function.

Epigenetic marks are widely used to study changes in the epigenome, and they are distinctive for each type of chromatin. Euchromatin is characterised by chromatin acetylation (H3K9Ac, H3K27Ac, H4K16Ac), and by other histone marks like H3K4me1/3, H3K79me2, and H3K36me3. In contrast, heterochromatin is mainly characterised by global histone hypoacetylation, but there are also other methylation marks enriched in this type of chromatin, including tri-methylation of several lysine residues of histone H3 (H3K9me3, H3K27me3, H3K64me3) and histone H4 (H4K20me3) (Noma, Allis & Grewal, 2001, Peters et al., 2001, Kourmouli et al., 2004, Schotta et al., 2004, Daujat et al., 2009) (summarized in Table 1-1). Several histone methyltransferases are involved in these methylations. H3K9 methylation is driven by several enzymes, including GLP, G9A, SETDB1, SUV39H1 and SUV39H2. While GLP and G9A are usually responsible for mono- and di-methylation of H3K9 (Tachibana et al., 2002), SETDB1 and SUV39H are responsible for telomeric and pericentromeric trimethylation of H3K9, respectively (Gauchier et al., 2019). H3K9me3 serves as anchoring sites for heterochromatin protein 1 (HP1), a heterochromatin mark that leads to transcriptional silencing (Lachner et al., 2001). In contrast, only one methyltransferase is known to methylate H3K27, the PRC2 complex through the EZH2 enzyme (Kim & Kim, 2012). Table 1-1 summarises the main differences between euchromatin and heterochromatin in regards to their epigenetic landscape.

Epigenetic information needs to be maintained from mother to daughter cells and potentially from generation to generation to ensure proper genome function. However, during cell division chromatin undergoes a wave of rearrangements followed

by subsequent restoration after the passage of the replication fork (Probst et al., 2009) and mitosis (Vagnarelli, 2013). These rearrangements that enable changes in epigenetic states and that are important for cell differentiation need to be restored and maintained for cell lineage preservation, and thus refined mechanisms have been established to ensure both stability and plasticity of the epigenetic marks. Although DNA methylation inheritance occurs readily and rapidly through replication, some histone methylation patterns including H3K9, H3K27, H4K20 and H3K79 are re-established gradually during the cell cycle in a DNA replication-independent fashion. Chromatin Assembly Factor 1 (CAF-1) is a replication-specific histone chaperone important for the inheritance of H3K9me3 in pericentric heterochromatin during DNA replication, as it also acts as a chaperone for HP1 (Quivy et al., 2004). CAF-1 sequesters the released HP1 during DNA replication and forms a CAF-1-HP1 complex that will recruit SETDB1 to monomethylate H3K9 during S phase (Sarraf and Stancheva, 2004). H3K9me1 acts as a substrate for further di- and trimethylation by Suv39H, generating H3K9me3 marks that will in turn recruit HP1 back to the chromatin. There are other factors involved in the re-establishment of H3K9me3 in heterochromatin, such as small RNAs that are processed from heterochromatin encoded transcripts (Muchardt et al., 2002, Maison et al., 2002, Li, 2014). In the case of H3K27me3, polycomb (PcG) proteins and H3K27me3 accumulate at polycomb response elements prior to DNA replication in early S phase (Lanzuolo et al., 2011). In late S phase, by the time these regions are replicated, PcG levels at those sites are reduced, indicating that PcG-dependent H3K27me3 mark is inherited by dilution through replication. The replication protein proliferating cell nuclear antigen (PCNA) is also important for recruiting histone deacetylases and DNA methylases to the replication fork to ensure proper inheritance of these epigenetic marks. For an extensive review of how the epigenome is re-established after DNA replication please refer to Budhavarapu et al., 2013. During mitosis, chromatin also rearranges and many epigenetic marks are removed to allow proper chromosome segregation. However, some chromatin marks persist through mitosis, including as H3K27me3, H3K9Ac, H3K27ac, and H3K4me3 (Terrenoire et al., 2010).

Table 1-1. List of epigenetic marks for euchromatin vs heterochromatin.

Euchromatin	Heterochromatin
H3K4me1/3	H3K9me3
H3K9Ac	H3K27me3
H3K27Ac	H3K64me3
H3K36me3	H4K20me3
H3K79me2	HP1
H4K16Ac	

1.2.1. Heterochromatin protein 1 (HP1)

1.2.1.1. HP1 structure and domains

HP1 is a family of proteins crucial for the formation of transcriptionally inactive heterochromatin, and therefore it has been used as a marker for heterochromatin for many years. In mammals, there are three distinct HP1 proteins: HP1 α , HP1 β , and HP1 γ . HP1 α is encoded by the Chromobox homolog 5 (CBX5) gene, which, in humans, is located on chromosome 12q13.13; HP1 β is encoded by CBX1 on human chromosome 17q21.32; and HP1 γ is encoded by CBX3 on human chromosome 7p15.2. CBX5, CBX1 and CBX3 null mutant mice revealed different phenotypic effects for the three isoforms. While loss of HP1 α did not result in any phenotype in mice, HP1 β and HP1 γ mutants led to perinatal lethality and infertility, respectively (Aucott et al., 2008, Brown et al., 2010). Interestingly, Suv39h1 and Suv39h2 mutants are viable, indicating that the essential function of HP1 β is independent of its interaction with H3K9me3 (Peters et al., 2001).

The HP1 family belongs to a larger superfamily of proteins that contain conserved chromatin organization modifier (chromo) domains. The chromodomain (CD) is situated in the amino-terminal half of HP1 proteins, consists of approximately 30-60 amino acids (Jones et al., 2000) and gives the proteins the ability to alter the chromatin

structure to make heterochromatin. For instance, the chromodomain of HP1 share 60% similarity with that of Polycomb, another repressive complex (Paro, Hogness, 1991). Within the chromodomain superfamily, HP1 proteins form their own family characterized by the presence of a second unique conserved domain in the carboxy-terminal half of the protein, known as the chromoshadow domain (CSD) (Lomber et al., 2006). Both domains share high level of similarity in their amino acid sequence, but they have different functions. The CD is responsible for binding to chromatin at H3K9me2 and H3K9me3, whereas the CSD is involved in homo- and heterodimerization and interaction with other proteins. These domains are separated by a variable hinge region that contains a nuclear localization signal (NLS) (Figure 1.5.A). In HP1 α , interactions between the C-terminus and the hinge domain stabilize the dimer in a compact auto-inhibited state (Larson et al., 2017).

The CD and CSD of HP1 are highly conserved among species (Figure 1.5.B) as seen by alignment of the sequences and suggested by cross-species experiments. The CD from mouse HP1 β can functionally replace the one of *S. pombe* HP1 (Wang et al., 2000) and expression of human HP1 α can rescue the lethality of homozygous mutants in the *Drosophila* HP1-encoding gene *Su(var)2-5* (Norwood et al., 2004), suggesting that both domains are crucial for HP1 function.

HP1 binds specifically to chromatin containing the H3K9me3 mark, where it mainly maintains a heterochromatic environment (Bannister et al., 2001, Lachner et al., 2001, Nakayama et al., 2001, Jacobs, Khorasanizadeh, 2002). While HP1 α is located predominantly in constitutive heterochromatin, HP1 γ and HP1 β are uniformly distributed in the nucleus and are found in both hetero- and euchromatic regions (Horsley et al., 1996, Minc et al., 2000, Fanti et al., 2003).



Figure 1.5. HP1 α protein structure and alignment. A) HP1 α presents an N-terminal chromo domain and a C-terminal chromoshadow domain separated by a variable hinge region containing a nuclear localisation signal (NLS). **B)** Both the chromodomain and the chromoshadow domain of HP1 α are highly conserved among vertebrate species.

1.2.1.2. HP1 binding to chromatin and heterochromatin formation

Several models have been proposed to explain how HP1 is bound to H3K9me3 and how it is able to maintain a silent chromatin environment. As mentioned earlier, HP1 binds to H3K9me2/3 through its CD, although it has been shown that the CSD is also important to adopt the proper conformation. The first models proposed that the CDS binds to H3 sites different from H3K9me2/3 of the nucleosome and the CD binds to H3K9me3 residues, and both contribute to HP1-chromatin binding (Lavigne et al., 2009, Dawson et al., 2009a). Another model suggests that two CD bind to two H3K9me3 residues in the same nucleosome (Canzio et al., 2011, Canzio et al., 2013, Azzaz et al., 2014, Hiragami-Hamada et al., 2016, Machida et al., 2018, Watanabe et al., 2018). However, the most recent model, known as the nucleosome-bridge model,

postulates that HP1 α is able to dimerize through the CSD and that these HP1 α dimers are able to bind through their CD to two H3K9me3 marks in different nucleosomes and form a bridge that compacts chromatin (Canzio et al., 2011, Canzio et al., 2013, Azzaz et al., 2014, Hiragami-Hamada et al., 2016, Machida et al., 2018, Watanabe et al., 2018) (Figure 1.6). Actually, mutation of the CD at tryptophan 40 to alanine (HP1 α W40A) inhibited HP1 binding to H3K9me3 (Jacobs, Khorasanizadeh, 2002), and mutation of the CSD at isoleucine 165 to glutamic acid (HP1 α I165E), which inhibits dimerization of HP1 α , was able to bind to H3K9me3 but adopted an aberrant conformation (Brasher et al., 2000, Machida et al., 2018). The structure of the bridge between H3K9me3-containing nucleosomes by HP1 was nicely shown by cryoelectron microscope by the Kurumizaka lab (Machida et al., 2018) (Figure 1.6). Although some studies reported that the ability of HP1 α to bind chromatin was weaker than that of HP1 β and HP1 γ (Fischle et al., 2005, Watanabe et al., 2018), Machida et al. (Machida et al., 2018) showed that the three HP1 isoforms form a similar nucleosome-bridge structure.

Further studies revealed that the lower affinity of HP1 α in binding H3K9me3 was due to the lack of HP1 α phosphorylation in the *E. coli* recombinant HP1 α , and that phosphorylation of HP1 α at S11-S14, lacking on HP1 β and HP1 γ , increased the affinity to chromatin binding (Hiragami-Hamada et al., 2011, Nishibuchi, G. et al., 2014, Watanabe et al., 2018). This exemplifies how important post-translational modifications are on HP1; the known HP1 PTM have been summarized in Figure 1.7. Likewise, studies on flies (Zhao et al., 2001) and fission yeast (Shimada et al., 2009) demonstrated that mutations on specific phosphorylatable sites of HP1 lead to defective heterochromatin silencing. In addition, HP1 α phosphorylation in the hinge domain was reported to be critical for mitotic progression and shugoshin (Sgo1) (a protein that prevents premature cohesion dissociation and protects the centromere cohesion during mitosis) loading into centromeres. Moreover, inability to phosphorylate HP1 either by decreasing the responsible kinase or by introducing a non-phosphorylatable HP1 mutant, led to prometaphase arrest and several mitotic defects (Chakraborty, Prasanth, 2014, Chakraborty et al., 2014). Although several protein kinases responsible for phosphorylation of HP1 α at distinct residues have been identified, including

nuclear dbf2-related (NDR) kinase and casein kinase II (CK2), the counteracting phosphatases still remain elusive (Shimada et al., 2009, Nishibuchi et al., 2014, Chakraborty, Prasanth, 2014, Chakraborty et al., 2014).

Recent studies on human and fly HP1 α led to the identification of liquid droplets on phosphorylated HP1 α solutions (Phos-HP1 α), but not on wild type HP1 α , HP1 β , nor HP1 γ . The ability of Phos-HP1 α to phase separate was linked to the ability to form higher order oligomers beyond dimers (Larson et al., 2017, Strom et al., 2017). Altogether, these points out to the idea that HP1 α is phosphorylated in its N-terminal tail, which triggers HP1 α dimerization, followed by binding to H3K9me3, further HP1 α recruitment and higher-order oligomer formation: this ultimately leads to intrinsic disorder and phase separation. Within the HP1 α droplets, repressive factors might accumulate and might be able to physically sequester and compact the nearby chromatin, forming HP1 foci visibly detectable by fluorescent microscopy (Larson et al., 2017, Strom et al., 2017). A recent paper by Sanulli et al. (Sanulli et al., 2019) suggested that HP1 binding to H3K9me3 loosens histone-histone and histone-DNA interactions, exposing trapped histone core residues. These residues would be able to interact with the neighboring nucleosome, increasing intrinsic histone core dynamics and accessibility that leads to nucleosome disorganization and phase separation.

Another known modification of HP1 is peptidyl citrullination, where an arginine residue is converted to citrulline, a non-encoded amino acid, losing a positive charge and reducing the hydrogen bonding ability. Wiese and colleagues (Wiese et al., 2019) found that the CD of HP1 γ gets citrullinated in embryonic stem cells (ESC) at R38 and R39, modifying its chromatin binding during stem cell differentiation. In ESC HP1 γ is citrullinated to reduce its binding to H3K9me3 and maintain an open chromatin conformation. Upon differentiation, HP1 γ citrullination is reduced and allows HP1 γ binding to chromatin and heterochromatin formation.

SUMOylation of the hinge domain of HP1 α by SUMO1 is another HP1 PTM important for targeting *de novo* HP1 to pericentric heterochromatin (Maison et al., 2011). HP1 α SUMOylation is enhanced by the Suv39h paralogue Suv39h1, but not Suv39h2, by directly interacting with Ubc9, an E2-conjugated enzyme necessary for SUMOylation of several protein (Maison et al., 2016).

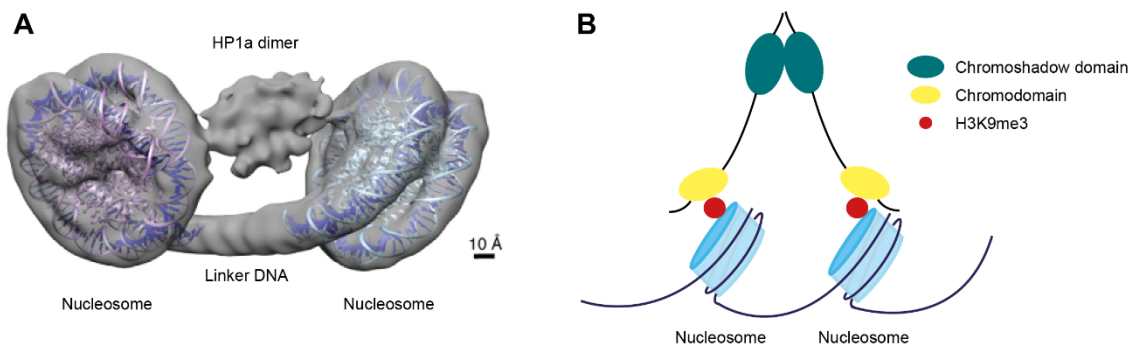


Figure 1.6. Structure of the HP1-dinucleosome bridge complex. A) 3D structure of the HP1 α -dinucleosome complex (from (Machida et al., 2018)). **B)** Schematic representation of the HP1 α -dinucleosome bridge. The chromodomain of HP1 recognizes the H3K9me3 mark while the chromoshadow domain dimerises with another HP1 molecule that is attached to another nucleosome.

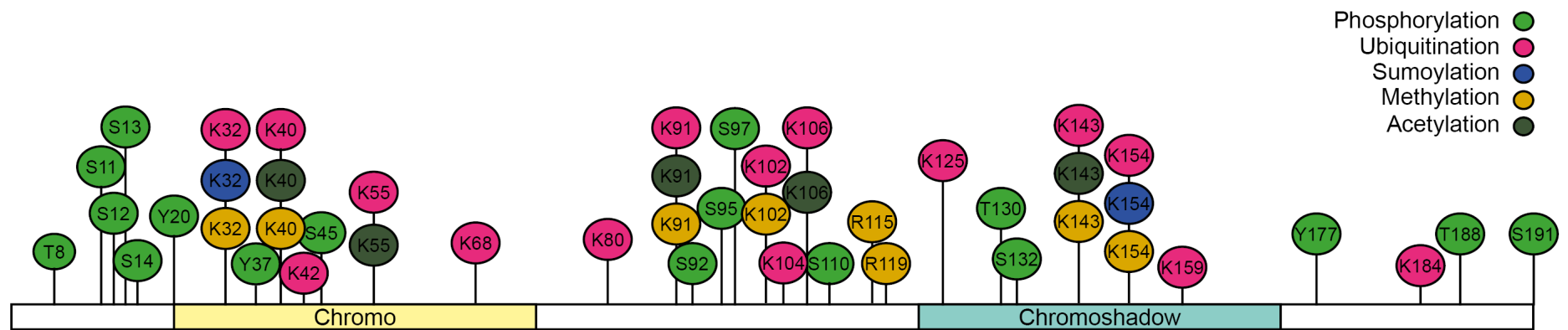


Figure 1.7. HP1 post-translational modifications sites. Known HP1 α PTMs sites are highlighted in light green (phosphorylation), pink (ubiquitination), blue (sumoylation), yellow (methylation), and dark green (acetylation). Figure adapted from Phosphosite.

1.2.1.3. HP1 during mitosis

During mitosis, HP1 dissociates from the H3K9me3 chromatin marker to allow chromatin restructuring required for proper chromosome segregation. Fischle et al. (Fischle et al., 2005) observed that levels of H3K9me3 during mitosis remain stable, thus HP1 dissociation from the chromatin is independent from H3K9me3 levels. They observed that the phosphorylation status of the nearby Ser10 (H3S10) is crucial to regulate HP1 binding to H3K9me3. In fact, H3S10 phosphorylation by Aurora B at mitotic entry ejects HP1 from its chromatin binding sites. At mitotic exit the Repo-man/PP1 complex, as explained later on in more detail, dephosphorylate H3S10ph, enabling HP1 binding to H3K9me3 and maintaining a chromatin repressive environment after each cell cycle (Vagnarelli et al., 2011, de Castro et al., 2017). Consistently, Aurora B inhibition or knockdown retains HP1 proteins on mitotic chromosomes but does not alter the localization of HP1 in interphase (Fischle et al., 2005). It is accepted, then, that Aurora B and Repo-man/PP1, which regulate the H3S10 phosphorylation status, are the main regulators of HP1 binding to chromatin during mitosis. However, if there are other phosphatases involved in this HP1 dynamics still remains unknown. In addition, as I have mentioned earlier, HP1 can be phosphorylated, and whether these phosphorylations, or other modifications, are important for HP1 reorganization through mitosis is still not known.

Although the majority of HP1 α is removed from the chromatin during mitosis, it has been shown that a small amount of HP1 α remains bound to the centromeric chromatin. There is now some evidence suggesting a role of HP1 α on protecting centromeric cohesion, as well as other studies showing the importance of HP1 α for proper mitotic progression (Inoue et al., 2008, De Koning et al., 2009). HP1 α was one of the first known binding partners of the chromosomal passenger complex (CPC) (Ainsztein et al., 1998). It has been suggested that Aurora B-mediated phosphorylation of HP1 α at S92 in early prophase is important for HP1 α localization at the centromeres and interaction with the CPC, increasing Aurora B activity at the centromere (Liu et al., 2014, Abe et al., 2016, Ruppert et al., 2018, Nishibuchi et al., 2018, Williams et al., 2019). In fact, a non-phosphorylatable HP1 α mutant (HP1 α S92A) results in increased anaphase bridges and micronuclei formation (Williams et al., 2019). H3T3 phosphorylation by Haspin phosphorylate H3T3 is also important for CPC

accumulation at mitotic centromeres (Jeyaprakash et al., 2007, Kelly et al., 2010, Wang et al., 2010, Yamagishi et al., 2010). At the centromere, CPC-HP1 interaction protects centromeric cohesion by promoting Haspin localization at the centromeres (Yi et al., 2018, Yi et al., 2019). Likewise, CPC-HP1 binding was shown to be important for Aurora B-mediated kinetochore phosphorylation, which prevents errors of kinetochore-microtubule attachment and subsequent chromosome segregating defects (Abe et al., 2016). The main HP1 functions at the centromere are summarised in Figure 1.8.

In fission yeast, the HP1 homologue Swi6 have been shown to interact with cohesin and be necessary for proper centromeric targeting and stabilization of cohesin (Bernard et al., 2001, Nonaka et al., 2002). However, siRNA-mediated depletion of the three HP1 isoforms independently in human cells did not show any effect on cohesin accumulation at pericentric chromatin (Serrano et al., 2009).

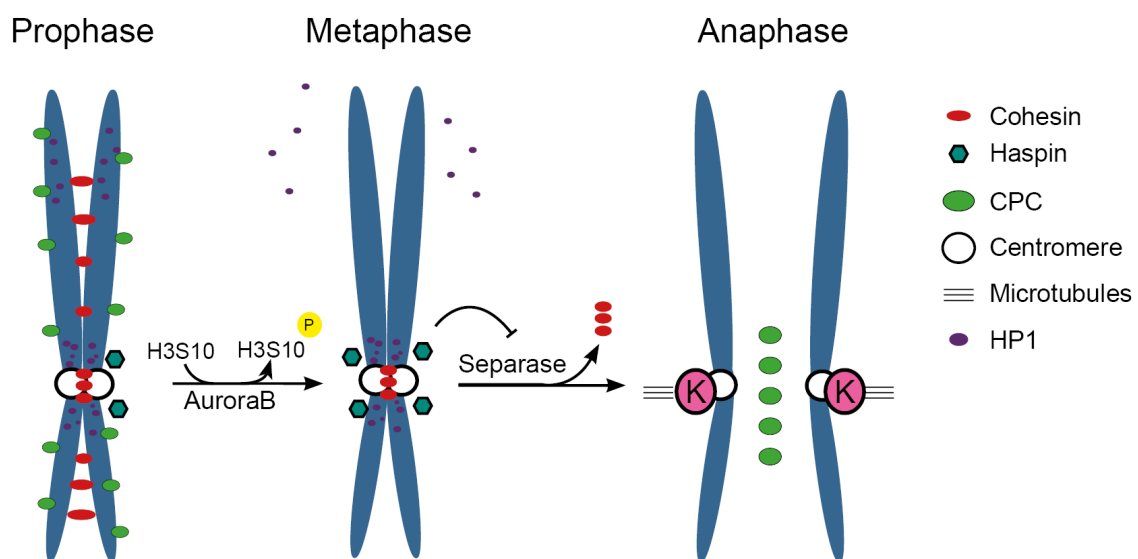


Figure 1.8. Role of HP1 at the centromere. During mitotic entry, Aurora B from the CPC is responsible for phosphorylation H3S10 from the chromatin, which will eject HP1 from the chromosomes. However, a portion of HP1 is retained at the centromeres where it is important to keep Haspin nearby, which protects cohesin release until microtubules are properly attached. Only proteins relevant to HP1 function at the centromere are shown.

1.2.2. Other heterochromatin marks: H3K27me3

Another important mark for heterochromatin is the trimethylation of lysine 27 on histone H3 (H3K27me3). Methylation of H3K27 seems to be gradual (from mono-methylation, to di- and finally tri-methylation) and more abundant than H3K9 methylation; embryonic stem cells (ESCs) have about 80-90% of total H3K27 methylated (20% mono-methylated, 50% di-methylated, and 10-20% tri-methylated) compared to about 50% of H3K9 being methylated (Peters et al., 2003). H3K27me_{2/3} is found in facultative heterochromatin, while H3K27me₁ is found in constitutive heterochromatin (telomeres and centromeres). However, enrichment of H3K27me₁ throughout the gene body associates with actively transcribed genes (Cui et al., 2009, Margueron, Reinberg, 2011).

H3K27 methylation is carried out by Enhancer of Zeste 2 (EZH2), a methyltransferase member of the Polycomb Repressing Complex 2 (PRC2) (Czermin et al., 2002, Kuzmichev et al., 2002, Cao et al., 2002). PRC2, together with Polycomb Repressing Complex 1 (PRC1), belongs to the polycomb group (PcG) proteins, a family that epigenetically alters chromatin in order to repress gene expression, mainly of genes related to proliferation and differentiation. PRC2 is well conserved among several species and loss of function during development results in early embryonic lethality in mice (O'Carroll et al., 2001). Interestingly, loss of H3K27 methylation results in increased H3K27 acetylation in ESC, indicating that PRC2 prevents H3K27Ac, a mark of active chromatin (Tie et al., 2009, Pasini et al., 2010).

There is some evidence that H3K27me₃ and H3K9me₃ are somehow linked and that the levels of one might affect the other. Some studies have shown that knockdown of Suz12, an important component of the PRC2 complex, results in loss of H3K9me₃ (Cecile et al., 2007). Likewise, several studies in animal cells and plants have shown that altered H3K9me₃ lead to changes in the H3K27me₃ distribution (Peters et al., 2003, Mathieu et al., 2005, Lindroth et al., 2008, Deleris et al., 2012, Hagarman et al., 2013, Reddington et al., 2013, Jamieson et al., 2016). Similarly, studies in fungi showed that HP1 knockout or simple mutations on the HP1 CD results in a dramatic redistribution of H3K27me₃, suggesting that HP1 binding to H3K9me₃ is required to affect H3K27me₃ organization (Jamieson et al., 2016). At the same

time, H3K27me_{2/3} has been proved to regulate HP1 binding to chromatin. Actually, either loss of EZH2 or Suz12, or overexpression of H3K27me₃ demethylases resulted in HP1 proteosomal degradation and are therefore important for HP1 stability (Boros et al., 2014). In addition, H3K27me₃ enhances HP1 α binding to H3K9me₃ and loss of H3K27me₃ is sufficient to dissociate HP1 α from chromatin (Boros et al., 2014).

The behaviour of H3K27me₃ during mitosis is similar to H3K9me₃; the phosphorylation status of the nearby amino acid (H3S28) is important for PRC2 binding to H3K27 and further lysine methylation. H3S28 is phosphorylated in early mitosis by Aurora B, an action counteracted by Repo-man/PP1 phosphatase complex at anaphase, which mediates H3S28 dephosphorylation and subsequent PRC2-driven methylation of H3K27, playing a role in gene expression regulation (Vagnarelli et al., 2011, de Castro et al., 2017). NIPP1 (Nuclear inhibitor of PP1), a PP1 regulatory subunit that inhibits PP1, also plays an important role on H3K27me₃ regulation through mitosis. NIPP1 can bind to phosphorylated EZH2 and block its dephosphorylation (normally carried out by PP1), thus keeping EZH2 bound to chromatin (Minnebo et al., 2012, Van Dessel et al., 2010). Altogether this evidence demonstrates the presence of a tightly regulated interplay between different histone modifications and heterochromatin marks to form and maintain a repressive environment.

1.3. Histone variant H2A.Z

The histone variant H2A.Z was originally identified in 1980 in mouse cells (West, Bonner, 1980), and the human *H2A.Z* gene was cloned ten years later by the same lab (Hatch, Bonner, 1990). Later studies in *Drosophila* (van Daal, Elgin, 1992) and mice (Faast et al., 2001) showed an essential role of this histone variant, since H2A.Z knockout led to early embryonic lethality. However, in *S. cerevisiae* H2A.Z depletion was not lethal (Jackson, Gorovsky, 2000), possibly pointing out to a difference on the role of H2A.Z within species.

As most proteins, H2A.Z is subject to PTM, including acetylation, methylation, phosphorylation, sumoylation, and ubiquitination. H2A.Z PTMs dictate its loading to the

chromatin as well as its transcriptional output. The residues that are subjected to modifications are summarised in Figure 1.10.

H2A.Z shares around 60% homology with H2A, with the main differences lying in the amino- and carboxy-terminal regions and the L1 loop. The overall structure of the H2A.Z and H2A containing nucleosomes are quite similar, although some differences at the C-terminal domain result in an extended acidic patch that extends across the surface of the H2A.Z octamer and exposes the cavity in the center of the nucleosome (Figure 1.10.A). Studies in *Drosophila* and *Xenopus* indicated that the acidic patch is important for development. Studies in ESCs showed that a mutant form of H2A.Z, with the three distinct amino acids from the acidic patch are mutated to the H2A ones, is less associated with chromatin and have increased mobility. Cells transfected with this mutant also failed to differentiate properly (Subramanian et al., 2013). Another significant difference between the H2A and H2A.Z structures is at the L1 loop, which is linked to an increase of flexibility in the H2A.Z variants (Horikoshi et al., 2013) (Figure 1.9.B).

1.3.1. H2A.Z variants

H2A.Z in vertebrates is present as two isoforms, known as H2A.Z.1 and H2A.Z.2 encoded by the *H2AFZ* and *H2AFV* genes, respectively. At the same time, H2A.Z.2 has two alternatively spliced variants, termed H2A.Z.2.1 and H2A.Z.2.2. The two H2A.Z variants only differ in three amino acids (Figure 1.10), they have similar nuclear distribution and PTMs with a similar, though not identical, genome distribution (Dryhurst et al., 2009). Furthermore, H2A.Z.1 and H2A.Z.2 are differentially expressed among human tissues: H2A.Z.1 expression is high in the brain of adult and foetal tissues, while H2A.Z.2 is higher in adult liver and kidney samples (Dryhurst et al., 2009). The promoters of both H2A.Z.1 and H2A.Z.2 also differ: while H2A.Z.1 presents a usual promoter similar to other histone variants, H2A.Z.2 promoter lacks a TATA box and the CAAT regions and CG elements do not correspond with those identified in H2A.Z.1 (Dryhurst et al., 2009). In addition, there are structural differences in the L1 loop of both variants, and they present different nucleosome mobility in cells (Horikoshi et al., 2013).

These differences between both variants might seem small, but they are rather significant in terms of functionality. One of the first differences on their individual activity was shown early in this decade by Matsuda and colleagues (Matsuda et al., 2010), who were able to individually knockout each of the H2A.Z variants in DT40 chicken cells. They showed that H2A.Z.2-deficient cells present a slower cell proliferation rate compared to WT and H2A.Z.1-deficient cells, and that this is due to an increased apoptotic rate. Later on, other studies aimed at deciphering differences between H2A.Z.1 and H2A.Z.2 have been conducted, although many studies nowadays still study these two variants as one. In agreement with Matsuda et al., knockdown of H2A.Z.2 in human metastatic melanoma cells led to downregulation of cell—cycle promoting genes (Vardabasso et al., 2015).

Not so many studies have been conducted on H2A.Z.2.2, a shorter spliced variant of H2A.Z.2 (Figure 1.10). However, it has been shown that, although it interacts with Tip60 and SRCAP chaperones, H2A.Z.2.2 gets only partially incorporated into the chromatin. This seems to not be caused by the shortened length, but rather to its unique amino acid sequence at the C-terminus domain (Bönisch et al., 2012a). Due to its difference on the C-terminus sequence, studies comparing H2A.Z.2.1 and H2A.Z.2.2 might be important to determine specific roles and characteristics of this C-terminal domain.

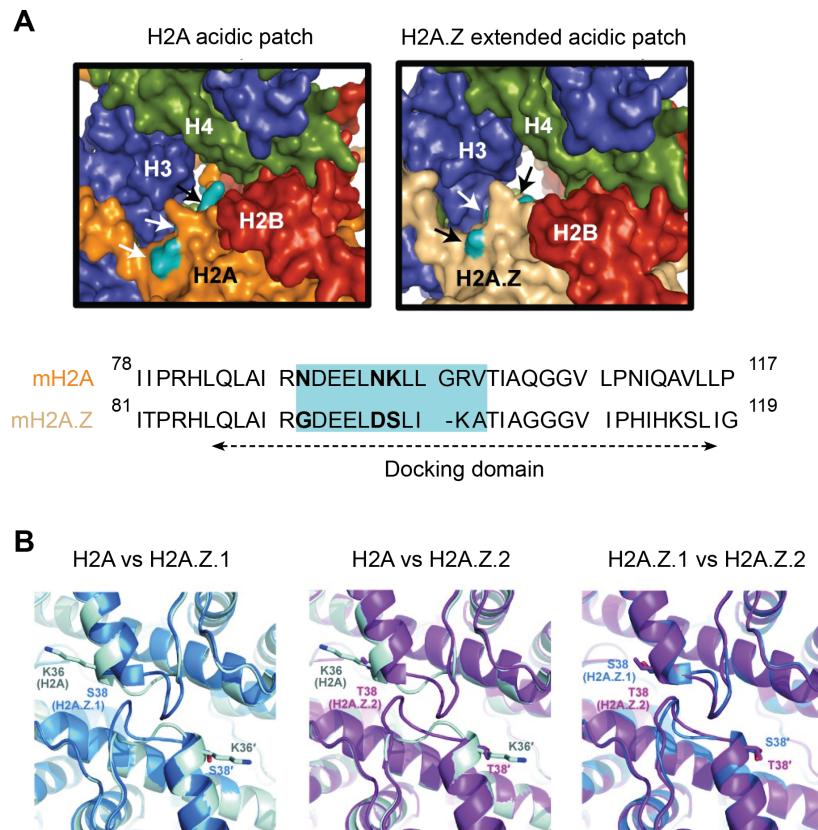


Figure 1.9. Main differences between H2A and H2A.Z. **A)** Surface rendering of the H2A and H2A.Z nucleosome center. The H2A (orange) and H2A.Z (light brown) structures are shown with H2B (red), H3 (blue), and H4 (green). The divergent residues (turquoise) are highlighted with arrows. Below, the C-terminal sequences of H2A and H2A.Z with the acidic patch highlighted in turquoise. From (Subramanian et al., 2013). **B)** Structural comparison of the L1 loop of H2A, H2A.Z.1 and H2A.Z.2 nucleosomes. From (Horikoshi et al., 2013).

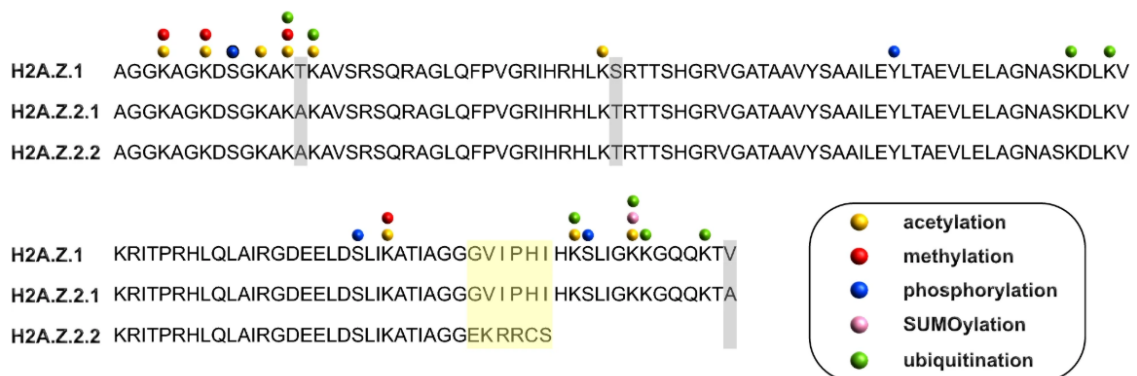


Figure 1.10 Alignment of the three human H2A.Z protein sequences. Highlighted in grey, the three different amino acids between H2A.Z.1 and H2A.Z.2.2; highlighted in yellow, amino acids not conserved between H2A.Z.2.1 and H2A.Z.2.2. Colour dots represent the sites for post-translational modifications (from (Giaino et al., 2019)).

1.3.2. Mechanisms of H2A.Z loading

Incorporation of H2A.Z onto chromatin is a complex mechanism involving the coordination of many proteins. In yeast, the loading is driven by the ATP-dependent chromatin-remodelling complex, Swi2/snif2-related 1 (SWR1) (Mizuguchi et al., 2004, Kobor et al., 2004, Wu et al., 2005, Luk et al., 2007, Zhou, Z. et al., 2008, Wu, W. et al., 2009, Ranjan et al., 2013). SWR1 is composed by several subunits (Figure 1.11) and its 3D structure has been determined by electron microscopy (Nguyen et al., 2013). The SWR1 complex partially unwraps the DNA from the histone core, and the subunit Swr1 acts as a chaperone to exchange one H2A at a time, forming a transient heterotypic nucleosome composed of H2A, H2A.Z and H2B (Luk et al., 2010, Hong et al., 2014). A H2A.Z-specific chaperone has been identified, Chz1, although it can be replaced by other chaperon-like proteins for histone replacement, as Chz1 knockout in yeasts do not present impaired H2A.Z deposition (Luk et al., 2007, Dronamraju et al., 2017, Wang, Y. et al., 2019). Other complexes are also necessary for the loading of H2A.Z, including NuA4 and Ino80. Esa1 (Tip60 in mammals) is an acetyltransferase from the NuA4 complex that acetylates the N-terminal domain of canonical H4 and H2A, required for SWR1 recruitment to the nucleosomes (Keogh et al., 2006, Auger et al., 2008, Altaf et al., 2010, Ranjan et al., 2013).

In mammals, there are two homologues of SWR1: Snf2-related CBP activator protein (SRCAP) and the Protein 400/60kDa Tat-interactive protein (p400-Tip60) complexes, both able to mediate the exchange (Doyon, Côté, 2004, Mizuguchi et al., 2004, Ruhl et al., 2006). YL1, the Chz1 homologue, is a subunit of both the p400-Tip60 and SRCAP complexes that binds to H2A.Z-H2B dimers through its N-terminal domain allowing the interchange between dimers H2A-H2B and H2A.Z-H2B (Cai et al., 2005, Latrick et al., 2016). YL1 has been reported to be involved in both H2A.Z.1 and H2A.Z.2 loading to the same extent, as the same decrease in deposition of both variants is observed in DT40 cells depleted of Arp6, an actin-related protein present in the SRCAP complex (Matsuda et al., 2010, Yoshida et al., 2010, Maruyama et al., 2012).

The mechanistic removal of H2A.Z from the chromatin has been less studied, although ANP32E, a member of the p400/Tip60 complex, has been identified as a chaperone

responsible for this removal (Obri et al., 2014). Due to the high degree of regulation on H2A.Z deposition, it is expected that other proteins involved in regulating its removal exist, although this aspect is still in need of further analysis.

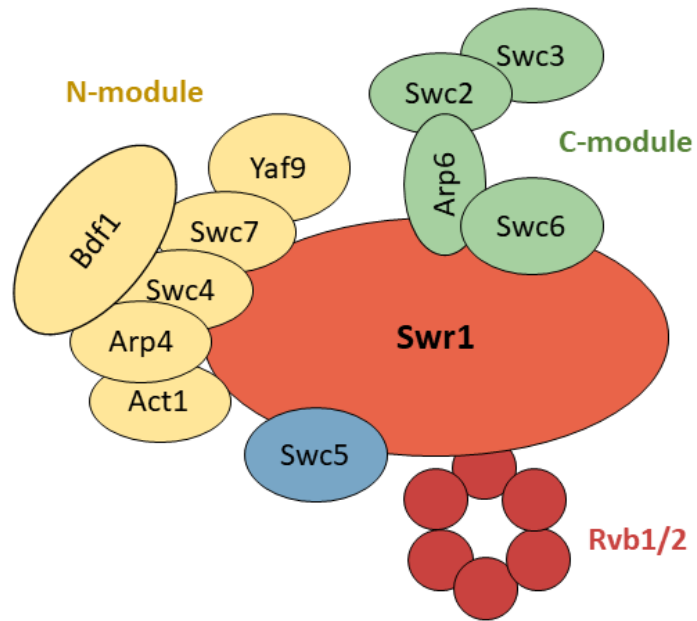


Figure 1.11. Schematic representation of the yeast SWR1 complex (from (Nguyen et al., 2013)).

Table 1-2. Composition of the NuA4, SWR1, p400/tip60 and SRCAP complexes (from (Giaimo et al., 2019))

Yeast		Mammalian	
NuA4	SWR1	P400/Tip60	SRCAP
Tra1		TRRAP	
Eaf1	Swr1	Ep400	SRCAP
	Bdf1	BRD8 (TRCp120)	BRD8 (TRCp120)
Epl1		EPC-like (EPC2)	
		ECP1	
Esa1		Tip60	
Eaf2	Eaf2	DMAP1	DMAP1
Rvb2	Rvb2	Tip49b (Ruvbl2)	Tip49b (Ruvbl2)
Rvb1	Rvb1	Tip49a (Ruvbl1)	Tip49a (Ruvbl1)
Arp4	Arp4	BAF53a (Actl6a)	BAF53a (Actl6a)
Yng2		ING3	
			ARP6
Eaf7		MRGBP	
Act1	Act1	Actin	
Eaf3		MRG15(Morf4l1)	
		MRGX(Morf4l2)	
	Vps72	YL1	YL1
Eaf5			
Yaf9	Yaf9	GAS41(Yeats4)	GAS41(Yeats4)
Eaf6		FLJ11730(Meaf6, hEaf6)	
	Vps71		Znf-HIT1

1.3.3. H2A.Z localization in the genome

H2A.Z is highly enriched at transcriptional start sites (TSS), mainly at the +1 nucleosome, of active and repressive genes, as showed by genome-wide localisation experiments in several organisms (Guillemette et al., 2005, Li et al., 2005, Petter et al., 2011, Raisner et al., 2005, Whittle et al., 2008, Bagchi et al., 2020). Enrichment and proximity of H2A.Z-containing nucleosomes to the TSS, as well as the PTMs of H2A.Z, influences gene expression (Bargaje et al., 2012). H2A.Z has been linked to RNA polymerase II (RNAPolII) and it was shown to be excluded from gene bodies by RNAPolII-related remodelers, as FACT and Spt6 mutants increased H2A.Z levels at coding regions in budding yeast (Jeronimo et al., 2015). Additionally, H2A.Z depletion led to impaired RNAPolII recruitment at TSS in specific

conditions (Adam et al., 2001, Hardy et al., 2009). Some studies also reported enrichment of H2A.Z at promoters, enhancers, and intergenic regions marked by H3K4me3 (alone or by coexistence with H3K27me3), but it was absent from nucleosomes of differentiated cells marked solely by H3K27me3 (Dryhurst et al., 2009, Ku et al., 2012, Hu et al., 2013, Creighton et al., 2008, Illingworth et al., 2012). However, it seems to be the opposite in embryonic stem cells, where H2A.Z associates with transcriptionally repressed genes marked by H3K27me3 and it colocalizes with the Polycomb complex, (Creighton et al., 2008, Illingworth et al., 2012).

H2A.Z is excluded from regions with high DNA methylated sites, and H2A.Z-enriched nucleosomes displayed low levels of DNA methylation in several organisms (Zilberman et al., 2008, Conerly et al., 2010, Zemach et al., 2010, Murphy et al., 2018). Loss of global DNA methylation associates with a gain of H2A.Z occupancy, while increased H2A.Z occupancy, obtained via loss of function of ANP32E, leads to reduced DNA methylation (Murphy et al., 2018, Zilberman et al., 2008). Valdés-Mora and colleagues (Valdés-Mora et al., 2012) showed that it is mainly the acetylated H2A.Z which anticorrelates with DNA methylation, as well as with H3K27me3. Other studies also showed the link between H2A.Z acetylation and active chromatin (Bruce et al., 2005), while H2A.Z ubiquitination is associated with transcriptional repression (Sarcinella et al., 2007, Draker et al., 2011).

1.3.4. Roles of H2A.Z

H2A.Z has been associated with several biological processes. Many studies revealed an important role of H2A.Z in transcription regulation; however, whether it promotes or represses transcription appears to depend on the gene, chromatin complex, and PTMs of H2A.Z itself. In *Drosophila*, H2A.Z acetylation and subsequent incorporation onto the chromatin are involved in the regulation of the Notch (Giaino et al., 2018) and Wnt (Chevallard-Briet et al., 2013, Rispoli et al., 2019) signalling pathways, directly linked to cell proliferation. In human cells, H2A.Z depletion induced p21 expression in a p53-dependent manner and led to premature senescence (Gévry et al., 2007, Bellucci et al., 2013). In

addition, H2A.Z was shown to be incorporated at the promoter regions of oestrogen receptor target genes, and its depletion led to defects on oestrogen-signalling, including cell proliferation (Gévry et al., 2009).

H2A.Z seems also to play a role in DNA repair mechanisms. H2A.Z was found to deposit at Double Strand Breaks (DSB) soon after DNA damage occurs (Kalocsay, Hiller & Jentsch, 2009, Xu, Y. et al., 2012), but it was rapidly removed by the chaperone Anp32. This exchange of H2A.Z nucleosomes is important to trigger a conformational change on the nearby chromatin necessary for the DNA damage checkpoint activation. The early deposition of H2A.Z to DSBs required the sumoylation of H2A.Z (Kalocsay et al., 2009) and it appeared to be specific for H2A.Z.2 (Nishibuchi et al., 2014). Damaged chromatin has been long reported to re-localize to the nuclear periphery to finalize the repair, and this also seems to be dependent on sumoylation of H2A.Z (Kalocsay et al., 2009, Horigome et al., 2014).

A role of H2A.Z in cognitive function has also been reported. H2A.Z mice knockouts have learning and memory difficulties (Shen et al., 2018), and H2A.Z is incorporated in the hippocampus and the cortex of mice in response to fear conditioning, where it regulates gene expression and prevents recent and remote memory formation (Stefanelli et al., 2018, Zovkic et al., 2014, Narkaj et al., 2018).

Possibly related to its role on the regulation of several cell cycle-related genes, overexpression of H2A.Z has been reported in many cancers, including breast (Hua et al., 2008), prostate (Slupianek et al., 2010, Valdés-Mora et al., 2012), bladder (Kim et al., 2013), liver (Yang, B. et al., 2018), and malignant melanoma (Vardabasso et al., 2015), and it is being investigated as a possible target for cancer therapy (Rangasamy, 2010). Accordingly, H2A.Z has been shown to play a role on the epithelial-mesenchymal transition (EMT), a feature of cancer cells (Domaschenz et al., 2017).

Another studied role of H2A.Z is on heterochromatin regulation. HP1 α , but not HP1 β or HP1 γ , was found to preferentially interact with nucleosomes containing H2A.Z and H2A.Z-depleted cells disrupted HP1 α binding (Rangasamy et al., 2004, Fan et al., 2004). Recent evidence suggests that H2A.Z and H3K9me3 can cooperate to enhance the binding of HP1 α to chromatin and that surprisingly, H2A.Z can substitute for H3K9me3 on promoting HP1 α -chromatin binding (Ryan, Tremethick, 2018). On chromosomes, H2A.Z is enriched at

pericentric heterochromatin, where it interacts with some centromere binding proteins like INCENP (Rangasamy et al., 2003, Greaves et al., 2007, Boyarchuk et al., 2014). This enrichment of H2A.Z at centromeres might explain the role of H2A.Z in chromosome segregation reported by Rangasamy and colleagues (Rangasamy et al., 2004).

1.4. Protein phosphatases

1.4.1. Protein kinases and phosphatases in chromatin regulation

Many factors are involved in controlling chromatin organization, ranging from ATP-dependent chromatin remodelling complexes to non-histone chromosome proteins.

One of the most important post-translational modifications is the reversible protein phosphorylation, with more than 70% of eukaryotic cellular proteins being regulated by this modification (Olsen et al., 2010). Phosphorylation mainly occurs at serine (Ser), threonine (Thr), tyrosine (Tyr) and Histidine (His) residues. This switch in the phosphorylation status is regulated by the activity of protein kinases and phosphatases. While kinases add a phosphate group to its substrate, phosphatases counteract these actions by removing the group. Alterations of the levels or activity of these enzymes could therefore alter the phosphorylation status of proteins leading to several pathological conditions.

Kinases and phosphatases are classified depending on whether they act at a Tyr or at a Ser/Thr residue. The number of Tyr kinases is similar to that of Tyr phosphatases (around 100 each). However, in the case of Ser/Thr, there are around ten times more kinases (about 400) than phosphatases (about 40) (Moorhead et al., 2009). These Ser/Thr phosphatases are highly regulated by regulatory protein subunits that bind to the catalytic domain and influence the localization, specificity and activity of the phosphatase catalytic subunit (Rebelo et al., 2015, Bollen et al., 2010a). The complex between catalytic and regulatory subunit is referred to as “holoenzyme” and represents the specific phosphatase within the cells.

When cells enter mitosis, chromatin is subjected to several changes that allow its condensation and re-modelling into distinct rod-shaped structures known as mitotic chromosomes. Phosphorylation of histone H3 at Ser10 and Ser28 by Aurora B kinase have been correlated with chromosome condensation and are crucial events during mitotic entry; however, Aurora B knockdowns have normal chromosome structure, indicating that it is not directly involved in the chromatin condensation process (Ajiro, Yasuda & Tsuji, 1996, Van Hooser et al., 1998, Hendzel et al., 1997, Goto et al., 1999). Phosphorylation of histone H3 at Thr3 by Haspin is also an important event during mitotic entry but not affecting chromatin condensation (Markaki et al., 2009, Dai, Higgins, 2005). All these mitotic phosphosites of Histone H3 (T3, S10 and S28) are removed during mitotic exit by the Repo-man/PP1 holoenzyme (Vagnarelli, P. et al., 2011, Qian et al., 2011). This complex gets fully activated and stabilised at anaphase onset and PP1 is recruited to the chromatin via its targeting subunit Repo-Man. Despite the importance of these phosphorylations during mitosis, studies on different species indicate that the role of these modifications might vary between organisms. In vertebrates, phosphorylation of H3S10 and H3S28 was shown not to be required for chromosome condensation (Xu et al., 2009). Moreover, studies in fission yeast proved that mutation of H3S10 to a non-phosphorylatable residue leads to impaired chromosome segregation but not chromosome condensation (Mellone et al., 2003). On the contrary, the same mutation in *S. cerevisiae* did not show any mitotic defect (Hsu et al., 2000). Similar to H3S10ph, H3Y41ph by JAK2 kinase has also been reported to be involved in HP1 release from chromatin, as there are reports that indicate that HP1 α is able to bind this residue via its chromodomain (Dawson et al., 2009b).

Histone H1 is also phosphorylated during mitosis and S phase and it has been related with chromatin decondensation, rather than with chromatin condensation (Roth, 1992). CDK2 phosphorylates H1, which disrupts H1-HP1 binding and destabilizes compacted chromatin, enabling proper cell cycle-progression (Halmer, Gruss, 1996, Hale et al., 2006). To our knowledge, the phosphatases involved in H1 dephosphorylation are still not known. Histone H2A and H2B phosphorylations at specific sites have also been related to chromatin organization. In particular, H2AY119ph by Aurora B is thought to regulate chromatin structure and function during mitosis (Brittle et al., 2007), and H2BS14ph facilitated apoptosis-related chromatin condensation (Cheung et al., 2003). Finally, phosphorylation of

histone H4S1 was also correlated with chromatin condensation during mitosis (Barber et al., 2004).

Altogether it is clear that histone modifications, and phosphorylations specifically, are very important for gene expression regulation. Several studies have been conducted to determine the specific roles of the phosphorylation sites that regulate transcription; however, new studies should focus on the identification of the phosphatases responsible for removing phosphorylations from histones and chromatin remodelling proteins, in order to have a better picture on how chromatin is maintained and regulated.

1.4.2. Protein phosphatase 1

Protein phosphatase 1 (PP1) belongs to the protein phosphatase subgroup of Serine/Threonine phosphatases (PPP), together with PP2A, PP2B and PP4, PP5, PP6, and PP7. All PPP subunits have a catalytic subunit with the same structural fold and catalytic mechanism, and have at least one regulatory subunit (Shi, 2009). PP1 and PP2A are the most characterized PPP proteins and are responsible for 90% of the protein phosphatase activity in eukaryotic cells (Bollen et al., 2010, Heroes et al., 2013). In mammals, three genes encode PP1 isoforms: PPP1CA, PP1CB and PP1CC, which encode for PP1 α , PP1 β , and PP1 γ , respectively (Sasaki et al., 1990, Barker et al., 1993, Barker et al., 1994). The amino acid sequence of the three isoforms is 90% identical, with slightly differences especially in the N- and C-terminal domains.

PP1 can interact with many different proteins. Traditionally, these proteins have been known as PP1 interacting proteins (PIPs), which are able to form stable complexes; recently, a new term for these PP1 subunits have emerged: RIPPOs (Regulatory Interactor of Protein Phosphatase One) (Wu et al., 2018), due to the possibility of confusing PIP with the acronym for phosphatidylinositol phosphates. It is not known the exact number of RIPPOs identified to date, although it has been suggested that PP1 can form complexes with around 650 mammalian proteins (Bollen et al., 2010). These proteins have been classified in 4 categories: i) inhibitors of the catalytic subunit; ii) substrate-specifying subunits; iii) targeting

subunits; iv) substrates. As indicated by the name, the catalytic subunit inhibitors block the access to the docking site of PP1 and inhibit the dephosphorylation of all substrates. Substrate-specifying subunits, also known as poor inhibitors, inhibit selectively the dephosphorylation of only a subset of substrates. The targeting subunits can target PP1 to different compartments including plasma membrane, mitochondria, nucleoli and chromatin, bringing PP1 into close proximity to specific substrates. PP1 substrates can be classified depending on their affinity for the catalytic subunit. Some substrates have high affinity for PP1 and are able to form stable complexes. However, there are others that only interact weakly with the catalytic subunit, and they require additional binding sites provided by RIPPOs. Substrates can be selectively dephosphorylated on a single site or at multiple sites. Some RIPPOs are both substrates and regulators of PP1 (Bollen et al., 2010).

How PP1 is able to interact with so many different proteins depends on a specific surface groove, which is mediated by docking motifs of about four to eight residues long known as SLiMs (short linear motifs). However, PP1 surface would only allow the interaction with about 30 non-overlapping proteins simultaneously, much lower than the total of RIPPOs, indicating that some must share docking sites on PP1. Nevertheless, a unique combination of the PP1 binding motifs and the exact sequence allows a high specific RIPPO-PP1 interaction (Figure 1.12) (Egloff et al., 1997, Hurley et al., 2007, Bollen et al., 2010). Altogether, it seems that selectively blocking specific docking sites of PP1 with small-molecule compounds could be an approach to disrupt a subset of PP1 holoenzymes and may have a therapeutic potential for different disease, including HIV (Ammosova et al., 2012, Lin et al., 2017). Inhibiting the catalytic subunit would have profound implications as it might block all PP1 functions; with this approach PP1 docking sites can be selectively targeted to disrupt only a subset of interactions and functions (Bollen et al., 2010).

The most common PP1 SLiM is the RVxF motif, present in about 90% of the validated RIPPOs (Bollen et al., 2010). It generally conforms to the consensus sequence K/R - x_{0-1} - V/I - y - F/W, where x is any residue and y usually a phosphorylatable residue (Wakula et al., 2003, Nasa et al., 2018). Although the binding of the RVxF motif in itself does not change the PP1 conformation and activity of PP1, it serves to anchor the RIPPO and bring it closer to PP1, allowing the interaction of the other SLiMs with PP1 to form the final holoenzyme complex (Egloff et al., 1997, Hurley et al., 2007, Ragusa et al., 2010, Carmody et al., 2008).

Interestingly, not all proteins that present the RVxF motif can bind PP1, thus the presence of an RVxF consensus sequence is not sufficient to classify a protein as a RIPPO (Wakula et al., 2003).

Other SLiMs comprise the SILK-type docking motif and the myosin phosphatase N-terminal element (MyPhoNE). The SILK domain is found in seven RIPPOs and contains the consensus sequence G/S I L R/K. SILK is always positioned N-terminal to the RVxF motif and, similarly, it serves as an anchoring site (Wakula et al., 2003, Hendrickx et al., 2009, Hurley et al., 2007). MyPhoNE, present in six RIPPOs, serves another function and it provides substrate selection. The consensus sequence is R x x Q V/I/L K/R x Y/W, where x can be any residue, and it is also always N-terminal to the RVxF motif (Hendrickx et al., 2009, Bollen et al., 2010). The detailed study of the interaction between PP1 and Spinophilin, a neuronal PP1 regulator, led to the identification of a new SLiM, also present in neurabon, termed SpiDoC (Spinophilin Docking site for the C-terminal groove), which blocks the recruitment of other substrates via the C-terminal groove of PP1 (Ragusa et al., 2010). In addition, studies on Inhibitor-2, another PP1 interactor, identified a conserved docking site for the hydrophobic and acidic grooves (IDoHA), which emanates from the catalytic subunit and inhibits phosphatase activity allosterically (Hurley et al., 2007).

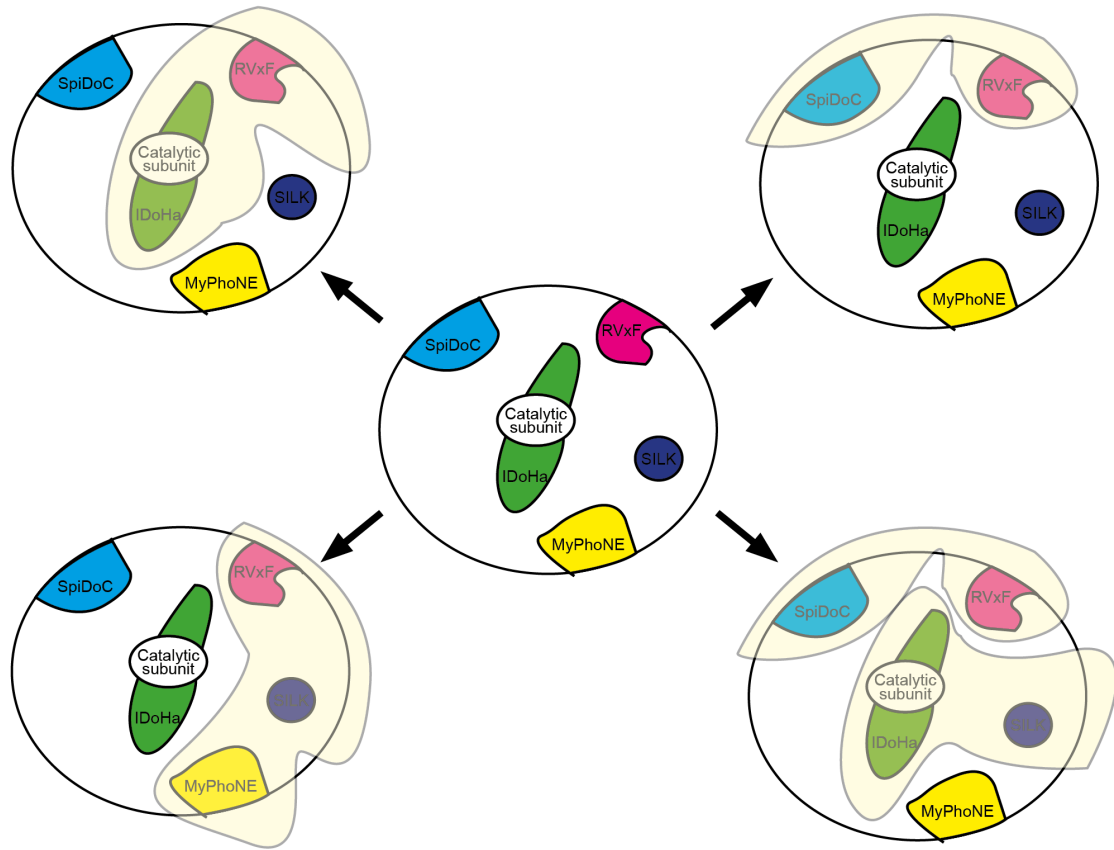


Figure 1.12. The PP1 binding code. PP1 presents multiple surface grooves that interact with RIPPOs SLiMs (middle). The most abundant ones are shown. RIPPOs adopt different combinations of docking sites to form unique PP1 holoenzymes. Adapted from (Heroes et al., 2013).

Studies on position-effect variegation (PEV) in *Drosophila* identified PP1 as a suppressor of variegation, *Su(var)3-6* (Baksa et al., 1993), which support the idea of PP1 as heterochromatin regulator. Chromosomal rearrangements or transpositions can lead to euchromatic genes being moved to nearby heterochromatic regions, which might suppress the expression of genes that are usually activated. Diverse mutagenesis experiments identified several genes that enhanced the expression of variegated genes (enhancers of variegation, *E(var)*), and some that suppressed its expression (suppressors of variegation, *Su(var)*). *Su(var)3-6*, which encodes for PP1, was one of these genes that, once mutated, suppressed the expression of variegated genes, meaning that in normal conditions *Su(var)3-6* acts as an enhancer of heterochromatin formation (Baksa et al., 1993).

Taken together, it is clear that protein phosphatases play crucial roles in the regulation of chromatin structure and dynamics. For a recent review on the role of protein phosphatases on chromatin organization please refer to (Gil, Vagnarelli, 2018). However, only a few phosphatase complexes and related molecular mechanisms have been identified to date. Considering the broad spectrum of phosphatase holoenzymes present, it is “normal” to think that these studies are just the tip of the iceberg and many more complexes are yet to be discovered.

1.4.3. Repo-man/PP1 holoenzyme

1.4.3.1. Repo-man as a PP1 targeting subunit

Repo-man is a PP1 targeting subunit encoded by the CDCA2 (Cell Division cycle Associated 2) gene, localized on chromosome 8 (8p21.2) in humans. CDCA2 was first identified as a cell cycle gene (Walker, 2001) until 2006, when Trinkle-Mulcahy et al. (Trinkle-Mulcahy et al., 2006) identified Repo-man as a targeting subunit of PP1, responsible for recruiting PP1 onto the chromatin at anaphase onset (Recruits PP1 onto Mitotic chromatin at anaphase). As the majority of PP1 targeting subunits, Repo-man possesses the conserved RVXF (RVTX in humans), which mediates PP1 binding. Mutation of the RVXF motif of Repo-man disrupts PP1 binding, although it does not affect Repo-man binding to chromatin (Trinkle-Mulcahy et al., 2006). Repo-man binds specifically to the β - and γ -isoforms (the latter more efficiently), but not the α -isoform of PP1 (Kumar et al., 2016, Trinkle-Mulcahy et al., 2006, Vagnarelli et al., 2011). Repo-man also possesses a conserved PP2A binding domain through which it forms the phosphatase complex Repo-man/PP2A (Qian et al., 2013) (Figure 1.13).

Studies using isothermal titration calorimetry (ITC) showed that Ki-67 and Repo-man bind PP1 $_{\gamma 7-323}$ following an identical mechanism with nearly equivalent affinities. They form a classical β -hairpin on the top of PP1 that extends from the PP1 RVxF binding pocket towards the PP1 N-terminal domain and then back again. This novel interaction domain, not found in

any other RIPPO, is known as the KiR-SLiM (Ki-67-Repoman Small Linear Motif) (Kumar et al., 2016) (Figure 1.14).

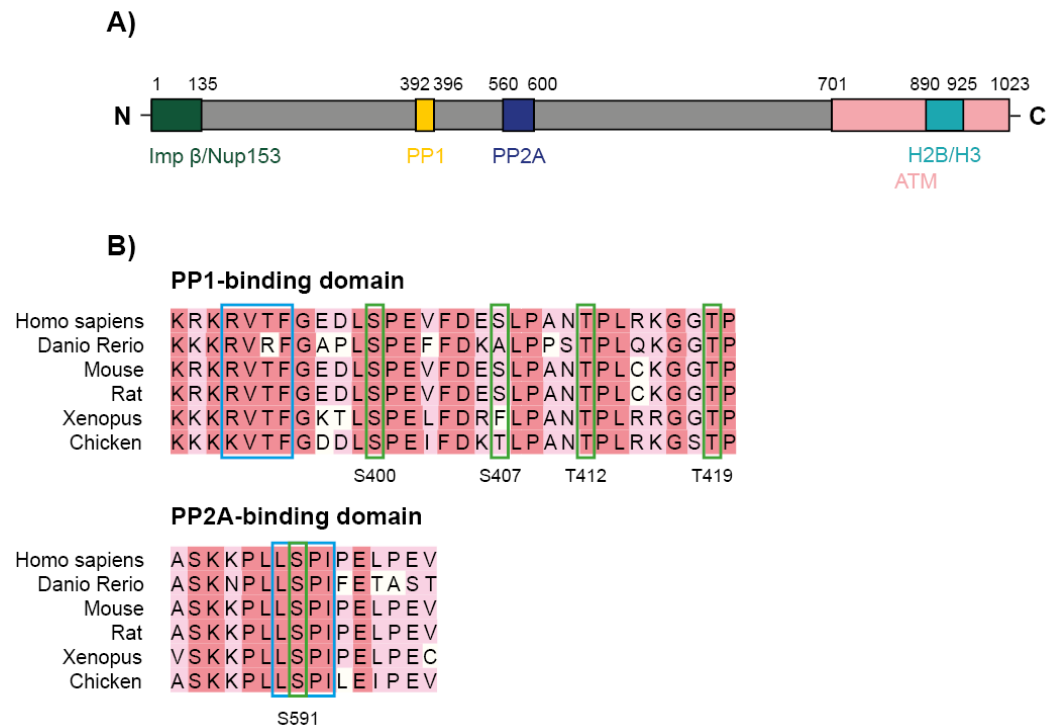


Figure 1.13. Repo-man structure and alignment of different species. **A)** A diagram showing the main functional domains of human Repo-man. **B)** The PP1-binding and the PP2A-binding motifs (blue) are highly conserved in vertebrates, as well as their main phosphorylation sites (green).

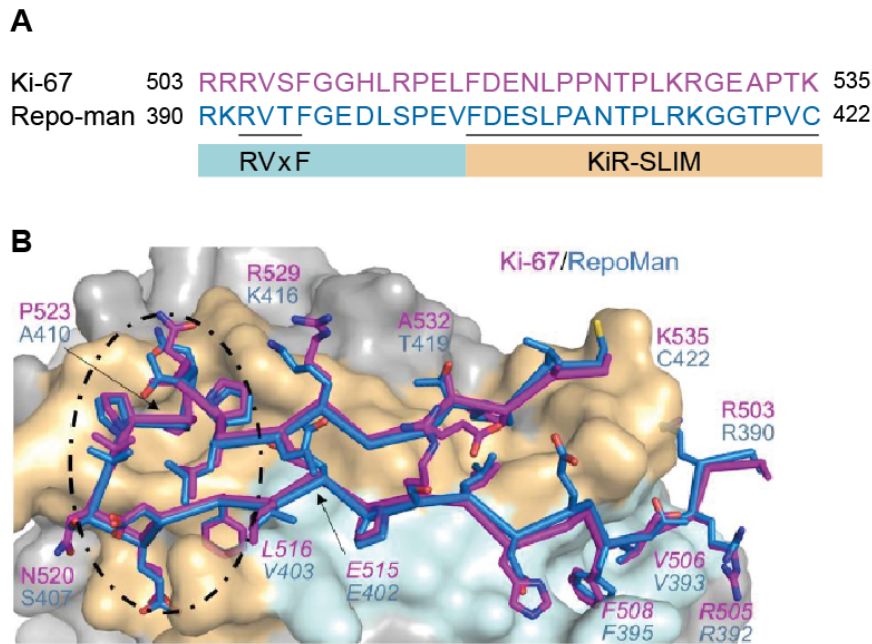


Figure 1.14. Repo-man:PP1 and Ki-67:PP1 holoenzyme complex (from (Kumar et al., 2016)). **A)** Ki-67 and Repo-man present a similar PP1 binding domain. The sequences corresponding to the RVxF domain (blue) and the KiR-SLiM domain (beige) are underlined in grey. **B)** Close-up of the Ki-67 (pink) and Repo-man (blue) interaction with PP1. Ki-67 residues 503–516 and Repo-man residues 390–403 bind the PP1 RVxF and $\Phi\Phi$ binding pockets (cyan surface; the Ki-67 and Repo-man RVxF and $\Phi\Phi$ SLiM residues are labelled). Ki-67 residues 517–535 and Repo-man residues 404–422 bind the KiR-SLiM binding pocket (beige surface).

1.4.3.2. Regulation of Repo-man throughout mitosis

In interphase, 20% of Repo-man/PP1 is localised on chromatin (De Castro et al, 2017), closely associated with histone H2B (Vagnarelli et al., 2011) and it has been proposed to play an important role in regulating the DNA damage response (Peng & Maller, 2010). Upon mitotic entry, Repo-man disperses in the cytoplasm and re-locates to the segregating chromatin at anaphase onset, where it de-phosphorylates histone H3 at three major sites: Thr3 (Vagnarelli et al., 2011, Qian et al., 2011), Ser10 (Vagnarelli et al., 2011), and Ser28 (de Castro et al., 2017). During mitosis, Repo-man/PP1 contributes to chromosome organisation and dynamics, and nuclear envelope reassembly during mitotic exit (Vagnarelli et al., 2011, de Castro et al., 2017).

Repo-man activity and localisation is controlled by CDK1-Cyclin B phosphorylation. At the beginning of mitosis, CDK1-Cyclin B phosphorylates Repo-man on different sites, including S400, T412, and T419 (Vagnarelli et al., 2011, Qian et al., 2011), which decrease Repo-man affinity for PP1 (Kumar et al., 2016) and chromatin, thus preventing Repo-man early binding to chromosomes. It was shown that, when T412 is mutated to an Alanine (cannot be phosphorylated by CDK1), Repo-man could bind to chromosomes in early mitosis (Vagnarelli et al., 2011). T412 phosphorylation also prevents PP1 from binding to the RVTF motif (Vagnarelli et al., 2011), making sure Repo-man is not fully activated before anaphase onset. Phospho-deficient mutations on all three CDK1 sites together (S400, T412, T419) increased the binding to PP1, suggesting that phosphorylation at these sites opposes the Repo-man/PP1 interaction. Aurora B kinase also contributes to Repo-man localisation and PP1-binding regulation via phosphorylation at Ser893 and T394, respectively (Qian et al., 2015, Kumar et al., 2016). Phosphorylation of Ser893, which can be counteracted by Repo-man/PP2A blocks Repo-man binding to mitotic chromatin (Vagnarelli et al., 2011, Qian et al., 2011), whereas T394ph inhibits PP1 γ binding (Kumar et al., 2016). At anaphase onset, CDK1 levels drop, and different phosphatases are involved in the fully activation of the complex. Firstly, a yet-unidentified phosphatase dephosphorylates T412 and allows Repo-man/PP1 complex formation. Ser893 is dephosphorylated by PP2A (Vagnarelli et al., 2011, Qian et al., 2011), and other phosphatases, including PP1, dephosphorylate other sites, contributing to Repo-man targeting to chromatin (Vagnarelli et al., 2011).

As mentioned, Repo-man/PP1 dephosphorylates different sites on histone H3. H3T3 represents a docking site for the Chromosome Passenger Complex (CPC), an important complex for the regulation of the spindle assembly checkpoint (SAC); therefore, dephosphorylation of this site is important for the re-location of the CPC from the centromere to the spindle and proper progression through mitosis (Jeyaprakash et al., 2007, Kelly et al., 2010, Wang et al., 2010, Yamagishi et al., 2010). H3S10 is important for HP1 binding to chromatin. HP1 recognizes tri-methylation of H3K9 but, in early mitosis, Aurora B phosphorylates H3S10, which ejects HP1 from the chromatin (Fischle, et al., 2005). Repo-man/PP1 is responsible for removing the phosphate group of H3S10 and is necessary for HP1 binding to chromatin at the end of mitosis, participating in the generation of a repressive chromatin environment within the nucleus (Castro, et al., 2017) (Figure 1.15).

Finally, Repo-man/PP1 is also responsible for dephosphorylation of H3S28. H3S28ph helps to modulate the binding of PRC2 and the expression of polycomb-regulated genes (Sawicka, Seiser, 2012), contributing to cell cycle progression (Figure 1.15).

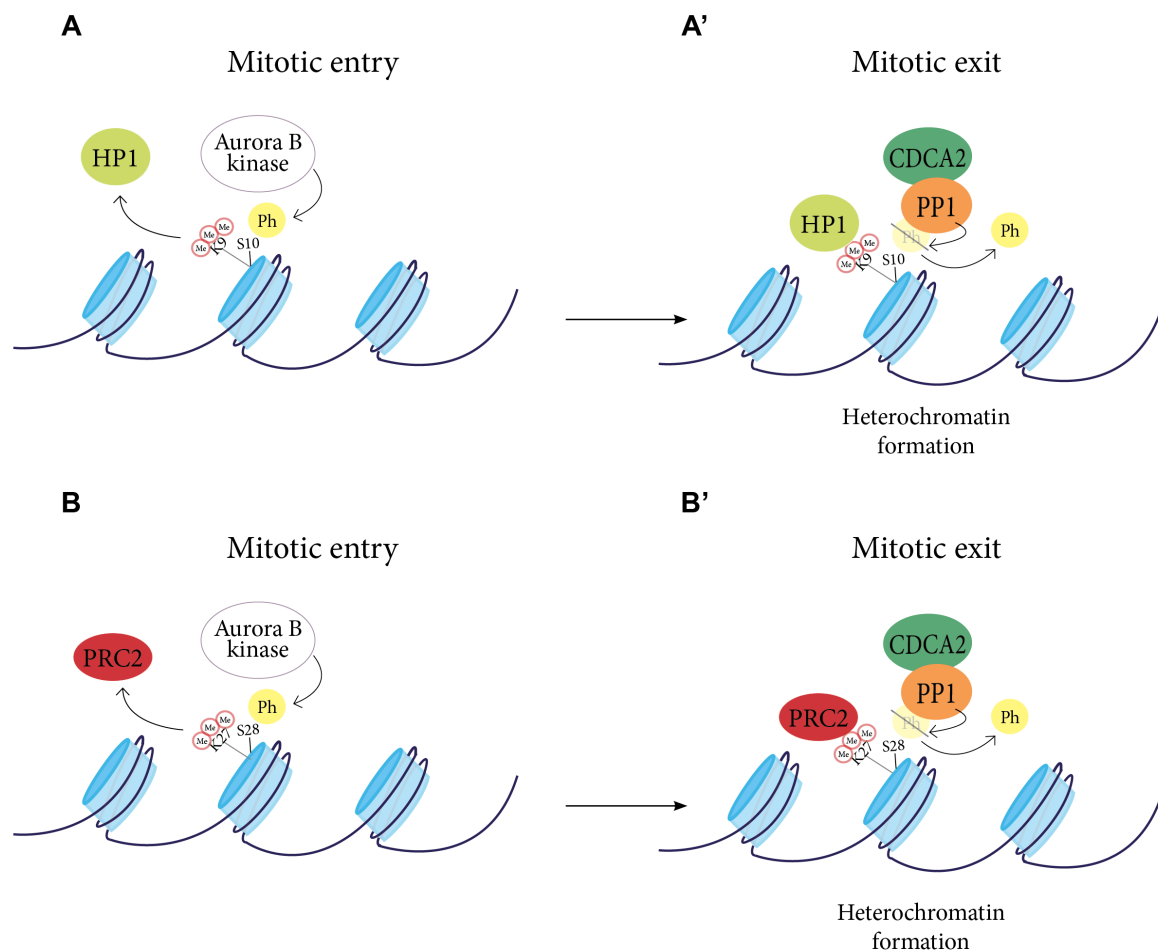


Figure 1.15. Module of CDCA2/PP1 function during mitosis. A) The cartoon represents the dynamics of HP1 during mitosis. At mitotic entry (**A**), Aurora B kinase phosphorylates H3S10, which ejects HP1 from the chromatin. During mitotic exit (**A'**), CDCA2/PP1 phosphatase complex dephosphorylates H3S10, enabling HP1 binding to chromatin and triggering heterochromatin formation. **B)** The cartoon represents the dynamics of PRC2 during mitosis. At mitotic entry (**B**), Aurora B phosphorylates H3S28, which ejects PRC2 from the chromatin. During mitotic exit (**B'**), CDCA2/PP1 is responsible for dephosphorylating H3S28, enabling PRC2 binding to chromatin and gene silencing.

1.5. Aims of the thesis

Chromatin organization has become a crucial area of study on cell biology for its impact on gene expression. Understanding how chromatin is organized and regulated might not only increase our knowledge on fundamental aspects of cell biology, but it might also shed light into understanding the origin of some diseases and identify new targets for drug therapy. In this research project I aimed to identify new regulators of heterochromatin formation and maintenance by:

- Developing a HeLa GFP:HP1 α cell line to use as a screening tool to identify new regulators of heterochromatin maintenance.
- Studying the role of protein phosphatase 1 (PP1) on HP1 α organization.
- Analysing CDCA2, a PP1 subunit involved in heterochromatin regulation, during development, using zebrafish as a model organism.
- Examining and distinguishing the two H2A.Z variants (H2A.Z.1 and H2A.Z.2) on their role on chromatin organization, gene expression and cell cycle.

2. MATERIALS AND METHODS

Cell culture methodology

2.1. Tissue culture

HeLa Kyoto (human cervical cancer cells) and MRC5 (human fibroblasts) cells were cultured in DMEM high glucose, GlutaMAX™ supplement (Gibco, 10566016), with addition of 10% foetal bovine serum (FBS) (Labtech, FB-1001-500), and 5% penicillin/streptomycin (Gibco, 15140122) at 37°C in 5% CO₂ humid incubator. Cells at 80-90% confluence were passaged (1:10) by trypsinization with TrypLE Express (Gibco, 12604013) to de-attach the adherent cells.

Zebrafish PAC2 fibroblasts cells, acquired from 24-hpf (hours post-fertilization) zebrafish embryos, were a kind gift from Peter Ceniijn (University of Vrije, The Netherlands). They were cultured in Leibovitz L-15 medium (Gibco, 11415) supplemented with 15% FBS, 5% penicillin/streptomycin at 28°C in a 0% CO₂ incubator. Cells at 80-90% confluence were passaged (1:5) by trypsinization with TrypLE Express.

Chicken B cell lymphoma DT40 cells carrying a LacO array integrated at a single locus (Vagnarelli, P. et al., 2006) were cultured in RPMI Medium 1640, GlutaMAX (Gibco, 61870036) supplemented with 10% FBS, 1% penicillin/streptomycin and 1% chicken serum, at 39°C in 5% CO₂ humid incubator. The cells were passaged 1:20 two to three times a week.

2.1.1. DNA and siRNA Transfection

For RNAi and transient DNA transfection, the JetPRIME® transfection reagent (refer to Table 7-1) was used. 1.5×10^5 cells were plated in 6-well plates 24 hrs before transfection in order to get 70-80% confluence at the time of transfection. 5µL of siRNA (stock solution 20 µM) (Table 1-1) and/or 1µL of DNA, depending on the experiment and unless otherwise

specified, were mixed with 200 μ L of JetPRIME[®] buffer and 4 μ L of JetPRIME[®] reagent and incubated at room temperature (RT) for 15 min. The reaction was added to 2 mL of fresh medium and the old medium was replaced. Cells were grown at 37°C for 24, 48 or 72 hrs, depending on the experiment.

Table 2-1. siRNA sequences used for the knockdown experiments.

Target mRNA	siRNA name	siRNA sequence (5' to 3')
	Control	CGUACGCGAAUACUUCGAdTdT
G9A	G9A.1	GAGUUUGGCAUGAGGCUA
	G9A.2	GAGUUUGGCUAUGAGGCUA
Ki-67	Ki-4	4392420 (Thermo Fisher Scientific)
	Ki-5	GCAUUUAAGCAACCUGCAA
	Ki-G	CGUCGUGUCUCAAGAUCUAtt
PP1 α	PP1 α	CCGCAUCUAUGGUUUCUAC
PP1 β	PP1 β	UUAUGAGACCUACUGAUGU
PP1 γ	PP1 γ	GCAUGAUUUGGAUCUUAUA
PNUTS	PNUTS (pool)	ACAAUUGGCUGACGUAUUC GCAGACCCGUUCACCAGAA GAACGAGUAAAUGUGAAUA GAAACAACCAGACUAUUCG
PTEN	PTEN	GUUAGCAGAAACAAAAGGAGUAUUC
Sds22	Sds22	AGUUCUGGAUGAACGACAATT
CDCA2	Repo-man	UGACAGACUUGACCAGAAA
NIPP1	NIPP1	GGAACCUCACAAGCCUCAGCAAUU
H2A.Z.1	H2A.Z.1_1	GUACCUACCCGACAGAGGUA
	H2A.Z.1_2	GCCGUAUUCAUCGACACCU
H2A.Z.2	H2A.Z.2_1	AUUUGUAUGUUCUAGACU
	H2A.Z.2_2	CUUAGACUCGAAGUUUGAU
	H2A.Z.2_3	UUUGUAUGUUCUAGACUC

Target mRNA	siRNA name	Target sequence (5' to 3')
MYH9	MYH9_2	CACGGAGATGGAGGACCTTAT
	MYH9_3	AACCGGGACGAAGCCATCAAA
RBL2	RBL2_6	ACCCTATATTAGGAAACTTTA
	RBL2_8	CTCCAACCACATTATACGATA

2.1.2. Transfection with Neon electroporation system

PAC2 cells and DT40 cells were transfected by electroporation using the Neon™ transfection system. 10^5 cells (PAC2) or 2.5×10^5 cells (DT40) were used in each transfection. The correct volume of cells was harvested and washed with PBS. Cells were pelleted at 1500 g for 5 mins, and the cell pellet was re-suspended in 10 μ l of buffer R (provided in the kit) and 1 μ g of DNA. Cells mixed with the DNA were picked up with the Neon pipette and placed in a cuvette filled with 3ml of Buffer E (provided in the kit), where an electric current (1600V, 10ms, 3 pulses) was applied. Cells were left overnight to grow in 24 well plates with 400 μ l of media.

2.1.3. Generating stable cell lines

GFP:HP1 α stable cell lines were performed using the GFP:HP1 α construct, a gift from Prof Eric Schrimmer, WTCCB, Edinburgh. This plasmid is cloned into the pEGFP-C1 vector (shown below, Figure 2.1) using the BamHI and EcoRI restriction sites. HeLa and MRC5 cells were transfected with 1 or 2.5 μ g/ml of the GFP:HP1 α plasmid with the JetPRIME® transfection reagent, as described previously. After 24 hrs, cells were plated at low density in selective medium containing 2mg/ml of geneticin (Gibco, G418) in 10cm dishes. After 10 days, single clones were collected and analysed for expression of GFP:HP1 α using a fluorescent microscope. Positive clones were grown in selection until the cell line was established and the medium was changed to standard conditions.

2.1.4. Drug treatments

The drugs in this study were used as follows: chaetocin (Sigma Aldrich, C9492) was used at a final concentration of 1 μ M for 48 hrs; 5-azacytidine (sigma Aldrich, A2385) was used at a final concentration of 4 μ M for 48 hrs; nocodazole (Sigma Aldrich, M1404) was used at a final concentration of 100ng/ml for 3 hrs.

2.2. Immunofluorescence

HeLa GFP:HP1 α cells were fixed in 1ml of ice-cold 100% methanol for 5 min at RT for HP1 analysis. Otherwise, cells were fixed in 1ml of freshly-made 4% PFA for 5 min at RT. Once fixed, cells were permeabilized in PBS / 0.2% triton for 2 min at RT and blocked with PBS / 1% bovine serum albumin (BSA) for 30 min at 37°C. Blocked cells were then incubated for 30 min at 37°C with the specific antibodies in 1% BSA (Table 2-2), and washed 3 times in PBS before exposure to the fluorescence-labelled secondary antibodies in 1% BSA (1:200) for 30 min at 37°C. Coverslips were then mounted in Vectashield mounting medium (Vector labs, H-1200) containing DAPI, and analysed in the NIKON Ti-E super research Live Cell imaging system.

Table 2-2. List of antibodies used for immunofluorescence

Antibody	Species	Company	Cat. number	Dilution
CDCA2	Rabbit	Abcam	Ab45129	1:250
CDCA2 58A	Rabbit	(Vagnarelli et al., 2006)		1:250
Zebrafish CDCA2 21	Rabbit		Home made	1:200
Zebrafish CDCA2 22	Rabbit		Home made	1:200
α -tubulin	Mouse	Sigma Laboratories Ltd	T5168	1:1000
HP1 α	Mouse	Merck	MAB3584	1:500

H2A.Z	Rabbit	Cell Signaling Technology	2718	1:200
H3K27me2/3	Mouse	Active Motif	39535	1:500
H3K9me3	Rabbit	Active Motif	39161	1:500
Lamin A+Lamin C	Rabbit	Abcam	ab108595	1:2500
mAb414	Mouse	Covance	MMS-120R	1:500
Texas Red	Rabbit	Jackson ImmunoResearch	711-585-152	1:200
	Mouse		115-076-062	
FITC	Rabbit	Jackson ImmunoResearch	715-095-150	1:200
	Mouse		715-545-150	

2.3. Immuno-fiber FISH

DT40 cells were transfected with the NeonTM transfection system as explained earlier. The following day, cells were spin down at 1000 g for 5 min, resuspended in 300µl of 75mM KCl and added to the cytospin at 100 g 5 min. The cells were collected in a slide and treated with 50ml of ULB buffer (see below) for 13 min before being fixed with 4% formaldehyde in PBS at RT, washed, and permeabilized in 0.2% Triton/PBS for 2 min at RT. Cells were washed and blocked in 1% BSA for 1h. Cells were then immunostained as explained earlier. Once the staining was finished, cells were incubated in 0.1M HCl for 10 min at RT, washed in 2xSSC for 3 min, and incubated in 70% ethanol for 3 min. LacO probe was labelled with fluorescein-12-dUTP by someone else using the Nick translation kit. 6µl of labelled LacO probe were mixed with 14µl of hybridization buffer (Fischer Scientific, 89-028-827) and incubated for 5 min at 73°C. Without allowing the slide to dry, 10µl of probe + hybridization buffer were applied and it was covered with a square coverlip and closed with rubber cement. The slide was incubated for 5 min at 85°C and overnight at 39°C in a humid box. The next day, the slide was incubated in 2xSSC for 10 min at RT, followed by 10 min at 60°C with 0.4x SSC. Chromatin was finally stained with Vectashield and cells were mounted for the microscope.

2.3.1. List of solutions

ULB buffer

- 25mM Tris pH 7.5 (Invitrogen, 15504-020)
- 0.5M NaCl (Sigma Aldrich, S3014)
- 1% Triton (Fischer Scientific, BP151-100)
- 0.5mM Urea (Acros Organics, 424585000)

2.4. Fluorescent microscopy and statistical analysis

All cell images presented were taken using the Nikon Eclipse Ti-E inverted microscope system. Images were taken with 100x objective in Z stacks (0.3 μm steps), deconvolved using the Nikon ElementAS software to eliminate the out of focus light, and presented as maximum intensity projection. For the intensity and nuclear shape analyses, the Nikon software ElementAS was used. For fluorescence intensity analyses, nuclei were automatically detected by the program and the ROI sum intensity in the area was recorded for each channel. All the analyses were conducted by first subtracting the background from a region of the same area within each image. For the circularity studies, nuclei were also selected automatically and the circularity ratio tools were used for each object.

For analysing the accumulation at the nuclear periphery, the 25 first and last data points obtained from the line scan analyses on the DAPI channel were considered “the periphery”. A mean was taken from the centre and the periphery/centre intensity ratio was calculated.

2.4. Fluorescence-activated cell sorting (FACS)

Cells were cultured in 6-well plates and transfected with siRNA as explained earlier. Once the cells were ready, they were detached with TrypleExpress and washed with PBS. Cells

were pelleted at 4°C and the supernatant was removed, leaving a few μl to resuspend the cells. Cells were vortexed and 5ml of 70% ice-cold ethanol were added dropwise. After the samples were incubated 30 min at RT, they were centrifuged at 1000g for 4 min, washed with 1ml of PBS and the supernatant was discarded. The pellet was resuspended in 200 μl of RNase A/PBS (100 $\mu\text{g}/\text{ml}$) and incubated for 2 hrs at 37°C in the dark. Propidium iodide (Fisher Scientific, P3566) was added at a final concentration of 5 $\mu\text{g}/\text{ml}$ just before analysing the samples by flow cytometry using the ACEA Novocyte flow cytometer. The analysis was performed using the NovoExpress® software.

2.5. Statistical analyses

The statistical analyses for the HP1 distribution studies were done by using the chi-square test, whereas for the nuclear intensity and the circularity, the Mann-Whitney U test was used. P values were represented as follows: ns ($p > 0.05$), * ($P \leq 0.05$), ** ($P \leq 0.01$), *** ($P \leq 0.001$).

2.6. RNA extraction

The RNeasy PowerLyzer Tissue & Cells Kit was used for RNA extraction (refer to Table 7-1). Cells were collected in culture media and counted using a haemocytometer. Cells were pelleted at 2000 x g for 5 min and the supernatant was discarded. 300 μL of solution TR1 containing 1% of β -mercaptoethanol were used to re-suspend the cells. The lysate was transferred to a 2mL tube and vortexed for 2 min. Solution TR1 lyses the cells, releasing the RNA. 300 μL of solution TR2 (70% ethanol) was added to establish optimal binding conditions for RNA on the Spin Filter membrane. The lysate was then transferred onto the Spin Filter and centrifuged for 1 min at 10000 x g. The Spin Filter was washed with 500 μL of solution TR3 (wash buffer) by centrifugation for 1 min at 10000 x g, in order to remove the proteins from the column. To remove the salts, the solution was washed twice with 500 μL

of solution TR4 by centrifugation for 1 min at 10000 x g. The Spin Filter was then centrifuged for 2 min at 13000 x g to dry the membrane completely and RNA was finally eluted with RNase-free water by centrifugation for 1 min at 10000 x g. RNA was stored at -80°C until needed.

2.7. Differential gene expression

2.7.1. cDNA retro-transcription

Thermo Scientific RevertAid First Strand cDNA synthesis kit (refer to Table 7-1) was used for cDNA synthesis. Before cDNA synthesis, genomic DNA was removed from the sample by mixing 1 µg of RNA with 1 µL of 5X Reaction Buffer with MgCl₂ and 1 µL of DNase I (RNase-free) and up to 10 µL of RNase-free water, and incubated at 37°C for 30 min. The reaction was finished by adding 1 µL of 50mM EDTA and incubating at 65°C for 10 min. Total RNA was then combined into a sterile tube on ice with the reagents indicated in Table 2-3. Components were added in the indicated order.

Table 2-3. Reverse transcription reaction

Component	Volume
Template DNA	1-2 µg
Oligo(dT)18 or Random Hexamer primer	1 µl
N-free water	Up to 12 µl
5x Reaction Buffer	4 µl
RiboLock RNase Inhibitor (20U/µL)	1 µl
10 mM dNTP Mix	2 µl
RevertAid M-MuLV RT (200U/µL)	1 µl

The components were mixed gently and centrifuged briefly. For oligo(dT)₁₈ synthesis, the mix was incubated for 60 min at 42°C, whereas for the Hexamer primed synthesis, the mix was first incubated for 5 min at 25°C followed by 60 min at 42°C. The reaction was terminated by heating at 70°C for 5 min. cDNA was stored at -80°C until used.

2.7.2. Quantitative Polymerase Chain Reaction (qPCR)

Gene expression was analysed by qPCR using primers designed with the Primer BLAST tool from NCBI website (Table 2-4). The melting temperature of all primers was set at 60°C, its length was about 20 nucleotides, and the target sequence to be amplified no longer than 200bp. Primers were synthesized by Eurofins Genomics (Germany).

The qPCR master mix for each gene was prepared by following reaction components in Table 2-5. 20ul of master mix was added into a 96 well plate and the plate was placed in a QuantStudio 7 Flex Real-Time PCR Machine with the parameters shown in Table 2-6.

Table 2-4. Set of qPCR primers

Target gene	Primers	Sequence (5' to 3')
H2A.Z.1	Forward	GCTGGAAAGGACTCCGGAAA
	Reverse	GTTCAAGTACCTCTGCGGTGA
H2A.Z.2	Forward	GAGAGCTGGGCTACAGTTTC
	Reverse	AGCACCTCTGCAGTGAGGTA
RBL2	Forward	TGACTCCCAGAAGGGTGA
	Reverse	CCCTCCATCAGAGGGGCTAT
MYH9	Forward	AGGGCTCATCTACACCTATT
	Reverse	CATCTCGTGCCTCTTCTTG

Table 2-5. qPCR reaction mix

Component	Volume
Maxima SYBR Green Master mix (2X)	12.5µL
Primer mix (10µM)	0.75µL
cDNA	1µL
N-free water	Up to 25 µL

Table 2-6. QuantStudio 7 qPCR reaction parameters

Temperature	Time	Number of cycles
50°C	2'	1
95°C	10'	1
95°C	15''	40
60°C	1'	
95°C	15''	1
60°C	1'	1
95°C	15''	1

2.7.3. Statistical analysis

For quantification of gene expression the cycle of threshold (Ct) for each gene transcript was determined and the relative expression (RE) was calculated in Excel as follows:

$$RE = 2^{-\Delta\Delta Ct}$$

$$\Delta\Delta Ct = \Delta Ct_{\text{sample}} - \Delta Ct_{\text{control}}$$

$$\Delta Ct = Ct_{\text{target gene}} - Ct_{\text{reference gene (GAPDH)}}$$

The mean and standard deviation (SD) of RE values was calculated from three biological replicates for each condition and a one-sample Student's t-test was performed to compare gene expression between control and treated samples.

2.8. Western Blotting

2.8.1. Cell lysate preparation

Cells were transfected with siRNA in 6-well plates as explained earlier. Once ready, cells were counted and collected by centrifugation at 1200g. Cells were washed in PBS, centrifuged, and re-suspended in PBS + protease and phosphatase inhibitors (refer to the section 2.7.4). Cells were centrifuged again for 5 min at 4^oC and the pellet was re-suspended in 1X Laemmli buffer (refer to the section 2.7.4); 30µl of Laemmli buffer was used for every 5x10⁵ cells. Cells were homogenised by hand pestle for 1 min and boiled at 95^oC for 5 min. This was repeated 3 times for each sample. The protein lysate was kept at -20^oC until needed and the samples were boiled 5 min at 95^oC before loaded on the gel.

2.8.2. Mouse tissues lysate preparation

Mouse tissues were a kind gift from Dr. Su-Ling Li from Brunel University London.

Protein extraction from mice tissue was performed using a TissueLyzer machine (Qiagen, 85300). Samples were mixed with a solution of PBS and protease and phosphatase inhibitors (refer to the section 2.7.4), put on the TissueLyzer machine, spined down for 20 min at 4^oC, and the supernatant was kept in the -80^oC fridge until used. A Coomassie Bradford protein assay (ThermoFisher, 23200) was used to determine the protein concentration of each sample. Briefly, a set of diluted albumin (BSA) standards was prepared as indicated in the kit and a standard curve was plotted with the measurements for each BSA standard, acquired with a spectrophotometer set to 595nm vs. its concentration. Our sample was mixed with the Coomassie reagent and measured on the spectrophotometer, and its concentration was determined using the previous standard curve. 20µg of each tissue mixed with 1x Laemmli sample buffer (refer to the section 2.7.4) were loaded on a SDS-PAGE electrophoresis gel.

2.8.3. SDS-PAGE gel electrophoresis, transfer and visualization

Proteins were separated with 7.5% polyacrylamide gel, run in 1X running buffer (refer to the section 2.7.4) at 135V, and transferred onto the nitrocellulose blotting membrane (GE Healthcare Life Science, 10600003) for 2 hrs in 1X transfer buffer (refer to the section 2.7.4) at 200mA. The membrane was blocked overnight with 5% milk in PBS-Tween at 4°C. The next day, the primary antibody (Table 2-7) was diluted in 3% milk in PBS-0.1%Tween (PBT) and applied to the membrane for 1 hr at RT. The membrane was washed three times with PBT for 5 min at RT. The appropriate HRP secondary antibody (Table 2-7) was diluted in 1% milk in PBT and applied for 1 hr at RT. The membrane was washed three times with PBT for 5 mins at RT. Pierce® ECL substrate (Thermo Scientific, 32209) was used to detect the HRP secondary antibodies. The membrane was visualized by using the Curix 60 processor, Agfa.

Table 2-7. List of antibodies used for Western Blots

Antibody	Species	Company	Cat. number	Dilution
CDCA2	Rabbit	Proteintech	17701-1-AP	1:300
CDCA2	Rabbit	Sigma Laboratories Ltd	HPA030049	1:500
CDCA2	Rabbit	Abcam	Ab45129	1:1000
ZfCDCA2 21	Rabbit	Home made	-	1:500
ZfCDCA2 22	Rabbit	Home made	-	1:500
α -tubulin	Mouse	Sigma Laboratories Ltd	T5168	1:3000
Histone H2A.Z	Rabbit	Cell Signaling Technology	2718	1:1000 (in BSA)
Goat anti-Rabbit IgG		Thermo Fisher Scientific	31460	1:5000
Goat anti-Mouse IgG		Thermo Fisher Scientific	31444	1:5000

2.8.4. List of solutions

RIPA buffer

- 150mM NaCl (Sigma Aldrich, S3014)
- 1% Igepal[®]CA-630 (Sigma Aldrich, I8896)
- 0.5% Sodium deoxycholate (Sigma Aldrich, D6750)
- 0.1% SDS (Fisher Scientific, 10593335)
- 50mM Tris-HCl pH 8.0 (Invitrogen, 15504-020)

Laemmli buffer

- 4% SDS (Fisher Scientific, 10593335)
- 20% Glycerol (Fisher Scientific, G/0650/08)
- 0.125M Tris-HCl (Invitrogen, 15504-020)
- 0.004% Bromophenol blue (Sigma Aldrich, B0126)
- 10% β-mercaptoethanol (Fisher Scientific, M/P200/05)

CLAP inhibitors (final concentration 1µg/ml)

- Chymostatin (Sigma Aldrich, C7268)
- Antipain (Sigma Aldrich, E13)
- Leupeptin (Sigma Aldrich, L2884)
- Pepstatin (Sigma Aldrich, P4265)

Phosphatase inhibitors (final concentration 1mM)

- Sodium orthovanadate (Sigma Aldrich, S6508)
- Sodium fluoride (Sigma Aldrich, S7920)
- B-Glycerolphosphate (Sigma Aldrich, G9422)

10X Running buffer

- 144g Glycine (Sigma Aldrich, G8790)
- 30g UltraPure[™] Tris (Invitrogen, 15504-020)
- Up to 1L dH₂O

1X Running buffer

- 100mL 10X running buffer
- 5mL SDS (Fisher Scientific, 10593335)
- Up to 1L dH₂O

10X Transfer buffer

- 144g Glycine (Sigma Aldrich, G8790)
- 30g UltraPure™ Tris (Invitrogen, 15504-020)
- Up to 1L dH₂O

1X Transfer buffer

- 100mL 10X transfer buffer
- 5mL SDS (Fisher Scientific, 10593335)
- 200mL Methanol (Fisher Scientific,
- Up to 1L dH₂O

SDS Gel buffer for running gel

- 1.5M Tris-HCl pH 8.8 (Invitrogen, 15504-020)
- 0.4% SDS (Fisher Scientific, 10593335)

SDS gel buffer for stacking gel

- 0.5M Tris-HCl pH 6.5 (Invitrogen, 15504-020)
- 0.4% SDS (Fisher Scientific, 10593335)

10% APS

- 10g APS (Fisher Scientific, BP179-100)
- 100 mL dH₂O

7.5% Proteingel

- 2.5mL SDS gel buffer for running gel
- 2.5mL 30% acrylamide (Severn Biotech, 20-2100-10)
- 5 mL dH₂O

- 100µL 10% APS (Fisher Scientific, BP179-100)
- 10µL TEMED (Sigma Aldrich, T9281)

Stacking gel

- 1.25mL SDS gel buffer for stacking gel
- 0.75mL 30% acrylamide (Severn Biotech Ltd, 20-2100-10)
- 3mL dH₂O
- 50µL 10% APS (Fisher Scientific, BP179-100)
- 5µL TEMED (Sigma Aldrich, T9281)

PBS-Tween

- 1X PBS (Severn Biotech Ltd, 20-7461-01)
- 0.1% TweenTM 20 (Fisher Scientific, BP337-100)
- Up to 1L dH₂O

2.9. Molecular cloning

2.9.1. Primer design and PCR

Primers were designed manually for each cloning experiment and synthesized by Eurofins Genomics, Germany. A restriction enzyme was added (with overhangs if appropriate) and care was taken to ensure the gene would be in frame with any possible tags (Table 2-8). The PCR mixture was prepared (Table 2-9) for each condition and run following the conditions in Table 2-10. After amplification, 5µl of each sample was run on a 1% agarose gel at 90V and analysed under UV light.

Table 2-8. PCR primer sequences for cloning

Name	Primer	Sequence (5' to 3')	Enzyme	TM
CDCA2_pCS2+	Forward	CGCGGATCCATGAATGTTACTGAAGCCATG	BamHI	60°C
	Reverse	CCGGAATTCTTACTCTCCCAAGTTTGTGTTAGTTC	EcoRI	
CDCA2_pEGFP	Forward	CTCGAGAAATGGATGTTACTGAAGCCATG	XhoI	55°C
	Reverse	GGATCCTTACTCTCCCAAGTTTGTGTTGT	BamHI	
YL1	Forward	AAGCTTTTATGAGTTTGGCTGGGGGCC	HindIII	58°C
	Reverse	GGATCCTCATTTAATGACAATTTTCTGGCGC	BamHI	
RFP	Forward	GCCTACAAGACCGACATCAA		

Table 2-9. PCR reaction components

Component	Volume	Final concentration
10x Standard Taq Buffer	5µl	1x
10mM dNTPs	1 µl	0.2mM
Primer mix (10µM each)	2 µl	400mM each
cDNA/plasmid	Variable (~1µg)	-
Taq polymerase	0.25 µl	25units/ml
N-free water	Up to 50 µl	-

Table 2-10. PCR reaction parameters

Temperature	Time	Number of cycles
95°C	5'	1
95°C	1'	30
TM	1'	
68°C	1min/Kb	
72°C	5'	1

2.9.2. Cloning into pGEM[®]-T Easy vector

Zebrafish CDCA2 cloned in pME18S-FL3 was obtained from Dharmacon (MDR1734-202795967). CDCA2 was amplified by PCR as explained before and run in an agarose gel. Gel extraction was performed using the QIAquick gel extraction kit (refer to Table 7-1) and DNA was ligated into pGEM[®]-T-easy vector system (Promega, A137A) (Table 2-11). The reaction was incubated 1h at RT followed by overnight incubation at 4°C.

Table 2-11. Ligation into pGEM[®]-T Easy vector

Component	Volume
2X Rapid Ligation Buffer	7.5µL
pGEM [®] -T Easy vector	0.5µL
DNA (PCR product)	6µL
T4 DNA ligase	1µL

After the overnight incubation, all 15µl of the ligation reaction were used to transform *E. coli* DH5α competent cells. The ligation reaction was added directly on top of 100µl of the competent cells and mixed gently. Cells were then incubated on ice for 30 min, heat shocked at 42°C for 30 sec, put back on ice for 5 min and diluted in 250µl of SOC medium (see section 2.8.5 for recipe). 100µl of the transformation reaction were plated on LB agar plates (see section 2.8.5 for recipe) with Ampicillin (50µg/µl, Sigma, A0166), X-gal (1.25%, Invitrogen, B1690) and IPTG (1M, Fisher Scientific, DP1755-10) and left overnight at 37°C to grow. The next day white colonies were collected to be grown overnight in LB with 1% Ampicillin. Plasmid DNA was extracted from grown cultures using the Qiagen plasmid Mini kit (refer to Table 7-1). The extracted plasmid DNA was then digested to check if the insert was successfully ligated into pGEM[®]-T Easy vector system (Table 2-12). The reaction was incubated at 37°C for 3 hrs and run on 1% agarose gel. Positive clones were grown further to get high quality DNA.

Table 2-12. Digestion reaction

Component	Volume
Restriction enzyme (NEB)	1 μ L
CutSmart buffer (NEB, B7204)	6 μ L
Plasmid DNA	1 μ g
N-free water	Up to 50 μ l

2.9.3. Subcloning from a vector to another plasmid

To clone a fragment from one vector to another, both plasmids were digested separately with the appropriate restriction enzymes (as in Table 2-12). The reaction was incubated at 37°C for 2 hrs. Digested fragments were run in a 1% agarose gel to verify the size. The remaining digestion product was run in another gel and the correct size band was gel-purified. After extraction, 5 μ l were run on an agarose gel to decide the quantity of the vector and the insert, and an overnight ligation with T4 ligase (NEB, M0202) was performed at 16°C (Table 2-13). The next day, a transformation into *E. coli* (DH5 α strain) cells was performed as described previously and colonies were grown overnight on 5ml of LB media with appropriate antibiotic. DNA was extracted, digested to identify the correct insert and sent to Source Bioscience (Cambridge, UK) for DNA sequencing. The positive clones were grown further into 100 ml of LB agar with the appropriate resistant antibiotic to obtain high concentration of plasmid DNA.

Table 2-13. Ligation reaction with T4 ligase

Component	Volume
Insert	x (1:3 bp ratio to the vector)
Vector	50ng
10x T4 DNA ligase buffer	2 μ l
T4 DNA ligase	1 μ l
Water	Up to 20 μ l

2.9.4. Preparation of *E. coli* competent cells

E. coli DH5 α strain cells were plated on an antibiotic free LB-Agar plate and incubated overnight at 37°C. A single colony was inoculated in 3mL of LB and incubated overnight at 37°C in a shaker. The culture was diluted 1:100 in 250mL of LB and 5mL of 1M MgSO₄ were added. It was left in the shaker at 37°C until OD₆₀₀=0.4-0.6. The culture was centrifuged at 2500 g for 10 min at 4°C and the supernatant was removed. The pellet was resuspended in 100mL of TFB1 and incubated on ice for 5 min. It was then centrifuged at 2500 g for 5 min at 4°C and the supernatant was removed. The pellet was resuspended in 10mL of TFB2 and incubated on ice for 30 min and aliquoted into 1.5mL Eppendorfs tubes (200 μ L). The tubes were then flash frozen in liquid nitrogen and stored at -80°C.

2.9.5. List of solutions

TFB1 (pH 5.8):

- 30Mm KAc (Fisher Scientific, P/3760/53)
- 100mM RbCl (Acros Organics, 193920100)
- 10mM CaCl₂ (Fisher Scientific, BP510-250)
- 50mM MnCl₂ (Acros Organics, 10096063)
- 15% Glycerol (Fisher Scientific, G/0650/08)

TFB2 (pH 6.5):

- 10mM MOPS (Fisher Scientific, BP308-100)
- 75mM CaCl₂ (Fisher Scientific, BP510-250)
- 10mM RbCl (Acros Organics, 193920100)

2.9.6. Map of plasmids used for the study

GFP plasmids were conducted using the pEGFP-C1 vector shown in Figure 2.1. Table 2-14 shows the main restriction enzymes used to generate each plasmid. Th, a gift from Eric Schirmer (Edinburgh, UK), was also cloned into the pEGFP-C1 vector shown below with BamHI and EcoRI.

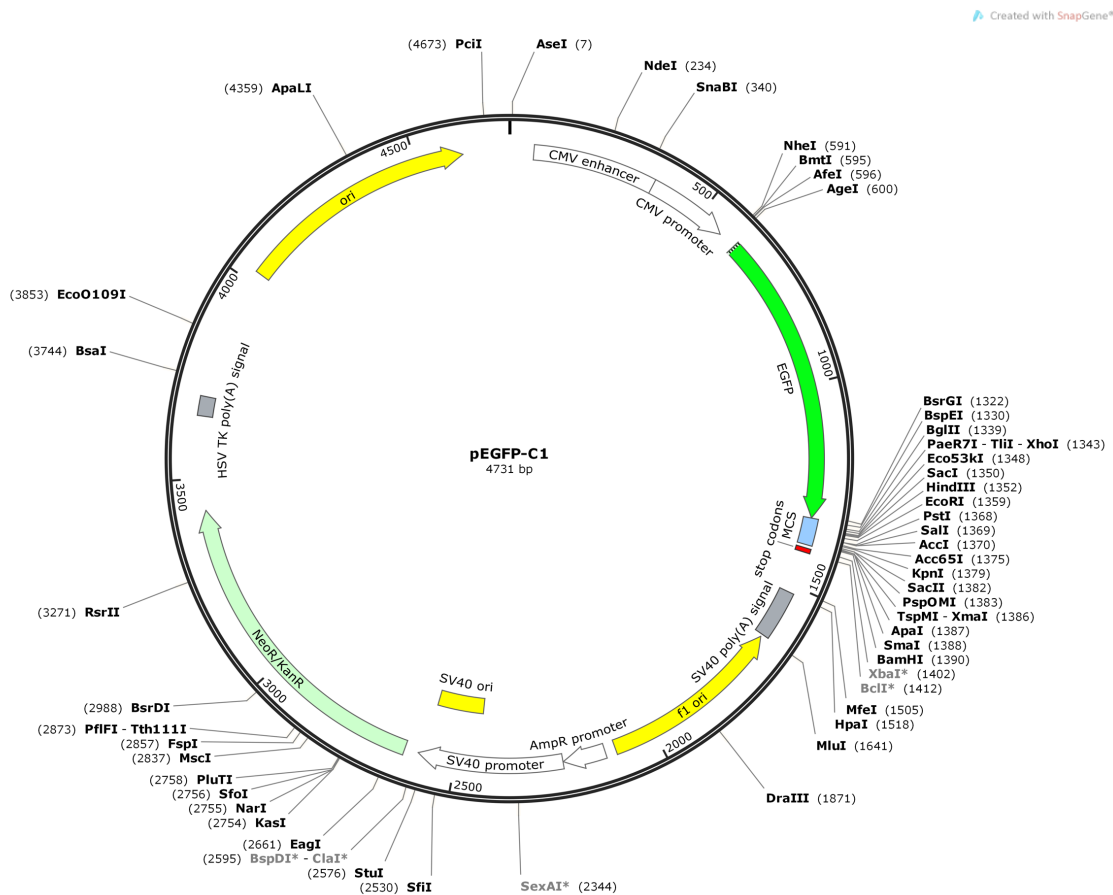


Figure 2.1. Map of pEGFP-C1 vector. The map shows the pEGFP-C1 vector with the unique restriction enzymes, the promoter and the antibiotic resistance sequence.

Table 2-14. List of restriction enzymes used for the cloning experiments

Plasmid	Restriction enzymes
CDCA2:GFP	XhoI and BamHI
Lacl:GFP	XhoI
YL1:Lacl:GFP	HindIII and BamHI
RFP	NheI and BglII

H2A.Z.1 and H2A.Z.2.1 and H2A.Z.2.2 resistant plasmids were obtained from Proteogenix (La Haye, France). They were cloned into pEGFP-C1 using XhoI and KpnI, BglII and BamHI, and BglII and EcoRI, respectively.

2.10. RNA sequencing

HeLa cells were transfected with the appropriate oligonucleotides using the transfection reagent JetPrime[®], and RNA was extracted after 48 hrs using the RNeasy PowerLyzer Tissue & Cells Kit from Qiagen, as described in Materials and Methods section 2.5. Only RNA with 260/230 and 260/280 ratios close to 2 were diluted to 100ng/μl and sent to Oxford Genomics Centre for whole-genome sequencing, using the Illumina HiSeq4000.

RNAseq data was kindly processed by Dr. Cristina Sisu from Brunel University. In brief, Tophat was used to align the reads from the Fastq. files to the human reference genome hg19/38, followed by a quantification to get the expression levels of the transcripts by Cufflinks. As we were interested in the differential expression between the two siRNA, Cuffdiff was used to acquire differences in expression levels. RStudio and Microsoft Excel were both used to analyse the obtained results and perform the appropriate graphs.

Zebrafish methodology

2.11. Zebrafish husbandry and egg line collection

Zebrafish were raised and maintained at Brunel University of London as described in the Zebrafish Book (Westerfield, 2000) according to the United Kingdom Animals (Scientific Procedures) Act 1986. All experiments were conducted under the Project licence (PPL) number PC883B4D6, and the Personal licence (PIL) number I03728908. The technicians in the animal facility, Julie Walker and Neil Brodigan, conducted all zebrafish maintenance. Adults (strain AB) were used for breeding to obtain embryos for several purposes. Embryos were collected and kept in E3 medium (see below) in batches of 100 eggs at 28°C until needed.

Embryos from sperm carrying a point mutation on CDCA2 were obtained from the Zebrafish International Resources Centre (ZIRC, Oregon) (CDCA2^{sa17504}, catalogue ID ZL10636.05) and raised in house. Embryos were raised to adulthood and genotyped as explained elsewhere for either CDCA2^{+/+} or CDCA2^{+/-}. CDCA2^{+/-} zebrafish were used for breeding to obtain embryos CDCA2^{-/-} to analyse protein function.

2.11.1. List of solutions

50x E3 medium

- 15µM NaCl (Sigma Aldrich, S3014)
- 2.2mM KCl (Fisher Scientific, P/4280/53)
- 14mM CaCl₂ (Fisher Scientific, BP510-250)
- 26.6mM MgSO₄ (Fisher Scientific, M/1100/53)

2.12. Immunofluorescence

Zebrafish embryos were collected at different post-fertilization time points and fixed with 4% PFA overnight at 4°C. Embryos were washed and kept at 4°C in 1% PBS ϕ -Tween until needed. Embryos < 24hpf were dechorionated with Dumont n.5 forceps before starting the protocol. Embryos were washed 3 x 10 min with PBS-Triton, permeabilized in ice cold acetone at -20°C for 10 min, washed again with PBS-Triton and blocked for 2 hrs at RT in blocking solution. Embryos were incubated overnight at 4°C with the primary antibodies (Table 2-2) anti-CDCA2 58A and anti- α -tubulin antibody in blocking solution. The next day, embryos were washed 6 x 10 min with PBS-Triton, blocked for 30 min and incubated for 2hrs at RT with secondary antibody in blocking solution. Embryos were counter-stained with DAPI and analysed in a microscope NIKON Ti-E super research Live Cell imaging system using 20X lenses.

2.13. Differential gene expression

Zebrafish cDNA from different differentiation stages and adult tissues was a kind gift from Marjo Den Broeder, University of Utrecht, the Netherlands.

The differential expression of CDCA2 was analysed in the qPCR QuantStudio 7 Flex Real-Time PCR Machine as previously described (Section 2.7) by using the following primers:

Name	Sequence
CDCA2 zf Forward	5' TGCTGAGGACACATGGAAGC 3'
CDCA2 zf Reverse	5' GCCTCTACAGAGAGAGCCAGT 3'

2.13.1. RNA extraction from zebrafish embryos

A pool of 50 2-3hpf embryos was transferred to a 1.5ml tube. As much water as possible was removed with a pipette and 250µl of TRIzol reagent (Ambion, 10296010) was added immediately. Embryos were lysed with a pestle until the tissue was completely disrupted. When cells were sufficiently homogenized, TRIzol was added to equal a total volume of 1ml. To allow complete dissociation of nucleoprotein complexes, samples were incubated for 5 min at RT. To continue, 200µl of chloroform was added and the tube was mixed for 15 seconds and later incubated for 2 min at RT. Tubes were centrifuged at 12000g for 15 min at 4°C. The upper layer containing RNA was transferred to a new tube and RNA precipitated by adding 500µl of isopropanol and allowing it to rest for 10 min at RT. The tubes were centrifuged at 12000g for 10 min at 4°C. The supernatant was removed and the pellet, corresponding to the RNA was washed with 75% ethanol and centrifuged at 7500g for 5 min at 4°C. After centrifugation, ethanol was removed with a pipette and the sample was air dried for 10 min. The pellet was resuspended in 40µl of RNase-free water and incubated at 55°C for 10 min, while finger vortexing often.

2.13.2. cDNA retro-transcription

Genomic DNA was removed from the samples and cDNA synthesized as described earlier in chapter 2.7. In this case, oligo (dT) primers were used for reverse transcription to obtain mRNA only.

2.13.3. Quantitative Polymerase Chain Reaction (qPCR)

The differential expression of CDCA2 was analysed in the qPCR QuantStudio 7 Flex Real-Time PCR Machine as previously described (Section 2.7) by using the following primers:

Target gene	Primers	Sequence (5' to 3')
CDCA2	Forward	TGCTGAGGACACATGGAAGC
	Reverse	GCCTCTACAGAGAGAGCCAGT
EF1 α	Forward	TTGAGAAGAAAATCGGTGGTGCTG
	Reverse	GGAACGGTGTGATTGAGGGAAATTC
HPRT1	Forward	CAGCGATGAGGAGCAAGGTTATG
	Reverse	GTCCATGATGAGCCCGTGAGG

2.14. Western Blotting

Zebrafish embryos were collected and, if necessary, dechorionated with Dumont n.5 forceps. Embryos younger than 2dpf were de-yolked with Ginzburg solution by pipetting up and down with a narrow tip and shaking at 1000g for 5 min. Embryos were centrifuged at 300g for 30 sec and the supernatant (containing the yolk sac) was discarded. Embryos were washed twice with washing buffer and either frozen at -20°C or processed directly for Western Blot.

PBS combined with protease and phosphatase inhibitors (as previously described) was added (1 μ l of PBS/embryo) and mixed with 2x Sample Buffer (1:1). Embryos were pestled for 1 min, boiled at 95°C for 5 min, and pestled again. Embryos were then pelleted at 13000g for 2 min at 4°C, sonicated twice for 30 sec, and heated again at 95°C for 5 min. Embryos were pelleted and the supernatant was transferred to a new tube. If kept at -20°C, the sample was boiled again at 95°C for 5 min before loading on the gel.

2.14.1. List of solutions

½ Gizburg Fish ringer:

- 55 mM NaCl (Sigma Aldrich, S3014)
- 1.8 mM KCl (Fisher Scientific, P/4280/53)
- 1.25 mM NaHCO₃ (Sigma Aldrich, S5761)

Wash buffer:

- 110 mM NaCl (Sigma Aldrich, S3014)
- 3.5 mM KCl (Fisher Scientific, P/4280/53)
- 2.7 mM CaCl₂ (Fisher Scientific, BP510-250)
- 10 mM Tris/HCl pH 8.5

2.15. In Situ Hybridization of zebrafish embryos

2.15.1. Probe synthesis

CDCA2 zebrafish was amplified by PCR as described before and using the following primers: 5' AAT TAA CCC TCA CTA AAG GGA TGA ATG TTA CTG AAG CCA TG 3' and 5' AAT ACG ACT CAC TAT AGG GAG ATA CTT CAT CGC TGT ACA GAA 3'. Underlined nucleotides correspond to the T3 and T7 promoters, respectively. PCR product was cleaned up with the PCR clean-up kit and RNA was labelled with DIG using the DIG RNA labelling mix (Roche Applied Science). 200 ng of PCR product was incubated with the transcription mix (see 2.15.3) for 2 hrs at 37°C, followed by digestion of the DNA template by adding 1µL RNase-free DNase for 15 min at 37°C. The synthesis reaction was stopped and RNA precipitated by adding 2µL of EDTA. The mix was cleaned with the RNA clean-up kit centrifuged at 4°C for 30 min at 13K, washed with 70% ethanol, centrifuged for 20 min at 4°C and let it dry. Afterwards, the pellet was re-suspended in 24µL of sterile water and run on a 1% agarose gel to check the quality.

2.15.2. In situ hybridization

Zebrafish at several stages of development were fixed in 4% PFA overnight at 4°C. The next day embryos were taken to 100% MeOH in serial dilutions with PBSØ – 0.1%Tween (PBT) and the samples were kept at -20°C until use. Zebrafish were rehydrated to PBT at RT by incubating them for 10 min in each dilution (75%, 50%, and 25% MeOH in PBT) to allow for equilibration, followed by 4 washes with PBT for 5 min. Embryos older than 24hpf were digested with Proteinase K (10 µg/mL) for 20 min. The embryos were re-fixed in 4% PFA, washed 5 times in PBT for 5 min and prehybridized in 500 µL of HM⁺ for at least 3 hrs at 70°C. HM⁺ was replaced with HM⁻ containing 1µg of digoxigenin-labelled antisense probe (a sense probe was used as a control) and they were incubated overnight at 70°C.

Non-hybridised probe was washed out by the following washing steps:

- 100% HM⁻ at 70°C, 15 min
- 75% HM⁻/25% 2x SSC at 70°C, 15 min
- 50% HM⁻/50% 2x SSC at 70°C, 15 min
- 25% HM⁻/75% 2x SSC at 70°C, 15 min
- 2x SSC at 70°C, 15 min
- 0.2x SSC at 70°C, 2x 30 min
- 75% 0.2x SSC/25% PBT at RT, 10 min
- 50% 0.2x SSC/50% PBT at RT, 10 min
- 25% 0.2x SSC/75% PBT at RT, 10 min
- PBT at RT, 10 min
- Blocking buffer at RT at least 2 h

Zebrafish were incubated overnight with an alkaline phosphatase-conjugated antibody against DIG in blocking buffer (1:2000) at 4°C in the dark.

The following day embryos were washed extensively 6 times with PBT for 15 min at RT and equilibrated in AP⁻ buffer 2 times for 30 min at RT. Embryos were incubated in NBT/BCIP staining solution (200µL NBT/BCIP stock solution in 8 mL AP⁻) at RT in the dark until they were stained. NBT/BCIP allows detection of the probe, as once catalysed by alkaline

phosphatase, the product of BCIP reacts with NBT to produce a precipitate that is dark blue to purple in color. In zebrafish up to 24hpf, staining was stopped by re-fixing the embryos with 4% PFA for 20 min at RT. Zebrafish older than 2dpf were bleached prior to re-fixation: zebrafish were brought to 100% methanol and left overnight at 4°C to ensure the staining solution was completely inactivated. The next day embryos were re-hydrated to PBT and incubated with bleaching solution for about 20 min. Bleaching was stopped by washing the embryos with PBT.

2.15.3. List of solutions

Transcription mix (Roche, 11277073910):

- 300 ng PCR product
- 4 µL 5x transcription buffer for T7/T3 RNA polymerase
- 2 µL 10x DIG mix
- 2 µL RNA polymerase
- Up to 20 µL sterile water

Hybridization mix minus (HM-):

- 25 mL deionized formamide (Sigma Aldrich, S4117)
- 12.5 mL 20x SSC (Sigma Aldrich, S6639)
- 0.1% TweenTM 20 (Fisher Scientific, BP337-100)
- 460 µL 1M citric acid pH 6.0
- Up to 50 mL N-free water

Hybridization mix plus (HM+):

- HM-
- 50 µL/mL Heparin (Sigma Aldrich, 84020)
- 500 µg/mL tRNA

Blocking buffer (in PBS/0.1% Tween):

- 2 mg/mL BSA (Sigma Aldrich, A7284)
- 10% lamb serum (Thermo Fisher Scientific, 16070096)

Alkaline Phosphatase (AP-) buffer:

- 10 mL Tris HCl pH 9.5 (Invitrogen, 15504-020)
- 2 mL 5M NaCl (Sigma Aldrich, S3014)
- 100 µL Tween™ 20 (Fisher Scientific, BP337-100)
- Up to 100 mL water

Bleaching solution:

- 0.5 mL deionized formamide (Molekula, 11651936)
- 0.25 mL 20x SSC (Sigma Aldrich, S6639)
- 1.65 mL 30% H₂O₂ (Sigma Aldrich, 95313)
- Up to 10 mL water MQ

2.16. Genotyping of zebrafish larvae and adults

Genotyping of zebrafish larvae and adults was performed using the fluorescence-based KASP (Kompetitive Allele- Specific PCR) assay technology (LGC Genomics, Teddington, UK). Genomic DNA was extracted from caudal fin clips of adult zebrafish and 4dpf larvae. Fin-clipped zebrafish were kept in individual tanks (adults) or 96 well plates (larvae) until genotyping was performed (maximum 5 days). Clipped fins were mixed with lysis buffer + proteinase K (1:400), heated to 60°C for 1 hr and heat inactivated for 10 mins at 95°C. DNA was added to the KASP assay mix as shown in Table 2-14 and the reaction was run and read using the Applied Biosystems QuantStudio™ 7 Flex Real-Time PCR system (Table 2-15).

The CDCA2 specific KASP primers were generated against the following target sequence:

5' GAGCAWGRATGTTACTGAAGCCATGGACWGCAGACCAGCACTTGCAGACT[T/A]GTCTCCCT CTCAGCAGAACACTGAAGCTGSGGATGTGGATTTCTCYAAAC 3'.

Table 2-14. KASP reaction

Component	Volume
2x KASP mix	5 μ L
CDCA2 assay mix	0.14 μ L
DNA	5 μ L

Table 2-15. KASP thermal cycling conditions

Procedure	Temperature	Time	Cycles
Activation	94°C	15min	1
Denaturation	94°C	20sec	10
Annealing/Elongation	61°C (Δ T: -0.6°C/cycle)	1min	
Denaturation	94°C	20sec	26
Annealing/Elongation	55°C	1min	
Reading	30°C	1min	1
Denaturation	94°C	20sec	3
Annealing/Elongation	55°C	1min	
Re-reading	30°C	1min	1

2.17. CDCA2 mutant line analysis

2.17.1. Behavioural study

4dpf zebrafish were placed individually in 24 well plates with 1 mL of E3 medium and left overnight to adapt to the environment. The next morning, the plates were placed in the behavioural study machine (ViewPoint, ZebraBox Revolution), which applies four 10 min-long dark/light cycles and records the distance and speed achieved by every individual. Data was processed using ViewPoint, Fast Data Monitor software.

2.17.2. Cardiovascular and growth analysis

The cardiovascular system was analysed by counting the heartbeats at 5dpf. Larvae were anesthetized with MS-222 (Sigma Aldrich, E10521) and the heartbeats were counted for 15 seconds (n=25). The average of three measurements per fish was calculated and multiplied by four to get the bpm (heartbeats per minute).

To analyse zebrafish growth, adult zebrafish were placed on a scale and their weight was recorded. At the same time, a ruler was placed next to the baker and a picture was taken for each fish. The length of each fish was then calculated on Photoshop.

2.17.3. Fertility study

Adult zebrafish (WT, CDCA2^{+/-}, and CDCA2^{-/-}) were transferred into a breeding tank at a 1:1 ratio (one male and one female) as following: WT male x WT female (n=9); CDCA2^{+/-} male x CDCA2^{-/-} female (n=6); CDCA2^{+/-} female x CDCA2^{-/-} male (n=6); CDCA2^{-/-} male x CDCA2^{-/-} female (n=6). Next morning, 1 hr after the dividers removal, eggs were collected and the total number of eggs laid, the fertilization rate and the mortality rate were calculated for each pair. If a female did not spawn, mating with another male was repeated after 3 days. Females were considered sterile after three failed attempts.

3. ROLE OF PHOSPHATASES AS REGULATORS OF HETEROCHROMATIN MAINTENANCE

3.1. Introduction

The eukaryote proteome is subject to post-translational modifications (PTM), chemical modifications that can occur at any time throughout the lifespan of proteins and regulate their localization, function, and interaction with other molecules. Phosphorylation is one of the most important PTM, and it is carried out by protein kinases that can add a phosphate group to either Threonine, Serine, Tyrosine, or Histidine residues. This modification is counteracted by the activity of protein phosphatases such as PP1 and PP2A, which form holoenzymes with regulatory subunits to acquire specificity. The biology of protein kinases has been extensively studied over the years and they have been widely used as drug targets for many diseases. However, the protein phosphatases have received less attention due to the difficulties in generating specific tools.

Protein phosphatases are involved in many aspects of cell biology and they play a crucial role during mitotic entry, when key protein phosphatases are inactivated to allow phosphorylation and activation of proteins involved in mitotic progression. Accordingly, at the onset of anaphase, phosphatases are re-activated to remove all the mitotic marks and ensure proper mitotic exit. During mitosis, chromatin is hugely rearranged to form chromosomes and ensure proper chromosome segregation, but it needs to be reorganized to protect chromatin structure and architecture once the new daughter cells have formed. In this aspect, a protein phosphatase holoenzyme, Repo-man/PP1, has emerged as a regulator of the epigenetic landscape, maintaining heterochromatin organization throughout cell division (de Castro et al., 2017).

Gene silencing by heterochromatin is proposed to occur partly as a result of the ability of heterochromatin protein 1 (HP1) to bind H3K9me3. Out of the three HP1 isoforms in mammals, HP1 α is the only one found almost exclusively in heterochromatin and it has been used as a marker for heterochromatin for many years (Smothers and Henikoff, 2001). HP1 α is able to form homodimers that bind to H3K9me3 regions that, through sequestration of compacted chromatin in phase-separated HP1 droplets, mediates heterochromatin formation and subsequent gene silencing (Larson et al., 2017, Strom et al., 2017). These characteristics are regulated by PTM of HP1 α itself. For instance, HP1 α

phosphorylation on several N-terminus residues (S11-14) was shown to enhance HP1 α binding to H3K9me3 (Hiragami-Hamada 2011) and that these and other phosphorylations can drive a conformational change in the protein and promote the formation of the phase-separated droplets (Larson et al., 2017, Strom et al., 2017). Also, lack of HP1 α phosphorylation in the hinge region resulted in mitotic defects, with cells arrested in prometaphase (Chakraborty et al., 2014). These data highlight the importance of studying protein regulation by phosphorylation in order to understand the molecular mechanisms underlying heterochromatin formation and maintenance.

In this chapter, we aimed to screen the major chromatin-associated PP1 holoenzymes in respect to a possible contribution towards the maintenance of heterochromatin. Since one of the markers for heterochromatin is HP1 α , we generated a stable GFP:HP1 α cell line to use as a screening tool and performed a screening on HP1 α localisation with different chromatin-related PP1 subunits siRNAs.

3.2. Results

3.2.1. Development of stable GFP:HP1 α cell lines

In order to establish a new cellular model to study heterochromatin changes, we chose two different human cell lines, HeLa (immortalized cervical cancer cells) and MRC5 (immortalized fibroblasts) together with the embryonal zebrafish cell line PAC2. However, the transfection efficiency of the PAC2 cell line was rather low (<10%), and no resistant clones were obtained, discarding the development of a GFP:HP1 α PAC2 cell line. MRC5 transfection was also low, but five positive clones were isolated and the MRC5 GFP:HP1 α cell line was successfully established. HeLa cells gave a much higher transfection rate and twelve positive clones were isolated. Although the PAC2 GFP:HP1 α could not be developed, we stained the PAC2 cells with a human anti-HP1 α antibody to test whether it recognized the CBX5 zebrafish protein to see if we could still use this cell line to test HP1 disruption (Figure 3.1). However, the human antibody or the fixation conditions used did not show any typical HP1 α pattern in the cells and the possibility to use a zebrafish cell line to study HP1 α distribution was rejected. Although we cannot discard the fact that this embryonic cell line might still have not fully assembled heterochromatin, it was recently reported that heterochromatin establishment is driven by the maternal to zygotic transition in zebrafish (about 4hpf) (Laue et al., 2019) , and thus this cell line, obtained from 24hpf embryos, should have already assembled heterochromatin.

In order to validate the stable cell lines and to demonstrate that they could be used as useful tools for the analyses of heterochromatin maintenance, cells were transfected with two different siRNA to deplete the G9 methyltransferase, the enzyme responsible for methylating lysine 9 on histone H3 (H3K9), enabling HP1 binding to chromatin. Therefore, it is expected that the knock down of this enzyme abolish the accumulation of HP1 at the major heterochromatic sites.

Although the G9 siRNAs have not been validated, both oligonucleotides were able to disrupt HP1 organization already at 48h (Figure 3.2.A) in the HeLa GFP:HP1 α cell line. However, in the MRC5 GFP:HP1 cells, the number of HP1 α foci was just altered by one of the

oligonucleotides (Figure 3.2.B). This latter result is probably due to the low efficiency of transfection in the MRC5 cell line (<10%). To test whether this cell line could be used for chemical screening, we treated the cells with two known DNA methyltransferase inhibitors, chaetocin and 5-Azacididine. However, at the concentrations tested, just chaetocin was able to have a small effect on HP1 α distribution. Therefore, we decided not to use this cell line to perform any experiments involving transient transfection or drug treatment, and the following experiments were just performed on the GFP:HP1 α HeLa cell line.

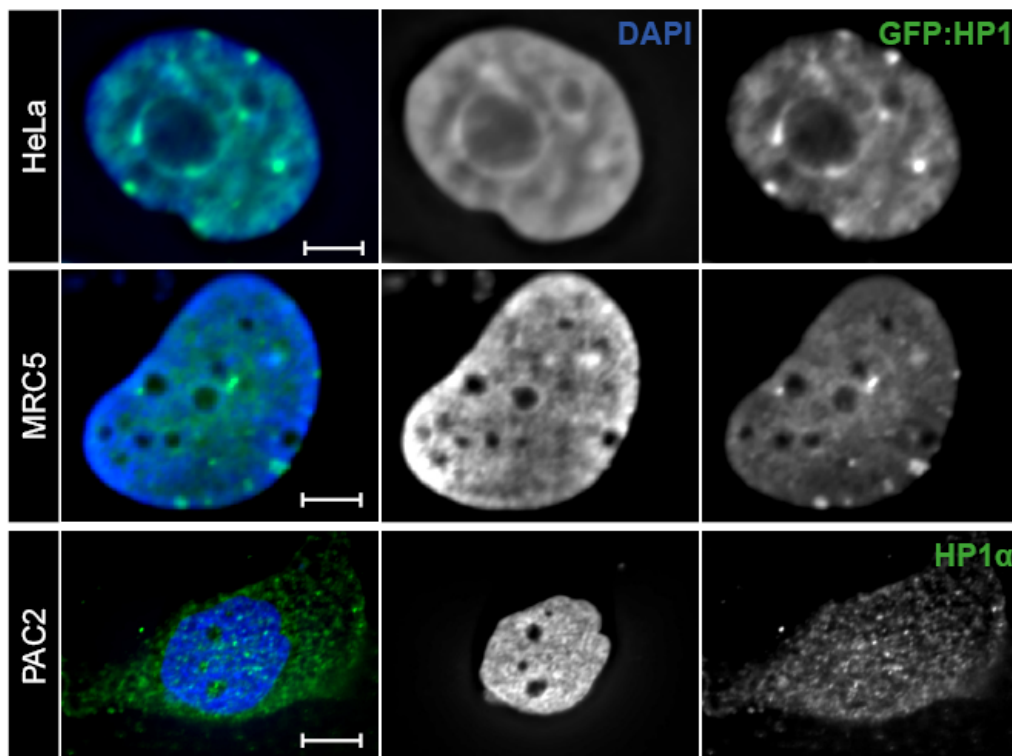


Figure 3.1. GFP:HP1 stable cell lines. Both HeLa GFP:HP1 cells (top panel) and MRC5 GFP:HP1 cells (middle panel) were successfully established and more than 5 HP1 foci can be observed in the nucleus. Immunofluorescence of PAC2 with the human anti-HP1 α antibody did not show specificity for the zebrafish HP1 homologue (CBX5) protein. Scale bar: 5 μ m.

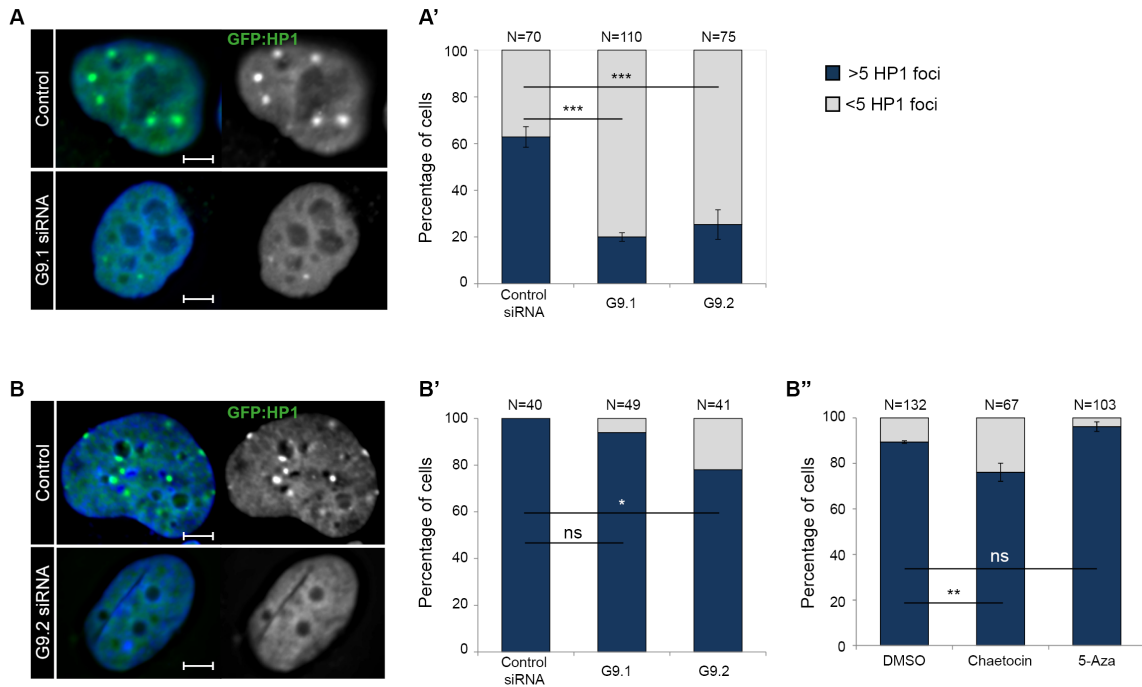


Figure 3.2 HeLa and MRC5 GFP:HP1 validation. A) HeLa GFP:HP1 cell lines were transfected with a control siRNA that does not target any gene product and two siRNA oligonucleotides against the G9 methyltransferase (G9.1, G9.2) for 48h. G9 siRNA were not validated in my cell line. **A')** HP1 foci analysis of cells in A. Three biological replicates were counted in this statistical test (Chi-square t test). **B)** The same experiment was conducted in MRC5 GFP:HP1 cells. **B')** HP1 foci analysis of cells in B. Just on replicate was analysed in this case. **B'')** MRC5 GFP:HP1 cells were also treated with chaetocin (10^{-7} M) and 5-Azacytidine (4μ M) for 48h and the HP1 foci were analysed. Two biological replicates were counted in this statistical test (chi-square t test). N represents the total number of cells counted. Green: GFP:HP1, blue: DAPI. Scale bar: 5μ m.

3.2.2. Screening of PP1 subunits on HP1 distribution

Published work from our lab has shown that Repo-man/PP1 is important to maintain HP1 foci after mitosis (de Castro et al., 2017). However, several PP1 targeting subunits are chromatin-linked and could possibly play a role in the epigenetic mechanisms that converge to regulate heterochromatin maintenance. We therefore decided to conduct a small siRNA screen for chromatin-associated PP1 targeting subunits.

In order to expand the study and to identify other PP1 targeting subunits involved in HP1 disruption, we performed additional siRNA experiments with several PP1 isoforms and subunits, including PP1 α , PP1 β , PP1 γ , PNUTs, AKAP, Sds22, NIPP1, Ki-67 and Repo-man (Figure 3.3.A). siRNA targeting PTEN was used as a positive control because it was previously reported to be involved in heterochromatin maintenance and HP1 α stabilization (Gong et al., 2015a). Our data shows that the PP1 β and PP1 γ isoforms are able to disrupt the number of HP1 foci, as well as Repo-man. In the PP1 α and NIPP1 depleted cells, there is an increase in the number of cells with more than five HP1 foci compared with the control. In the conditions used, Sds22, AKAP, and PNUTs knockdowns were not able to alter HP1 distribution.

The results with Ki-67 did cause some problems. Previous work (Michal et al., 2016) has shown that Ki-67 depletion causes a decrease of H3K9me3 in human and mouse cells. Three oligonucleotides were used to interfere with Ki-67 RNA (Ki-4, Ki-5 (Booth et al, 2014), and Ki-G (from (Cuylen et al., 2016a)). Although two oligonucleotides did not alter the HP1 pattern after 48h of transfection, one (Ki-5) showed a strong decrease in the number of HP1 foci (Figure 3.3.B). In order to investigate a possible off-target effect of Ki-5, we performed a rescue experiment with a plasmid carrying RFP:Ki-67 resistant to the oligonucleotide Ki-5 (Figure 3.3.C). To some extent, the RFP:Ki-67 plasmid resistant to Ki-5 was able to rescue the phenotype produced by Ki-5. However, the fact that the other two siRNAs targeting Ki-67 did not show any effect on HP1 distribution was puzzling and we could not reach a strong conclusion. We therefore decided to analyse differentially expressed genes by RNA sequencing analysis to understand the specific targets of these oligonucleotides.

Altogether, these results show that several phosphatase complexes are involved in the regulation of heterochromatin during the cell cycle, and the identification of their mechanism of action, as well as any other phosphatase complex involved, could be an important aspect to investigate in the future.

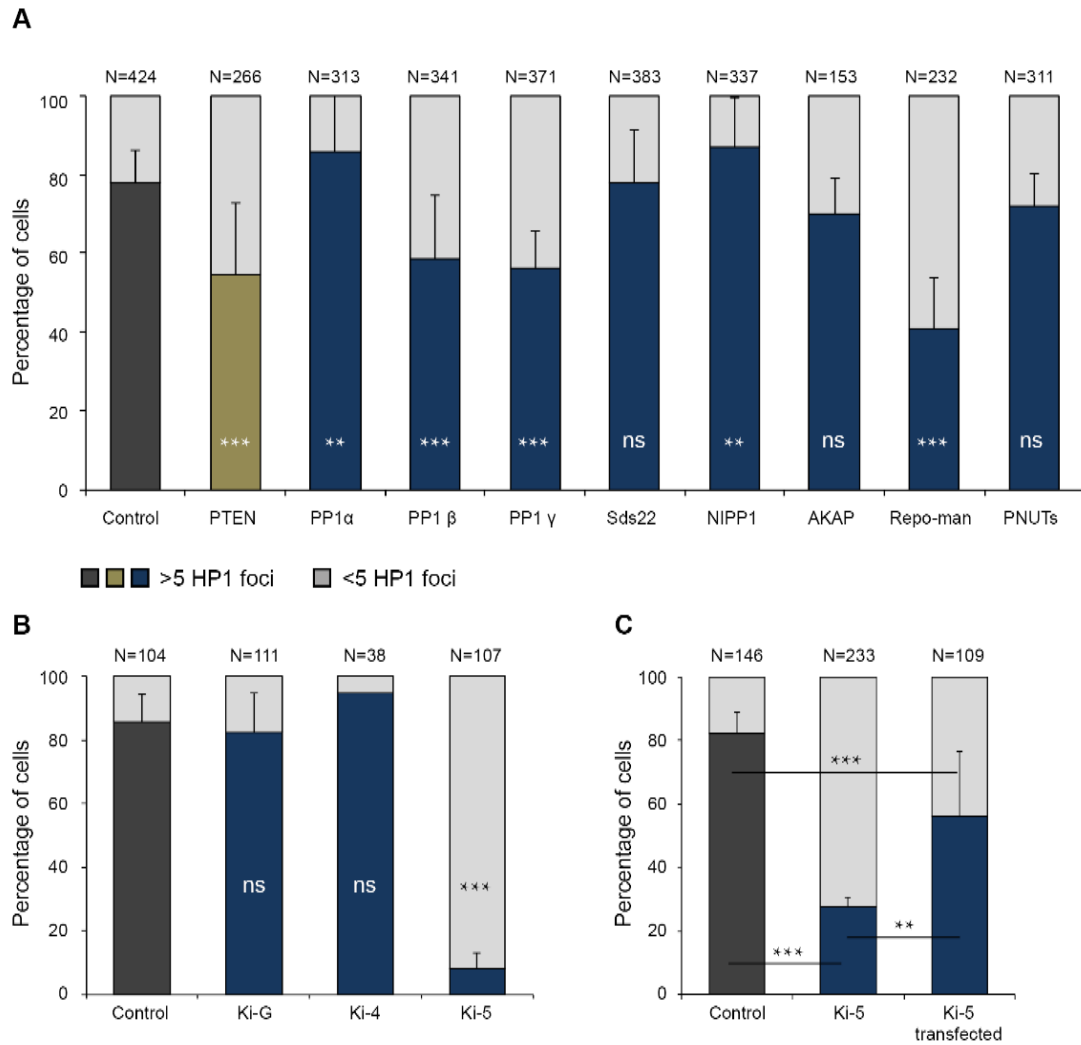


Figure 3.3. Screening of PP1 subunits on HP1 distribution. A) HeLa GFP:HP1 cells were transfected for 48 hours with siRNA oligonucleotides against a control sequence, PTEN, the three PP1 isoforms, and several PP1 subunits that have been linked to chromatin. Whereas depletion of PP1 β , PP1 γ , and Repo-man clearly decrease the number of cells with more than five foci, depletion of PP1 α and NIPP1 seem to increase it. Depletion of Sds22, AKAP, and PNUTs do not affect HP1 distribution. **B)** HeLa GFP:HP1 cells were transfected with three different siRNA targeting Ki-67 for 48h. One of the oligonucleotides (Ki-5) was able to disrupt HP1 organization, while the other two did not. Three replicas were analysed in the statistical test. **C)** HeLa GFP:HP1 cells were transfected with a control siRNA, the Ki-5 siRNA, and the Ki-5 siRNA in combination with a GFP:Ki-67 plasmid resistant to the Ki-5 siRNA, for 72h. Transfection with the resistant plasmid was able to somewhat rescue the phenotype. Three biological replicas were analysed. Chi-square test was used for the statistics. N represents the total number of cells counted from four biological replicates.

3.2.3. Differential expression analyses of Ki-67-depleted cells

In order to unravel a possible explanation on the difference between Ki-G and Ki-5 siRNA transfected cells, RNA isolated from cells transfected with a control siRNA, the Ki-G, and the Ki-5 siRNAs was sent to sequence (Oxford Genomics, UK) and a differential expression analysis was performed.

Both siRNAs are able to decrease Ki-67 gene expression to the same extent, as shown by RNAseq and qPCR data (Figure 3.4), ruling out the possibility that the difference on the effect was due to a more efficient siRNA compared to the other two oligonucleotides. However, the gene expression profile is significantly different for each siRNA transfection. Transfections with Ki-G and Ki-5 siRNAs alter the expression of 885 and 684 genes, respectively; only 116 of these genes are common for both siRNAs (Figure 3.4.A). Out of these differentially expressed genes, 605 in the Ki-5 and 441 in the Ki-G siRNAs are downregulated, and only 78 are common between samples (Figure 3.4.B). These represent real target genes that are affected by Ki-67 depletion. However, these analyses gives us the potential to identify other genes involved in HP1 regulation. Among the 527 downregulated genes in the Ki-5 siRNA transfected cells we could not find any candidate that is already known to be involved in HP1 regulation at any level. Therefore, this dataset offered us the potential to discover additional factors that could be implicated in HP1 localisation. In order to narrow down this number, we only focused on the genes with a high significant difference ($p < 0.001$). Out of those, two genes, MYH9 (myosin) and RBL2 (Retinoblastoma-like protein 2), were previously reported to be linked to chromatin, and therefore they were further tested on the GFP:HP1 α cell line for HP1 deregulation. The RNA sequencing data was also compared to the one from Sobecki et al. (Sobecki et al., 2016) (Figure 3.4.E).

As seen in Figure 3.5. A and B, MYH9 and RBL2 are only downregulated in the Ki-5 samples. In order to study if they could explain the difference seen in HP1 distribution, we used two siRNAs for each gene. We analysed the efficiency of the siRNAs by qPCR (Figure 3.5. C and D) and we counted the HP1 foci in our HeLa GFP:HP1 α (Figure 3.5. E and F). In the case of MYH9, both siRNAs were able to decrease the number of cells with more than five HP1 foci, indicating a potential role for this protein on HP1 regulation.

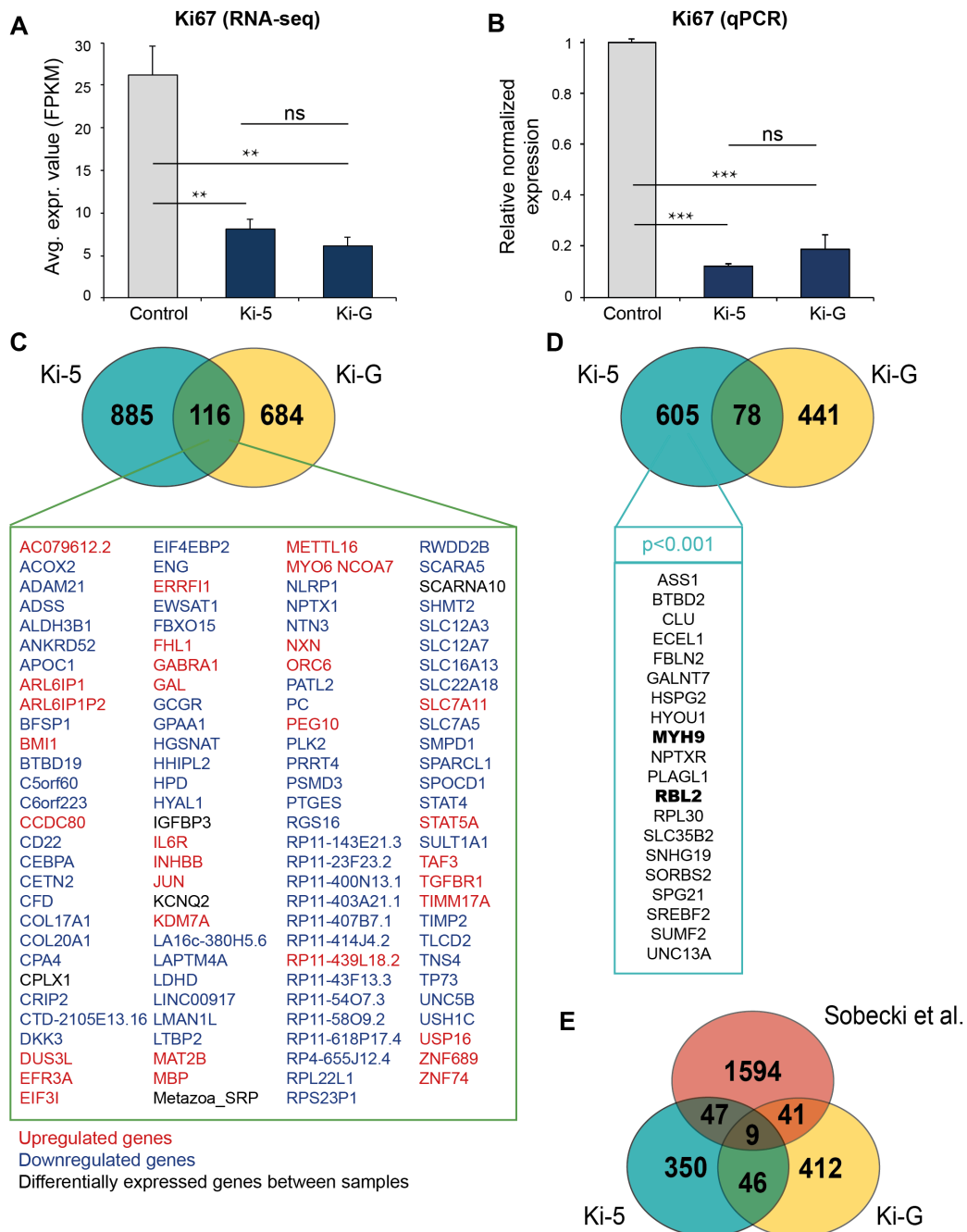


Figure 3.4. Differential expression analysis between Ki-G and Ki-5 siRNA-mediated knockdown cells. RNA from HeLa cells transfected with Ki-5 and Ki-G siRNAs were sequenced and the differentially expressed genes were analysed. **A, B)** Ki67 average expression values from the RNA-seq data (A) and by qPCR (B). Three biological replicates were analysed for each experiment. However, MKI67 was not the most downregulated gene in any of the siRNA-treated samples. **C)** Venn diagram showing the number of altered genes in Ki-67-depleted cells using the two different siRNAs, with the list of common genes up/down regulated in both samples. In red, upregulated genes in both samples; in blue, downregulated genes in both samples; in black, genes that are upregulated in one sample but downregulated in the other. **D)** Venn diagram showing only the downregulated genes, with the list of genes with $p < 0.001$ only downregulated in the Ki-5 siRNA transfected cells. In bold, genes that have been previously linked to chromatin. **E)** Comparison of our data with the RNA sequencing data obtained by Sobecki et al. (Sobecki et al., 2016) of genes with $p < 0.02$.

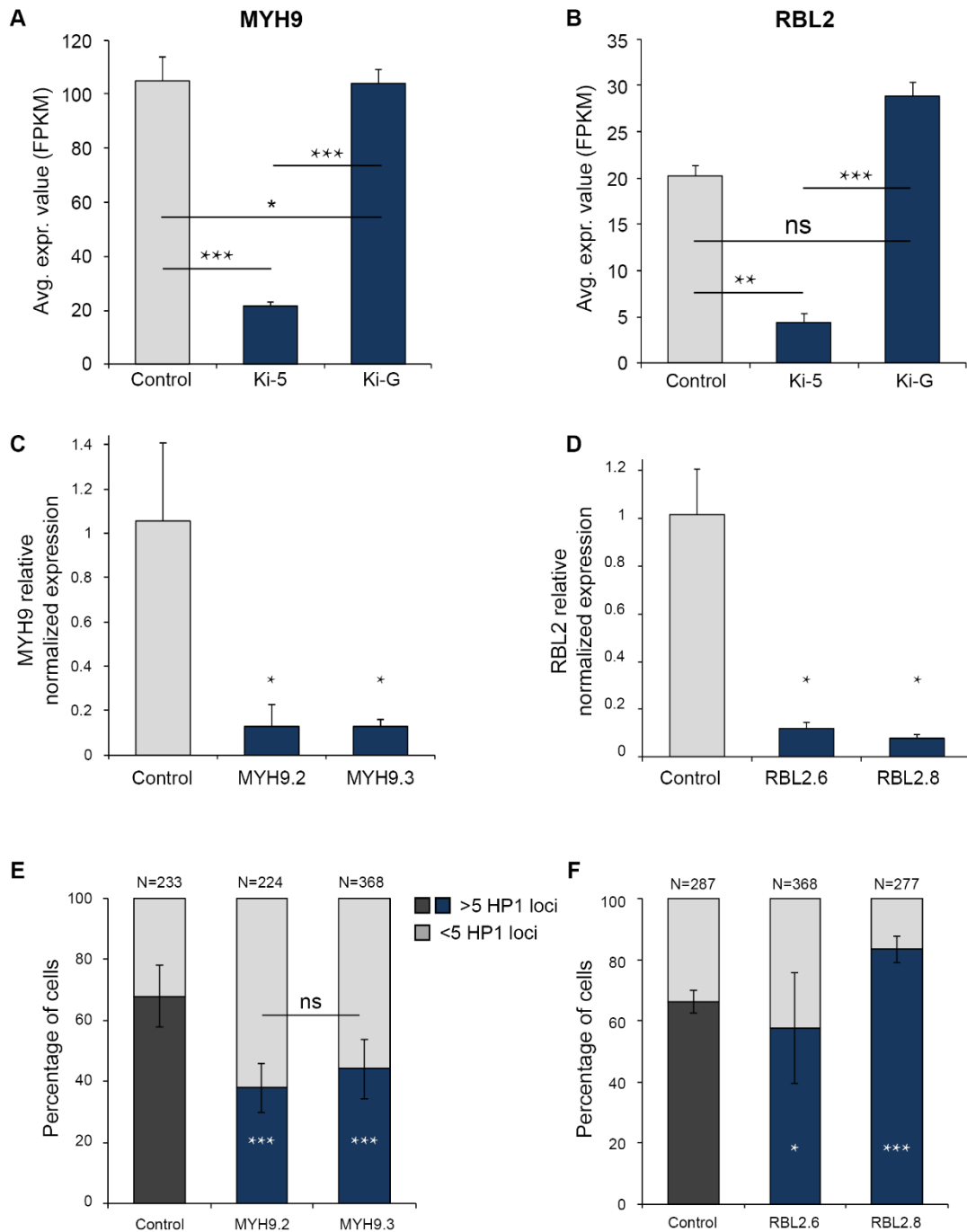


Figure 3.5. MYH9 knockdown, but not RBL2, regulates HP1 distribution. **A, B)** MYH9 and RBL2 are downregulated in Ki-5 transfected cells but not in the Ki-G transfected ones, as shown by RNA sequencing data. **C, D)** HeLa GFP:HP1 α cells were transfected with two different siRNA targeting MYH9 (**C**) and RBL2 (**D**) and efficiency of siRNA transfection was assessed by qPCR. The graphs show the average of three biological replicates. **E, F)** HP1 distribution was analysed for both MYH9-depleted cells (**E**) and RBL2-depleted ones (**F**) of three biological replicates. N represents the total number of cells counted. Chi-square t test was used for the statistics.

Overall, in this chapter, we identified Repo-man (CDCA2) as a major PP1-subunit regulator of heterochromatin maintenance in human cells. Furthermore, using different siRNAs against Ki-67 we reported different effects on HP1 regulation and, by RNA sequencing analysis, we were able to identify a potential new player on heterochromatin regulation, MYH9.

3.3. Discussion

This chapter aimed to identify chromatin-linked PP1 subunits as regulators of heterochromatin maintenance throughout cell cycle. For this purpose, a cell line that permanently expresses GFP:HP1 α was developed to use as a screening tool. The original plan was to develop three different cell lines, two human lines (HeLa and MRC5 fibroblast) and one zebrafish line (PAC2) in order to test our hypothesis in different cell types and organisms. However, only the HeLa GFP:HP1 α and MRC5 GFP:HP1 α cell lines were successfully developed. The zebrafish cell line could not be efficiently transfected with the GFP:HP1 α plasmid with any of the methods used, so the PAC2 GFP:HP1 α was not developed. However, in order to be able to use the PAC2 cells to study HP1 organization, I tested if the human anti-HP1 α antibody recognized the CBX5 protein of the zebrafish by immunofluorescence. However, at the conditions used, the antibody did not show the typical HP1 staining pattern expected in mitosis. It is also possible that this cell line that has been established from embryos, does not yet have the high level of heterochromatin organisation that is required for the establishment of HP1 α foci. Therefore, for all these reasons, we decided to discard the PAC2 cell line as a model to study HP1 regulation.

Validation of the HeLa GFP:HP1 α cell line was conducted by depleting G9A, a methyltransferase responsible for di-methylation of H3K9 (H3K9me₂), an anchoring site for HP1. Inhibition of the enzyme decreases the levels of H3K9me₂, reducing the HP1 chromatin binding sites. Two different oligonucleotides against G9A were used to validate the new established transgenic cell line. The same experiment was conducted in the MRC5 GFP:HP1 cell line, although in this case a reduction on HP1 α foci was not observed and the MRC5

GFP:HP1 α cell line could not be further used for transfection-related experiments. Another test to validate this cell line was done with two different drugs that are known to alter DNA methylation, chaetocin and 5-azacytidine, although again at the conditions used they were not able to affect HP1 organization. This cell line was then discarded for any future work regarding heterochromatin studies.

Once the HeLa GFP:HP1 cell line was validated and ready to use as a screening tool, we selected some siRNAs that target chromatin-linked PP1 subunits and performed a small screening for HP1 distribution; some of them have already been associated with chromatin organization (Van Dessel et al., 2010, Landsverk et al., 2005, O'Connell et al., 2012). siRNA targeting PTEN was used as a positive control, as it has been shown previously to regulate HP1 distribution (Gong et al., 2015b). In addition, siRNAs targeting the three PP1 isoforms were used. The results show that only Repo-man is able to decrease the number of cells with more than five HP1 foci, which was already shown previously in the lab (de Castro et al., 2017).

Ki-67 is widely known as a proliferative marker. However, other roles for this PP1 subunit have been described, including heterochromatin regulation (Booth et al., 2014, Sobecki et al., 2016a). Furthermore, due to its similarities with Repo-man regarding PP1 binding (Kumar et al., 2016, Booth et al., 2014) we wanted to study whether Ki-67 would also affect HP1 α organization in our system. We used three siRNAs targeting different Ki-67 sequences and, to our surprise, two different phenotypes were clearly observed. Two siRNAs (here referred to as Ki-G (from (Cuylen et al., 2016b)) and Ki-4) did not show any effect on HP1 distribution. This is in agreement with the results obtained in the Fisher's lab (Sobecki et al., 2016b) indicating that, although ki-67 mutant mouse cells decreased the number of H3K9me3 foci compared to the control, none of the three HP1 isoforms was affected. Sobecki et al. (Sobecki et al., 2016b) also showed that Ki67 mutant mice were viable and fertile. However, in the case of Ki-67 depletion using the Ki-5 siRNA, the number of cells with more than five HP1 α foci drastically decreased. Although the resistant plasmid rescued the phenotype to some extent, an off-target effect could not be excluded and RNA from cells treated with a control, the Ki-G and the Ki-5 siRNA were sent to sequence. Unexpectedly, the expression pattern on both siRNAs was very different and only a low percentage of genes were differentially expressed in both samples compared to the control. This clearly

indicates that mRNA knockdowns using siRNAs should be always validated with more than one siRNA targeting different sequences of the gene, and that any studies using this technique should be carefully analysed.

The difference in HP1 organization in the Ki-5 transfected cells could be due to a gene being differentially expressed in this sample compared to the Ki-G transfected one. Looking at the differential expression, we recognized two genes that meet the description and could account for the phenotypical difference: RBL2 (encodes for retinoblastoma-like protein 2) and MYH9 (encodes for myosin 9). These two genes were also not found downregulated in the RNA sequencing experiments performed by Sobecki et al. (Sobecki et al., 2016), in where Ki67 depletion did not affect HP1 α organization. RBL2 has been previously linked to heterochromatin regulation (Gonzalo et al., 2005, Benetti et al., 2008). Specifically, triple RB1^{-/-}/RBL1^{-/-}/RBL2^{-/-} knockout was seen to alter DNA methylation and decrease the levels of H4K20me3, a marker for heterochromatin; however, in this experiment, the triple knockout did not alter the levels of H3K9me2/3 or HP1 (Gonzalo et al., 2005). Still, we tested if RBL2 knockdown was able to disrupt HP1 distribution in our cell lines. In agreement with the previous study, RBL2 was not able to alter HP1 distribution and therefore it could not be the one responsible for the difference in the phenotype. To our knowledge, a direct link between MYH9 and heterochromatin has never been observed. However, the role of myosin on the cytoskeleton, microtubule stabilization, and cell shape maintenance could suggest a possible role on chromatin structure. Therefore, we also knockdown MYH9 independently with two siRNAs and, in both cases, HP1 distribution could not be maintained, identifying a new regulator for HP1 maintenance. A rescue experiment using a MYH9 resistant plasmid should be performed to claim that the results obtained are due to MYH9 knockdown. Moreover, heterochromatin might be altered due to defects on the cell cycle; in order to discard this hypothesis, cell cycle progression should be analysed by fluorescence-activated cell sorting (FACS). The influence of actin cytoskeleton and microtubules on nuclear integrity and chromatin organization is well known, thus we hypothesize that MYH9 might regulate heterochromatin indirectly by affecting the cytoskeleton structure. Further experiments could be focused on analysing several cytoskeleton factors and identifying the specific pathway by which MYH9 affects

heterochromatin regulation, and whether MYH9 is involved in regulation of other heterochromatin markers, namely H3K9me3 and H3K27me2/3.

4. ANALYSES OF CDCA2/PP1 COMPLEX DURING ZEBRAFISH DEVELOPMENT

4.1. Introduction

In the previous chapter, we confirmed CDCA2 (Repo-man) as the major phosphatase implicated in the regulation of heterochromatin maintenance in human cells. However, heterochromatin is disassembled in the gametes prior to the formation of the zygote, and it needs to be re-established in early development as cells differentiate. We hypothesised that CDCA2 could also be important for these early steps of chromatin organization and thus in this chapter we aimed to unravel the functions of this mitotic protein in early development, using zebrafish as a model organism. The function of CDCA2 in a model organism has never been studied and its role as an essential gene for cell proliferation has only been assessed in cultured cells.

4.1.1. Zebrafish

Danio rerio, commonly known as zebrafish, is a tropical freshwater fish that belongs to the order of Cypriniformes and it is native to the Southeast Asia. Due to its major advantages compared to other model organisms, zebrafish has been widely used as a vertebrate model organism in biomedical and environmental research since the 1960s. One of the main advantages is its affordability in terms of space and money, as zebrafish are considerably smaller and cheaper to maintain than other organisms such as rodents. For the purposes of this research, another major advantage is the fact that the embryos develop outside the mother's body and are transparent until larval stages, making them a powerful model to study embryo development. Furthermore, a single female can produce as many as 50 to 300 eggs a day, increasing the statistical power for downstream experiments, and they reach sexual maturity in about 3 months after fertilization. Finally, the zebrafish genome shares about 70% identity with that of humans, and the complete genome sequence was published in 2013, enabling scientist to study zebrafish genetics. The full zebrafish genome sequence can be found in the Zebrafish Genome Project in the Sanger website (Wellcome Sanger Institute, 2013). Altogether, these characteristics have made zebrafish a really suitable

model system to study a variety of scientific areas, including developmental biology, cancer, epigenetics, and toxicology (Mudbhary, Sadler, 2011).

4.1.1.1. Zebrafish development

Zebrafish embryos develop optimally in incubators at 28°C, although they appear to develop normally at temperatures between 25°C and 33°C. Development starts by cleavages every 15 minutes periods in regular orientations, until the mid-blastula transition (MBT) at around 2-3hpf, when gene transcription is activated. From there, the embryo starts gastrulation, (5-10hpf) followed by a segmentation period (10-24hpf) where the rudiments of the primary organs become visible. At 24hpf the main organs are already visible, and at 48hpf, some embryos start to hatch and by day 3 most of the morphogenesis is already completed and the larvae start to swim (Figure 4.1). Larvae are still kept developing in incubators until around day 5, when they start to be fed externally and they can be transferred to the normal water system.

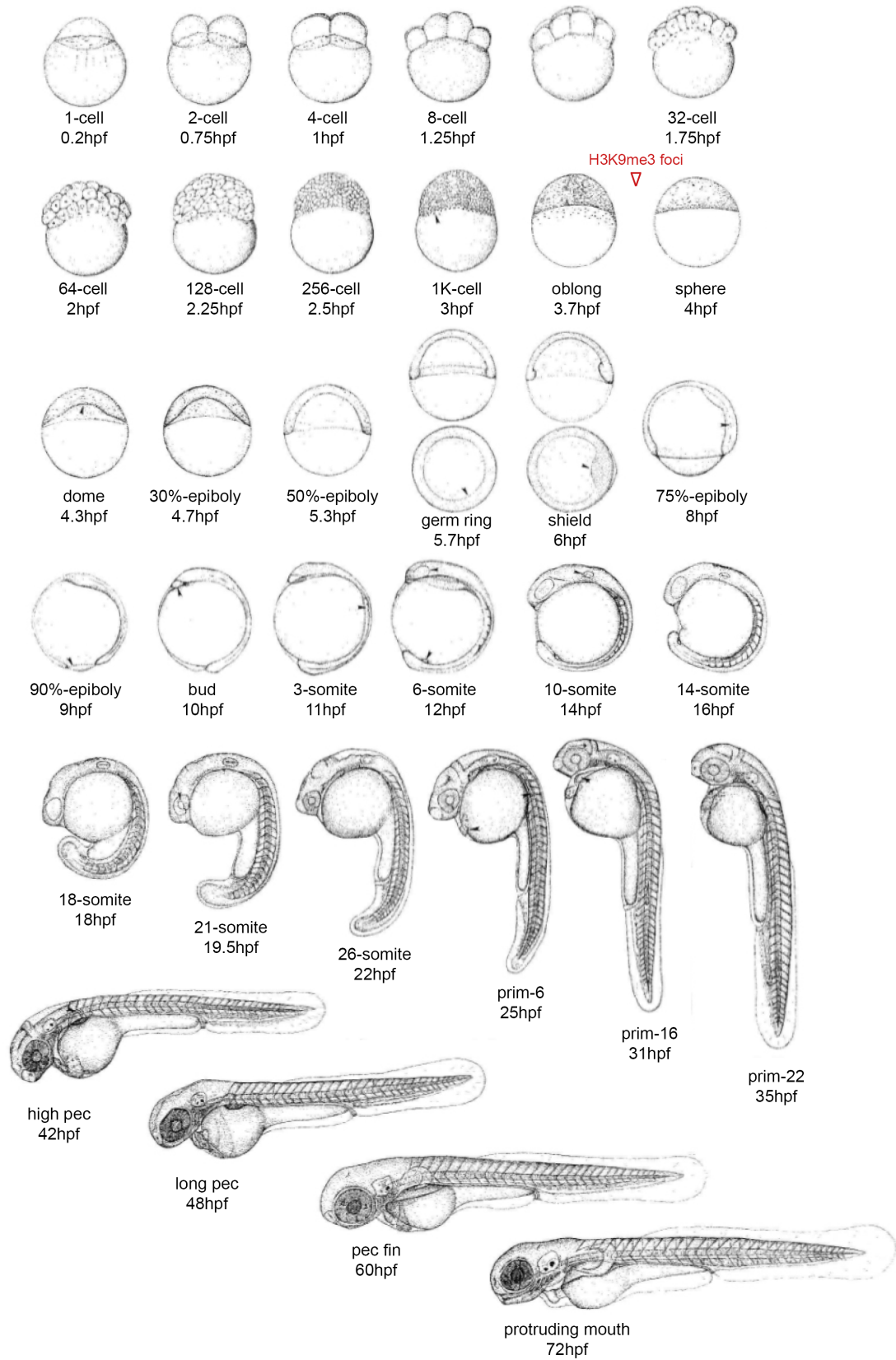


Figure 4.1. Zebrafish developmental stages (adapted from (Kimmel, et al., 1995), indicating when H3K9me3 foci are first apparently visible (Laue et al., 2019).

4.1.2. Epigenetics in zebrafish development

Zebrafish embryos start developing from maternal mRNAs and proteins stored in the egg, and it is not until the 6th-10th cleavage cycle (2-3 hours post fertilization (hpf)) that they undergo mid-blastula transition (MBT) and gene transcription activation (Kane, Kimmel, 1993, Tadros, Lipshitz, 2009). This stage corresponds with an increase on global DNA methylation and histone modification marks, which evolve to become more and more complex as the embryo develops (Mhanni, McGowan, 2004, Lindeman et al., 2010). These proteins involved in DNA methylation pathways as well as the main epigenetic mechanisms in zebrafish are generally preserved in mammals, making it a great system to study epigenetics during development (Lindeman et al., 2010, Goll, Halpern, 2011). However, there are some epigenetic differences between zebrafish and mammalian development, summarized in Table 4-1 (Balasubramanian, Raghunath & Perumal, 2019)

Many experiments have been performed to study the genes involved in epigenetics during zebrafish development. One of the most studied set of epigenetic genes are the group of DNA methyltransferases (Dnmt), which can be easily studied via inhibition with 5-Azacytidine. Zebrafish treated with this drug during the blastula stage showed impaired somite, muscle, and cardiac development (Martin et al., 1999, Goll, Halpern, 2011, Yang, W. et al., 2019). Studies on each of the eight Dnmt present in zebrafish showed that Dnmt1 is important for some, but not all, organs development, including pancreas, intestine, and retina (Rai et al., 2006, Anderson et al., 2009). In contrast, Dnmt2 knockdown was essential for retina, liver, and brain development (Rai et al., 2007), and the Dnmt3 orthologue, for neurogenesis (Rai et al., 2010, Smith, Collins & McGowan, 2011). Histone modifications have also been extensively studied in zebrafish, as they play crucial roles during development. Heterochromatin is established in the zebrafish only after MZT, therefore the heterochromatic mark H3K9me3 is absent from the zebrafish genome until after this transition (Laue et al., 2019). The histone deacetylase Hdac1 was reported to be important for neurogenesis, ear and pancreas development (Cunliffe, 2004, Zhou, B. et al., 2011, He et al., 2016), whereas Hdac3 plays a role on liver development. From histone variants, H2AFV was shown to restrict DNA methylation during MZT by crosstalk with Dnmt1 (Madakashira

et al., 2017), and macro H2A regulates neuronal differentiation (Buschbeck et al., 2009, Gonzalez-Munoz et al., 2019).

Table 4-1. Major epigenetic differences between mammalian and zebrafish development (adapted from (Balasubramanian, Raghunath & Perumal, 2019).

Epigenetic mechanism	Zebrafish	Mammals
DNA methylation	Global DNA methylation remodelling absent	Global DNA methylation remodelling present
	Imprinting absent	Imprinting present
	DNA methylation from sperm is inherited	DNA methylation undergoes two rounds of reprogramming
	ZGA happens during blastula stage	ZGA happens at earlier stage
Histone modifications	Histone modifications are globally removed before ZGA	Histone modifications play an important role during ZGA
	Sperm genome is packed into nucleosome	Sperm genome is packed into protamine

4.1.3. CDCA2 in zebrafish

CDCA2 is found on chromosome 5 of the zebrafish genome. It is a long gene that encodes a mRNA of 3440bp and a protein of 807 amino acids. An alignment of different binding domains of human and zebrafish CDCA2, together with other species, has been performed, indicating a high conservation among species (Figure 1.13). To our knowledge, this protein has never been studied before in zebrafish, thus the importance of this research chapter. More information about the gene can be found with the following ID: ZDB-GENE- 030131-3271. A full alignment between human and zebrafish CDCA2 is shown in Figure 4.2.

BAD AVG GOOD



Figure 4.2. Human CDCA2 and zebrafish CDCA2 full protein alignment. Human and zebrafish CDCA2 protein sequences were aligned using the T-Coffee website. Highly conserved sequences are shown in red, followed by medium conserved sequences in yellow and poorly conserved sequences in green.

4.2. Results

4.2.1. CDCA2 characterization during zebrafish development

As previously mentioned, CDCA2 has never been studied in zebrafish before, thus we first had to characterize the expression levels and patterns of this protein in zebrafish, as well as to optimize antibodies to recognize the zebrafish protein.

First of all, we analysed CDCA2 gene expression at different developmental stages by quantitative PCR (qPCR) (Figure 4.2.A), and then performed whole-mount RNA *in situ* hybridization (ISH) at three time points of early development (Figure 4.2.B) in order to investigate expression patterns. In the initial stages of development, we can observe a huge expression of CDCA2, which drops considerably after the embryos undergo mid-blastula transition (MBT) and start transcribing their own genes. After the primary organs have been established, CDCA2 expression levels decrease and remain low throughout the larval stages (Figure 4.2.A.) Early stages of zebrafish development are driven by maternal mRNA, and thus the high expression observed at the 4-16 cells stage and, to some extent, the one at 4hpf, correspond to transcripts from the mother.

Whole-mount ISH revealed a ubiquitous expression of CDCA2 at 2-cell and 4hpf stages, although at 24hpf strong signals were detected in the brain area (Figure 4.2.B). As far as we could tell, these signals are located mainly in the midbrain, hindbrain, and the cerebellum, and they are absent from brain areas such as the epiphysis (or pineal gland) and the telencephalon (or fore brain). To evaluate whether CDCA2 was particularly important for brain function, we also analysed the expression levels of different adult tissues (Figure 4.2.C). Surprisingly, CDCA2 expression was no longer concentrated in the brain, but rather in both the male and female reproductive system. We also studied CDCA2 at protein level in mice tissues (a kind gift from Dr. Su-Ling Li, Brunel University). In mice, CDCA2 was more expressed in the liver than in the other tissues tested (Figure 4.2.D). However, it would be interesting to have some ovaries or testis tissue from the mice to be able to compare it with the data from the zebrafish. The zebrafish expression data is in agreement with human data

available in the Expression Atlas or the NCBI website, from genome-wide transcriptomics experiments (Szabo et al., 2015, Fagerberg et al., 2014). Those experiments also show a very high expression on the testis compared to other tissues, and a decrease on CDCA2 expression in most tissues as the foetus develops (Figure 4.3).

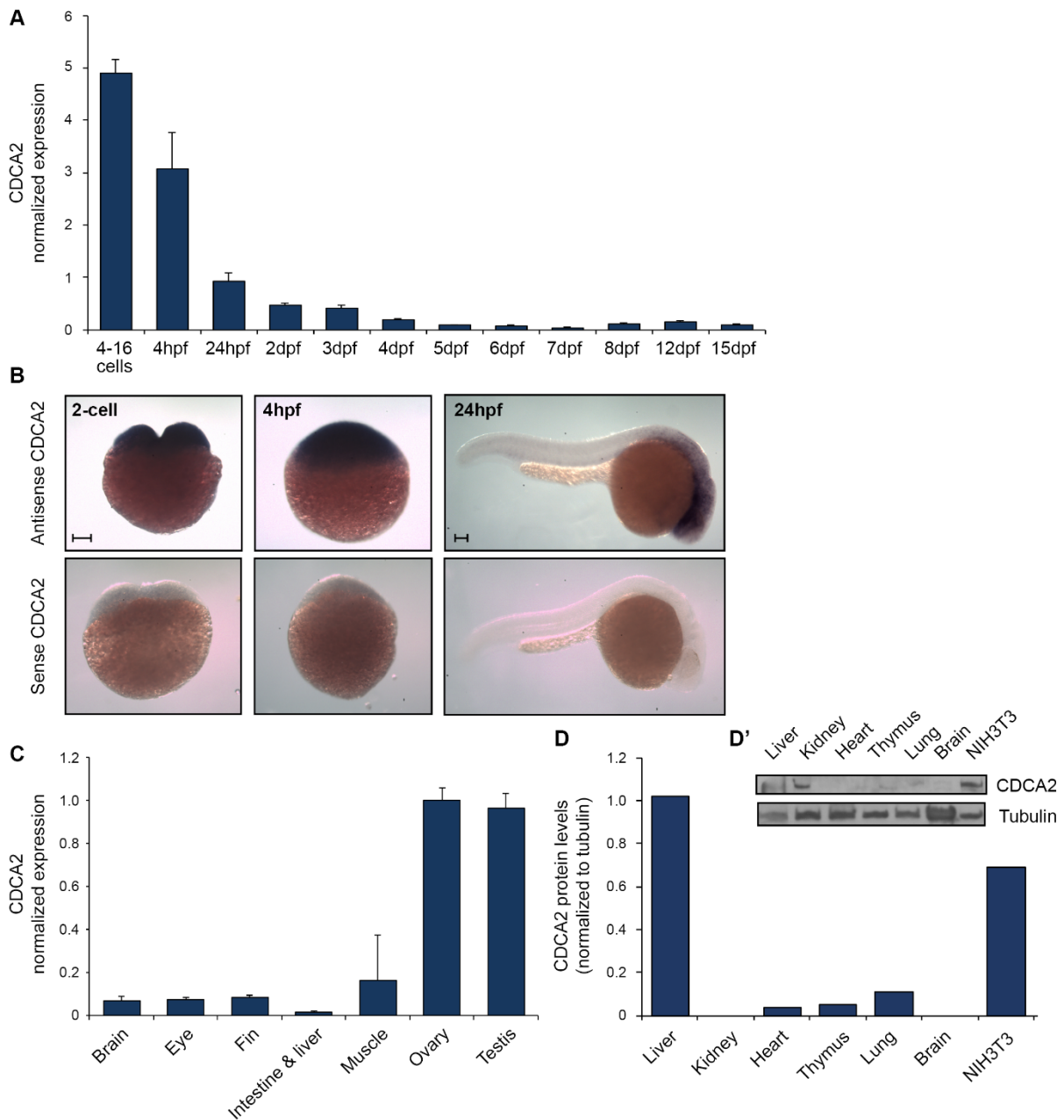


Figure 4.2. CDCA2 expression analysis in zebrafish. A) CDCA2 gene expression levels during zebrafish development by qPCR. Error bars represent the standard deviation of three technical replicates. **B)** Whole-mount in situ hybridization of zebrafish embryos at 2-cell, 4hpf, and 24hpf stages. The lower panel represents a negative control using a sense CDCA2 mRNA probe. Scale bars: 0.1mm. **C)** CDCA2 gene expression of adult zebrafish tissues. Error bars represent the standard deviation of three technical replicates. **D)** Quantification of CDCA2 protein levels in several mice tissues normalized to tubulin. **D')** Western Blot of the different mice tissues using a human CDCA2 antibody and tubulin.

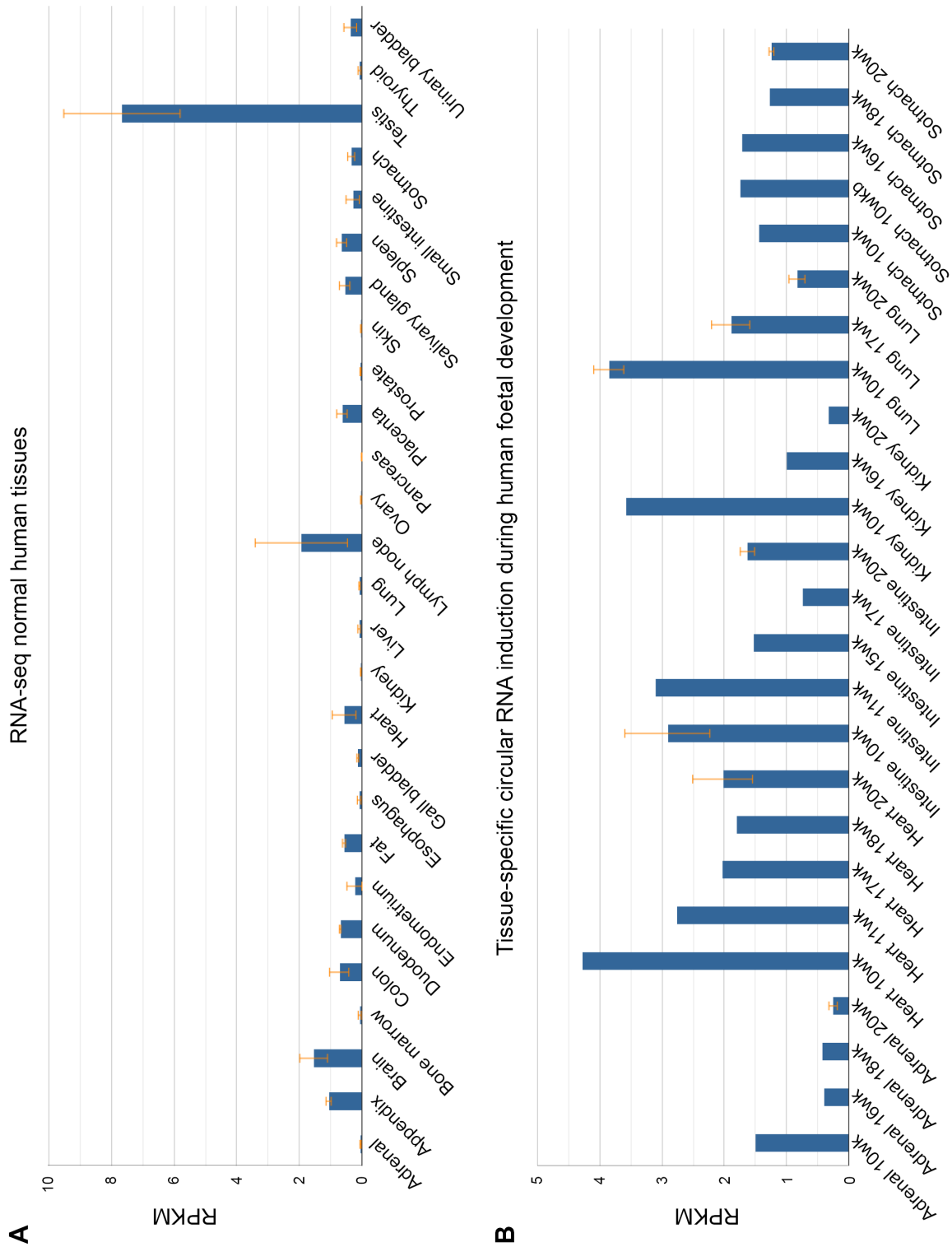


Figure 4.3. CDCA2 RNA expression data in human tissues. **A)** RNA of tissue samples from 95 human individuals representing 27 different tissues was sequenced and the levels of CDCA2 represented in the graph (Fagerberg et al., 2014). **B)** RNA from 35 human foetal samples from 6 tissues (3 - 7 replicates per tissue) collected between 10 and 20 weeks gestational time were sequenced using Illumina TruSeq Stranded Total RNA (Szabo et al., 2015). Both graphs were available in the NCBI website.

In order to study CDCA2 at protein level, we first had to find an antibody that recognized the zebrafish protein sequence. Our first attempt was to test the human antibodies that were already available in our laboratory. For this purpose, a zebrafish cell line, PAC2, was grown and fixed for immunofluorescence. However, the epitopes used for both the Proteintech and Sigma CDCA2 antibodies are not present in the zebrafish protein, thus we should expect no recognition. For the other available antibody, from Abcam, we did not have the epitope sequence but only that it was designed from the C-terminus of the human CDCA2 protein, which is less than 40% similar to that of the zebrafish. Nevertheless, we tested whether this antibody and another one that was previously developed in the lab also raised against the C-terminus, were able to detect CDCA2 by immunofluorescence. CDCA2 is a mitotic protein that gets dispersed at the beginning of mitosis and relocates to the chromatin at anaphase; therefore, the staining pattern at the different stages of mitosis was analysed. Both antibodies showed a similar pattern, with relocalization of CDCA2 onto chromosomes during anaphase (Figure 4.4), therefore we tested the antibody that appeared more specific, 58A, on whole zebrafish embryos at 4, 18, and 24hpf (Figure 4.5). However, analysing the specificity by immunofluorescence in a whole zebrafish embryo is somehow challenging; due to the three-dimensional aspects, detecting cells at different stages of mitosis is complicated and, due to the multiple layers of cells, it is difficult to distinguish between background and staining at different focus. The antibodies were also tested by Western Blot (WB), although no specific band was detected in any of the conditions used (data not shown). Altogether, all these experiments made it rather difficult to assure antibody specificity and, considering that there are no antibodies targeting the zebrafish CDCA2 available, two new antibodies specifically designed to recognize the zebrafish CDCA2 protein were developed by Eurogentec. The zebrafish CDCA2 protein sequence was uploaded to the Eurogentec website and two out of the three best proposed peptide sequences were used to develop the antibodies. One of the antibodies targets the very end of the C-terminal tail, from amino acid 793 to 807, with the following sequence: H – CFI PQP SEE LTT NLG E – OH. The other targets from amino acid 674 to 688 with the following sequence: H – CQK TPS NKR PGQ GQK V – NH₂. They were both polyclonal developed in rabbits.

Once more, we first tested the new antibodies by immunofluorescence on the PAC2 cell lines, but several conditions tested did not show any signal corresponding to CDCA2 (data

not shown). Afterwards, an immunofluorescence of the whole embryo was performed (Figure 4.6) and, although some specificity was detected compared to a negative control, it was again hard to distinguish. Much effort has been put on optimizing the new antibodies, also by Western Blot as we would see in the next subchapter, though, until now, we were not able to demonstrate their specificity.

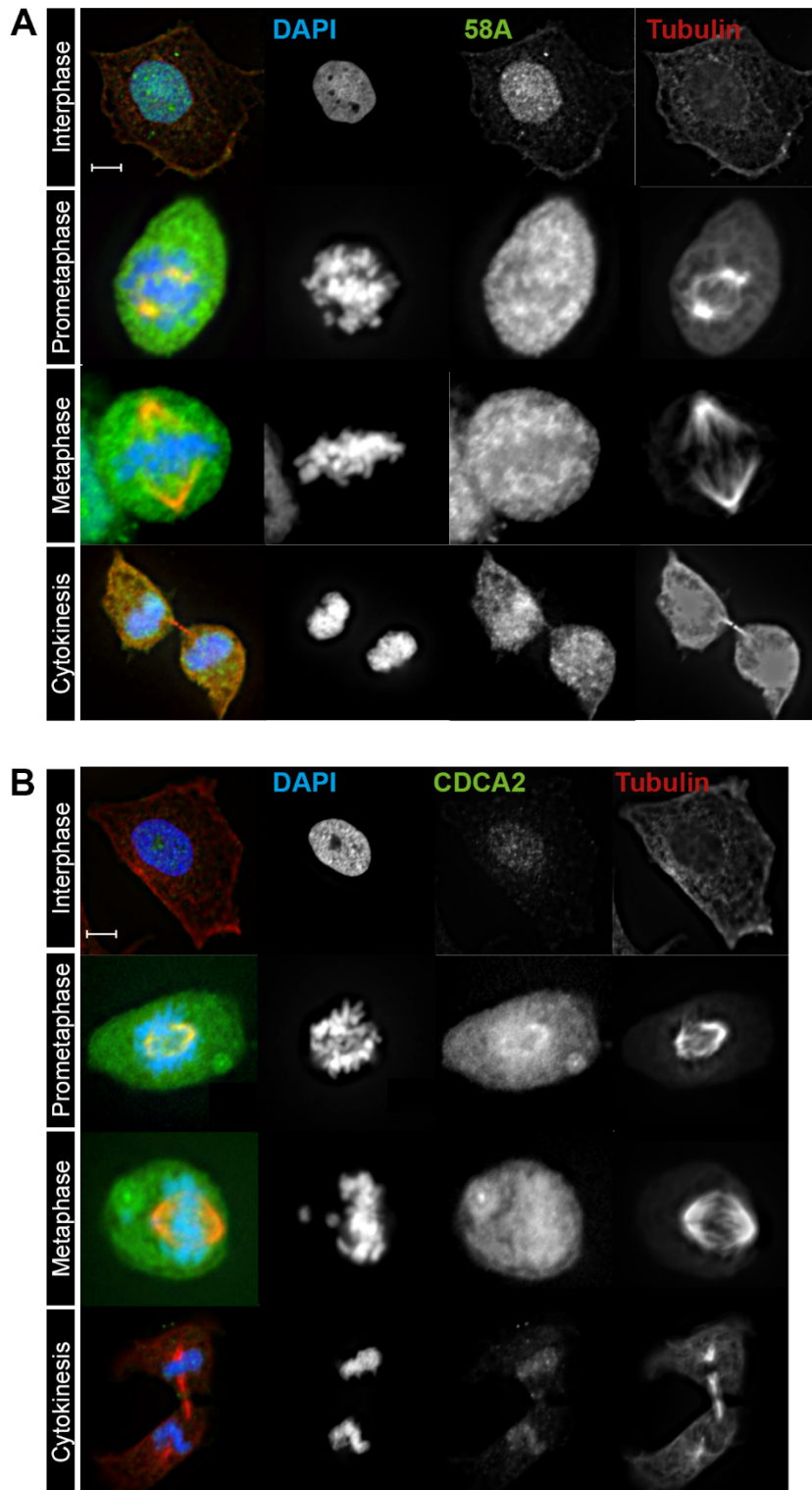


Figure 4.4. Anti-human CDCA2 specificity testing against the zebrafish protein. PAC2 cells were immunostained using two different antibodies targeting the human CDCA2 protein: an antibody specific for the N-terminus of CDCA2, 58A (**A**) and anti-CDCA2 from Abcam (**B**). Scale bar: 5µm.

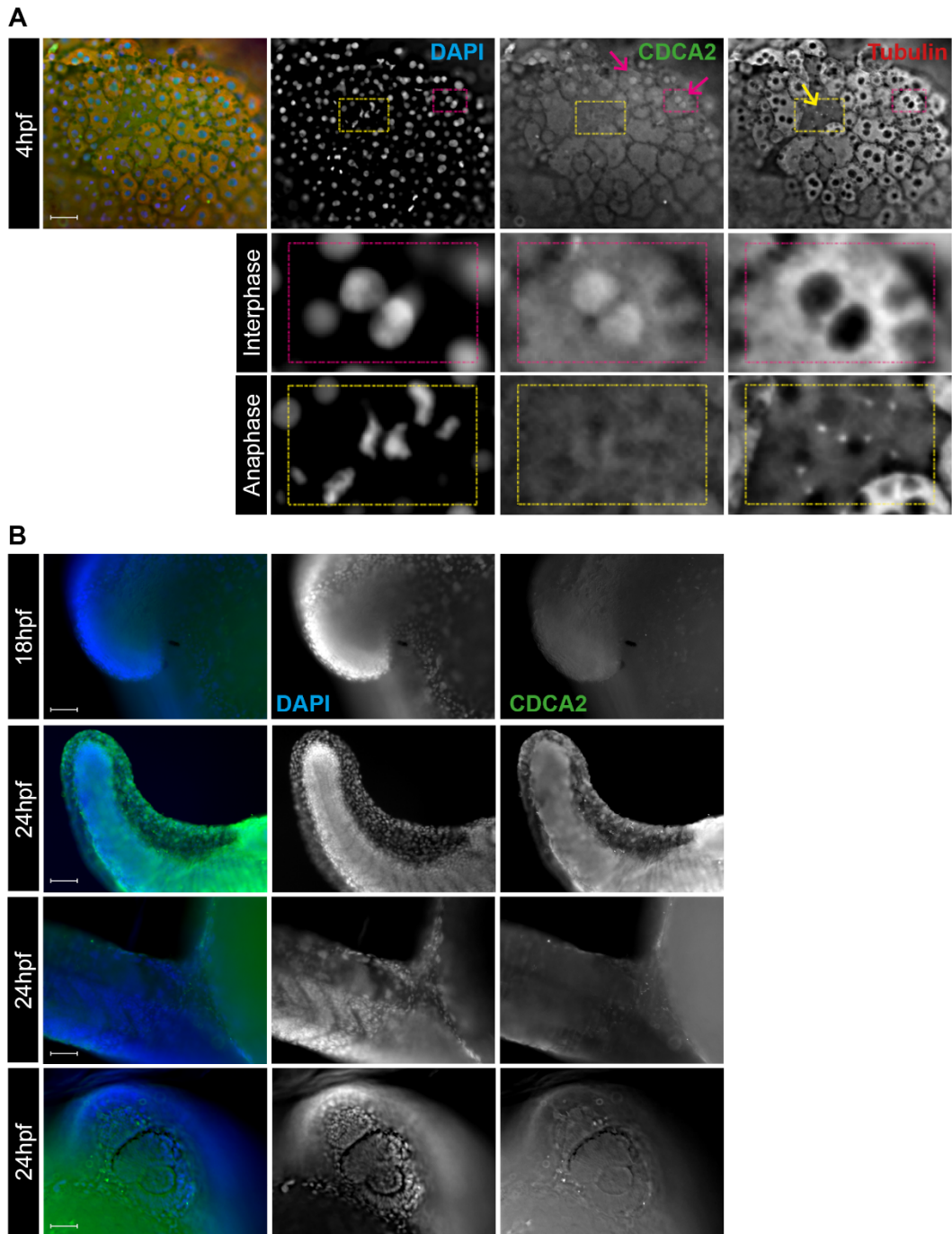


Figure 4.5. Whole zebrafish embryo immunofluorescence. Zebrafish embryos at 4hpf (**A**), 18hpf and 24hpf (**B**) were immunostained using the 58A CDCA2 antibody to evaluate antibody specificity. At 4hpf, cells in interphase and anaphase were zoomed in in order to detect specificity. Scale bars: 100 μ m.

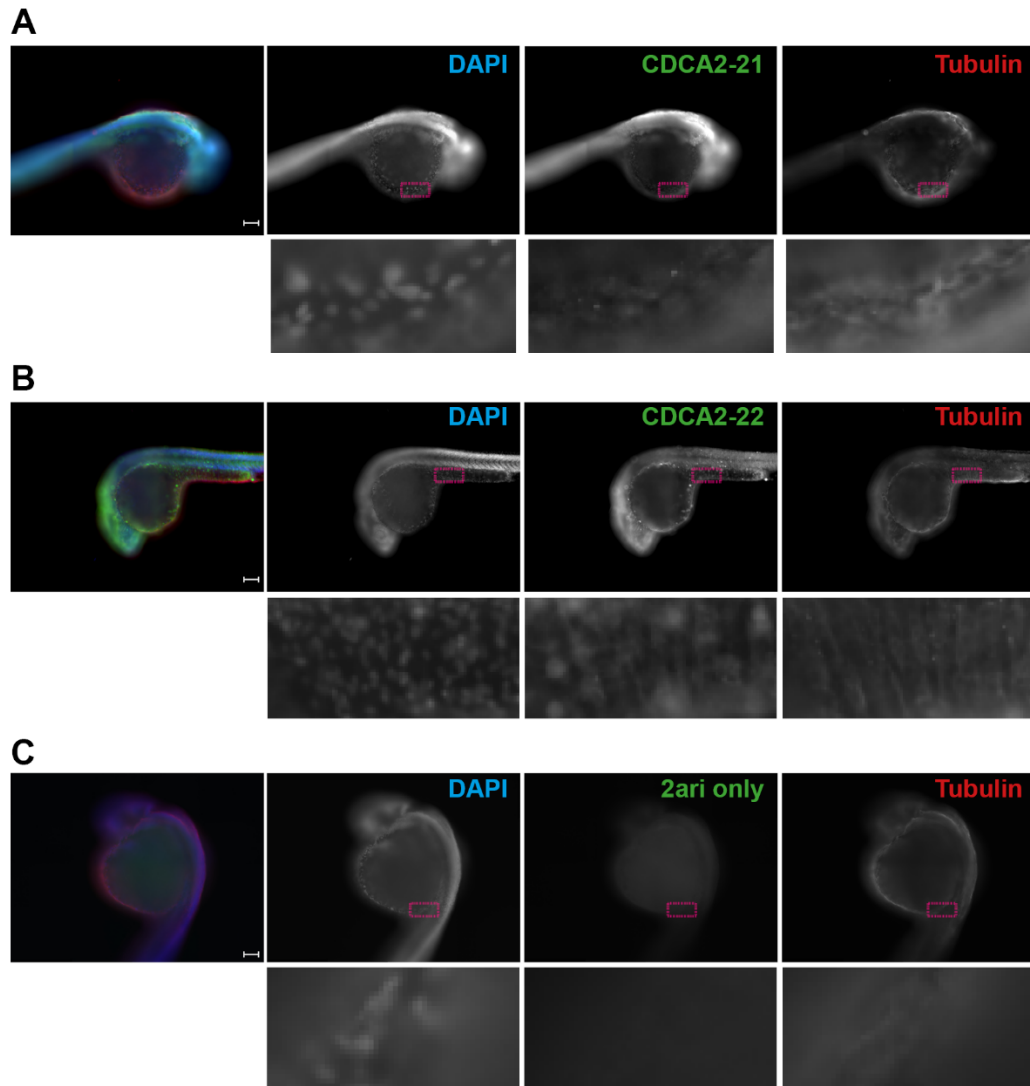


Figure 4.6. Whole zebrafish embryo immunofluorescence with antibodies specific for the CDCA2 zebrafish protein. 24hpf zebrafish embryos were stained using the two antibodies specifically design to recognize the CDCA2 zebrafish protein (**A**, **B**). Embryos only stained with the secondary antibody were used as a negative control (**C**). Scale bars: 100µm.

4.2.2. Mutant CDCA2 zebrafish line analysis

In 2011, The Sanger Institute aimed to create a knockout allele in all protein-coding genes of zebrafish in the so-called Zebrafish Mutation Project (ZMP). In the case of CDCA2, a nonsense mutation in the base pair number 47 was produced, where a Thymine was replaced by an Adenosine, producing a stop codon at amino acid 16 (Figure 4.7.A). The distribution of the lines is carried out by the Zebrafish International Resource Center (ZIRC), where wild type eggs were in vitro fertilized with frozen mutated sperm and the eggs were shipped for further analysis. No previous researchers have ever analysed this line before, so the efficiency and effectivity has never been validated. When the eggs reached adulthood (about 4 months after receiving them), we genotyped them, obtaining 35 zebrafish with both WT alleles and 36 with one mutated allele, consistent with the expected Mendelian distribution. These heterozygous zebrafish were crossed to obtain a second generation; this also follows the expected Mendelian distribution: 100 zebrafish had both wild type alleles (CDCA2^{+/+}), 202 were heterozygous (CDCA2^{+/-}), and 98 were homozygous for the mutation (CDCA2^{-/-}) (Figure 4.7.B).

In order to verify the mutation efficiency, the second-generation zebrafish were crossed, and the eggs were analysed for CDCA2 gene expression levels, as transcripts with premature stop codons should undergo non-sense mediated mRNA decay. Figure 4.8.A shows a clear decrease on mRNA levels in eggs from heterozygous and mutant crosses, compared to the ones from WT. This difference was not observed at protein level (Figure 4.8.B). Nevertheless, as mentioned previously, we cannot be sure that the antibody works and there is no validated antibody that specifically recognizes the zebrafish protein, thus no comprehensive conclusions could be done at this time with the blot obtained.

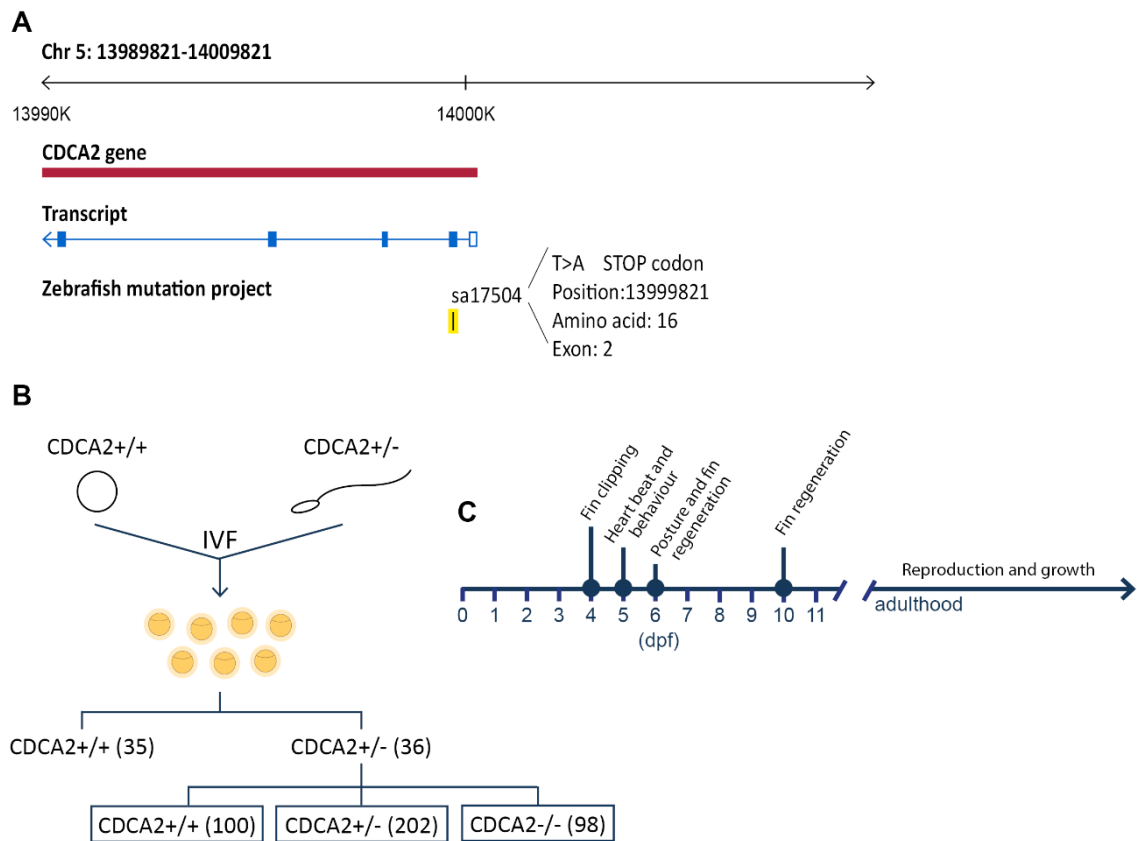


Figure 4.7. Mutant CDCA2 zebrafish line. A) Graphical representation of the mutation in the CDCA2 gene. **B)** Explanation of the mutant CDCA2 zebrafish line production. CDCA2^{+/+} oocytes were in vitro fertilized with spermatozooids carrying a point mutation on one allele of the CDCA2 gene. These eggs were grown to adulthood and genotyped, obtaining a Mendelian distribution. Heterozygous zebrafish were crossed, and a Mendelian distribution was obtained. These eggs were further genotyped, and the fish were used for analyses. **C)** Timeline of the experiments carried out in the mutant zebrafish line.

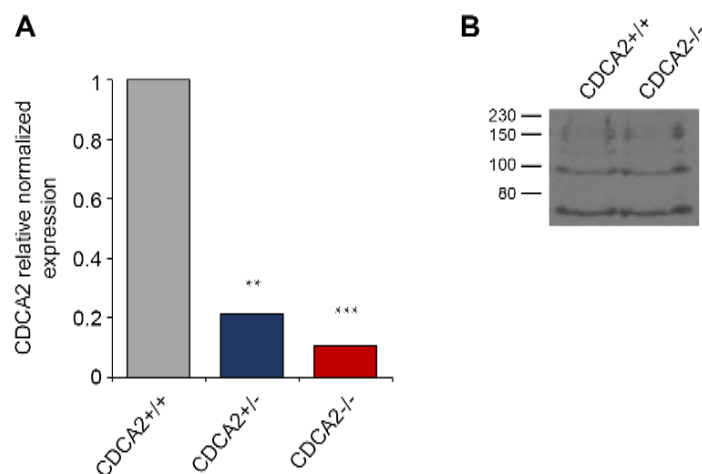


Figure 4.8. CDCA2 mutant lines undergo non-sense mediated mRNA decay. A) CDCA2 gene expression of 2hpf embryos from CDCA2^{+/+}, CDCA2^{+/-}, and CDCA2^{-/-} crosses. Only one replicate, with a pool of 50 embryos, was analysed. T test was used for the statistics. **B)** Western blot of 3dpf embryos from CDCA2^{+/+} and CDCA2^{-/-} crosses using one of the newly synthesized antibodies against zebrafish CDCA2.

This second generation of zebrafish was used to study the function of CDCA2. Since visual analysis of the embryos did not show any phenotype, we developed a timeline to analyse several systems (Figure 4.7.C). At 4dpf, zebrafish were genotyped by clipping a part of the caudal fin and separated by genotype. The regeneration of the fin was observed at 6dpf and 10dpf, with no apparent difference between the three genotypes (data not shown). At 5dpf, zebrafish were submitted to a behavioural study to analyse the central nervous system (CNS) (**Error! Reference source not found.9**). The statistical analyses show a significant difference in the response of the heterozygous and the homozygous to the light/dark cycles compared to the control, although the biological significance of these results remains unclear, as no significant difference is observed in the distance run and the speed achieved in the same experiment. In another analysis, the heartbeats from 5dpf embryos were manually recorded in order to analyse the cardiovascular system but with no significant difference between the WT and the homozygous fish was observed (Figure 4.10.A). The next day, the posture and response to stimuli were annotated, with again no difference spotted. Measurements during their adulthood did not show any difference in their weight or length either (Figure 4.10.B,C), as well as in their reproductive capability (Figure 4.11). In the

fertility study, the different lines were crossed 1:1 (one male paired with one female), and the next morning the total number of eggs were counted, together with the number of fertilized and dead embryos. Statistically, no significant difference was observed. However, there was a huge variability between replicates and the wild type females had repetitive difficulties to spawn. Further experiments and replicates should be performed in order to validate the results, although it would be optimal to enlarge the number of zebrafish available, which is not feasible in the timeline of this research project at this time.

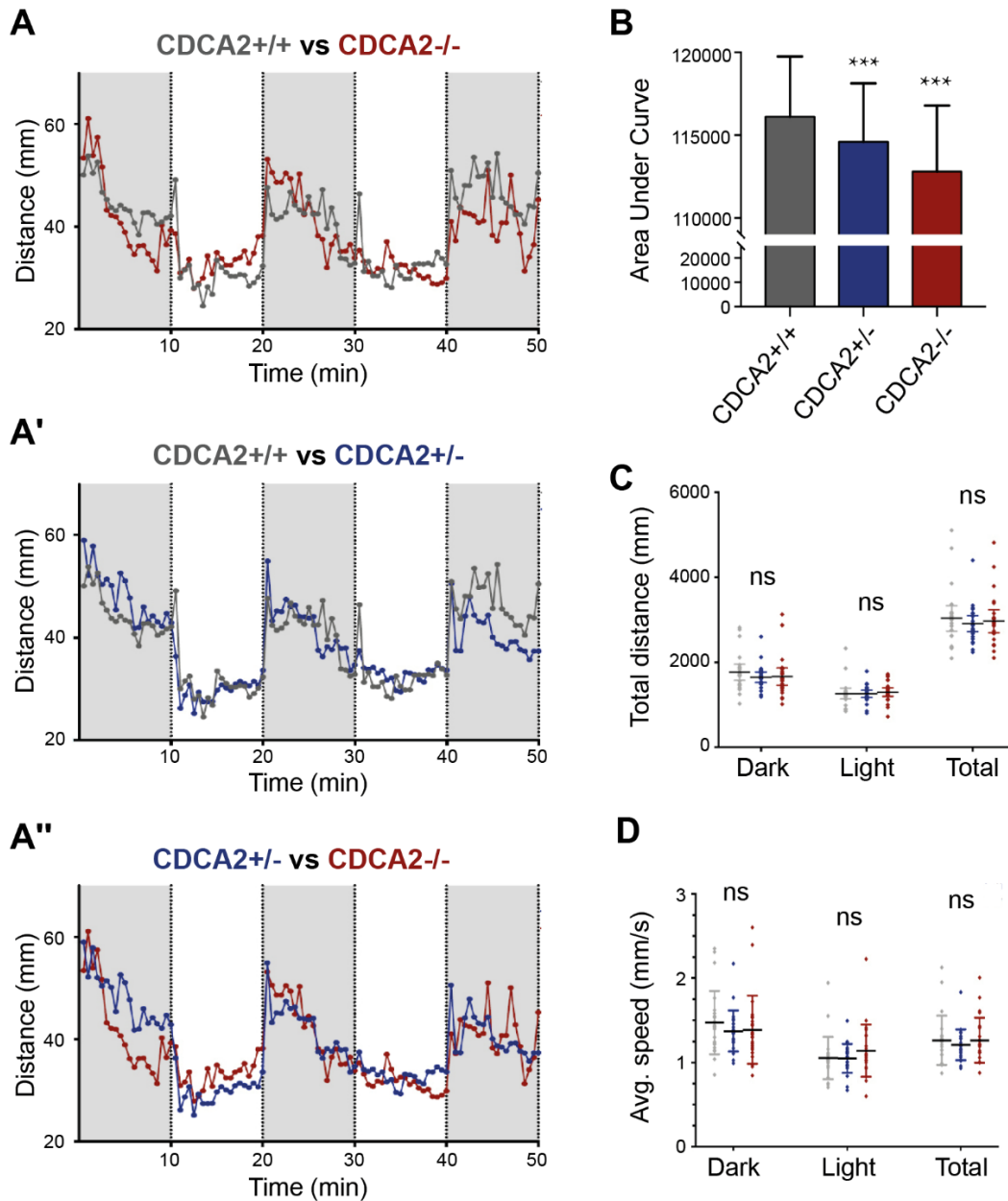


Figure 4.9. Central nervous system analysis on the CDCA2 mutant zebrafish line. **A)** Graph showing the distance run by the zebrafish in 10 minutes long dark/light cycles. Comparison between the CDCA2^{+/+} and CDCA2^{-/-} (A), CDCA2^{+/+} and CDCA2^{+/-} (A') and CDCA2^{+/-} and CDCA2^{-/-} (A''). Each point corresponds to the average of 24 zebrafish. **B)** Area Under the Curve (AUC) from experiments in A. Bar represents standard deviation. **C)** Total distance run in each cycle and in total from experiment A. **D)** Average speed in each cycle and in total from experiment A. Mann-Whitney U test was used for the statistics. Grey represents CDCA2^{+/+}, blue CDCA2^{+/-}, and red CDCA2^{-/-}.

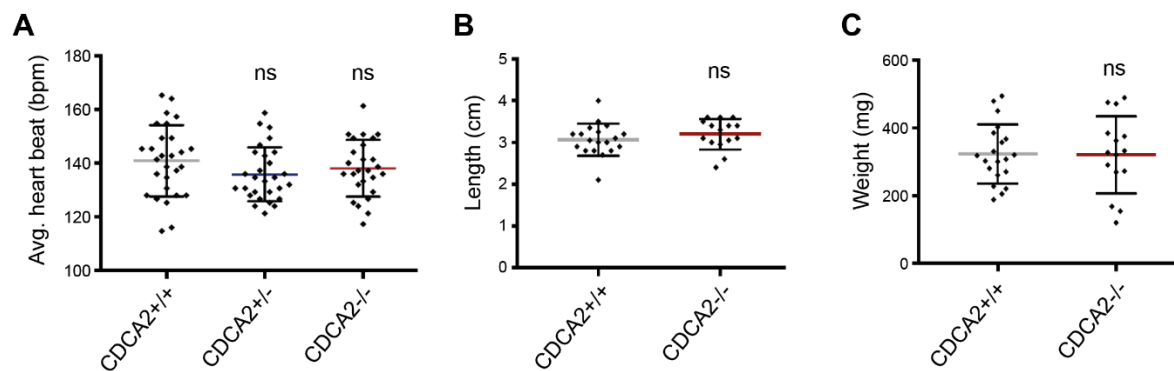


Figure 4.10. Cardiovascular system analysis on the CDCA2 mutant zebrafish line. A) Average heartbeat. Each dot represents the average of three counts for each 5dpf embryo. **B, C)** Length (B) and weight (C) of adult zebrafish. Mann-Whitney U test was used for the statistics.

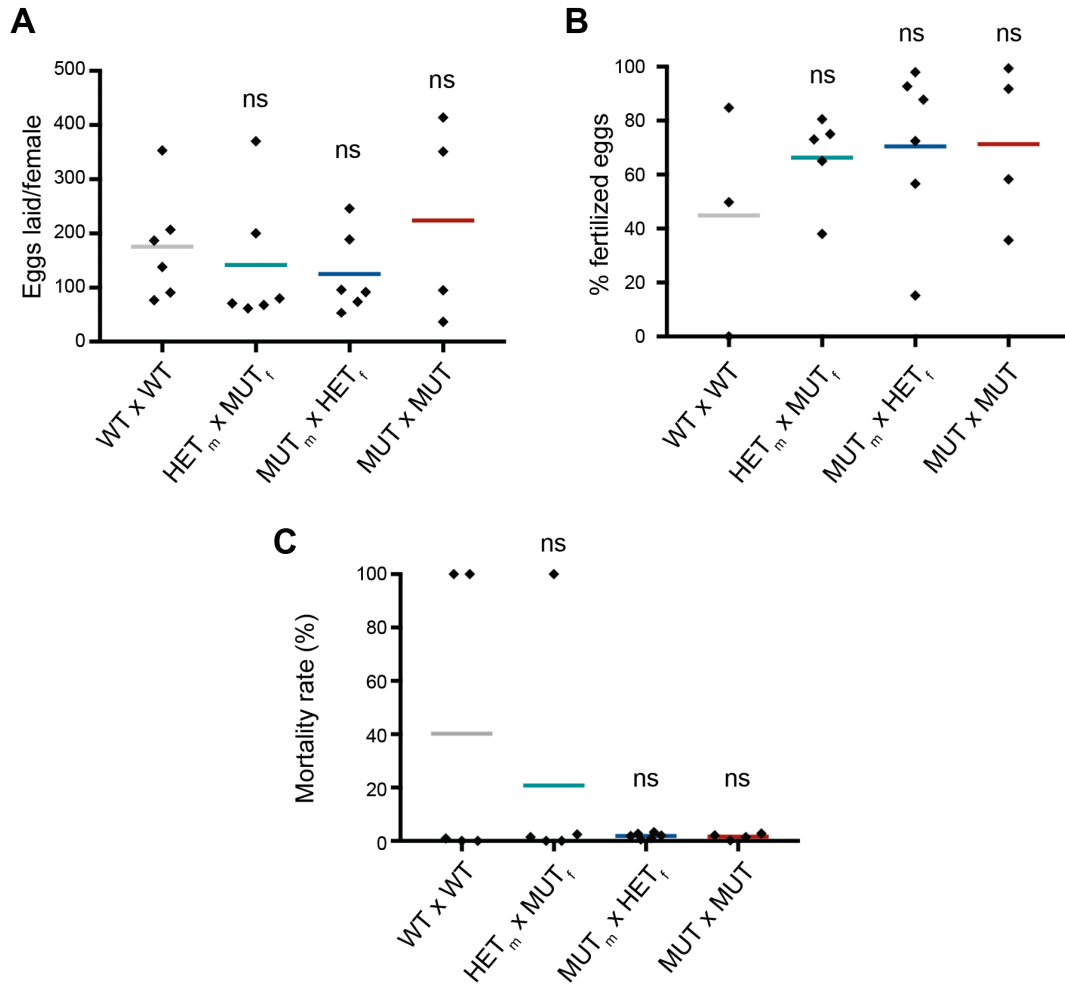


Figure 4.11. Fertilization analysis on the CDCA2 mutant fish line. Graph representing the total number of eggs laid/female (H), the fertility rate (I), and the mortality rate (J) after 1:1 crosses. For readability purposes, CDCA2^{+/+} = WT, CDCA2^{+/-} = HET, CDCA2^{-/-} = MUT. The subscript letter m stands for male and f for female. The coloured bar represents the mean and each dot represents a biological replicate. Mann-Whitney U test was used for the statistics.

4.3. Discussion

Studies in cells have shown that Repo-man/PP1 is essential for cell viability (Trinkle-Mulcahy et al., 2006). In this study, knockdown and overexpression of Repo-man led cells to apoptosis and cell death. Also, Repo-man has been linked to PP1-dependent regulation of DNA damage response, and that might be why it is upregulated in many types of cancer. Despite its studies in cells and its importance in cell cycle regulation, Repo-man has never been studied in any animal model. Therefore, in this chapter, we aimed to unravel the properties and function of CDCA2 (Repo-man orthologue) in vivo, using zebrafish as a model organism. As CDCA2 has been identified as a heterochromatin regulator (de Castro et al., 2017) and heterochromatin is established in early development through epigenetic processes, we ought to study this gene during the development of zebrafish.

The first objective was to analyse the expression levels of the gene and the protein at different stages of development. Gene expression experiments showed high levels of CDCA2 expression in the very early stages of development, and then a decrease in the expression from 24hpf, which is kept stable until at least 15dpf, the last stage analysed. However, it is important to remember that until the mid-blastula transition, about 4hpf, zebrafish do not start to transcribe their own genes, and therefore any gene expression detected before that stage corresponds to maternal transcripts. This does not mean that we should omit any gene expression detected at those stages, as it could be still critical for those early steps.

In order to localize where CDCA2 was being expressed, we performed in situ hybridization experiments in a whole zebrafish embryo and, as far as we could tell, identified that CDCA2 is expressed mainly in the brain area, except for the forebrain and pineal gland. Later stages were also tested (2 and 3dpf); however, at 2dpf the embryos start to develop pigment cells and the cells are more complicated to penetrate, making it more difficult to achieve a successful whole-mount in situ hybridization. Several trials were attempted, also using a positive control probe against the PCNA gene (Hu, Z., Holzschuh & Driever, 2015), although no signal was detected. This could be due to the low CDCA2 expression after 24hpf, although at this point this is just extrapolation.

Finally, the expression levels of CDCA2 were also analysed in zebrafish adult tissues. Surprisingly, CDCA2 expression is no longer focused on the brain, but rather on the reproductive tissues such as the ovaries and testis. This finding is in accordance to the fact that this protein is involved in the cell cycle and should be expressed in proliferative tissues, such as the gonads. Online databases like the Expression Atlas (EMBL-EBI, 2019), NCBI (NCBI, 2019) or Bgee (SIB, 2019) also report CDCA2 expression in testis and/or ovaries of adult humans, and in in the foetal brain, in accordance with our findings.

Following gene expression, the next step was to find a good antibody that could detect the zebrafish CDCA2 protein. As nobody has ever studied this protein in the zebrafish before, there are no commercial antibodies specifically designed to recognize the zebrafish protein. In the first attempt, we tested the anti-human CDCA2 antibodies available in our lab in an embryonic zebrafish cell line, PAC2. CDCA2 expression levels increase during anaphase, where it localizes to the chromatin. However, although some specificity was seen with both antibodies tested in regards of chromatin loading at anaphase, when I tested the antibodies in a whole zebrafish embryo and by western blot, specificity was very difficult to visualize. For these reasons, two new antibodies specifically targeting the zebrafish CDCA2 were developed by Eurogentec. Again, some specificity was gained over a negative control, but due to the 3D effect of a whole zebrafish embryo, it is difficult to differentiate between background and cells in other planes. Probably a good approach in this case would be to test the antibodies in zebrafish sections in order to remove the 3D component.

After characterizing the expression levels during development, we aimed to study the function of CDCA2 in vivo. The idea was to use two techniques: 1) knockdown of the protein by morpholino microinjection, and 2) knockout of the protein with a mutant line. However, microinjection is a laborious technique that requires high level of practice and precision, and in all the trials made, the mortality rate in all the conditions was too high to be able to conduct any analysis. For this reason, and due to being tight on time, all the efforts were focused on raising and analysing the mutant zebrafish line.

After raising the eggs received from ZIRC and genotyping them, adult heterozygous fish were cross to obtain a new generation with CDCA2^{WT}, CDCA2^{-/+} and CDCA2^{-/-}. As no major phenotype was observed by naked eye, and following gene expression, tissue and system ranks from the online databases mentioned earlier, we identified a few systems that could

potentially be affected by CDCA2 knockout and performed a few experiments comparing the three genotypes. In our conditions, CDCA2 knockout did not affect the heart or the growth of the zebrafish and, even though there seems to be a slight difference in the way they respond to the dark/light periods, the overall swimming performance, as judged by distance and speed, was not affected. Surprisingly, despite the high expression levels of CDCA2 in the ovaries and testis, the fertility of the mutant fish did not seem to be strongly affected. It is important to notice, though, that during the studies wild type fish were not able to produce and fertilize as many eggs as the other lines, making the analysis complicated and difficult to trust.

Nevertheless, the main question about this mutant fish line still remains unclear: does this mutation affect protein levels? The mutation was produced to generate a stop codon in the amino acid 16, and therefore protein levels should not be detectable in the mutant lines. As commented earlier, the lack of antibodies specific for the zebrafish protein make this question rather difficult to resolve. However, a western blot performed in embryos obtained from the second generation did not show any difference in any of the bands observed. However, the specificity and relevance of these bands cannot be guaranteed, and further experiments to either identify the specific band or prove protein decrease should be performed. Nonetheless, gene expression levels in the mutant lines are significantly decreased due to a phenomenon known as non-sense mediated decay, a pathway conserved among eukaryotes that eliminates mRNA containing premature stop codons.

In all the systems that have been analysed, CDCA2 protein levels follow its mRNA expression level thus making it plausible that in the homozygotes fish with reduced CDCA2 mRNA level, the protein will also be depleted.

However, organisms have ways to compensate for protein loss and there are several studies reporting lack of differences between mutants and gene knockdowns due to genetic compensation in the mutant lines (Rossi et al., 2015, El-Brolosy, Stainier, 2017, El-Brolosy et al., 2019). Therefore, it is critically important to be able to knockdown the protein at the first stages of development by morpholinos to discard any possible genetic compensation that might account for the no-phenotype in the mutant line. Another interesting approach would be to sequence the RNA from the wild type and mutated lines to be able to analyse if there is any genes that upregulate to compensate for the loss of CDCA2.

Any findings on this aspect are very important, as there are still no phenotypes associated with CDCA2 in any in vivo model. This is according to the Monarch Initiative, a bioinformatics web source focused on gathering information that relates genotypes with phenotypes (Monarch, 2019).

However, if it is really correct that an organism can survive in the absence of CDCA2, this knowledge will have important applications for human health. As CDCA2 overexpression has been linked to some types cancers (you need lots of references) and it has been shown that its depletion in these cancer cell lines leads to apoptosis, the clear demonstration that CDCA2 protein knockout might not have any potential harmful phenotype could point to the direction of using this protein as target for cancer therapies.

5. ROLE OF H2A.Z VARIANTS IN HETEROCHROMATIN REGULATION

5.1. Introduction

The importance of specific histones variants as a way of regulating gene expression during cell cycle progression has been known for a few decades. A well-known histone variant is H2A.Z, a highly conserved H2A-type variant with important roles during development and differentiation (Subramanian, Fields & Boyer, 2015). Although several studies have been conducted to assess the role of this variant, there is still a lot of uncertainty regarding the link between H2A.Z and gene transcription regulation, since different experimental data have linked it to both transcriptional repression and activity. H2A.Z is mainly localized at TSS and enhancers of active and silent genes, but its specific localisation within the gene, as well as its PTMs, seem to dictate its role on gene expression (Sura et al., 2017, Bargaje et al., 2012).

Several studies have shown a role of H2A.Z in heterochromatin establishment, and a link between H2A.Z and HP1 has been suggested in many organisms. For instance, in *Drosophila*, mutation of the H2AZ orthologue, *H2Av*, showed a reduction of the heterochromatic marks H3K9me2/3 and HP1 during development (Swaminathan, Baxter & Corces, 2005). In addition, H2Av was shown to interact with HP1, and the loss of this gene resulted in decreased HP1 binding at centromeres during mitosis, leading to defects on chromosome segregation and cell proliferation in *Drosophila* (Vernì, Cenci, 2015). Studies in mice showed that the expression of H2A.Z is switched on during development, it becomes enriched at pericentric heterochromatin (Rangasamy et al., 2003) but it is excluded from constitutive heterochromatin in differentiated cells (Sarcinella et al., 2007). HP1 α was found to preferentially interact with nucleosomes containing H2A.Z in vivo (Rangasamy, Greaves & Tremethick, 2004, Fan et al., 2004) and H2A.Z-depleted cells presented disrupted HP1 α binding in mouse cells (Rangasamy, Greaves & Tremethick, 2004, Fan et al., 2004). Recently, Ryan and Tremethick (Ryan, Tremethick, 2018), using nucleosome arrays, showed that H2A.Z is able to mimic the effect of H3K9me3 by enhancing HP1 α binding in vitro, possibly suggesting that H2A.Z is responsible for maintaining a proportion of HP1 α bound to pericentric heterochromatin during mitosis despite H3S10 phosphorylation.

Unpublished data obtained in our lab using a proteogenomic approach coupled to SILAC and Mass spectrometry to identify histone variants specifically enriched in chromatin capable of binding to HP1 α *in vitro*, has clearly identified the H2A.Z variant as one of the major features of such chromatin (**Figure 5.1. Histone variants enriched at HP1-bound chromatin regions. A)** Recombinant GST or GST:HP1 α or GST:SAP18 (a chromatin binding protein non-associated with HP1 used as control) were incubated with HeLa nucleosomes (see procedure in De Castro et al., 2017) labelled with heavy amino acids. The calibration input (I) was labelled with light amino acids in order to allow to calculate enrichment quantification by mass spectrometry. The yellow boxes indicate the regions from each pull down that were cut out and sent for mass spectrometry analyses together with the same region from the Light Input. M=Molecular weight marker; E= glutathione elution; U= unbound. **B)** Histones enrichment over GST for HP1 and SAP18. **C)** Comparison of the enrichment in the HP1 fraction over SAP18 (Figure 5.1). Another histone enriched on HP1 α -chromatin was H3.3, a marker for active chromatin. A study from van Steensel lab (de Wit et al., 2007) showed that although nonpericentric genes with low levels of HP1 showed strong enrichment of H3.3 along the entire transcription unit, pericentric genes with high HP1 levels presented an enrichment of H3.3 levels just upstream of the TSS. Also, the link between H2A.Z and H3.3 is well established and H3.3 has been shown to be colocalized with H2A.Z at active promoters and many other regulatory regions (Jin et al., 2009, Chen et al., 2013, Chen et al., 2014), which might explain the enrichment of H3.3 on HP1 α -chromatin.

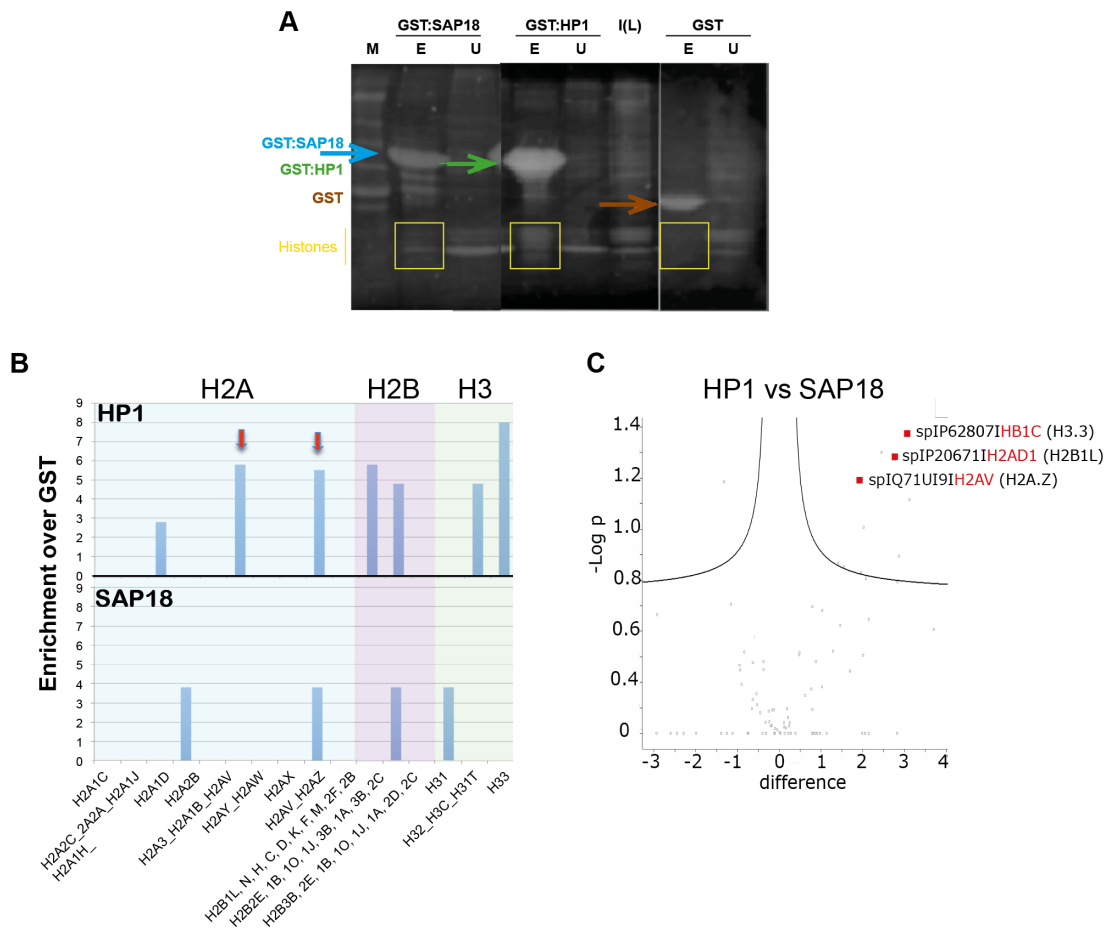


Figure 5.1. Histone variants enriched at HP1-bound chromatin regions. A) Recombinant GST or GST:HP1 α or GST:SAP18 (a chromatin binding protein non-associated with HP1 used as control) were incubated with HeLa nucleosomes (see procedure in De Castro et al., 2017) labelled with heavy amino acids. The calibration input (I) was labelled with light amino acids in order to allow to calculate enrichment quantification by mass spectrometry. The yellow boxes indicate the regions from each pull down that were cut out and sent for mass spectrometry analyses together with the same region from the Light Input. M=Molecular weight marker; E= glutathione elution; U= unbound. **B)** Histones enrichment over GST for HP1 and SAP18. **C)** Comparison of the enrichment in the HP1 fraction over SAP18.

In vertebrates, H2A.Z is present as two variants: H2A.Z.1 (encoded by the *H2AFZ* gene) and H2A.Z.2 (encoded by the *H2AFV* gene). They only differ in three amino acids, they are distributed similarly around the nucleus and they are subjected to the same PTMs. However, they present some differences in their 3D structures, genome localization and tissue distribution (Dryhurst et al., 2009, Horikoshi et al., 2013). Although some studies have been conducted in the attempt of analysing possible distinct roles for H2A.Z.1 and H2A.Z.2 (Faast et al., 2001, Matsuda et al., 2010, Dunn et al., 2017, Dryhurst et al., 2009) and seem to indicate that the two isoforms have different properties, the majority of the research on H2A.Z still does not distinguish between the two variants. In particular there are no clear studies evaluating their distinct roles during cell cycle and chromatin organisation.

Certainly, many of the discrepancies found on transcriptional regulation might be clarified by distinguishing between the two variants, and it will clearly direct us to a better understanding of epigenetic regulation. H2A.Z overexpression has been observed in many cancers; therefore, unravelling the specific individual functions will also be critical if we can consider the possibility of H2A.Z as target for cancer therapy. By knowing which variant is involved and its specific role will surely help in optimising drug efficiency. In this chapter, I aimed to analyse the individual roles of H2A.Z.1 and H2A.Z.2, if any, on several aspects of heterochromatin regulation and cell cycle progression.

5.2. Results

5.2.1. H2A.Z.1 and H2A.Z.2 knockdown

In order to knockdown each H2A.Z variants independently, two siRNA (from Sigma Aldrich, Table 2-1) targeting different regions of each H2A.Z variant were used. The HeLa GFP:HP1 α cell line was transfected with the JetPrime[®] reagent for 72h with each siRNAs and the H2A.Z.1 or H2A.Z.2 gene expression levels were analysed by quantitative PCR (qPCR) (Figure 5.2.A,B). In each case, only one of the siRNA used was able to significantly knockdown the gene of interest (siRNA2 for H2A.Z.1 and siRNA1 for H2AZ.2) therefore these SiRNAs were chosen for the rest of the experiments designed to analyse individual histone variant function. In order to prove that the siRNAs were specific for each histone variant, the cDNA was re-analysed by qPCR using primers for both H2A.Z variants; both siRNAs were indeed specific for each H2A.Z variant (Figure 5.2.C). These results were later confirmed with the RNA sequencing data (Figure 5.2.D), explained later. All the data taken together clearly demonstrate that I can significantly reduce the mRNA level of each variant without affecting the expression of the other.

In order to test that the siRNA knockdown was also efficient at protein level, I analysed the siRNA-treated cells by western blot. Unfortunately, there are not known commercial antibodies specific for each variant. I first used an H2A.Z antibody that was already available in the lab (CST, 2718). However, in the data sheet, there was neither specification regarding which H2A.Z variant this antibody recognizes nor information about the antigen used. The results suggest that this antibody preferentially recognizes variant H2A.Z.1; in fact, in H2A.Z.1-depleted cells, where H2A.Z.2 remains expressed, no band is identified. On the contrary, in H2A.Z.2-depleted cells, where H2A.Z.1 is still expressed, a band at 17KDa is observed (Figure 5.2.E). This band is fainter than the one in the control sample, which might indicate that H2A.Z.1 is also slightly downregulated in H2A.Z.2-depleted cells, as seen in the qPCR analysis as well, although the difference seems not to be significant. I later acquired another antibody that should recognize specifically H2A.Z.2, although at the conditions

tested, the antibody did not work. These results seem to indicate that there is a decrease also at protein level but also point toward the need of generating more specific antibodies for the community to conduct further studies.

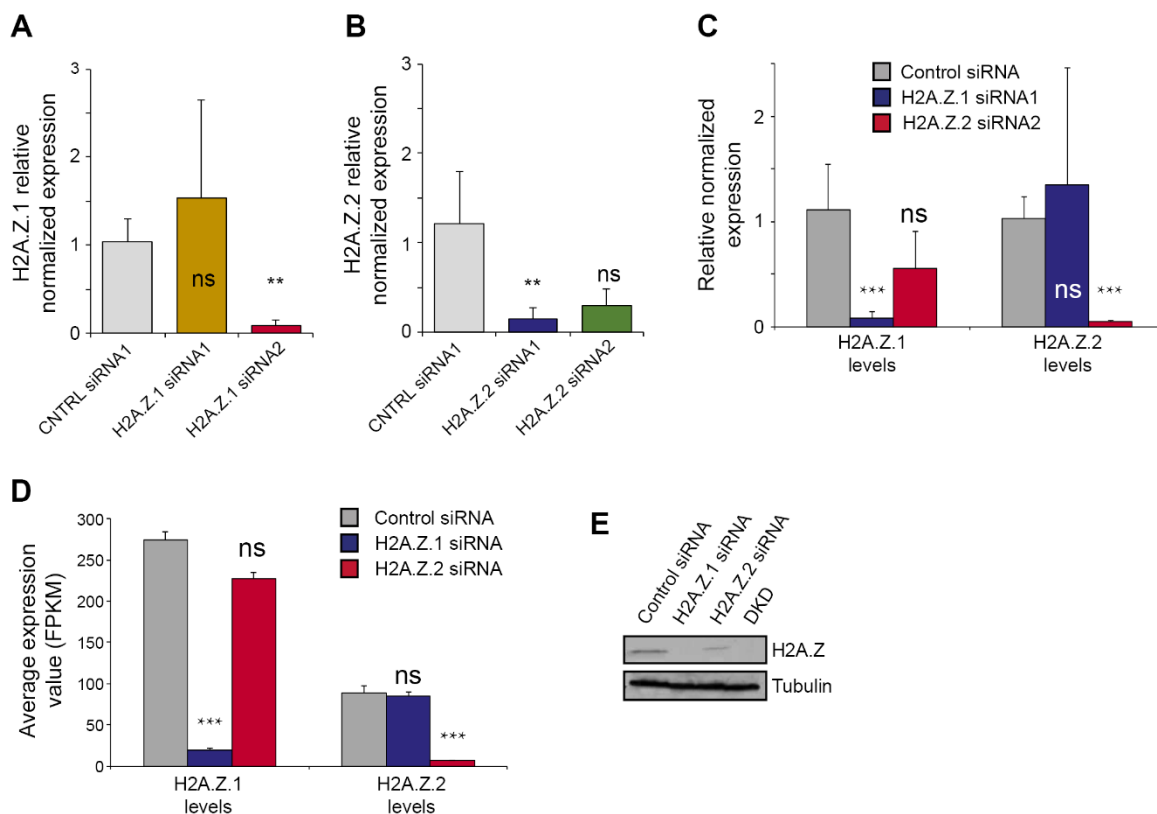


Figure 5.2. Validation of the H2A.Z siRNA-mediated knockdowns. The knockdown efficiencies for siRNA targeting either H2A.Z.1 or H2A.Z.2 were examined in HeLa GFP:HP1 cells. **A)** Expression levels of H2A.Z.1 after transfection with two different oligonucleotides against H2A.Z.1 (H2A.Z.1 SiRNA1 and H2A.Z.1 SiRNA2). Error bars indicate standard deviation between three biological replicates. **B)** Expression levels of H2A.Z.2 after transfection with two different oligonucleotides against H2A.Z.2 (H2A.Z.2 SiRNA1 and H2A.Z.2 SiRNA2). Error bars indicate standard deviation between three biological replicates. **C)** Expression levels of H2A.Z.1 and H2A.Z.2 after transfection with the siRNA from A and B, in order to check for variant specificity. Error bars indicate standard deviation between three biological replicates. **D)** Average expression value of the two variants in H2A.Z.1 and H2A.Z.2-depleted HeLa GFP:HP1 α cells after RNA sequencing analysis (FPKM: Fragments Per Kilobase Million). Error bars indicate standard deviation between three biological replicates. Student t test was used for the statistical analyses. **E)** H2A.Z protein expression of the individual and double (DKD) knockdowns. Anti-tubulin antibody was used as a reference.

5.2.2. Analyses of the effect of H2A.Z.1 or H2A.Z.2 depletion on HP1 α localisation

In order to analyse the effect of H2A.Z.1 and H2A.Z.2 individually on heterochromatin maintenance, I first analysed the HP1 α localization in the HeLa GFP:HP1 α cell line upon knockdown of H2A.Z.1 and H2A.Z.2. Depletion of H2A.Z.2 but not of H2A.Z.1 decreased the number of HP1 α foci in the interphase nuclei (Figure 5.3.A,B). In order to prove that this effect on HP1 was not due to an off-target effect of the siRNA, I have conducted rescue experiments using an oligo-resistant RFP:H2A.Z.2 plasmid. However, the usual set up for a rescue experiment (1 μ g of DNA) was highly toxic for the cells (Figure 5.4) and the conditions needed to be adjusted to determine a non-toxic concentration to use for the rescue experiment. In this condition, the number of HP1 α foci was not rescued by the overexpression of an oligo-resistant RFP:H2A.Z.2 plasmid (Figure 5.3.C). These results could mean that the HP1 mislocalisation is an off-target effect of the siRNA but it might also be that the concentration used or the timing of expression was not sufficient to rescue the HP1 α foci. It could also be that H2A.Z.2 overexpression results in the same phenotype, with altered HP1 α distribution, and the rescue conditions should be optimized. In order to confirm the results, I used another siRNA targeting H2A.Z.2 and obtained the same phenotype as in the previous siRNA used

As HP1 foci reform in G1 after each cell division, a block in early G1 could have an indirect effect on the foci formation. To discard a possible defect caused by an impaired cell cycle progression, I performed fluorescence-activated cell sorting (FACS) analysis on both H2A.Z.1 and H2A.Z.2 depleted cells. Although H2A.Z.2-depleted cells did not present any cell-cycle difference compared to the control, H2A.Z.1-depleted cells showed a significant increase of cells in G1 phase followed by a decrease of S phase cells, indicating a possible defect on cell cycle progression (Figure 5.5. A-D). I corroborated this phenotype by analysing the percentage of mitotic cells in each knockdown condition. Although both knockdowns showed a decrease in the number of mitotic cells, it was considerably more significant in the case of H2A.Z.1-depleted cells (Figure 5.5.E).

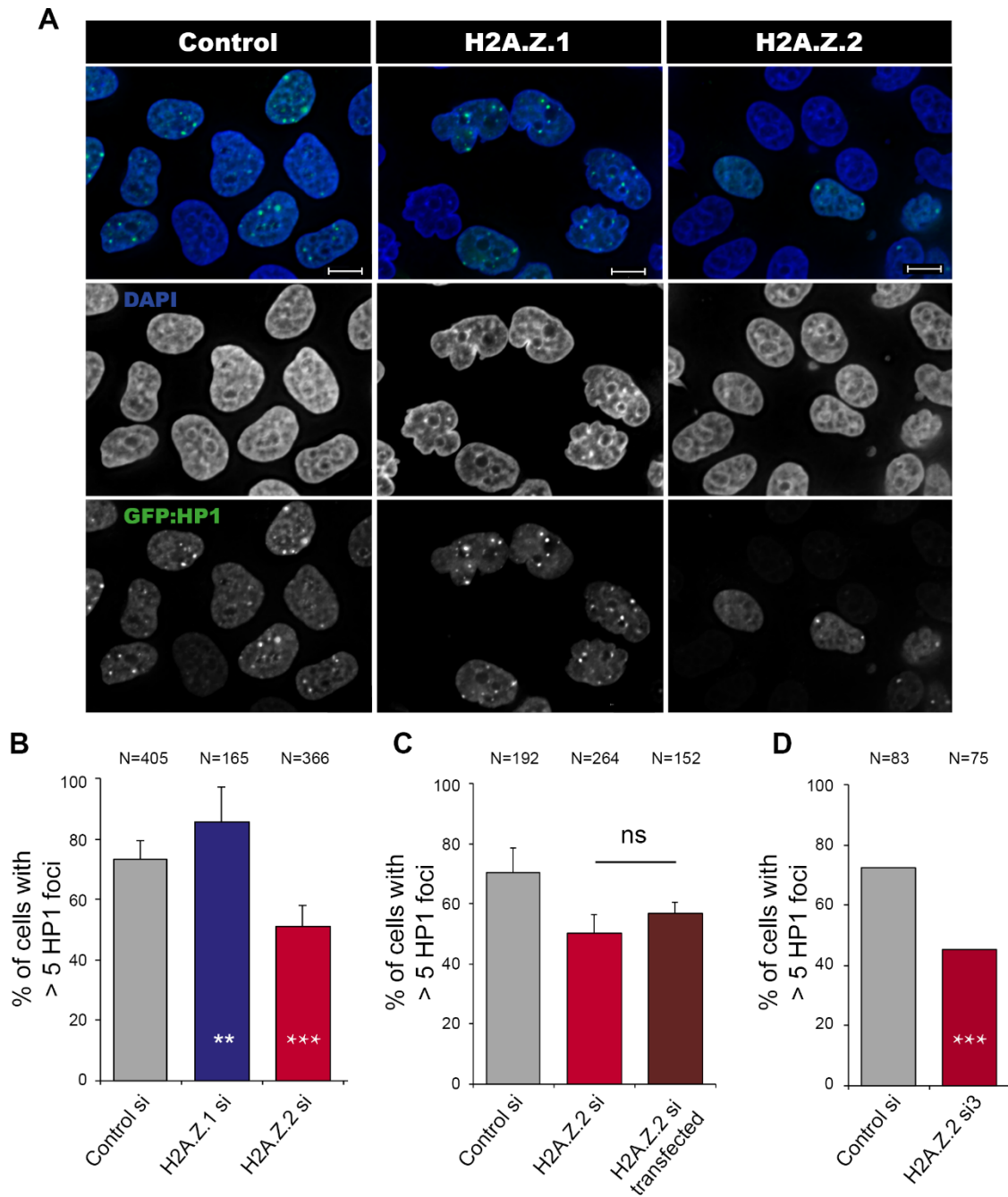


Figure 5.3. H2A.Z.2, but not H2A.Z.1, is possibly involved in heterochromatin maintenance. **A)** HeLa GFP:HP1 were transfected for 72h with a control siRNA and the successful siRNA against H2A.Z.1 or H2A.Z.2. Scale bar: 10 μ m. **B)** Quantification of the number of cells presenting more than five HP1 foci from experiment in A. Four replicates were analysed for the statistical test (chi square). **C)** HeLa GFP:HP1 cells treated with H2A.Z.2 siRNA were transfected with a RFP:H2A.Z.2.1 plasmid resistant to the siRNA and the HP1 foci were analysed as in B. Three replicates were analysed for the statistical test (chi square). Error bars indicate standard deviation. **D)** HeLa GFP:HP1 were transfected with another H2A.Z.2 siRNA (si3) and the HP1 foci were analysed. N: the total number of cells analysed.

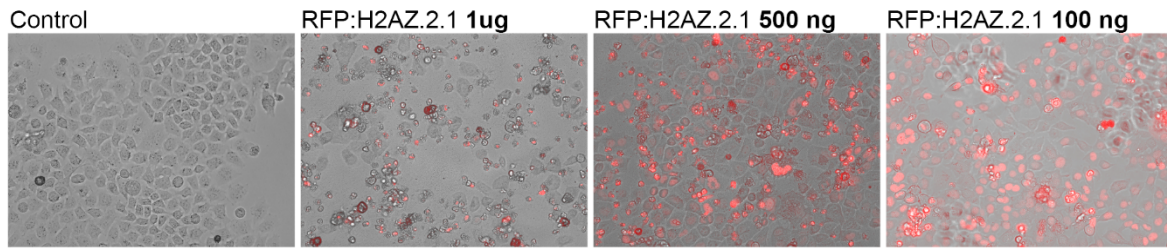


Figure 5.4. Overexpression of H2A.Z.2.1 is toxic for the cells. Starting from left to right, HeLa GFP:HP1 α cells were transfected with a control siRNA, and decreasing concentrations of RFP:H2A.Z.2.1 (1 μ g, 500ng and 100ng) to determine a non-toxic concentration to use for the rescue experiment. Phase contrast (grey) and fluorescence representative images of the transfection. Red cells indicate transfection of the RFP:H2A.Z.2.1 plasmid.

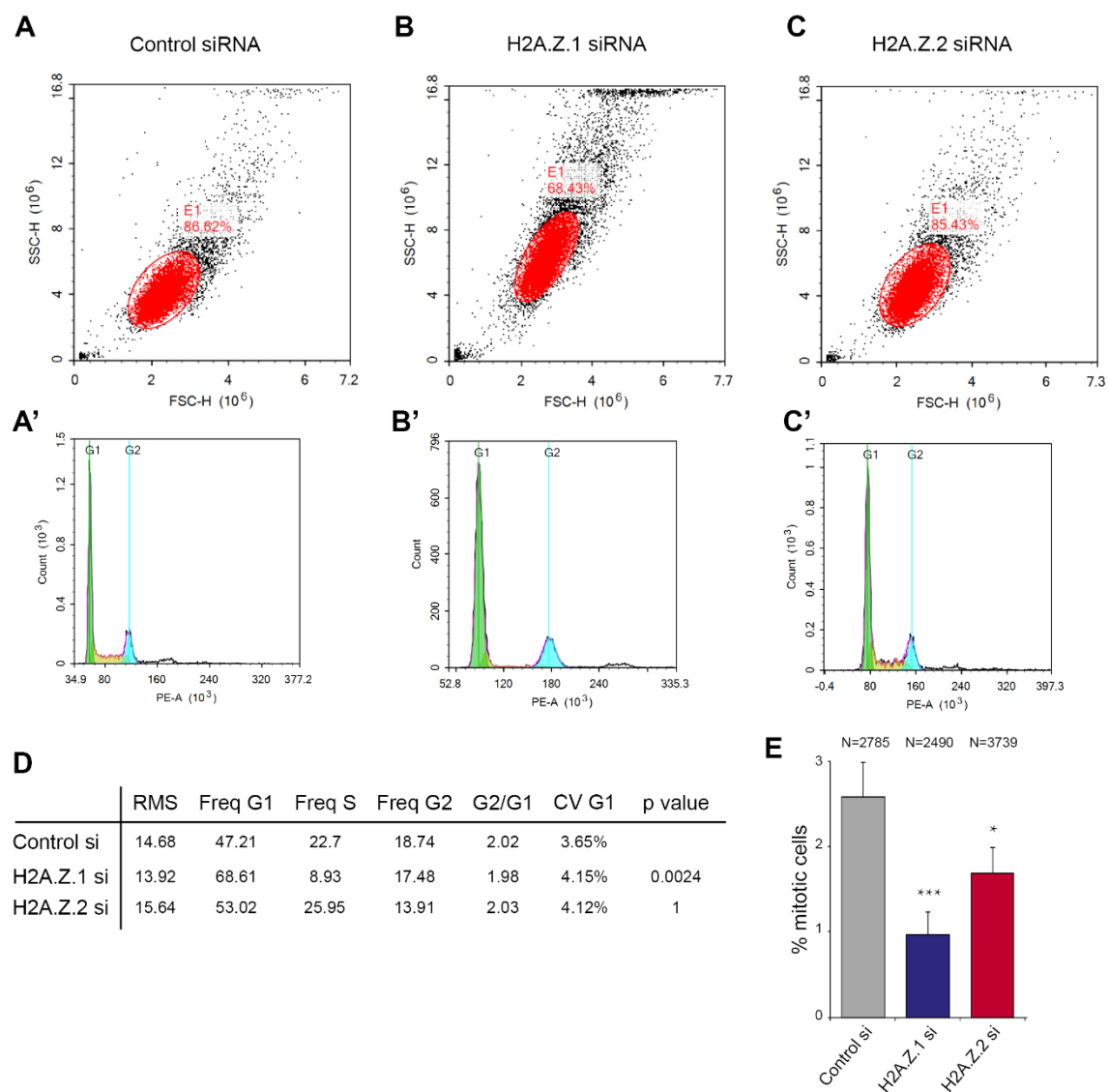


Figure 5.5. Cell cycle progression on H2A.Z knockdowns. HeLa cells transfected with either a control siRNA (**A**), H2A.Z.1 siRNA (**B**) or H2A.Z.2 siRNA (**C**) were analysed by flow cytometry. **D**) The frequency of cells on each cell cycle phase was recorded as an average of two experiments and presented on a table. Two replicates were counted for the statistical analyses (t test). **E**) The cells were analysed on a microscope and the number of cells in mitosis was counted and represented as a percentage of the total number of cells (mitotic index). Statistical analysis (chi square) from the result of three independent biological replicates. Error bars indicate standard deviation between three replicates. N: the total number of cells analysed.

5.2.3. Role of H2A.Z.1 and H2A.Z.2 on chromosome segregation

Published work has linked H2A.Z to chromosome segregation fidelity in yeast (Yamamoto et al., 2019) and in mammalian cells (Rangasamy et al., 2004). I therefore wanted to analyse this parameter in the individual isoforms knockdown to see if any or both isoforms were important for this aspect of cell division. A very prominent feature of the H2A.Z.2-depleted cells was the presence of micronuclei (MN) (Figure 5.6.A), small nuclei formed when a chromosome or a fragment of a chromosome fails to be incorporated into the main cell nuclei after mitosis. The most common cause of MN formation is the presence of chromatin bridges or lagging chromosomes clearly visible during anaphase (Utani et al., 2010) (Figure 5.6.B); thus, I counted both the percentage of anaphases with chromatin bridges and the total of cells with MN. H2A.Z.2 siRNA transfection led to an increase in the number of chromosome bridges and MN (Figure 5.6.C,D) compared to the control. To prove that this phenotype was actually due to a decrease of H2A.Z.2, I co-transfected the cells with an oligo-resistant H2A.Z.2.1 and H2A.Z.2.2 plasmid. Both H2A.Z.2 isoforms were able to rescue the MN phenotype (Figure 5.6.E), indicating that the formation of MN is due to a depletion of H2A.Z.2. In this case, the phenotype was more pronounced than in the case of HP1, which might explain why in this case the plasmids were able to rescue the phenotype. The presence of MN could be the result of either chromosome mis-segregation or DNA damage that results in double-strand breaks (DSB) and the production of chromosome fragments. In order to understand the most possible cause of this phenotype, I have analysed the progression through mitosis and the nature of the MN.

It has been shown that mitotic delays are often associated with chromosome segregation errors (Daum et al., 2011, Worrall et al., 2018) that might ultimately lead to the formation of MN. Although I did not observe an increased mitotic index that could indicate a delay in progressing through mitosis, I wanted to evaluate if, within the mitotic population, there was an aberrant distribution of mitotic phases. I therefore counted the percentage of cells at each stage of mitosis. Although there was a slight increase of the number of cells in anaphase, this difference was not significant, indicating that mitotic progression is not altered upon H2A.Z knockdown and cannot account for the chromosome segregation errors observed (Figure 5.7.A). However, a compromised Spindle Assembly Checkpoint (SAC) could

also be compatible with a lack of mitotic arrest and a progression through mitosis even in the presence of incorrect chromosome attachments.

In order to analyse whether the lagging chromatin and MN were due to missegregation errors, I used a stable cell line that expresses YFP:CENP-A. CENP-A is a histone H3 variant present at the centromeres that has been shown to be important for kinetochore assembly and chromosome segregation (Régnier et al., 2005, Allshire, Karpen, 2008, Catania, Pidoux & Allshire, 2015). I depleted H2A.Z.2 in this cell line and analysed the presence of CENP-A in the lagging chromosomes and the MN. As seen in Figure 5.7.B, the majority of the MN have a CENP-A signal indicating that they possibly contain chromosomes rather than DNA fragments. Some MN presents a single CENP-A signal (indicating the presence of only one sister chromatid), some present two CENP-A signals (indicating both sister chromatids are missegregated), and some have no signal (indicating some sort of DNA damage). It would be interesting to quantify exactly the percentage of MN with each CENP-A signal in order to extract more accurate conclusions. I have also analysed the mitotic figures where only few chromosomes were mis-aligned. In this case there are both chromosomes with two CENP-A signals and also single chromatids (with a single CENP-A signal) as sister chromatid separation had occur prematurely. This phenomenon of asynchronous chromatid separation is known as cohesion fatigue, and the balance between pulling microtubule forces and interchromatid cohesion plays a critical role. In order to address this, I have also analysed chromosome spreads and noticed that in some H2A.Z.2-depleted cells, sister chromatids are already separated (Figure 5.7.C) similarly to the depletion of cohesin. This indicates that in H2A.Z.2-depleted cohesion is not maintained, leading to premature chromosome segregation and consequently misaligned chromatin and MN formation.

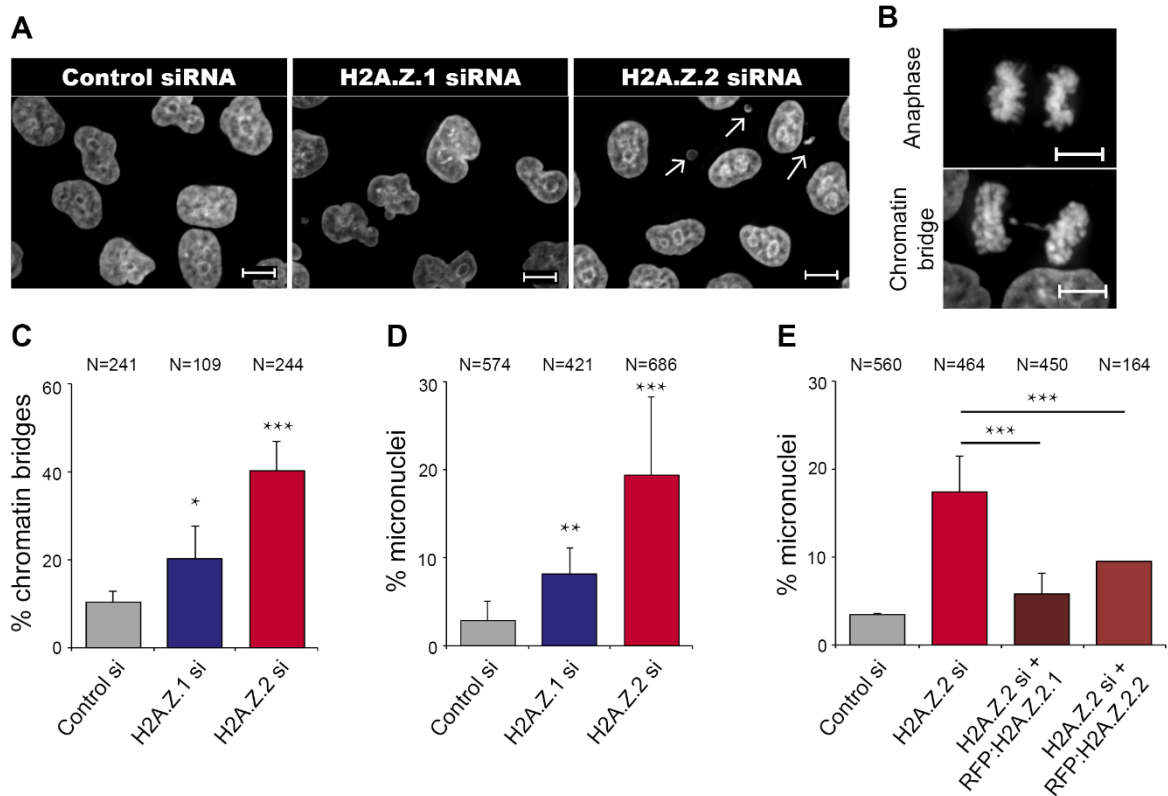


Figure 5.6. H2A.Z.2 knockdown leads to chromosome segregation defects. A) Image of HeLa cells depleted of H2A.Z.1 and H2A.Z.2 showing the presence of micronuclei (white arrows). Scale bar: 10 μ m. **B)** Example of a normal anaphase (top panel) and a chromatin bridge (lower panel). Scale bar: 10 μ m **C)** Graph showing the number of chromatin bridges on anaphase cells (as in B lower panel) over the total number of anaphases from experiment A. **D)** Graph showing the percentage of cells with MN over total number of cells from experiment A. **E)** Percentage of cell with MN over total number of cells in H2A.Z.2-depleted cells after rescue with RFP:H2A.Z.2.1 or RFP:H2A.Z.2.2. Error bars show standard deviation. Chi square statistical test between three replicates (except rescue with RFP:H2A.Z.2.2, where only one replicate was analysed). N: total number of cells analysed.

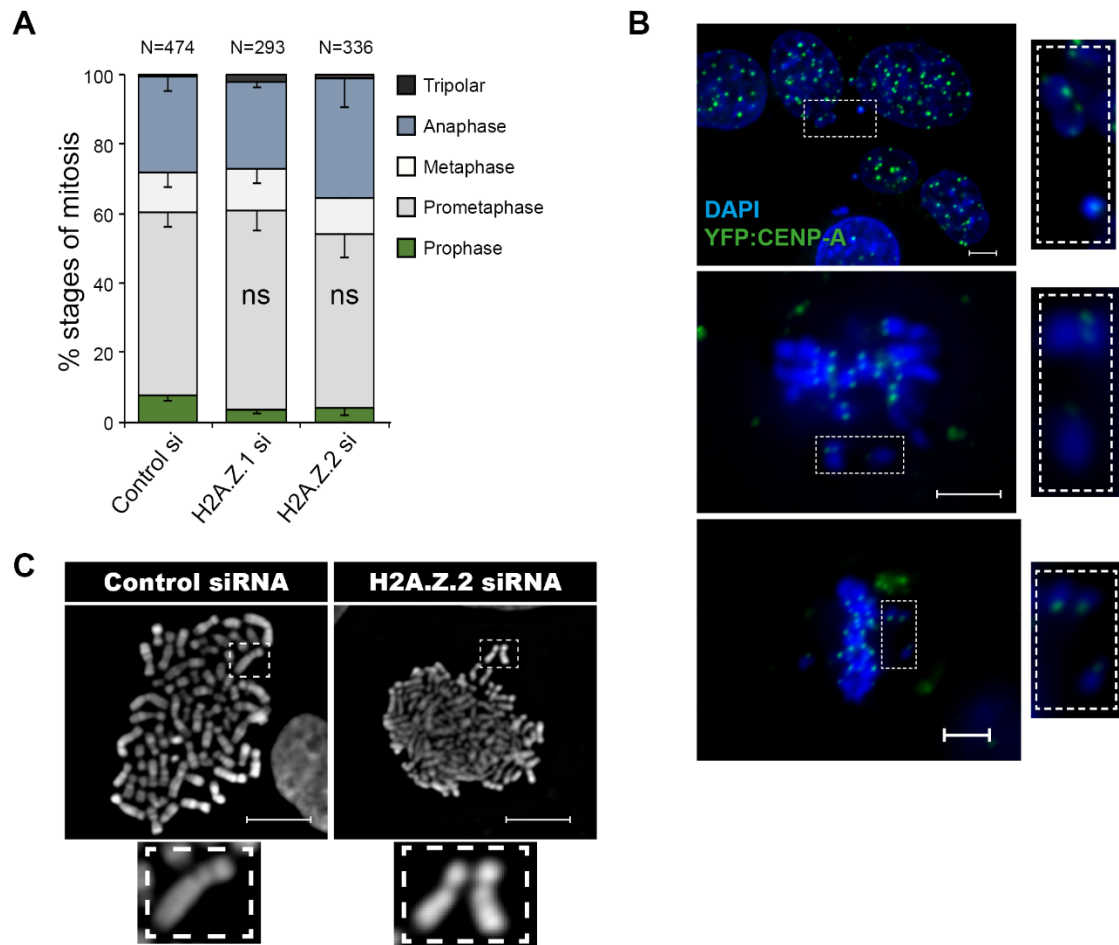


Figure 5.7. H2A.Z.2 knockdown results in cohesin impairment. **A)** Percentage of cells on each stage of mitosis over the total of cells in mitosis. N: total number of cells analysed. **B)** HeLa YFP:CENP-A cells were transfected with H2A.Z.2 siRNA and the presence of CENP-A in lagging chromosomes and in MN was observed. Scale bar: 5 μ m. **C)** Chromosome spreads from HeLa cells treated with control or H2A.Z.2 siRNA. At the bottom, amplification of an example of a joined pair of sister chromatids (left) and separated sister chromatids (right, after H2A.Z.2 siRNA transfection). Scale bar: 5 μ m

5.2.4. H2A.Z.2.1 regulates nuclear morphology

During the analyses of the H2A.Z siRNA, I observed prominent defects in nuclear shape in H2A.Z.1-depleted cells, therefore I analysed the circularity of the nuclei. This phenotype was highly significant and only associated with H2A.Z.1-knockdown cells, but not with H2A.Z.2-depleted cells (Figure 5.8.A). The nuclear circularity was fully rescued by co-transfection with a siRNA-resistant H2A.Z.1:GFP plasmid (Figure 5.8.B), indicating that it is a real phenotype due to the depletion of the histone variant H2A.Z.1. As the nuclear lamina and the nuclear pore complexes (NPCs) play crucial roles in determining the nuclear shape, I also wanted to analyse if these Nuclear Envelope components presented defects. I therefore stained the cells with lamina A/C and mAb414 (an antibody that recognizes a set of NPC proteins) antibody, although none of them seemed to be affected by H2A.Z.1 depletion (Figure 5.8.C,D).

A defect in morphology could also be caused by a compromised heterochromatin organisation present at the nuclear periphery. I therefore set out to analyse the effect of H2A.Z depletion on chromatin using several epigenetic markers as readouts.

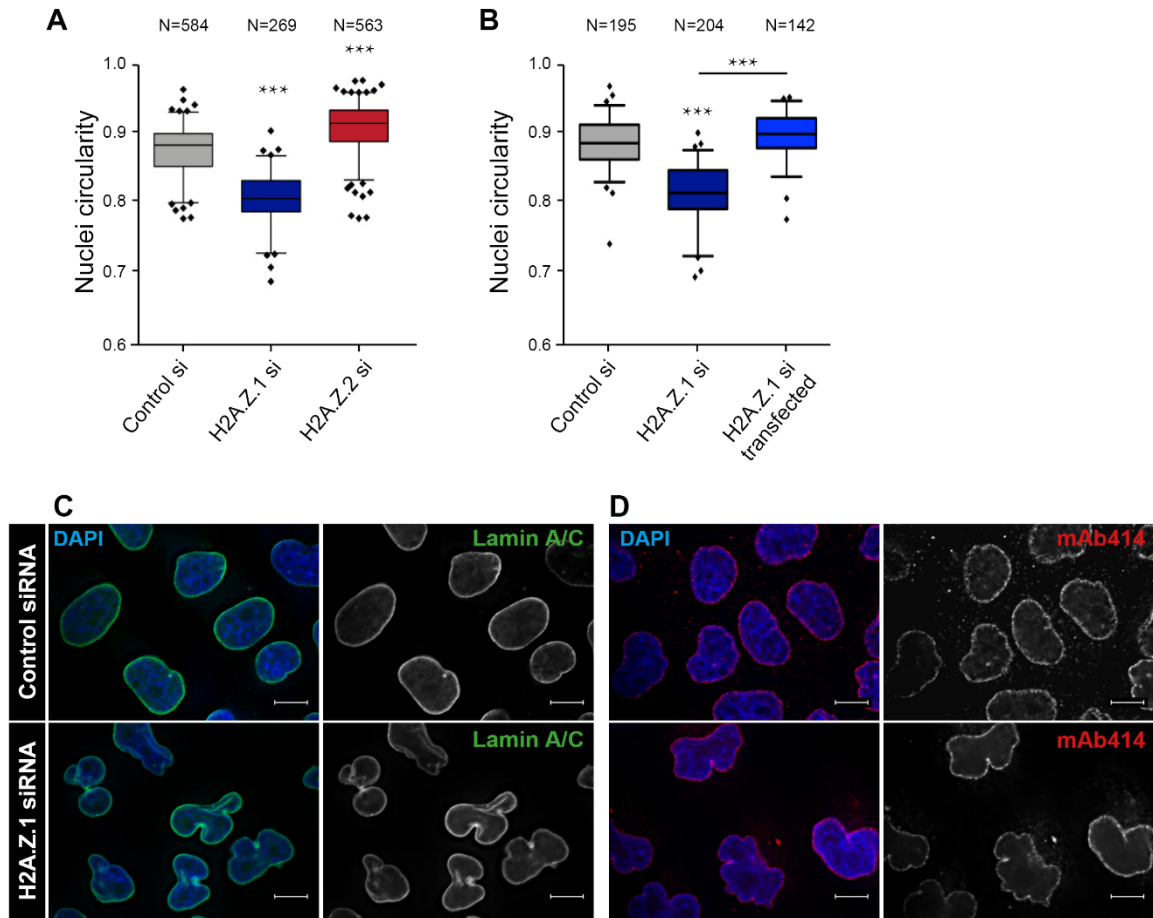


Figure 5.8. H2A.Z.1 knockdown results in aberrant nuclear shape. A) Nuclear circularity from cells transfected with H2A.Z.1 and H2A.Z.2 siRNA was analysed using the Nikon software ElementAS. **B)** The circularity from HeLa H2A.Z.1-depleted cells were rescued with an H2A.Z.1si-resistant plasmid. For both A and B, Mann-Whitney U test was used for the statistical analysis between three biological replicates. N: the total number of cells analysed. **C,D)** HeLa cells were transfected with control or H2A.Z.1 siRNA for 72h and stained for Lamin A/C (**C**) or a subset of nuclear pore complexes (mAb414) (**D**). Scale bar: 10µm

5.2.5. H2A.Z depletion compromises the repressive chromatin landscape

In order to study the chromatin landscape upon H2A.Z depletion, I treated HeLa cells with each H2A.Z isoforms siRNA and stained for well-known heterochromatin markers: H3K9me3 and H3K27me2/3. H3K9me3 acts as an anchoring site for HP1 α , thus I wondered whether H3K9me3 levels were also disrupted upon H2A.Z.2 depletion. In fact, this seems to be the case: H3K9me3 levels are significantly decreased in H2A.Z.2-depleted cells (Figure 5.9.A,B) but not in H2A.Z.1 siRNA. Although a Western Blot should have been performed to confirm the results, this observation could suggest that H2A.Z.2 incorporation in some chromatin sites is upstream of the H3K9me3 modification, or that H2A.Z.2 might stabilize the H3K9me3 mark on specific chromatin areas.

As H3K9me3 accumulates at the nuclear periphery (NP), we analysed whether its distribution around the nucleus was also impaired. However, I did not observe any changes in the enrichment of H3K9me3 around the NP in either variant siRNA, indicating that H3K9me3 distribution around the nucleus remains intact (Figure 5.9.C). This observation also rules out that the defect in nuclear morphology observed in H2A.Z.1 siRNA could be caused by a defect in the lamina-associated heterochromatin distribution. I also analysed the levels of H3K27me2/3, another heterochromatin marker. Surprisingly, H3K27me2/3 levels seem to increase upon depletion of either H2A.Z.1 or H2A.Z.2 (Figure 5.9.D), indicating that H2A.Z variants affect the chromatin landscape in different ways.

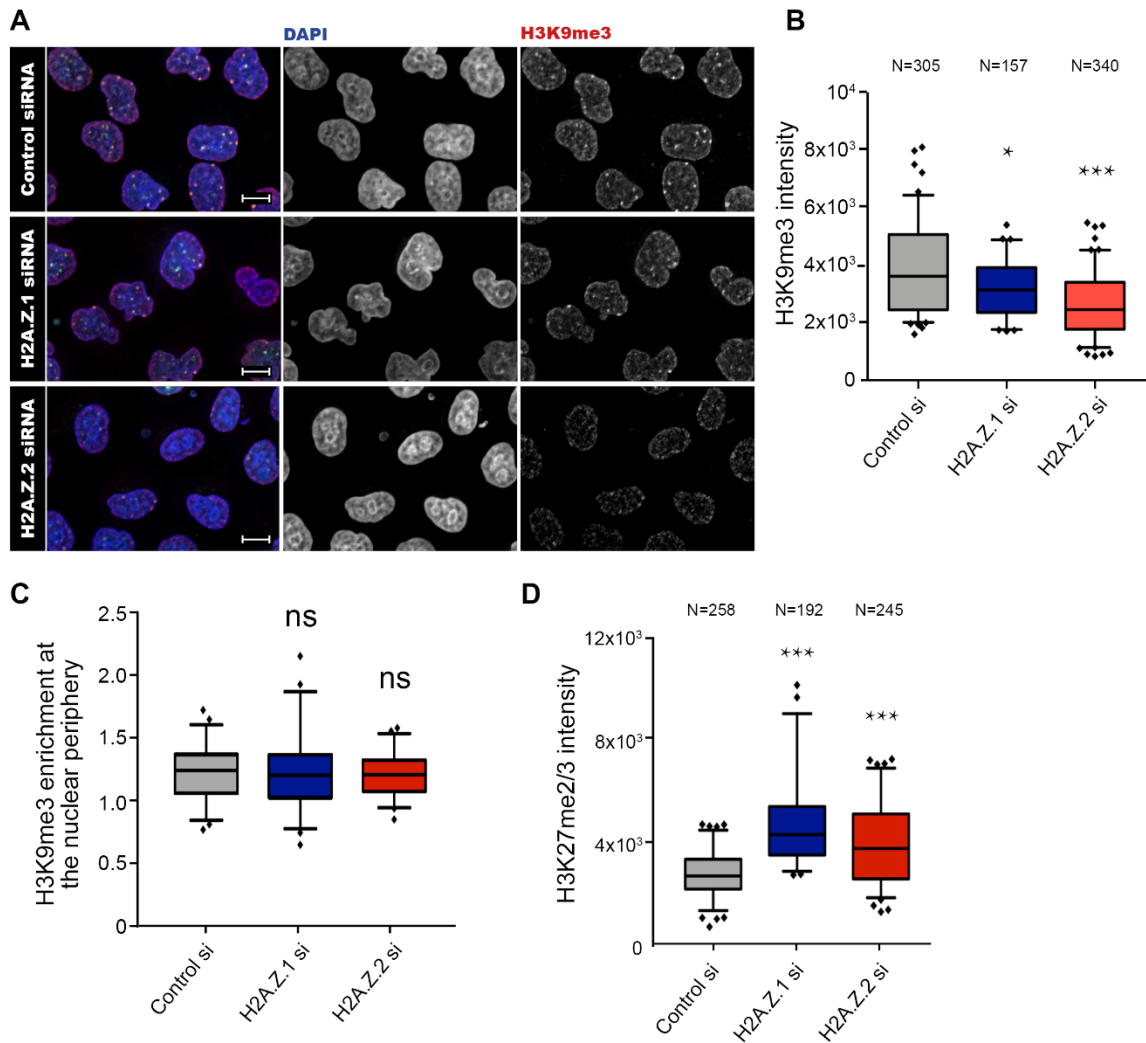


Figure 5.9. H2A.Z.1 and H2A.Z.2 have different effects on repressive chromatin. **A)** HeLa GFP:HP1 cells were transfected with H2A.Z.1 or H2A.Z.2 siRNA and stained for H3K9me3. **B)** Graph showing the intensity cy3 signal (H3K9me3) from cells in A obtained using the Nikon software ElementAS. **C)** Graph showing the enrichment of H3K9me3 intensity at the nuclear periphery. **D)** HeLa GFP:HP1 α were transfected as in A and stained for H3K27me2/3 and the intensity signals were measured as in B. Error bars represent standard deviation. Four replicates were counted for each statistical test (Mann-Whitney U test). N: the total number of cells analysed.

5.2.1. Distinct roles of the H2A.Z.1 and H2A.Z.2 variants on gene expression

From what we have learned so far, the two variants seem to have distinct roles in organising chromatin structure and function. However, some reports (Dryhurst et al., 2009) claim that their distribution in the genome is very similar. Therefore, I wanted to ask the question if their down-regulation could have different outcomes in the transcriptional programme. In order to analyse the effect on gene expression caused by depletion of each H2A.Z variant, HeLa cells were transfected with the siRNAs against H2A.Z.1 or H2A.Z.2 individually and in parallel with a control siRNA; the RNA was extracted and then sent to sequence. Three biological replicates were used.

The first analyses of the correlation between the three biological replicates detected a very low correlation coefficient (R value) between some replicates (Figure 5.10). However, a more careful analysis of the data revealed that there were three genes that appear to have an abnormal high value. These genes (MIR4767 in control 1, MT-TL1 in Control and H2A.Z.2si 2, and SNORD100 in control 3) were then removed from the analysis and the correlation was re-assessed. This time, the three biological replicates had a high correlation coefficient (Figure 5.11).

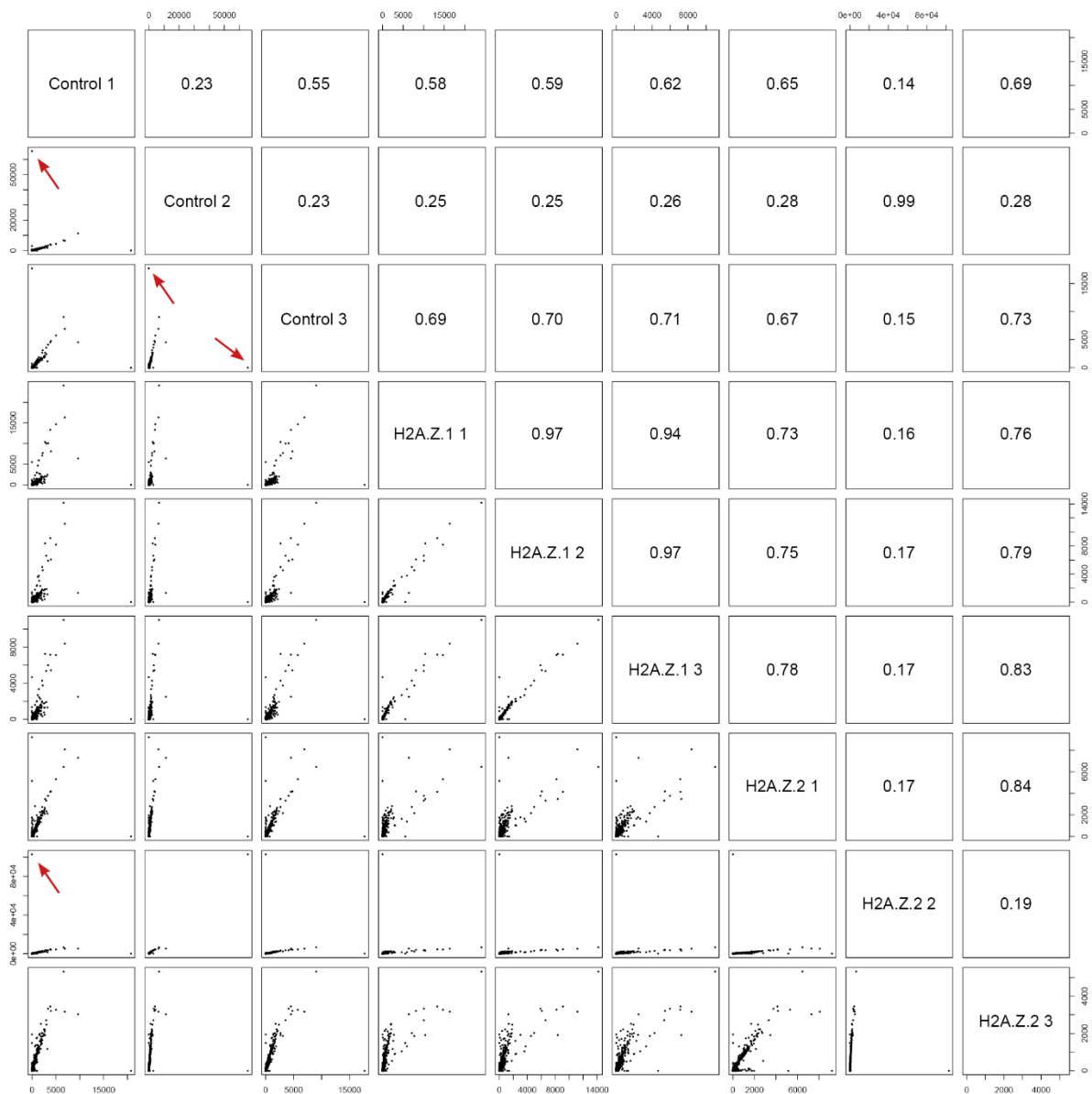


Figure 5.10. Biological replicates present low correlation coefficient. HeLa cells were transfected with a control H2A.Z.1 and H2A.Z.2 siRNA and the RNA was sent to sequence. **A)** Analysis of the correlation between samples. The numbers represent the R coefficient. Red arrows point at the extremely high values that were removed.

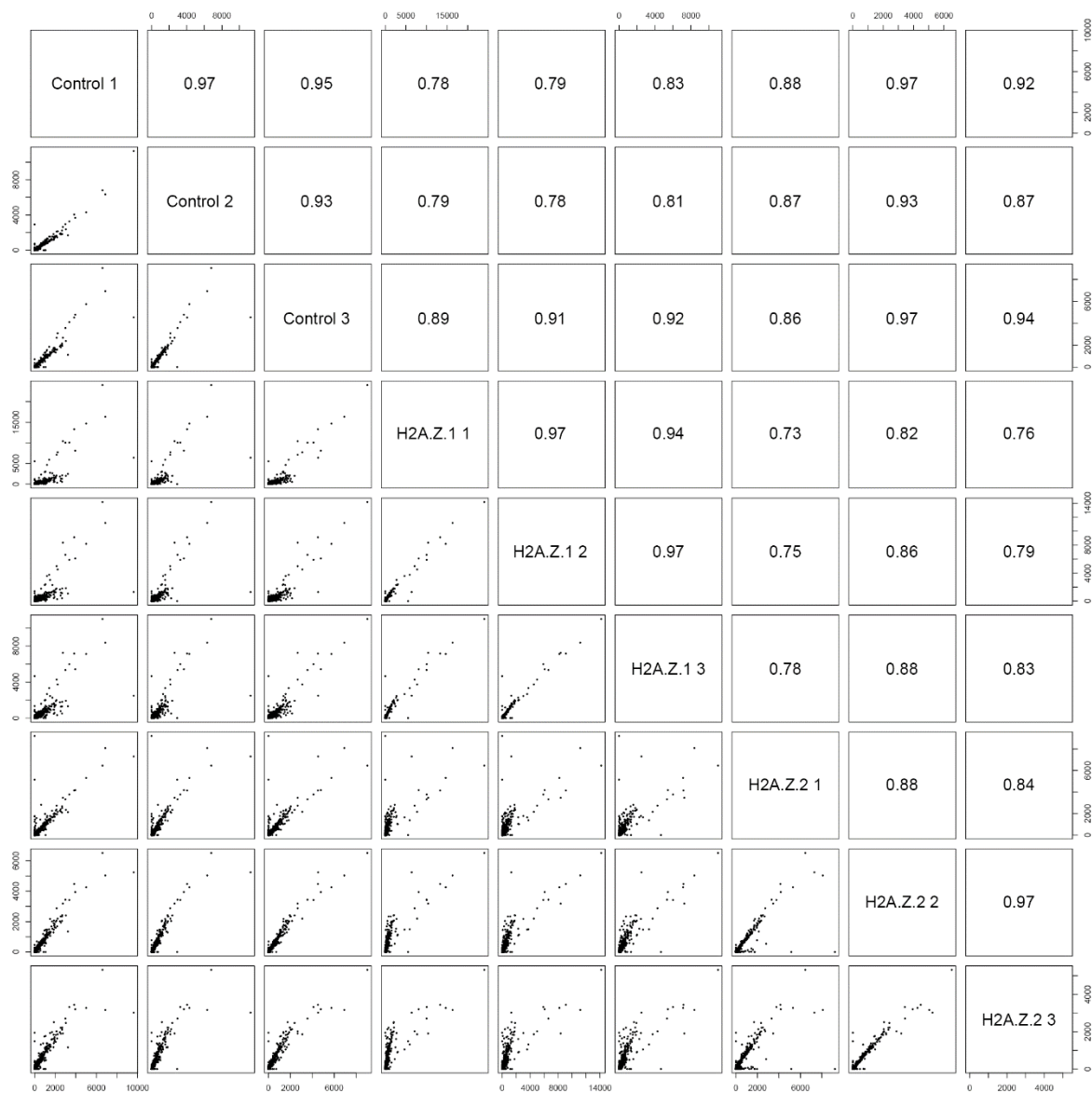


Figure 5.11. Correlation between replicates after removing outliers. The graph shows the correlation coefficient (R) values between samples after removing the three aberrantly high values.

The data obtained shows a clear difference on the gene expression pattern between the variants. I first analysed the number of up/downregulated genes in each conditions and their overlap in the two variants knockdown (Figure 5.12.A,B). Upon H2A.Z.1 depletion, 150 genes are downregulated ($p < 0.01$) and 109 genes are upregulated, whereas in H2A.Z.2-depleted cells 92 genes are downregulated and 122 upregulated. Among the downregulated genes, only 5 are found in both H2A.Z.1 and H2A.Z.2 depleted cells, while among the upregulates genes, only 13 are shared between the variants. This clearly shows a huge difference on gene expression regulation between the variants. Using a STRING analysis, I found a high protein-protein interaction (PPI) enrichment ($p = 10^{-16}$) on the downregulated genes of H2A.Z.1 depleted cells. Most of these genes were associated with gene ontologies (GO) associated with cell division and mitosis (Figure 5.12. C,D). This analysis strongly corroborate my data on a cell G1 cycle delay, suggesting a role of H2A.Z.1 in cell cycle regulation.

Using the RNAseq data, I also analysed if the down-regulated gene were clustered on specific chromosomes. I calculated the frequency of genes on each chromosome (gene density, in grey) and the frequency of altered genes for each chromosome (Figure 5.12.E). The data suggests that chromosomes 1 ($p < 0.05$), 9 ($p < 0.05$), and 17 ($p < 0.05$) are more affected by H2A.Z depletion than the other chromosomes.

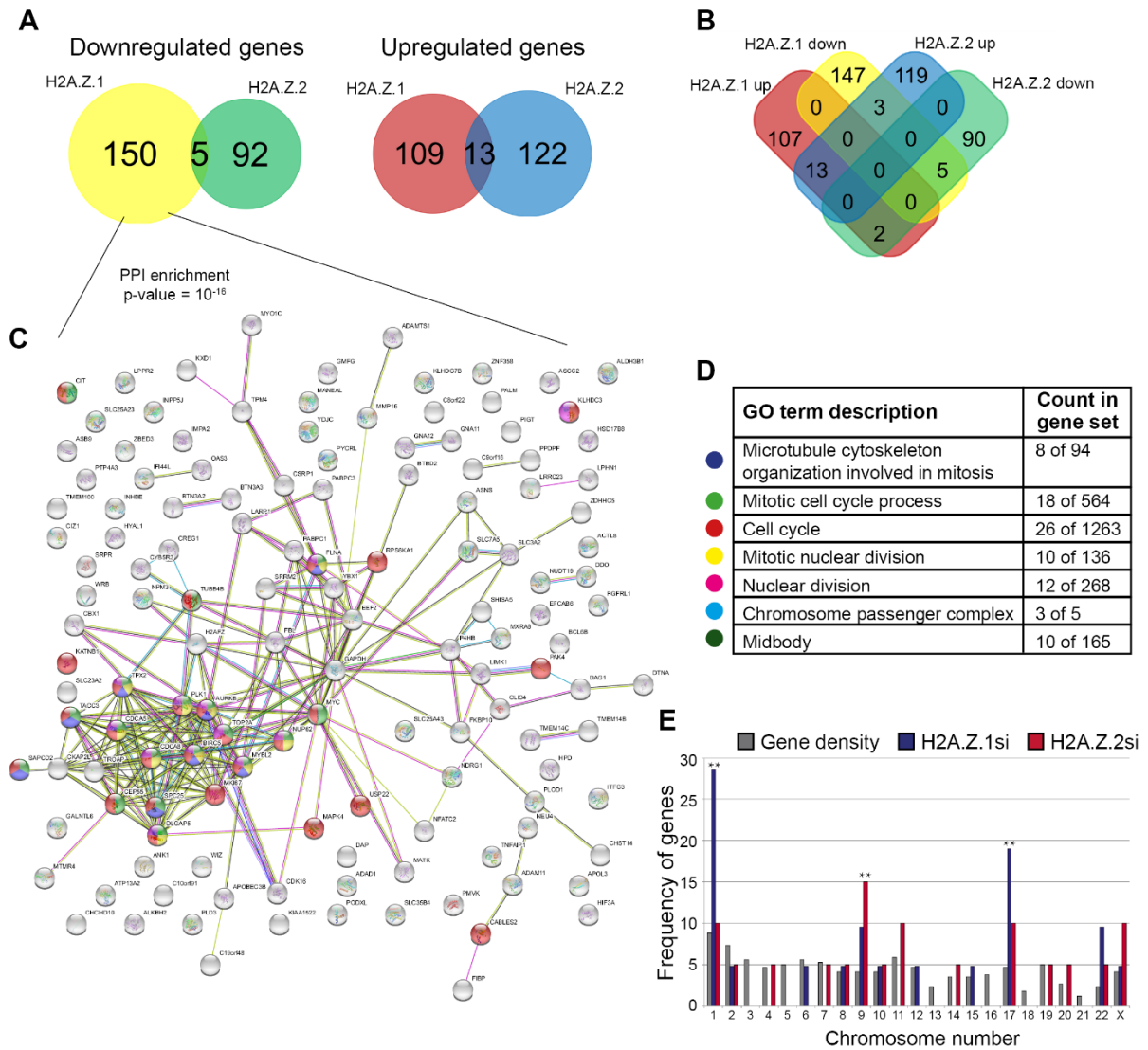


Figure 5.12. RNA sequencing analysis. A) Venn diagram of down (left) and up (right) regulated genes in H2A.Z.1 and H2A.Z.2 depleted cells compared to the control. Only genes with $p < 0.01$ were included. **B)** Venn diagram of up and downregulated genes combined together. **C)** STRING analysis of protein interactions of downregulated genes in H2A.Z.1 depleted cells. Genes with enriched functions have been highlighted as in figure legend D. **D)** Table showing the gene ontology (GO) descriptions for the enrichments detected, with the corresponding number of genes present in the STRING analysis out of the total number of genes found under that GO description. **E)** Frequency of altered genes per chromosome in H2A.Z.1 (blue) and H2A.Z.2 (red) depleted cells, as well as the gene density for each chromosome (grey).

5.2.2. Is H2A.Z sufficient to drive de novo heterochromatin assembly?

Since the data I have obtained on H2A.Z.2 depletion seems to suggest that this histone variant is upstream of H3K9me3 modification, I wanted to test if the recruitment of H2A.Z.2 at a specific locus is sufficient to establish heterochromatin. To this purpose, I transfected DT40 cells carrying a LacO array inserted at a single chromosomal locus (Vagnarelli et al., 2011) with YL1, the H2A.Z chaperone, fused to GFP:Lacl. As a control I used an established DT40 stable cell line expressing GFP:Lacl. By analysing the enrichment of the H2A.Z antibody on the LacO/Lacl locus, I could confirm that YL1 fusion protein was able to recruit H2A.Z (Figure 5.13. A, B). I also wondered whether YL1 was a chaperone for both H2A.Z.1 and H2A.Z.2, as to our knowledge there are no studies addressing this question. I therefore co-transfected the DT40 LacO cells with GFP:Lacl:YL1 and RFP:H2A.Z.1 or RFP:H2A.Z.2 and quantified the enrichment. The data shows that YL1 is able to recruit both H2A.Z variants to the same extent (Figure 5.13.C,D).

To analyse whether H2A.Z was sufficient to recruit other heterochromatin marks and form heterochromatin, we stained the DT40 LacO cells transfected with GFP:Lacl:YL1 with either HP1 α , H3K9me3 or H3K27me2/3. In our system, YL1 was not able to recruit any of these heterochromatin markers (Figure 5.13.E). This could be due to the fact that YL1 is able to recruit both variants to the same extent and, as they have different roles, co-recruitment of both might not be sufficient to nucleate heterochromatin. It could also be that, although we see accumulation of H2A.Z to the LacO locus, H2A.Z is not loaded onto the chromatin.

To test this hypothesis, I performed immune-fiber FISH experiments to see co-localization between H2A.Z and the LacO arrays in more depth. Similar to the previous experiments, I analysed the enrichment of H2A.Z staining on the LacO (with LacO probe) although this time, due to the chromatin fibers, I could precisely analyse the levels of H2A.Z on chromatin containing LacO arrays. I first checked if the procedure itself maintains or not the chaperone linked to the chromatin. I performed fiber FISH without immunostaining and analysed whether the cells still contained GFP. However, the GFP fluorescence was not observed,

concluding that the chaperone was removed from the chromatin. This was essential to avoid a mis-interpretation of the results after immunostaining.

Although the FISH was very efficient in those samples, the fiber stretching and/or the IF were not very consistent and limited the ability of analysing a sufficient number of fibers. Despite the limited analyses, the majority of the fibers do not have a specific enrichment for H2A.Z that follows the FISH signal (the enrichment follows the DAPI) (Figure 5.14. A-C). Only in one case I could see the H2A.Z staining following the signal of the FISH probe independent from the DAPI (Figure 5.14.D). Although more experiments should be conducted to obtain a firm conclusion on this aspect, the fact that the majority of fibres were not showing a positive correlation could point towards the fact that just recruiting the chaperone to the locus is not sufficient to drive active incorporation of the variant with high efficiency. Another method to test whether H2A.Z recruited via YL1 is loaded into the chromatin would be using a micrococcal nuclease to obtain only nucleosomes and check for the presence of H2A.Z.

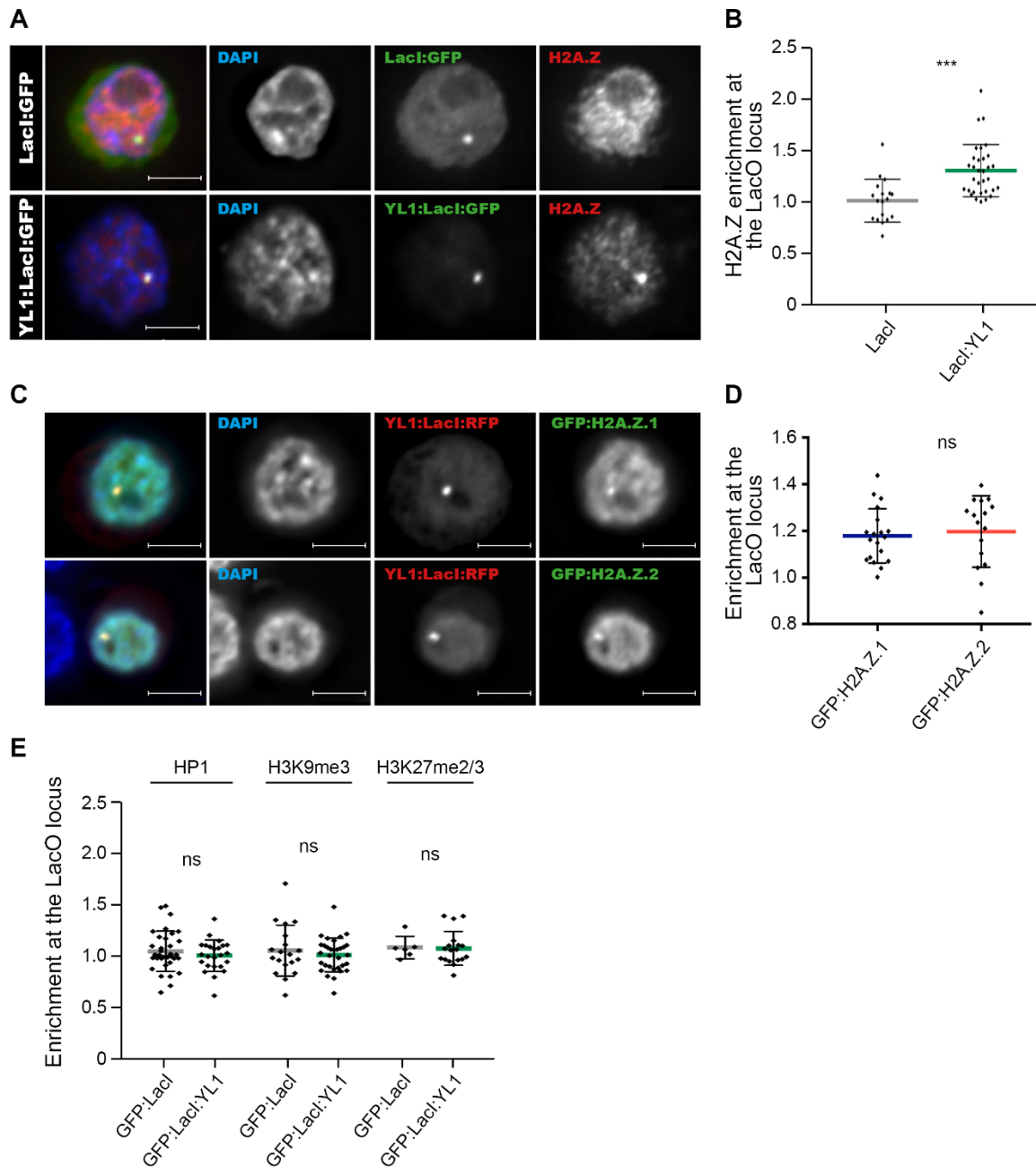


Figure 5.13. YL1 is sufficient to recruit H2A.Z.1 and H2A.Z.2. **A)** DT40 LacO cells were transfected with GFP:LacI:YL1 and stained for H2A.Z. A stable GFP:LacI DT40 cell line was used as a control. Scale bar: 5 μ m. **B)** Enrichment of H2A.Z at the LacO locus against another random locus on the nucleus of the cell was analysed. **C)** DT40 LacO cells were co-transfected with RFP:LacI:YL1 and GFP:H2A.Z.1 or GFP:H2A.Z.2. **D)** Enrichment of RFP signal at the LacO locus from experiment in C. Only one biological replicate was analysed. **E)** Enrichment of HP1, H3K9me3 and H3K27me2/3 at the LacO locus after GFP:LacI:YL1 transfection of DT40 LacO cells. Three biological replicates (only one in section E) were counted for the statistical test (Mann-Whitney U test).

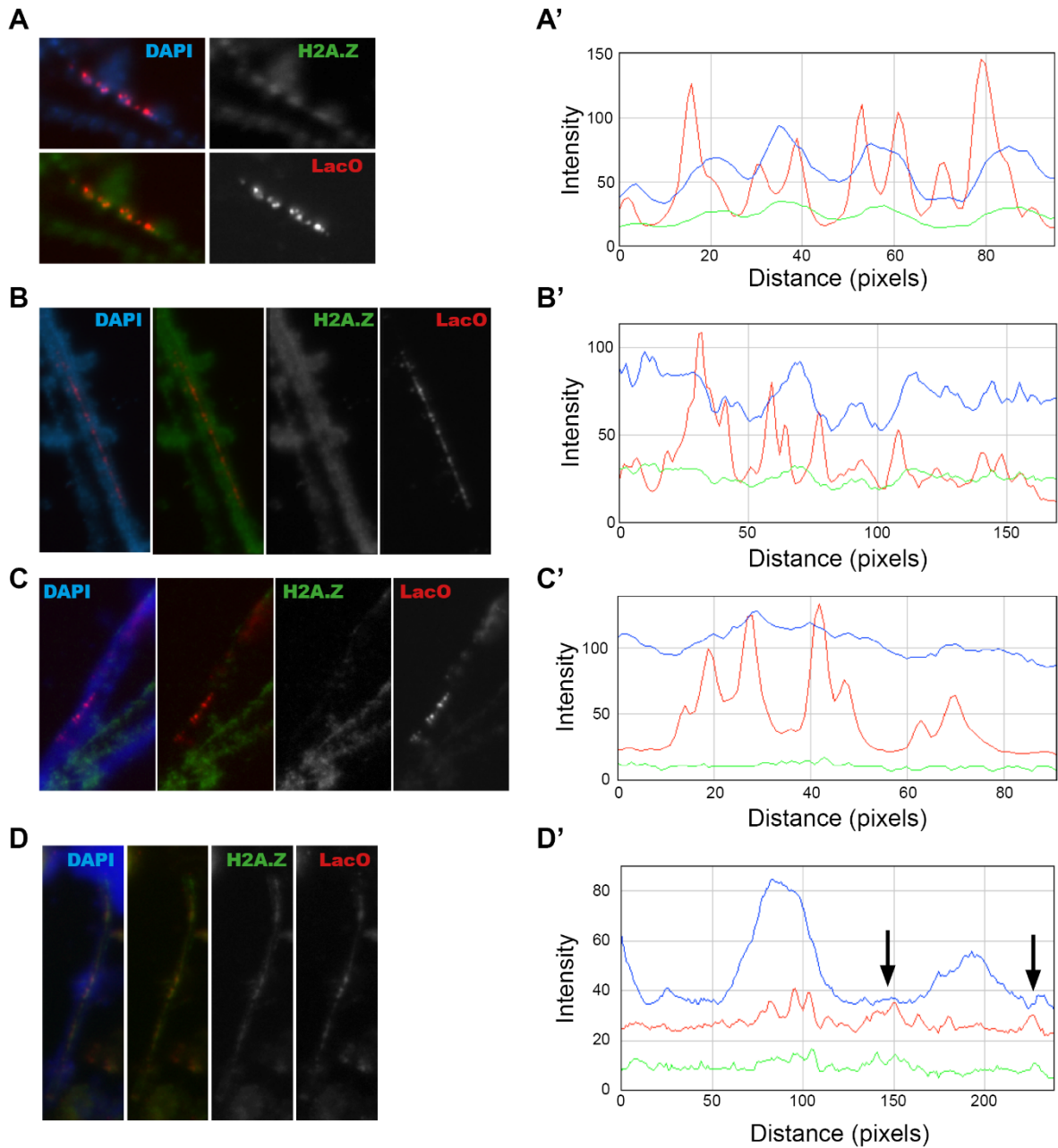


Figure 5.14. H2A.Z is not fully incorporated onto the chromatin by YL1. A-D) Extended DNA fibers from DT40 LacO9 cells transfected with GFP:LacI:YL1 were used to analyse H2A.Z incorporation onto the chromatin. Fibers were stained with H2A.Z (green) and hybridized with a LacO probe (red). **A'-D')** A line was drawn on top of the hybridized fibers and the intensity of the three channels was analysed. Black arrows indicate an example of a colocalization of H2A.Z and LacO when DAPI intensity is decreased.

5.1. Discussion

Histone variants play crucial roles in many aspects of cell biology, including gene expression and chromatin organization. H2A.Z has been involved in gene expression activation and repression, and its role on heterochromatin establishment and maintenance have been studied by several groups (Rangasamy et al., 2003, Rangasamy, Greaves & Tremethick, 2004, Fan et al., 2004, Swaminathan, Baxter & Corces, 2005, Sarcinella et al., 2007, Ryan, Tremethick, 2018). However, very little is known about the individual roles of the two H2A.Z variants, H2A.Z.1 and H2A.Z.2.

In order to study the individual roles, H2A.Z.1 and H2A.Z.2 were depleted independently using specific siRNAs. H2A.Z has been previously linked to HP1 α , and it has been suggested that HP1 α binds preferably to H2A.Z-containing nucleosomes and that H2A.Z-deficient cells disrupt HP1 α binding to chromatin (Fan et al., 2004, Rangasamy, Greaves & Tremethick, 2004). However, none of the previous studies distinguishes between the two H2A.Z variants. Therefore, I wondered whether there were any differences between the two H2A.Z variants in regards to HP1 α distribution. I used the HeLa GFP:HP1 cell line and analysed the HP1 α foci; in my analysis, only H2A.Z.2 downregulation decreased the number of HP1 α foci, suggesting a role of H2A.Z.2, but not H2A.Z.1, on heterochromatin regulation.

HP1 is dissociated from the chromatin during mitosis and it needs to reform in G1 (de Castro et al., 2016), thus an arrest in G1 might have an indirect effect on the HP1 foci reformation. Cell cycle sorting cytometry analysis did not show any impairment in cells depleted for H2A.Z.2. However, H2A.Z.1 depleted cells showed a significant increase on cells in G1 phase followed by a decrease on S phase cells, indicating a possible role of H2A.Z.1 on cell cycle progression. This was also corroborated by the decrease on the number of mitotic cells in H2A.Z.1 depleted cells, and by the RNA sequencing analysis, in where a variety of cell cycle-related genes were downregulated upon H2A.Z.1 knockdown. Recent studies have reported H2A.Z.1, but not H2A.Z.2, as an oncogene overexpressed in several types of cancer, including liver cancer (Yang et al., 2016) and neuroblastoma. Yang and colleagues showed that in liver cancer cells, depletion of H2A.Z.1 resulted in a decrease of several proteins that promote cell cycle progression, as well as the upregulation of some negative

cell cycle regulators (Yang et al., 2016); the majority of proteins analysed in the study were also up or downregulated, accordingly, in our RNA sequencing analysis. Other cancers (Hua et al., 2008) have been linked to overexpression of H2A.Z, although there was not distinction between the variants.

On the other side, H2A.Z.2 depleted cells presented a high percentage of cells with micronuclei (MN) and chromatin bridges, resulting from some mis-segregation defects. In order to understand the nature of MN I analysed the presence/absence of a centromeric protein, CENP-A, on the misaligned chromatin and MN. Although not fully quantified, my experiments indicated that MN are formed from lagging chromatin resulting from defects in chromatin segregation, rather than from DNA damage, as the majority of lagging chromatin had either one or two CENP-A signals (indicating that the chromosome or the sister chromatid remains intact). Cohesin is a protein complex that acts as a regulator of chromosome segregation, as it blocks sister chromatids separation until kinetochores are not attached to the microtubules. Thus, defects in cohesin have been reported to lead to defects in mitotic progression and metaphase chromosome alignment (Michaelis et al., 1997, Vass et al., 2003, Vagnarelli et al., 2004). By blocking cells in prometaphase with nocodazole and making chromosome spreads, I was able to observe that sister chromatid cohesion is impaired in H2A.Z.2-depleted cells, indicating that the chromosome misalignment defects are due to defects in the cohesin complex. It has been shown that HP1 localizes at the centromeres where it interacts with several centromere and kinetochore complexes (Inoue et al., 2008, De Koning et al., 2009). HP1 at the centromeres is necessary for the recruitment of cohesin to the centromere in fission yeasts and mammals (Nonaka et al., 2002, Yi et al., 2018) and it prevents chromosome segregation defects. As HP1 maintenance is compromised in H2A.Z.2-depleted cells, we hypothesise that H2A.Z.2 depletion may disrupt HP1 α interaction at the centromere during mitosis, compromising the retention of cohesin at the centromeres and resulting in premature sister chromosome separation and misalignment of chromosomes. It would be interesting to test if this is the case by quantifying the level of HP1 α or Shugoshin at the centromere in H2A.Z.2-depleted cells.

H2A.Z.1-depleted cells seem to struggle to maintain its nuclear shape. Alterations of the nuclear morphology are observed in some physiological processes, like cell differentiation,

as well as in some diseases like cancer and laminopathies. Although the lamina and the nuclear pore complexes (NPC) are crucial elements to support a proper nuclear shape (Schirmer, Guan & Gerace, 2001, Wiesel et al., 2008), neither the lamina nor the NPC were altered upon H2A.Z.1 depletion. Cytoskeleton forces might also trigger changes in the nuclear morphology (Olins, Olins, 2004, Lammerding et al., 2005, Zhang et al., 2007, Versaevel, Grevesse & Gabriele, 2012, Kim, Wirtz, 2015). Although a mild link between the *Drosophila* H2A.Z orthologue, H2A.V, and microtubules have been made (Vernì, Cenci, 2015), it might be interesting to analyse some cytoskeleton proteins in the H2A.Z.1-depleted cells. Finally, the degree of chromatin condensation as well as the histone modifications also determine the nuclear morphology independently of the lamina (Li et al., 2014, Stephens et al., 2018). Although H2A.Z.1 depletion does not appear to alter the HP1 foci, it does show an increase on the levels of H3K27me2/3, which might indicate some degree of alteration on chromatin organization. An interesting experiment would be to analyse the localization of some chromosomes by fluorescence in situ hybridization (FISH) to check for possible defects in chromosome spatial distribution upon H2A.Z.1 depletion. Most downregulated genes in the H2A.Z.1-depleted cells were located in either chromosome 1, 9, 17 and 22, thus it would be good to start studying the localization of these chromosomes in particular and see if there is any alteration.

My data indicate that H2A.Z.2 knockdown significantly decreases the levels of H3K9me3. A collaboration between H2A.Z and H3K9me3 to regulate HP1 α binding to chromatin has already been reported (Ryan, Tremethick, 2018) although again, there is no distinction between the two H2A.Z variants. I therefore hypothesise that H2A.Z.2 depletion might somehow impede H3K9 methylation, decreasing the ability of HP1 α to bind chromatin. H2A.Z was also seen to strongly correlate with H3K27me3, due to the fact that H2A.Z enhances PCR2-mediated H3K27 methylation (Dai et al., 2017, Wang et al., 2019). However, when I analysed the levels of H3K27me3, those were significantly increased upon individual knockdown of both variants. Although some aspects might differ from other studies, I clearly show that both variants affect chromatin in distinct ways and should be therefore studied separately. These differences between variants might be able to account for the differences observed on gene expression within the H2A.Z literature.

I next wondered whether H2A.Z alone is sufficient to assemble heterochromatin in H2A.Z-rich regions using DT40 cells carrying a LacO array inserted in the genome (Vagnarelli et al., 2011). YL1 was able to recruit H2A.Z to the LacO sites although it did not seem to be able to load H2A.Z to the chromatin efficiently. This could explain why any of the other heterochromatin marks tested (HP1 α , H3K9me3, and H3K27me3) was enriched at the LacO locus. YL1 has been reported to be the H2A.Z chaperone although, to our knowledge, there is no data reporting whether it is able to recruit both H2A.Z variants. The experiments here presented indicate that YL1 is a chaperone for both H2A.Z.1 and H2A.Z.2.

Overall, these results clearly show a difference on both H2A.Z variants on different aspects of cell biology and gene expression, and they highlight the importance of studying both variants independently, especially if the research community aims to use H2A.Z as a target for cancer therapy.

6. DISCUSSION

During the last few decades chromatin structure and dynamics has become a key area of study due to its relevance in many biological processes, including gene expression. The role of epigenetics on chromatin organization is well known, and it has arisen as an important focus of research because of its link to several diseases, including cancer, obesity, cardiovascular and autoimmune diseases. Many molecules have been shown to control the epigenome and thus chromatin structure, although there is still a lack of knowledge on the different pathways that converge to precisely regulate chromatin organization and the transcription programme in each cell type in complex organisms. Therefore, models to improve the identification of factors and mechanisms relevant to epigenetic alterations are required in order to speed up the so-much-needed knowledge in this area and provide tools to be able to manipulate these events in cases where this regulation becomes aberrant, such in cancer, or when there is need to generate iPSCs (induced pluripotent stem cells) or other specific and clinically-relevant cell lineages.

The aim of this project was to expand our current basic science knowledge on the mechanisms that maintain heterochromatin in development and adulthood. Heterochromatin refers to the tightly packed and transcriptional inactive type of chromatin that is established in early development and needs to be maintained throughout cell divisions to ensure proper cell function. A key marker used to study heterochromatin organization is HP1 (heterochromatin protein 1), a protein that binds di- and tri-methylated H3K9 during interphase and promotes heterochromatin formation (Lachner et al., 2001, Strom et al., 2017, Larson et al., 2017). However, the regulation of this process has been shown to be very complex, and many proteins have emerged as regulators of HP1-H3K9me3 binding and heterochromatin formation. For instance, HP1 is subject to several PTM that can influence its binding to the chromatin, thus all the proteins responsible for these modifications will play a role on heterochromatin regulation. Furthermore, the surrounding chromatin landscape is also important for the affinity of HP1 to H3K9me3. It is now apparent that H3K9me3 is not solely sufficient to recruit HP1 to the chromatin, and that additional factors are needed. In fact, studies in *Drosophila* showed that HP1 binding to promoters of active genes do not depend on H3K9me (Figueiredo et al., 2012), and studies in mouse cells revealed that, despite the loss of H3K9me3 in Ki-67 cells, HP1 isoform

maintain their localization (Sobecki et al., 2016). These findings clearly indicate that are other factors important for HP1-chromatin binding.

The initial idea was to develop new cell lines that stably express GFP:HP1 α to be used as model systems to identify novel regulators of heterochromatin establishment and maintenance. Although the idea was to develop several cell lines (mammalian and zebrafish), I could only successfully obtain human cell lines (MRC5 and HeLa) expressing GFP:HP1 α . However, the MRC5 cell line did not respond efficiently to transfection, rendering the screening approach not reliable. I therefore performed all the experiments using only the HeLa GFP:HP1 α cell line.

Identification of PP1 targeting subunits involved in heterochromatin maintenance in HeLa cells.

My first studies were focused on the role of protein phosphatases, in particular protein phosphatase 1 (PP1), on chromatin organization. PP1 was the first phosphatase linked to heterochromatin by studies conducted in *Drosophila* which identified PP1 as the suppressor of variegation gene *Su(var)3-6* (Baksa et al., 1993). Suppressors of variegation are genes that suppress the expression of euchromatic genes moved near to centromeric heterochromatin in chromosomal rearrangements or transpositions, and therefore have a role on gene expression. Not only PP1 has been related to chromatin biology, but also later studies revealed that other phosphatases, like PTEN (Phosphatase and tensin homolog), acts on chromatin organization. In fact, PTEN was seen to bind and stabilize HP1. Loss of PTEN resulted in impaired HP1 distribution, increased levels of H3K16 acetylation and chromatin decondensation (Chen et al., 2014, Gong et al., 2015c). Recently, in our lab was also revealed that Repo-man, a PP1 regulatory subunit, plays a role on HP1-chromatin binding regulation through the modulation of the phosphorylation status of H3S10 (de Castro et al., 2017). Aurora B kinase phosphorylates H3S10 at mitotic entry and weakens the affinity of HP1 for H3K9me3. Repo-man/PP1 counteracts Aurora B and dephosphorylates H3S10ph at mitotic exit, enabling HP1 α binding to H3K9me2/3 (de Castro et al., 2017). However, whether other PP1 subunits are also involved in this process remains unknown. Furthermore, the fact that HP1-chromatin binding not only depends on histone post-

translational modifications but also on post-translational modifications of HP1 itself, leads to the assumption that other protein phosphatases might be involved in heterochromatin formation and maintenance.

PP1, which accounts for the majority of the phosphatase activity in the cell, is regulated in space and time by other interacting proteins known as RIPPOs (Regulatory Interactor of Protein Phosphatase One). My aim was to study the role of PP1 on chromatin organization, therefore I performed a screening of several known chromatin-associated PP1 targeting subunits, as well as of the three different PP1 isoforms (α , β and γ). Using this visual screen, I identified that Repo-man was the only PP1 targeting subunit analysed that decreased the number of cells with normal HP1 foci. In vivo, Repo-man specifically bins to both PP1 β and PP1 γ isoforms (Trinkle-Mulcahy et al., 2006, Kumar et al., 2016), thus it was not surprising that siRNA-depletion of these two PP1 isoforms resulted in a decrease in the number of HP1 foci. However, since Repo-Man corresponds only to a small fraction of the PP1 targeting subunits, it cannot be excluded that other yet unknown PP1 binding proteins or its substrates could represent additional factors important for heterochromatin maintenance. Future studies using more extended libraries (such as a phosphatase siRNA library) could be used to identify all the phosphatases that influence HP1 α localisation. Other subunits could present an opposite effect and, in fact, NIPP1 siRNA transfection, as well as PP1 α knockdown, resulted in an increase in the number of cells with more than five foci. NIPP1, as the name indicates, is an inhibitor of PP1, thus its knockdown could enhance PP1 activity and result in an increased HP1-chromatin binding stabilization. Further studies would be needed to confirm this hypothesis.

The first round of screening actually revealed that Ki-67 was also a positive candidate. Ki-67 was identified as a PP1 regulatory protein in 2014 (Booth et al., 2014) and it was shown, as Repo-man, to interact preferentially with PP1 β and PP1 γ . It also plays a role on PP1 γ recruitment to chromatin during anaphase (Booth et al., 2014) and, although Ki-67-depleted cells still divide normally, daughter cells appear to have smaller nuclei, increased cell death, and delay in the following mitosis compared to control cells. Ki-67 shares the same PP1 binding sequence than Repo-man and they interact with the phosphatase at nearly equivalent affinities. Ki-67 has also been reported to interact with high affinity with HP1 members through its C-terminal domain and it was shown that HP1 α and HP1 β partially co-

localize with Ki-67 in early G1 phase (Takagi et al., 1999, Kametaka et al., 2002). Overexpression of a C-terminal fragment led to the formation of aberrant heterochromatin (Takagi et al., 1999), whereas overexpression of any of the three HP1 isoforms resulted in relocalization of Ki-67 in HeLa cells (Scholzen et al., 2002). Due to its similarities with Repoman and the fact that it has been linked to HP1 before, I hypothesised that it could also have a role on heterochromatin regulation. However, in a study conducted by the Fisher's lab (Sobecki et al., 2016), knockdown of Ki-67 did not affect the localization of any HP1 isoform.

However, to study more in detail the possible role of Ki-67 on HP1 regulation in my system, I used three different siRNAs targeting Ki-67. Strikingly, the three siRNAs did not show the same phenotype, and only one of them (Ki-5) presented a clear decrease of the number of cells with more than five foci. This could have been caused either by a greater potency of this oligo to reduce Ki-67 or by an off target effect. To investigate this, I used a rescue approach with an oligo resistant Ki-67 mRFP construct. This approach slightly rescued the phenotype but also produced toxic effects in control cells, thus making the experiment difficult to interpret. To solve this conundrum, I decided to undertake an RNA-sequencing approach. The RNA extracted from samples transfected with Ki-5 and one of the other siRNA that did not present the phenotype, Ki-G, was sent to sequence. The sequencing revealed that the Ki-67 depletion level was equivalent in both siRNAs treatments, thus allowing the conclusion that the striking HP1 mis-localisation obtained with Ki-5 was due to its off-target effects.

MYH9 as a new regulator of heterochromatin maintenance

Although disappointing, this investigation has opened new possibilities, as a unique protein (or more than one) depleted by this siRNA could be involved in HP1 biology. The list of differentially expressed genes did not show any known candidate involved in HP1 regulation. I could have conducted a wide siRNA screening approach on all the possible candidates however, due to the time restriction and resources, I decided to study two genes that could potentially be related to chromatin organization, RBL2 and MYH9.

RBL2 had been previously linked to heterochromatin, although it was shown to affect neither H3K9me2/3 levels nor HP1 distribution (Gonzalo et al., 2005, Benetti et al., 2008). Nevertheless, I wanted to test the effect of RBL2 knockdown in my cell line. In agreement with those reports, RBL2 knockdown with two different siRNAs did not alter HP1 α in my system either.

The other gene, MYH9, had never been reported to be involved in heterochromatin regulation. However, its role on the cytoskeleton, microtubule stabilization and cell shape maintenance could suggest a possible role on nuclear re-organisation after cell division that could also lead to defect on heterochromatin compartmentalization. When I knocked down MYH9 in the HeLa GFP:HP1 α cell lines, the localisation of HP1 α foci was disrupted. This was the case for two different siRNAs against MYH9, leading me to the identification of a new regulator of HP1 α maintenance. The mis-localisation does not seem to be caused by a delay of the cell to exit mitosis and progress in the cycle; FACS analyses does not show an accumulation in G1 and progression through mitosis via live cell imaging seems apparently normal. Therefore, the identification of the molecular mechanisms linking MYH9 and HP1 could be an interesting avenue to pursue.

CDCA2/PP1 characterization during zebrafish development

Heterochromatin is established early in development to determine gene expression in every cell type and tissue and it needs to be maintained throughout cell generations to ensure cell integrity. Using the GFP:HP1 α cell type model, I corroborated Repo-man as a regulator of the maintenance of heterochromatin, but its role on heterochromatin establishment was yet to be studied. Repo-man has also been reported to be essential for cell viability (Trinkle-Mulcahy et al., 2006), and overexpression has been found in some types of cancer, including melanoma, neuroblastoma, and triple negative breast cancer (Krasnoselsky et al., 2005, Ryu et al., 2007, Peng et al., 2010, Uchida et al., 2013).

However, an animal model for Repo-Man is not available and this protein has never been studied in any living organism. I therefore decided to use zebrafish as model system to study the function of Repo-Man during development.

Zebrafish has become an excellent model organism to study development for many reasons. Firstly, fish can be easily and inexpensively housed within a modest facility. Secondly, they reach sexual maturity in about 3 months, and a single female can lay up to 400 eggs in a week. Furthermore, fertilization occurs externally, the embryos are transparent until they start to develop pigment cells at about 2-3dpf, and the primary organs start to appear visible as soon as 24hpf. For all these reasons, and because a Repo-man orthologue has never been reported in *Drosophila*, zebrafish was chosen as a model to study the role of Repo-man (CDCA2 in zebrafish) during development and, ultimately, heterochromatin establishment. Data on the role of CDCA2 in zebrafish would also be important to understand the impact of this protein in humans and it could support, or undermine, the idea of using CDCA2 as a potential target for cancer therapy.

As the first team ever studying this protein in zebrafish, we encountered some difficulties along the way. One of the first barriers was the lack of antibodies that specifically recognise the CDCA2 zebrafish protein, hence the necessity of developing and optimizing new antibodies. Once the antibodies were acquired, some troubles were faced in extracting proteins from zebrafish embryos, as chromatin-bound proteins are harder to extract compared to others. All this led to an unexpected delay and we do not currently have a validated antibody for the CDCA2 zebrafish protein. However, many other experiments were conducted, and we learned some important aspects of CDCA2 biology in an organism. First, our findings revealed a high CDCA2 expression in the very early stages of development and a decrease in expression as the zygote gene expression programme is activated at around 4hpf. In early development, CDCA2 is expressed ubiquitously in all the cells, although as the main organs form it localizes in the brain area. However, during adulthood, CDCA2 expression is only high in the gonads, both ovaries and testis. These findings could indicate a potential role of CDCA2 on brain development, as well as on the reproductive abilities of the adult zebrafish.

Mutant CDCA2 do not present any visible phenotype

In order to study the function of CDCA2 *in vivo*, I acquired a mutant zebrafish line carrying a point mutation at the beginning of the CDCA2 gene. Embryos produced by *in vitro* fertilization from mutated sperm and wild type eggs were distributed by the Zebrafish International Resource Centre (ZIRC). Upon arrival, eggs were grown to adulthood, when I performed an extensive work in order to genotype each fish and classify it as control or heterozygous. The heterozygous fishes were crossed, and the embryos were genotyped again in order to identify the homozygous line. This genotyping was done at day 4 post fertilization (4dpf) in order to be able to analyse any developmental features of CDCA2. To our surprise, the survival rate of the CDCA2 double knockouts was similar to that of the WT and the heterozygous indicating that, contrary to what was shown in mammalian cells (Trinkle-Mulcahy et al., 2016), CDCA2 is not essential for life in zebrafish.

No obvious major phenotypes were observed by eye between the CDCA2^{+/+}, CDCA2^{+/-}, and CDCA2^{-/-} zebrafish lines, thus I selected a few systems to look at. Because of the data obtained on the tissue expression, and following gene expression, tissue and system ranks from online databases, I concentrated the attention on phenotypes that were related with the nervous, cardiovascular, and reproductive system. However, none of these systems was altered in our mutant fish.

Several reports in the last few years have highlighted the occurrence of “lack of phenotype” in zebrafish mutants generated by nonsense-mediated decay (El-Brolosy et al., 2019, Conti, Izaurralde, 2005), where the organisms degrade transcripts that carry a stop mutation. This seems to be the case in our mutants, as CDCA2 transcripts are reduced accordingly in both CDCA2^{+/-} and CDCA2^{-/-} lines but no phenotype is emerging. To be 100% sure, it would be important to analyse CDCA2 at protein level, although as previously mentioned we could not generate a suitable antibody. Some studies have also reported that mRNA degradation can lead to genetic compensation in many mutant zebrafish lines (Rossi et al., 2015, El-Brolosy, Stainier, 2017, El-Brolosy et al., 2019). The question now would be to understand whether our zebrafish undergoes genetic compensation for the loss of CDCA2, and which genes could be responsible for such compensation.

One possible control would be to knockdown CDCA2 in early development using morpholinos, as genetic compensation has not been observed in this case (Rossi et al., 2015). However, the effect of morpholinos only last up to five days, thus many of the experiments performed in the mutant fish would not be possible to test, such as the fertilization experiments. Nevertheless, the use of morpholinos would allow us to detect possible phenotypes in early development and might give us an idea about a possible genetic compensation occurring in our system. I did attempt to inject CDCA2 morpholinos, but I was faced with a high rate of mortality even in the ones injected with a control morpholino and, due to the lack of time, I had to put aside this approach at this point.

However, I have collected RNA from the wild-types and homozygote mutants therefore it would be possible to send these samples for RNA sequencing to identify if either a compensatory programme is in place or if really CDCA2 is dispensable for development in zebrafish. Any of these outcomes would be of extreme value to understand CDCA2 biology.

H2A.Z.1 and H2A.Z.2 knockdown present different phenotypes

Histone modifications and their role on chromatin regulation have been widely studied for decades. It is well accepted that heterochromatin is marked by the presence of specific histone modifications, namely H3K9me3 and H3K27me3, whereas euchromatin is enriched in histone acetylation. Not only histone modifications are involved on chromatin structure, but the replacement of some histones by their histone variant have also implications in chromatin regulation. For instance, replacement of H2A with macroH2A (Douet et al., 2017) or H2A.Z (Rangasamy et al., 2003, Rangasamy et al., 2004, Fan et al., 2004, Swaminathan et al., 2005, Sarcinella et al., 2007, Ryan, Tremethick, 2018) have been reported to alter chromatin organization and gene expression.

Linked to my research focus, I ought to add some more knowledge on the association between H2A.Z and heterochromatin. H2A.Z is present as two variants, H2A.Z.1 and H2A.Z.2, and although some reports indicated that they might have different functions (Faast et al., 2001, Matsuda et al., 2010, Dunn et al., 2017, Dryhurst et al., 2009), they have never been studied individually on their role on chromatin organization, cell cycle and gene

expression. At the same time, two splicing variants of H2A.Z.2 have been found, H2A.Z.2.1 and H2A.Z.2.2 (Bönisch et al., 2012b).

Unpublished data from the lab indicate that H2A.Z is enriched on chromatin that binds recombinant HP1 α . As mass spectrometry was not able to distinguish between the two variants, I successfully depleted both variants individually and analysed their role in heterochromatin maintenance using the HeLa GFP:HP1 α line. The study revealed that H2A.Z.2, but not H2A.Z.1, is involved in heterochromatin regulation. Although co-transfection with a siRNA-resistant plasmid did not fully rescue the phenotype, depletion of H2A.Z.2 with another siRNA also affected HP1 α localization, strongly suggesting a specific involvement of this variant in HP1 α biology.

I have also revealed major differences between the two isoforms knockdowns regarding chromatin segregation, nuclear shape and cell proliferation. For instance, H2A.Z.1 knockdown resulted in a decrease in mitotic cells and accumulation of cells in G1 phase, identifying H2A.Z.1 as a key regulator of cell cycle progression. These findings are in agreement with other studies that report H2A.Z.1 as an oncogene involved in liver tumorigenesis associated with poor prognosis (Yang et al., 2016). Using an RNA sequencing approach, I have revealed the molecular mechanism for this: a great number of cell-cycle related genes are downregulated in H2A.Z.1-depleted cells, including MYCN, MYBL2, Ki-67, and Aurora B. H2A.Z.1-depleted cells showed also the presence of highly mis-shaped nuclei that was rescued by an oligo-resistant construct; however, neither the lamina nor the nuclear pore complexes were altered. On the contrary, H2A.Z.2 knockdown cells presented a high number of MN and chromosome segregation defects that were successfully rescued by the co-transfection of both siRNA-resistant H2A.Z.2.1 and H2A.Z.2.2 plasmid. Chromosome segregation defects can be the result of cohesin impairment, and in fact this seems to be the case, as sister chromatids from H2A.Z.2-depleted cells fail to be kept together in chromosome spreads.

Overall, I have provided the first evidence for a distinct role of these two isoforms in chromatin segregation and nuclear organisation. I have clearly shown that H2A.Z.1 and H2A.Z.2 present different functions: while H2A.Z.1 plays a crucial role on cell cycle progression and nuclear shape, H2A.Z.2 is involved in heterochromatin regulation and

chromosome segregation. H2A.Z.1 depletion affects cell cycle through decreasing the expression levels of several cell cycle-related genes. How exactly this occurs still remains unknown, although it might be related to the position of H2A.Z.1 along these genes. H2A.Z.2, through a mechanism that is yet to be fully determined but that might be linked to HP1 α could affect cohesin maintenance, possibly via an impaired Shugoshin recruitment, at the centromere leading to a premature sister chromatids separation, mis-segregation and MN formation. All these aspects will be experimentally testable.

Although my study and other have reported differences between H2A.Z.1 and H2A.Z.2 (Faast et al., 2001, Matsuda et al., 2010, Dunn et al., 2017, Dryhurst et al., 2009), H2A.Z is still being studied mainly as one H2A variant. I would like to emphasize with this research chapter the importance to study both variants individually in order to contribute to a better understanding of this essential H2A variant. H2A.Z has been related to several diseases, including cancer, and its interest as a drug target has been increasing in the past years. It is critical, though, that we unravel first the differences between these two variants and study its individual roles in diseases, as it would minimise any secondary effects linked to the variant that might not be altered in the first place.

Concluding remarks

Overall, this research has contributed in the understanding of heterochromatin biology, and it introduces some new insights on regulators of chromatin structure. In the first chapter, studying the role of protein phosphatases on chromatin organization led us to the unexpected identification of a new regulator of HP1 α distribution, MYH9. This could be an interesting research to pursue as there is no evidence to date linking this gene to heterochromatin regulation. In the second chapter, I have analysed for the first time the role of a known HP1 α regulator, CDCA2, on a living organism, and the fact that CDCA2 mutants do not present any significant phenotype could have profound implications on the clinic, as it raises the possibility to use CDCA2 as target for several chemotherapeutic drugs. Finally, I have clearly demonstrated the biological differences between two H2A.Z variants, highlighting the importance of studying these two variants individually and expanding the knowledge of histone variants on gene expression and cell viability.

7. APPENDIX

Table 7-1. List of kits used in the project

Kit name	Company	Catalogue number
jetPRIMER®	Polyplus transfection	114-01
Neon transfection system	Invitrogen	MPK10025
Rneasy PowerLyzer Tissue & Cells kit	Qiagen	15055-50
DNase I, RNase-free (1 U/μL)	Thermo Fisher Scientific	EN0521
RevertAid First Strand cDNA synthesis kit	Thermo Fisher Scientific	K1622
Maxima SYBR Green/ROX qPCR Master Mix (2X)	Thermo Fisher Scientific	K0222
Taq DNA Polymerase with Standard Taq Buffer (5000U/mL)	New England Biolabs	M0273S
QIAquick gel extraction kit	Qiagen	28704
pGEM®-T-easy vector system	Promega	A1360
QIAGEN Plasmid Mini/Midi Kits	Qiagen	12943
QIAquick PCR Purification Kit	Qiagen	28104
QIAquick Gel extraction Kit	Qiagen	28704
RNeasy MinElute Cleanup Kit	Qiagen	74204
RNA clean up kit	Macherey-Nagel	740948

8. REFERENCES

- Abe, Y., Sako, K., Takagaki, K., Hirayama, Y., Uchida, K.S., Herman, J.A., DeLuca, J.G. & Hirota, T. 2016a, "HP1-assisted Aurora B kinase activity prevents chromosome segregation errors", *Developmental cell*, vol. 36, no. 5, pp. 487-497.
- Adam, M., Robert, F., Larochelle, M. & Gaudreau, L. 2001, "H2A. Z is required for global chromatin integrity and for recruitment of RNA polymerase II under specific conditions", *Molecular and cellular biology*, vol. 21, no. 18, pp. 6270-6279.
- Ainsztein, A.M., Kandels-Lewis, S.E., Mackay, A.M. & Earnshaw, W.C. 1998, "INCENP centromere and spindle targeting: identification of essential conserved motifs and involvement of heterochromatin protein HP1", *J Cell Biol*, vol. 143, no. 7, pp. 1763-1774.
- Ajiro, K., Yasuda, H. & Tsuji, H. 1996, "Vanadate Triggers the Transition from Chromosome Condensation to Decondensation in a Mitotic Mutant (tsTM13) Inactivation of P34cdc2/H1 Kinase and Dephosphorylation of Mitosis-Specific Histone H3", *European journal of biochemistry*, vol. 241, no. 3, pp. 923-930.
- Albig, W. & Doenecke, D. 1997, "The human histone gene cluster at the D6S105 locus", *Human genetics*, vol. 101, no. 3, pp. 284-294.
- Allshire, R.C. & Karpen, G.H. 2008, "Epigenetic regulation of centromeric chromatin: old dogs, new tricks?", *Nature Reviews Genetics*, vol. 9, no. 12, pp. 923.
- Altaf, M., Auger, A., Monnet-Saksouk, J., Brodeur, J., Piquet, S., Cramet, M., Bouchard, N., Lacoste, N., Utley, R.T. & Gaudreau, L. 2010, "NuA4-dependent acetylation of nucleosomal histones H4 and H2A directly stimulates incorporation of H2A. Z by the SWR1 complex", *Journal of Biological Chemistry*, vol. 285, no. 21, pp. 15966-15977.
- Ammosova, T., Platonov, M., Yedavalli, V.R., Obukhov, Y., Gordeuk, V.R., Jeang, K., Kovalsky, D. & Nekhai, S. 2012, "Small molecules targeted to a non-catalytic "RVxF" binding site of protein phosphatase-1 inhibit HIV-1", *PLoS One*, vol. 7, no. 6, pp. e39481.
- Anderson, R.M., Bosch, J.A., Goll, M.G., Hesselton, D., Dong, P.D.S., Shin, D., Chi, N.C., Shin, C.H., Schlegel, A. & Halpern, M. 2009, "Loss of Dnmt1 catalytic activity reveals multiple roles for DNA methylation during pancreas development and regeneration", *Developmental biology*, vol. 334, no. 1, pp. 213-223.
- Aucott, R., Bullwinkel, J., Yu, Y., Shi, W., Billur, M., Brown, J.P., Menzel, U., Kioussis, D., Wang, G., Reisert, I. and Weimer, J., 2008. "HP1- β is required for development of the cerebral neocortex and neuromuscular junctions". *The Journal of cell biology*, 183(4), pp.597-606.

- Auger, A., Galarneau, L., Altaf, M., Nourani, A., Doyon, Y., Utle, R.T., Cronier, D., Allard, S. & Côté, J. 2008, "Eaf1 is the platform for NuA4 molecular assembly that evolutionarily links chromatin acetylation to ATP-dependent exchange of histone H2A variants", *Molecular and cellular biology*, vol. 28, no. 7, pp. 2257-2270.
- Azzaz, A.M., Vitalini, M.W., Thomas, A.S., Price, J.P., Blacketer, M.J., Cryderman, D.E., Zirbel, L.N., Woodcock, C.L., Elcock, A.H. & Wallrath, L.L. 2014, "Human heterochromatin protein 1 α promotes nucleosome associations that drive chromatin condensation", *Journal of Biological Chemistry*, vol. 289, no. 10, pp. 6850-6861.
- Bagchi, D.N., Battenhouse, A.M., Park, D. and Iyer, V.R., 2020. "The histone variant H2A. Z in yeast is almost exclusively incorporated into the +1 nucleosome in the direction of transcription", *Nucleic acids research*, 48(1), pp.157-170.
- Baksa, K., Morawietz, H., Dombradi, V., Axton, M., Taubert, H., Szabo, G., Trk, I., Udvardy, A., Gyurkovics, H. & Szr, B. 1993, "Mutations in the protein phosphatase 1 gene at 87B can differentially affect suppression of position-effect variegation and mitosis in *Drosophila melanogaster*", *Genetics*, vol. 135, no. 1, pp. 117-125.
- Balasubramanian, S., Raghunath, A. & Perumal, E. 2019, "Role of epigenetics in zebrafish development", *Gene*, , pp. 144049.
- Bannister, A.J., Zegerman, P., Partridge, J.F., Miska, E.A., Thomas, J.O., Allshire, R.C. & Kouzarides, T. 2001, "Selective recognition of methylated lysine 9 on histone H3 by the HP1 chromo domain", *Nature*, vol. 410, no. 6824, pp. 120.
- Barber, C.M., Turner, F.B., Wang, Y., Hagstrom, K., Taverna, S.D., Mollah, S., Ueberheide, B., Meyer, B.J., Hunt, D.F. & Cheung, P. 2004, "The enhancement of histone H4 and H2A serine 1 phosphorylation during mitosis and S-phase is evolutionarily conserved", *Chromosoma*, vol. 112, no. 7, pp. 360-371.
- Bargaje, R., Alam, M.P., Patowary, A., Sarkar, M., Ali, T., Gupta, S., Garg, M., Singh, M., Purkanti, R. & Scaria, V. 2012, "Proximity of H2A. Z containing nucleosome to the transcription start site influences gene expression levels in the mammalian liver and brain", *Nucleic acids research*, vol. 40, no. 18, pp. 8965-8978.
- Barker, H.M., Brewis, N.D., Street, A.J., Spurr, N.K. & Cohen, P.T. 1994, "Three genes for protein phosphatase 1 map to different human chromosomes: sequence, expression and gene localisation of protein serine/threonine phosphatase 1 beta (PPP1CB)", *Biochimica et Biophysica Acta (BBA)-Molecular Cell Research*, vol. 1220, no. 2, pp. 212-218.
- Barker, H.M., Craig, S.P., Spurr, N.K. & Cohen, P.T. 1993, "Sequence of human protein serine/threonine phosphatase 1 gamma and localization of the gene (PPP1CC) encoding it to chromosome bands 12q24. 1-q24. 2", *Biochimica et Biophysica Acta (BBA)-Molecular Cell Research*, vol. 1178, no. 2, pp. 228-233.

- Beagrie, R.A., Scialdone, A., Schueler, M., Kraemer, D.C., Chotalia, M., Xie, S.Q., Barbieri, M., de Santiago, I., Lavitas, L.M., Branco, M.R. and Fraser, J., 2017. "Complex multi-enhancer contacts captured by genome architecture mapping", *Nature*, 543(7646), pp.519-524.
- Bellucci, L., Dalvai, M., Kocanova, S., Moutahir, F. & Bystricky, K. 2013, "Activation of p21 by HDAC inhibitors requires acetylation of H2A. Z", *PloS one*, vol. 8, no. 1, pp. e54102.
- Benetti, R., Gonzalo, S., Jaco, I., Muñoz, P., Gonzalez, S., Schoeftner, S., Murchison, E., Andl, T., Chen, T. & Klatt, P. 2008, "A mammalian microRNA cluster controls DNA methylation and telomere recombination via Rbl2-dependent regulation of DNA methyltransferases", *Nature structural & molecular biology*, vol. 15, no. 3, pp. 268.
- Bernard, P., Maure, J.F., Partridge, J.F., Genier, S., Javerzat, J.P. and Allshire, R.C., 2001. "Requirement of heterochromatin for cohesion at centromeres", *Science*, 294(5551), pp.2539-2542.
- Bickmore, W.A. & Teague, P. 2002, "Influences of chromosome size, gene density and nuclear position on the frequency of constitutional translocations in the human population", *Chromosome research*, vol. 10, no. 8, pp. 707-715.
- Birnstiel, M.L., Buslinger, M. & Strub, K. 1985, "Transcription termination and 3' processing: the end is in site!", *Cell*, vol. 41, no. 2, pp. 349-359.
- Bollen, M., Peti, W., Ragusa, M.J. & Beullens, M. 2010a, "The extended PP1 toolkit: designed to create specificity", *Trends in biochemical sciences*, vol. 35, no. 8, pp. 450-458.
- Bönisch, C., Schneider, K., Pünzeler, S., Wiedemann, S.M., Bielmeier, C., Bocola, M., Eberl, H.C., Kuegel, W., Neumann, J. & Kremmer, E. 2012a, "H2A. Z. 2.2 is an alternatively spliced histone H2A. Z variant that causes severe nucleosome destabilization", *Nucleic acids research*, vol. 40, no. 13, pp. 5951-5964.
- Bönisch, C., Schneider, K., Pünzeler, S., Wiedemann, S.M., Bielmeier, C., Bocola, M., Eberl, H.C., Kuegel, W., Neumann, J. & Kremmer, E. 2012b, "H2A. Z. 2.2 is an alternatively spliced histone H2A. Z variant that causes severe nucleosome destabilization", *Nucleic acids research*, vol. 40, no. 13, pp. 5951-5964.
- Booth, D.G., Takagi, M., Sanchez-Pulido, L., Petfalski, E., Vargiu, G., Samejima, K., Imamoto, N., Ponting, C.P., Tollervey, D. & Earnshaw, W.C. 2014, "Ki-67 is a PP1-interacting protein that organises the mitotic chromosome periphery", *Elife*, vol. 3, pp. e01641.
- Boros, J., Arnoult, N., Stroobant, V., Collet, J.-. & Decottignies, A. 2014, "Polycomb Repressive Complex 2 and H3K27me3 Cooperate with H3K9 Methylation To Maintain Heterochromatin Protein 1 at Chromatin", *Molecular and Cellular Biology*, vol. 34, no. 19, pp. 3662-3674.

- Boumendil, C., Hari, P., Olsen, K.C., Acosta, J.C. & Bickmore, W.A. 2019, "Nuclear pore density controls heterochromatin reorganization during senescence", *Genes & development*, vol. 33, no. 3-4, pp. 144-149.
- Boyarchuk, E., Filipescu, D., Vassias, I., Cantaloube, S. & Almouzni, G. 2014, "The histone variant composition of centromeres is controlled by the pericentric heterochromatin state during the cell cycle", *J Cell Sci*, vol. 127, no. 15, pp. 3347-3359.
- Boyle, S., Rodesch, M.J., Halvensleben, H.A., Jeddloh, J.A. & Bickmore, W.A. 2011, "Fluorescence in situ hybridization with high-complexity repeat-free oligonucleotide probes generated by massively parallel synthesis", *Chromosome research*, vol. 19, no. 7, pp. 901-909.
- Brasher, S.V., Smith, B.O., Fogh, R.H., Nietlispach, D., Thiru, A., Nielsen, P.R., Broadhurst, R.W., Ball, L.J., Murzina, N.V. & Laue, E.D. 2000, "The structure of mouse HP1 suggests a unique mode of single peptide recognition by the shadow chromo domain dimer", *The EMBO journal*, vol. 19, no. 7, pp. 1587-1597.
- Brittle, A.L., Nanba, Y., Ito, T. & Ohkura, H. 2007, "Concerted action of Aurora B, Polo and NHK-1 kinases in centromere-specific histone 2A phosphorylation", *Experimental cell research*, vol. 313, no. 13, pp. 2780-2785.
- Brown, J.M., Leach, J., Reittie, J.E., Atzberger, A., Lee-Prudhoe, J., Wood, W.G., Higgs, D.R., Iborra, F.J. & Buckle, V.J. 2006, "Coregulated human globin genes are frequently in spatial proximity when active", *J Cell Biol*, vol. 172, no. 2, pp. 177-187.
- Brown, J.P., Bullwinkel, J., Baron-Lühr, B., Billur, M., Schneider, P., Winking, H. and Singh, P.B., 2010. "HP1 γ function is required for male germ cell survival and spermatogenesis". *Epigenetics & chromatin*, 3(1), p.9.
- Bruce, K., Myers, F.A., Mantouvalou, E., Lefevre, P., Greaves, I., Bonifer, C., Tremethick, D.J., Thorne, A.W. & Crane-Robinson, C. 2005, "The replacement histone H2A. Z in a hyperacetylated form is a feature of active genes in the chicken", *Nucleic acids research*, vol. 33, no. 17, pp. 5633-5639.
- Budhavarapu, V.N., Chavez, M. and Tyler, J.K., 2013. "How is epigenetic information maintained through DNA replication?", *Epigenetics & chromatin*, 6(1), p.32.
- Buschbeck, M. & Hake, S.B. 2017, "Variants of core histones and their roles in cell fate decisions, development and cancer", *Nature reviews Molecular cell biology*, vol. 18, no. 5, pp. 299.
- Buschbeck, M., Uribealago, I., Wibowo, I., Rué, P., Martin, D., Gutierrez, A., Morey, L., Guigó, R., López-Schier, H. & Di Croce, L. 2009, "The histone variant macroH2A is an epigenetic regulator of key developmental genes", *Nature structural & molecular biology*, vol. 16, no. 10, pp. 1074.

- Cai, Y., Jin, J., Florens, L., Swanson, S.K., Kusch, T., Li, B., Workman, J.L., Washburn, M.P., Conaway, R.C. & Conaway, J.W. 2005, "The mammalian YL1 protein is a shared subunit of the TRRAP/TIP60 histone acetyltransferase and SRCAP complexes", *Journal of Biological Chemistry*, vol. 280, no. 14, pp. 13665-13670.
- Canzio, D., Chang, E.Y., Shankar, S., Kuchenbecker, K.M., Simon, M.D., Madhani, H.D., Narlikar, G.J. & Al-Sady, B. 2011, "Chromodomain-mediated oligomerization of HP1 suggests a nucleosome-bridging mechanism for heterochromatin assembly", *Molecular cell*, vol. 41, no. 1, pp. 67-81.
- Canzio, D., Liao, M., Naber, N., Pate, E., Larson, A., Wu, S., Marina, D.B., Garcia, J.F., Madhani, H.D. & Cooke, R. 2013, "A conformational switch in HP1 releases auto-inhibition to drive heterochromatin assembly", *Nature*, vol. 496, no. 7445, pp. 377.
- Cao, R., Wang, L., Wang, H., Xia, L., Erdjument-Bromage, H., Tempst, P., Jones, R.S. & Zhang, Y. 2002, "Role of histone H3 lysine 27 methylation in Polycomb-group silencing", *Science*, vol. 298, no. 5595, pp. 1039-1043.
- Carmena, M., Wheelock, M., Funabiki, H. & Earnshaw, W.C. 2012, "The chromosomal passenger complex (CPC): from easy rider to the godfather of mitosis", *Nature reviews Molecular cell biology*, vol. 13, no. 12, pp. 789.
- Carmody, L.C., Baucum, A.J., Bass, M.A. & Colbran, R.J. 2008, "Selective targeting of the $\gamma 1$ isoform of protein phosphatase 1 to F-actin in intact cells requires multiple domains in spinophilin and neurabin", *The FASEB Journal*, vol. 22, no. 6, pp. 1660-1671.
- Catania, S., Pidoux, A.L. & Allshire, R.C. 2015, "Sequence features and transcriptional stalling within centromere DNA promote establishment of CENP-A chromatin", *PLoS genetics*, vol. 11, no. 3, pp. e1004986.
- Cecile, C., Kirmizis, A., Simon, M.D., Isono, K., Koseki, H. & Panning, B. 2007, "The Polycomb group protein SUZ12 regulates histone H3 lysine 9 methylation and HP1 α distribution", *Chromosome research*, vol. 15, no. 3, pp. 299-314.
- Chakraborty, A., Prasanth, K.V. & Prasanth, S.G. 2014, "Dynamic phosphorylation of HP1 α regulates mitotic progression in human cells", *Nature communications*, vol. 5, pp. 3445.
- Chakraborty, A. & Prasanth, S.G. 2014, "Phosphorylation–dephosphorylation cycle of HP1 α governs accurate mitotic progression", *Cell cycle*, vol. 13, no. 11, pp. 1663-1670.
- Chambeyron, S. & Bickmore, W.A. 2004, "Chromatin decondensation and nuclear reorganization of the HoxB locus upon induction of transcription", *Genes & development*, vol. 18, no. 10, pp. 1119-1130.
- Chen, X., Miragaia, R.J., Natarajan, K.N. and Teichmann, S.A., 2018. "A rapid and robust method for single cell chromatin accessibility profiling", *Nature Communications*, 9(1), pp.1-9.

- Chen, Z.H., Zhu, M., Yang, J., Liang, H., He, J., He, S., Wang, P., Kang, X., McNutt, M.A. & Yin, Y. 2014, "PTEN interacts with histone H1 and controls chromatin condensation", *Cell reports*, vol. 8, no. 6, pp. 2003-2014.
- Chen, P., Zhao, J., Wang, Y., Wang, M., Long, H., Liang, D., Huang, L., Wen, Z., Li, W., Li, X. and Feng, H., 2013. "H3. 3 actively marks enhancers and primes gene transcription via opening higher-ordered chromatin", *Genes & development*, 27(19), pp.2109-2124.
- Cheung, W.L., Ajiro, K., Samejima, K., Kloc, M., Cheung, P., Mizzen, C.A., Beeser, A., Etkin, L.D., Chernoff, J. & Earnshaw, W.C. 2003, "Apoptotic phosphorylation of histone H2B is mediated by mammalian sterile twenty kinase", *Cell*, vol. 113, no. 4, pp. 507-517.
- Chevillard-Briet, M., Quaranta, M., Grézy, A., Mattera, L., Courilleau, C., Philippe, M., Mercier, P., Corpet, D., Lough, J. & Ueda, T. 2013, "Interplay between chromatin-modifying enzymes controls colon cancer progression through Wnt signaling", *Human molecular genetics*, vol. 23, no. 8, pp. 2120-2131.
- Chubb, J.R., Boyle, S., Perry, P. & Bickmore, W.A. 2002, "Chromatin motion is constrained by association with nuclear compartments in human cells", *Current Biology*, vol. 12, no. 6, pp. 439-445.
- Conerly, M.L., Teves, S.S., Diolaiti, D., Ulrich, M., Eisenman, R.N. & Henikoff, S. 2010, "Changes in H2A. Z occupancy and DNA methylation during B-cell lymphomagenesis", *Genome research*, vol. 20, no. 10, pp. 1383-1390.
- Conti, E. & Izaurralde, E. 2005, "Nonsense-mediated mRNA decay: molecular insights and mechanistic variations across species", *Current opinion in cell biology*, vol. 17, no. 3, pp. 316-325.
- Craig, J.M. & Bickmore, W.A. 1997, "The relationship between gene density and chromosome banding patterns in mammalian nuclei" in *Chromosomes Today* Springer, , pp. 65-83.
- Creyghton, M.P., Markoulaki, S., Levine, S.S., Hanna, J., Lodato, M.A., Sha, K., Young, R.A., Jaenisch, R. & Boyer, L.A. 2008, "H2AZ is enriched at polycomb complex target genes in ES cells and is necessary for lineage commitment", *Cell*, vol. 135, no. 4, pp. 649-661.
- Croft, J.A., Bridger, J.M., Boyle, S., Perry, P., Teague, P. & Bickmore, W.A. 1999, "Differences in the localization and morphology of chromosomes in the human nucleus", *The Journal of cell biology*, vol. 145, no. 6, pp. 1119-1131.
- Cui, K., Zang, C., Roh, T., Schones, D.E., Childs, R.W., Peng, W. & Zhao, K. 2009, "Chromatin signatures in multipotent human hematopoietic stem cells indicate the fate of bivalent genes during differentiation", *Cell stem cell*, vol. 4, no. 1, pp. 80-93.
- Cunliffe, V.T. 2004, "Histone deacetylase 1 is required to repress Notch target gene expression during zebrafish neurogenesis and to maintain the production of

- motoneurons in response to hedgehog signalling", *Development*, vol. 131, no. 12, pp. 2983-2995.
- Cuylen, S., Blaukopf, C., Politi, A.Z., Müller-Reichert, T., Neumann, B., Poser, I., Ellenberg, J., Hyman, A.A. & Gerlich, D.W. 2016a, "Ki-67 acts as a biological surfactant to disperse mitotic chromosomes", *Nature*, vol. 535, no. 7611, pp. 308.
- Cuylen, S., Blaukopf, C., Politi, A.Z., Müller-Reichert, T., Neumann, B., Poser, I., Ellenberg, J., Hyman, A.A. & Gerlich, D.W. 2016b, "Ki-67 acts as a biological surfactant to disperse mitotic chromosomes", *Nature*, vol. 535, no. 7611, pp. 308.
- Czermin, B., Melfi, R., McCabe, D., Seitz, V., Imhof, A. & Pirrotta, V. 2002, "Drosophila enhancer of Zeste/ESC complexes have a histone H3 methyltransferase activity that marks chromosomal Polycomb sites", *Cell*, vol. 111, no. 2, pp. 185-196.
- Dai, J. & Higgins, J.M. 2005, "Haspin: a mitotic histone kinase required for metaphase chromosome alignment", *Cell cycle*, vol. 4, no. 5, pp. 665-668.
- Daujat, S., Weiss, T., Mohn, F., Lange, U.C., Ziegler-Birling, C., Zeissler, U., Lappe, M., Schübeler, D., Torres-Padilla, M. & Schneider, R. 2009, "H3K64 trimethylation marks heterochromatin and is dynamically remodeled during developmental reprogramming", *Nature structural & molecular biology*, vol. 16, no. 7, pp. 777.
- Dawson, M.A., Bannister, A.J., Göttgens, B., Foster, S.D., Bartke, T., Green, A.R. & Kouzarides, T. 2009a, "JAK2 phosphorylates histone H3Y41 and excludes HP1 α from chromatin", *Nature*, vol. 461, no. 7265, pp. 819.
- Dawson, M.A., Bannister, A.J., Göttgens, B., Foster, S.D., Bartke, T., Green, A.R. & Kouzarides, T. 2009b, "JAK2 phosphorylates histone H3Y41 and excludes HP1 α from chromatin", *Nature*, vol. 461, no. 7265, pp. 819.
- de Castro, I.J., Budzak, J., Di Giacinto, M.L., Ligammari, L., Gokhan, E., Spanos, C., Moralli, D., Richardson, C., de Las Heras, J I, Salatino, S., Schirmer, E.C., Ullman, K.S., Bickmore, W.A., Green, C., Rappsilber, J., Lambie, S., Goldberg, M.W., Vinciotti, V. & Vagnarelli, P. 2017, "Repo-Man/PP1 regulates heterochromatin formation in interphase", *Nature communications*, vol. 8, pp. 14048.
- De Koning, L., Savignoni, A., Boumendil, C., Rehman, H., Asselain, B., Sastre-Garau, X. & Almouzni, G. 2009, "Heterochromatin protein 1 α : a hallmark of cell proliferation relevant to clinical oncology", *EMBO molecular medicine*, vol. 1, no. 3, pp. 178-191.
- De Wit, E., Greil, F. and van Steensel, B., 2007. "High-resolution mapping reveals links of HP1 with active and inactive chromatin components", *PLoS genetics*, 3(3).
- Dekker, J., Rippe, K., Dekker, M. & Kleckner, N. 2002, "Capturing chromosome conformation", *Science*, vol. 295, no. 5558, pp. 1306-1311.

- Deleris, A., Stroud, H., Bernatavichute, Y., Johnson, E., Klein, G., Schubert, D. & Jacobsen, S.E. 2012, "Loss of the DNA methyltransferase MET1 Induces H3K9 hypermethylation at PcG target genes and redistribution of H3K27 trimethylation to transposons in *Arabidopsis thaliana*", *PLoS genetics*, vol. 8, no. 11, pp. e1003062.
- Dixon, J.R., Selvaraj, S., Yue, F., Kim, A., Li, Y., Shen, Y., Hu, M., Liu, J.S. & Ren, B. 2012, "Topological domains in mammalian genomes identified by analysis of chromatin interactions", *Nature*, vol. 485, no. 7398, pp. 376.
- Domaschenz, R., Kurscheid, S., Nekrasov, M., Han, S. & Tremethick, D.J. 2017, "The histone variant H2A. Z is a master regulator of the epithelial-mesenchymal transition", *Cell reports*, vol. 21, no. 4, pp. 943-952.
- Douet, J., Corujo, D., Malinverni, R., Renaud, J., Sansoni, V., Marjanović, M.P., Cantariño, N., Valero, V., Mongelard, F. & Bouvet, P. 2017, "MacroH2A histone variants maintain nuclear organization and heterochromatin architecture", *J Cell Sci*, vol. 130, no. 9, pp. 1570-1582.
- Doyon, Y. & Côté, J. 2004, "The highly conserved and multifunctional NuA4 HAT complex", *Current opinion in genetics & development*, vol. 14, no. 2, pp. 147-154.
- Draker, R., Sarcinella, E. & Cheung, P. 2011, "USP10 deubiquitylates the histone variant H2A. Z and both are required for androgen receptor-mediated gene activation", *Nucleic acids research*, vol. 39, no. 9, pp. 3529-3542.
- Dronamraju, R., Ramachandran, S., Jha, D.K., Adams, A.T., DiFiore, J.V., Parra, M.A., Dokholyan, N.V. & Strahl, B.D. 2017, "Redundant Functions for Nap1 and Chz1 in H2A. Z Deposition", *Scientific reports*, vol. 7, no. 1, pp. 10791.
- Dryhurst, D., Ishibashi, T., Rose, K.L., Eirín-López, J.M., McDonald, D., Silva-Moreno, B., Veldhoen, N., Helbing, C.C., Hendzel, M.J. & Shabanowitz, J. 2009, "Characterization of the histone H2A. Z-1 and H2A. Z-2 isoforms in vertebrates", *BMC biology*, vol. 7, no. 1, pp. 86.
- Dunlevy, K.L., Medvedeva, V., Wilson, J.E., Hoque, M., Pellegrin, T., Maynard, A., Kremp, M.M., Wasserman, J.S., Poleshko, A. & Katz, R.A. 2019, "The PPR14 heterochromatin tether encodes modular domains that mediate and regulate nuclear lamina targeting", *bioRxiv*, , pp. 788356.
- Dunn, C.J., Sarkar, P., Bailey, E.R., Farris, S., Zhao, M., Ward, J.M., Dudek, S.M. & Saha, R.N. 2017, "Histone hypervariants H2A. Z. 1 and H2A. Z. 2 play independent and context-specific roles in neuronal activity-induced transcription of *Arc/Arg3. 1* and other immediate early genes", *eNeuro*, vol. 4, no. 4.
- Egloff, M., Johnson, D.F., Moorhead, G., Cohen, P.T., Cohen, P. & Barford, D. 1997, "Structural basis for the recognition of regulatory subunits by the catalytic subunit of protein phosphatase 1", *The EMBO journal*, vol. 16, no. 8, pp. 1876-1887.

- El-Brolosy, M.A., Kontarakis, Z., Rossi, A., Kuenne, C., Guenther, S., Fukuda, N., Kikhi, K., Boezio, G.L., Takacs, C.M. & Lai, S. 2019, "Genetic compensation triggered by mutant mRNA degradation", *Nature*, vol. 568, no. 7751, pp. 193.
- El-Brolosy, M.A. & Stainier, D.Y. 2017, "Genetic compensation: a phenomenon in search of mechanisms", *PLoS genetics*, vol. 13, no. 7, pp. e1006780.
- Eltsov, M., MacLellan, K.M., Maeshima, K., Frangakis, A.S. & Dubochet, J. 2008, "Analysis of cryo-electron microscopy images does not support the existence of 30-nm chromatin fibers in mitotic chromosomes in situ", *Proceedings of the National Academy of Sciences*, vol. 105, no. 50, pp. 19732-19737.
- Faast, R., Thonglairoam, V., Schulz, T.C., Beall, J., Wells, J.R., Taylor, H., Matthaei, K., Rathjen, P.D., Tremethick, D.J. & Lyons, I. 2001, "Histone variant H2A. Z is required for early mammalian development", *Current Biology*, vol. 11, no. 15, pp. 1183-1187.
- Fagerberg, L., Hallström, B.M., Oksvold, P., Kampf, C., Djureinovic, D., Odeberg, J., Habuka, M., Tahmasebpour, S., Danielsson, A. & Edlund, K. 2014, "Analysis of the human tissue-specific expression by genome-wide integration of transcriptomics and antibody-based proteomics", *Molecular & Cellular Proteomics*, vol. 13, no. 2, pp. 397-406.
- Fan, J.Y., Rangasamy, D., Luger, K. & Tremethick, D.J. 2004, "H2A. Z alters the nucleosome surface to promote HP1 α -mediated chromatin fiber folding", *Molecular cell*, vol. 16, no. 4, pp. 655-661.
- Fanti, L., Berloco, M., Piacentini, L. & Pimpinelli, S. 2003, "Chromosomal distribution of heterochromatin protein 1 (HP1) in *Drosophila*: a cytological map of euchromatic HP1 binding sites", *Genetica*, vol. 117, no. 2-3, pp. 135-147.
- Figueiredo, M.L., Philip, P., Stenberg, P. & Larsson, J. 2012, "HP1a recruitment to promoters is independent of H3K9 methylation in *Drosophila melanogaster*", *PLoS genetics*, vol. 8, no. 11, pp. e1003061.
- Fischle, W., Tseng, B.S., Dormann, H.L., Ueberheide, B.M., Garcia, B.A., Shabanowitz, J., Hunt, D.F., Funabiki, H. & Allis, C.D. 2005, "Regulation of HP1-chromatin binding by histone H3 methylation and phosphorylation", *Nature*, vol. 438, no. 7071, pp. 1116.
- Fraser, P. & Bickmore, W. 2007, "Nuclear organization of the genome and the potential for gene regulation", *Nature*, vol. 447, no. 7143, pp. 413.
- Fussner, E., Strauss, M., Djuric, U., Li, R., Ahmed, K., Hart, M., Ellis, J. & Bazett-Jones, D.P. 2012, "Open and closed domains in the mouse genome are configured as 10-nm chromatin fibres", *EMBO reports*, vol. 13, no. 11, pp. 992-996.
- Gan, L., Ladinsky, M.S. & Jensen, G.J. 2013, "Chromatin in a marine picoeukaryote is a disordered assemblage of nucleosomes", *Chromosoma*, vol. 122, no. 5, pp. 377-386.

- Gauchier, M., Kan, S., Barral, A., Sauzet, S., Agirre, E., Bonnell, E., Saksouk, N., Barth, T.K., Ide, S., Urbach, S. and Wellinger, R.J., 2019. "SETDB1-dependent heterochromatin stimulates alternative lengthening of telomeres", *Science advances*, 5(5), p.eaav3673.
- Gévry, N., Chan, H.M., Laflamme, L., Livingston, D.M. & Gaudreau, L. 2007, "p21 transcription is regulated by differential localization of histone H2A. Z", *Genes & development*, vol. 21, no. 15, pp. 1869-1881.
- Gévry, N., Hardy, S., Jacques, P., Laflamme, L., Svtelis, A., Robert, F. & Gaudreau, L. 2009, "Histone H2A. Z is essential for estrogen receptor signaling", *Genes & development*, vol. 23, no. 13, pp. 1522-1533.
- Gaiimo, B.D., Ferrante, F., Vallejo, D.M., Hein, K., Gutierrez-Perez, I., Nist, A., Stiewe, T., Mittler, G., Herold, S. & Zimmermann, T. 2018, "Histone variant H2A. Z deposition and acetylation directs the canonical Notch signaling response", *Nucleic acids research*, vol. 46, no. 16, pp. 8197-8215.
- Gil, R.S. & Vagnarelli, P. 2018, "Protein phosphatases in chromatin structure and function", *Biochimica et Biophysica Acta (BBA)-Molecular Cell Research*, .
- Gilchrist, S., Gilbert, N., Perry, P. & Bickmore, W.A. 2004, "Nuclear organization of centromeric domains is not perturbed by inhibition of histone deacetylases", *Chromosome Research*, vol. 12, no. 5, pp. 505-516.
- Goll, M.G. & Halpern, M.E. 2011, "DNA methylation in zebrafish" in *Progress in molecular biology and translational science* Elsevier, , pp. 193-218.
- Gong, L., Govan, J.M., Evans, E.B., Dai, H., Wang, E., Lee, S., Lin, H., Lazar, A.J., Mills, G.B. & Lin, S. 2015a, "Nuclear PTEN tumor-suppressor functions through maintaining heterochromatin structure", *Cell cycle*, vol. 14, no. 14, pp. 2323-2332.
- Gong, L., Govan, J.M., Evans, E.B., Dai, H., Wang, E., Lee, S., Lin, H., Lazar, A.J., Mills, G.B. & Lin, S. 2015b, "Nuclear PTEN tumor-suppressor functions through maintaining heterochromatin structure", *Cell cycle*, vol. 14, no. 14, pp. 2323-2332.
- Gong, L., Govan, J.M., Evans, E.B., Dai, H., Wang, E., Lee, S., Lin, H., Lazar, A.J., Mills, G.B. & Lin, S. 2015c, "Nuclear PTEN tumor-suppressor functions through maintaining heterochromatin structure", *Cell cycle*, vol. 14, no. 14, pp. 2323-2332.
- Gonzalez-Munoz, E., Arboleda-Estudillo, Y., Chanumolu, S.K., Otu, H.H. & Cibelli, J.B. 2019, "Zebrafish macroH2A variants have distinct embryo localization and function", *Scientific reports*, vol. 9, no. 1, pp. 1-17.
- Gonzalez-Sandoval, A., Towbin, B.D., Kalck, V., Cabianga, D.S., Gaidatzis, D., Hauer, M.H., Geng, L., Wang, L., Yang, T. & Wang, X. 2015, "Perinuclear anchoring of H3K9-methylated chromatin stabilizes induced cell fate in *C. elegans* embryos", *Cell*, vol. 163, no. 6, pp. 1333-1347.

- Gonzalo, S., García-Cao, M., Fraga, M.F., Schotta, G., Peters, A.H., Cotter, S.E., Eguía, R., Dean, D.C., Esteller, M. & Jenuwein, T. 2005, "Role of the RB1 family in stabilizing histone methylation at constitutive heterochromatin", *Nature cell biology*, vol. 7, no. 4, pp. 420.
- Goto, H., Tomono, Y., Ajiro, K., Kosako, H., Fujita, M., Sakurai, M., Okawa, K., Iwamatsu, A., Okigaki, T. & Takahashi, T. 1999, "Identification of a novel phosphorylation site on histone H3 coupled with mitotic chromosome condensation", *Journal of Biological Chemistry*, vol. 274, no. 36, pp. 25543-25549.
- Greaves, I.K., Rangasamy, D., Ridgway, P. & Tremethick, D.J. 2007, "H2A. Z contributes to the unique 3D structure of the centromere", *Proceedings of the National Academy of Sciences*, vol. 104, no. 2, pp. 525-530.
- Guelen, L., Pagie, L., Brasset, E., Meuleman, W., Faza, M.B., Talhout, W., Eussen, B.H., de Klein, A., Wessels, L. & de Laat, W. 2008, "Domain organization of human chromosomes revealed by mapping of nuclear lamina interactions", *Nature*, vol. 453, no. 7197, pp. 948.
- Guillemette, B., Bataille, A.R., Gévry, N., Adam, M., Blanchette, M., Robert, F. & Gaudreau, L. 2005, "Variant histone H2A. Z is globally localized to the promoters of inactive yeast genes and regulates nucleosome positioning", *PLoS biology*, vol. 3, no. 12, pp. e384.
- Haarhuis, J.H., van der Weide, R.H., Blomen, V.A., Yáñez-Cuna, J.O., Amendola, M., van Ruiten, M.S., Krijger, P.H., Teunissen, H., Medema, R.H., van Steensel, B. and Brummelkamp, T.R., 2017. "The cohesin release factor WAPL restricts chromatin loop extension", *Cell*, 169(4), pp.693-707.
- Hadjur, S., Williams, L.M., Ryan, N.K., Cobb, B.S., Sexton, T., Fraser, P., Fisher, A.G. & Merkenschlager, M. 2009, "Cohesins form chromosomal cis-interactions at the developmentally regulated IFNG locus", *Nature*, vol. 460, no. 7253, pp. 410.
- Hagarman, J.A., Motley, M.P., Kristjansdottir, K. & Soloway, P.D. 2013, "Coordinate regulation of DNA methylation and H3K27me3 in mouse embryonic stem cells", *PLoS one*, vol. 8, no. 1, pp. e53880.
- Hale, T.K., Contreras, A., Morrison, A.J. & Herrera, R.E. 2006, "Phosphorylation of the linker histone H1 by CDK regulates its binding to HP1 α ", *Molecular cell*, vol. 22, no. 5, pp. 693-699.
- Halmer, L. & Gruss, C. 1996, "Effects of cell cycle dependent histone H1 phosphorylation on chromatin structure and chromatin replication", *Nucleic acids research*, vol. 24, no. 8, pp. 1420-1427.
- Hardy, S., Jacques, P., Gévry, N., Forest, A., Fortin, M., Laflamme, L., Gaudreau, L. & Robert, F. 2009, "The euchromatic and heterochromatic landscapes are shaped by antagonizing effects of transcription on H2A. Z deposition", *PLoS genetics*, vol. 5, no. 10, pp. e1000687.

- Hatch, C.L. & Bonner, W.M. 1990, "The human histone H2A. Z gene. Sequence and regulation.", *Journal of Biological Chemistry*, vol. 265, no. 25, pp. 15211-15218.
- He, Y., Tang, D., Li, W., Chai, R. & Li, H. 2016, "Histone deacetylase 1 is required for the development of the zebrafish inner ear", *Scientific reports*, vol. 6, pp. 16535.
- Hendrickx, A., Beullens, M., Ceulemans, H., Den Abt, T., Van Eynde, A., Nicolaescu, E., Lesage, B. & Bollen, M. 2009, "Docking motif-guided mapping of the interactome of protein phosphatase-1", *Chemistry & biology*, vol. 16, no. 4, pp. 365-371.
- Henzel, M.J., Wei, Y., Mancini, M.A., Van Hooser, A., Ranalli, T., Brinkley, B.R., Bazett-Jones, D.P. & Allis, C.D. 1997, "Mitosis-specific phosphorylation of histone H3 initiates primarily within pericentromeric heterochromatin during G2 and spreads in an ordered fashion coincident with mitotic chromosome condensation", *Chromosoma*, vol. 106, no. 6, pp. 348-360.
- Heroes, E., Lesage, B., Görnemann, J., Beullens, M., Van Meervelt, L. & Bollen, M. 2013, "The PP1 binding code: a molecular-lego strategy that governs specificity", *The FEBS journal*, vol. 280, no. 2, pp. 584-595.
- Hiragami-Hamada, K., Shinmyozu, K., Hamada, D., Tatsu, Y., Uegaki, K., Fujiwara, S. & Nakayama, J. 2011, "N-terminal phosphorylation of HP1 α promotes its chromatin binding", *Molecular and cellular biology*, vol. 31, no. 6, pp. 1186-1200.
- Hiragami-Hamada, K., Soeroes, S., Nikolov, M., Wilkins, B., Kreuz, S., Chen, C., Inti, A., Zenn, H.M., Kost, N. & Pohl, W. 2016, "Dynamic and flexible H3K9me3 bridging via HP1 β dimerization establishes a plastic state of condensed chromatin", *Nature communications*, vol. 7, pp. 11310.
- Hong, J., Feng, H., Wang, F., Ranjan, A., Chen, J., Jiang, J., Ghirlando, R., Xiao, T.S., Wu, C. & Bai, Y. 2014, "The catalytic subunit of the SWR1 remodeler is a histone chaperone for the H2A. Z-H2B dimer", *Molecular cell*, vol. 53, no. 3, pp. 498-505.
- Horigome, C., Oma, Y., Konishi, T., Schmid, R., Marcomini, I., Hauer, M.H., Dion, V., Harata, M. & Gasser, S.M. 2014, "SWR1 and INO80 chromatin remodelers contribute to DNA double-strand break perinuclear anchorage site choice", *Molecular cell*, vol. 55, no. 4, pp. 626-639.
- Horikoshi, N., Sato, K., Shimada, K., Arimura, Y., Osakabe, A., Tachiwana, H., Hayashi-Takanaka, Y., Iwasaki, W., Kagawa, W. & Harata, M. 2013, "Structural polymorphism in the L1 loop regions of human H2A. Z. 1 and H2A. Z. 2", *Acta Crystallographica Section D: Biological Crystallography*, vol. 69, no. 12, pp. 2431-2439.
- Horsley, D., Hutchings, A., Butcher, G.W. & Singh, P.B. 1996, "M32, a murine homologue of Drosophila heterochromatin protein 1 (HP1), localises to euchromatin within interphase nuclei and is largely excluded from constitutive heterochromatin", *Cytogenetic and Genome Research*, vol. 73, no. 4, pp. 308-311.

- Hsu, J., Sun, Z., Li, X., Reuben, M., Tatchell, K., Bishop, D.K., Grushcow, J.M., Brame, C.J., Caldwell, J.A. & Hunt, D.F. 2000, "Mitotic phosphorylation of histone H3 is governed by Ipl1/aurora kinase and Glc7/PP1 phosphatase in budding yeast and nematodes", *Cell*, vol. 102, no. 3, pp. 279-291.
- Hu, G., Cui, K., Northrup, D., Liu, C., Wang, C., Tang, Q., Ge, K., Levens, D., Crane-Robinson, C. & Zhao, K. 2013, "H2A. Z facilitates access of active and repressive complexes to chromatin in embryonic stem cell self-renewal and differentiation", *Cell stem cell*, vol. 12, no. 2, pp. 180-192.
- Hu, Z., Holzschuh, J. & Driever, W. 2015, "Loss of DDB1 leads to transcriptional p53 pathway activation in proliferating cells, cell cycle deregulation, and apoptosis in zebrafish embryos", *PLoS one*, vol. 10, no. 7, pp. e0134299.
- Hua, S., Kallen, C.B., Dhar, R., Baquero, M.T., Mason, C.E., Russell, B.A., Shah, P.K., Liu, J., Khramtsov, A. & Tretiakova, M.S. 2008, "Genomic analysis of estrogen cascade reveals histone variant H2A. Z associated with breast cancer progression", *Molecular systems biology*, vol. 4, no. 1.
- Hurley, T.D., Yang, J., Zhang, L., Goodwin, K.D., Zou, Q., Cortese, M., Dunker, A.K. & DePaoli-Roach, A.A. 2007, "Structural basis for regulation of protein phosphatase 1 by inhibitor-2", *Journal of Biological Chemistry*, vol. 282, no. 39, pp. 28874-28883.
- Illingworth, R.S., Botting, C.H., Grimes, G.R., Bickmore, W.A. & Eskeland, R. 2012, "PRC1 and PRC2 are not required for targeting of H2A. Z to developmental genes in embryonic stem cells", *PLoS one*, vol. 7, no. 4, pp. e34848.
- Inoue, A., Hyle, J., Lechner, M.S. & Lahti, J.M. 2008, "Perturbation of HP1 localization and chromatin binding ability causes defects in sister-chromatid cohesion", *Mutation Research/Genetic Toxicology and Environmental Mutagenesis*, vol. 657, no. 1, pp. 48-55.
- Jackson, J.D. & Gorovsky, M.A. 2000, "Histone H2A. Z has a conserved function that is distinct from that of the major H2A sequence variants", *Nucleic acids research*, vol. 28, no. 19, pp. 3811-3816.
- Jacobs, S.A. & Khorasanizadeh, S. 2002, "Structure of HP1 chromodomain bound to a lysine 9-methylated histone H3 tail", *Science*, vol. 295, no. 5562, pp. 2080-2083.
- Jamieson, K., Wiles, E.T., McNaught, K.J., Sidoli, S., Leggett, N., Shao, Y., Garcia, B.A. & Selker, E.U. 2016, "Loss of HP1 causes depletion of H3K27me3 from facultative heterochromatin and gain of H3K27me2 at constitutive heterochromatin", *Genome research*, vol. 26, no. 1, pp. 97-107.
- Jeronimo, C., Watanabe, S., Kaplan, C.D., Peterson, C.L. & Robert, F. 2015, "The histone chaperones FACT and Spt6 restrict H2A. Z from intragenic locations", *Molecular cell*, vol. 58, no. 6, pp. 1113-1123.

- Jeyapragash, A.A., Klein, U.R., Lindner, D., Ebert, J., Nigg, E.A. & Conti, E. 2007, "Structure of a Survivin–Borealin–INCENP core complex reveals how chromosomal passengers travel together", *Cell*, vol. 131, no. 2, pp. 271-285.
- Jin, C., Zang, C., Wei, G., Cui, K., Peng, W., Zhao, K. and Felsenfeld, G., 2009. "H3. 3/H2A. Z double variant-containing nucleosomes mark 'nucleosome-free regions' of active promoters and other regulatory regions", *Nature genetics*, 41(8), p.941.
- Jones, D.O., Cowell, I.G. & Singh, P.B. 2000, "Mammalian chromodomain proteins: their role in genome organisation and expression", *Bioessays*, vol. 22, no. 2, pp. 124-137.
- Junqueira, L.C. & Mescher, A.L. 2013, *Junqueira's basic histology: text & atlas/Anthony L. Mescher*. New York [etc.]: McGraw-Hill Medical,.
- Kalocsay, M., Hiller, N.J. & Jentsch, S. 2009, "Chromosome-wide Rad51 spreading and SUMO-H2A. Z-dependent chromosome fixation in response to a persistent DNA double-strand break", *Molecular cell*, vol. 33, no. 3, pp. 335-343.
- Kametaka, A., Takagi, M., Hayakawa, T., Haraguchi, T., Hiraoka, Y. & Yoneda, Y. 2002, "Interaction of the chromatin compaction-inducing domain (LR domain) of Ki-67 antigen with HP1 proteins", *Genes to Cells*, vol. 7, no. 12, pp. 1231-1242.
- Kane, D.A. & Kimmel, C.B. 1993, "The zebrafish midblastula transition", *Development*, vol. 119, no. 2, pp. 447-456.
- Kelly, A.E., Ghenuiu, C., Xue, J.Z., Zierhut, C., Kimura, H. & Funabiki, H. 2010, "Survivin reads phosphorylated histone H3 threonine 3 to activate the mitotic kinase Aurora B", *Science*, vol. 330, no. 6001, pp. 235-239.
- Keogh, M., Mennella, T.A., Sawa, C., Berthelet, S., Krogan, N.J., Wolek, A., Podolny, V., Carpenter, L.R., Greenblatt, J.F. & Baetz, K. 2006, "The *Saccharomyces cerevisiae* histone H2A variant Htz1 is acetylated by NuA4", *Genes & development*, vol. 20, no. 6, pp. 660-665.
- Kim, K., Punj, V., Choi, J., Heo, K., Kim, J., Laird, P.W. & An, W. 2013, "Gene dysregulation by histone variant H2A. Z in bladder cancer", *Epigenetics & chromatin*, vol. 6, no. 1, pp. 34.
- Klein, U.R., Nigg, E.A. & Gruneberg, U. 2006, "Centromere targeting of the chromosomal passenger complex requires a ternary subcomplex of Borealin, Survivin, and the N-terminal domain of INCENP", *Molecular biology of the cell*, vol. 17, no. 6, pp. 2547-2558.
- Kobor, M.S., Venkatasubrahmanyam, S., Meneghini, M.D., Gin, J.W., Jennings, J.L., Link, A.J., Madhani, H.D. & Rine, J. 2004, "A protein complex containing the conserved Swi2/Snf2-related ATPase Swr1p deposits histone variant H2A. Z into euchromatin", *PLoS biology*, vol. 2, no. 5, pp. e131.

- Kohwi, M., Lupton, J.R., Lai, S., Miller, M.R. & Doe, C.Q. 2013, "Developmentally regulated subnuclear genome reorganization restricts neural progenitor competence in *Drosophila*", *Cell*, vol. 152, no. 1-2, pp. 97-108.
- Kourmouli, N., Jeppesen, P., Mahadevhaiah, S., Burgoyne, P., Wu, R., Gilbert, D.M., Bongiorno, S., Prantera, G., Fanti, L. & Pimpinelli, S. 2004, "Heterochromatin and trimethylated lysine 20 of histone H4 in animals", *Journal of cell science*, vol. 117, no. 12, pp. 2491-2501.
- Krasnoselsky, A.L., Whiteford, C.C., Wei, J.S., Bilke, S., Westermann, F., Chen, Q. & Khan, J. 2005, "Altered expression of cell cycle genes distinguishes aggressive neuroblastoma", *Oncogene*, vol. 24, no. 9, pp. 1533.
- Ku, M., Jaffe, J.D., Koche, R.P., Rheinbay, E., Endoh, M., Koseki, H., Carr, S.A. & Bernstein, B.E. 2012, "H2A. Z landscapes and dual modifications in pluripotent and multipotent stem cells underlie complex genome regulatory functions", *Genome biology*, vol. 13, no. 10, pp. R85.
- Kueng, S., Hegemann, B., Peters, B.H., Lipp, J.J., Schleiffer, A., Mechtler, K. and Peters, J.M., 2006. "Wapl controls the dynamic association of cohesin with chromatin", *Cell*, 127(5), pp.955-967.
- Kumar, G.S., Gokhan, E., De Munter, S., Bollen, M., Vagnarelli, P., Peti, W. & Page, R. 2016, "The Ki-67 and RepoMan mitotic phosphatases assemble via an identical, yet novel mechanism", *eLife*, vol. 5, pp. 10.7554/eLife.16539.
- Küpper, K., Kölbl, A., Biener, D., Dittrich, S., von Hase, J., Thormeyer, T., Fiegler, H., Carter, N.P., Speicher, M.R. & Cremer, T. 2007, "Radial chromatin positioning is shaped by local gene density, not by gene expression", *Chromosoma*, vol. 116, no. 3, pp. 285-306.
- Kurz, A., Lampel, S., Nickolenko, J.E., Bradl, J., Benner, A., Zirbel, R.M., Cremer, T. & Lichter, P. 1996, "Active and inactive genes localize preferentially in the periphery of chromosome territories.", *The Journal of cell biology*, vol. 135, no. 5, pp. 1195-1205.
- Kuzmichev, A., Nishioka, K., Erdjument-Bromage, H., Tempst, P. & Reinberg, D. 2002, "Histone methyltransferase activity associated with a human multiprotein complex containing the Enhancer of Zeste protein", *Genes & development*, vol. 16, no. 22, pp. 2893-2905.
- Lachner, M., O'carroll, D., Rea, S., Mechtler, K. & Jenuwein, T. 2001, "Methylation of histone H3 lysine 9 creates a binding site for HP1 proteins", *Nature*, vol. 410, no. 6824, pp. 116-120.
- Lachner, M., O'Carroll, D., Rea, S., Mechtler, K. & Jenuwein, T. 2001, "Methylation of histone H3 lysine 9 creates a binding site for HP1 proteins", *Nature*, vol. 410, no. 6824, pp. 116.

- Landsverk, H.B., Kirkhus, M., Bollen, M., Küntziger, T. & Collas, P. 2005, "PNUTS enhances in vitro chromosome decondensation in a PP1-dependent manner", *Biochemical Journal*, vol. 390, no. 3, pp. 709-717.
- Lanzuolo, C., Sardo, F.L. and Adamo Diamantini, V.O., 2011. "PcG complexes set the stage for epigenetic inheritance of gene silencing in early S phase before replication", *PLoS genetics*, 7(11).
- Larson, A.G., Elnatan, D., Keenen, M.M., Trnka, M.J., Johnston, J.B., Burlingame, A.L., Agard, D.A., Redding, S. & Narlikar, G.J. 2017, "Liquid droplet formation by HP1 α suggests a role for phase separation in heterochromatin", *Nature*, vol. 547, no. 7662, pp. 236.
- Latrick, C.M., Marek, M., Ouarrhni, K., Papin, C., Stoll, I., Ignatyeva, M., Obri, A., Ennifar, E., Dimitrov, S. & Romier, C. 2016, "Molecular basis and specificity of H2A. Z-H2B recognition and deposition by the histone chaperone YL1", *Nature structural & molecular biology*, vol. 23, no. 4, pp. 309.
- Laue, K., Rajshekar, S., Courtney, A.J., Lewis, Z.A. & Goll, M.G. 2019, "The maternal to zygotic transition regulates genome-wide heterochromatin establishment in the zebrafish embryo", *Nature communications*, vol. 10, no. 1, pp. 1551.
- Lavigne, M., Eskeland, R., Azebi, S., Saint-André, V., Jang, S.M., Batsché, E., Fan, H., Kingston, R.E., Imhof, A. & Muchardt, C. 2009, "Interaction of HP1 and Brg1/Brm with the globular domain of histone H3 is required for HP1-mediated repression", *PLoS genetics*, vol. 5, no. 12, pp. e1000769.
- Lenain, C., de Graaf, C.A., Pagie, L., Visser, N.L., de Haas, M., de Vries, S.S., Peric-Hupkes, D., van Steensel, B. & Peeper, D.S. 2017, "Massive reshaping of genome–nuclear lamina interactions during oncogene-induced senescence", *Genome research*, vol. 27, no. 10, pp. 1634-1644.
- Li, B., Pattenden, S.G., Lee, D., Gutiérrez, J., Chen, J., Seidel, C., Gerton, J. & Workman, J.L. 2005, "Preferential occupancy of histone variant H2AZ at inactive promoters influences local histone modifications and chromatin remodeling", *Proceedings of the National Academy of Sciences*, vol. 102, no. 51, pp. 18385-18390.
- Li, L.C., 2014. "Chromatin remodeling by the small RNA machinery in mammalian cells", *Epigenetics*, 9(1), pp.45-52.
- Lieberman-Aiden, E., Van Berkum, N.L., Williams, L., Imakaev, M., Ragoczy, T., Telling, A., Amit, I., Lajoie, B.R., Sabo, P.J. & Dorschner, M.O. 2009, "Comprehensive mapping of long-range interactions reveals folding principles of the human genome", *Science*, vol. 326, no. 5950, pp. 289-293.
- Lin, X., Ammosova, T., Kumari, N. & Nekhai, S. 2017, "Protein phosphatase-1-targeted small molecules, iron chelators and curcumin analogs as HIV-1 antivirals", *Current pharmaceutical design*, vol. 23, no. 28, pp. 4122-4132.

- Lindeman, L.C., Winata, C.L., Aanes, H., Mathavan, S., Aleström, P. & Collas, P. 2010, "Chromatin states of developmentally-regulated genes revealed by DNA and histone methylation patterns in zebrafish embryos", *International Journal of Developmental Biology*, vol. 54, no. 5, pp. 803-813.
- Lindroth, A.M., Park, Y.J., McLean, C.M., Dokshin, G.A., Persson, J.M., Herman, H., Pasini, D., Miro, X., Donohoe, M.E. & Lee, J.T. 2008, "Antagonism between DNA and H3K27 methylation at the imprinted Rasgrf1 locus", *PLoS genetics*, vol. 4, no. 8, pp. e1000145.
- Liu, X., Song, Z., Huo, Y., Zhang, J., Zhu, T., Wang, J., Zhao, X., Aikhionbare, F., Zhang, J. & Duan, H. 2014, "Chromatin protein HP1 α interacts with the mitotic regulator borealin protein and specifies the centromere localization of the chromosomal passenger complex", *Journal of Biological Chemistry*, vol. 289, no. 30, pp. 20638-20649.
- Luk, E., Ranjan, A., FitzGerald, P.C., Mizuguchi, G., Huang, Y., Wei, D. & Wu, C. 2010, "Stepwise histone replacement by SWR1 requires dual activation with histone H2A. Z and canonical nucleosome", *Cell*, vol. 143, no. 5, pp. 725-736.
- Luk, E., Vu, N., Patteson, K., Mizuguchi, G., Wu, W., Ranjan, A., Backus, J., Sen, S., Lewis, M. & Bai, Y. 2007, "Chz1, a nuclear chaperone for histone H2AZ", *Molecular cell*, vol. 25, no. 3, pp. 357-368.
- Machida, S., Takizawa, Y., Ishimaru, M., Sugita, Y., Sekine, S., Nakayama, J., Wolf, M. & Kurumizaka, H. 2018, "Structural basis of heterochromatin formation by human HP1", *Molecular cell*, vol. 69, no. 3, pp. 38-397. e8.
- Madakashira, B., Corbett, L., Zhang, C., Paoli, P., Casement, J.W., Mann, J., Sadler, K.C. & Mann, D.A. 2017, "Variant Histone H2afv reprograms DNA methylation during early zebrafish development", *Epigenetics*, vol. 12, no. 9, pp. 811-824.
- Mahy, N.L., Perry, P.E. & Bickmore, W.A. 2002, "Gene density and transcription influence the localization of chromatin outside of chromosome territories detectable by FISH", *J Cell Biol*, vol. 159, no. 5, pp. 753-763.
- Mahy, N.L., Perry, P.E., Gilchrist, S., Baldock, R.A. & Bickmore, W.A. 2002, "Spatial organization of active and inactive genes and noncoding DNA within chromosome territories", *J Cell Biol*, vol. 157, no. 4, pp. 579-589.
- Maison, C., Bailly, D., Peters, A.H., Quivy, J.P., Roche, D., Taddei, A., Lachner, M., Jenuwein, T. and Almouzni, G., 2002. "Higher-order structure in pericentric heterochromatin involves a distinct pattern of histone modification and an RNA component". *Nature genetics*, 30(3), pp.329-334.
- Maison, C., Bailly, D., Roche, D., de Oca, R.M., Probst, A.V., Vassias, I., Dingli, F., Lombard, B., Loew, D., Quivy, J.P. and Almouzni, G., 2011. "SUMOylation promotes de novo targeting of HP1 α to pericentric heterochromatin". *Nature genetics*, 43(3), p.220.

- Maison, C., Quivy, J.P. and Almouzni, G., 2016. "Suv39h1 links the SUMO pathway to constitutive heterochromatin", *Molecular & cellular oncology*, 3(6), p.e1225546.
- Makrantonis, V. & Marston, A.L. 2018, "Cohesin and chromosome segregation", *Current Biology*, vol. 28, no. 12, pp. R688-R693.
- Margueron, R. & Reinberg, D. 2011, "The Polycomb complex PRC2 and its mark in life", *Nature*, vol. 469, no. 7330, pp. 343.
- Markaki, Y., Christogianni, A., Politou, A.S. & Georgatos, S.D. 2009, "Phosphorylation of histone H3 at Thr3 is part of a combinatorial pattern that marks and configures mitotic chromatin", *Journal of cell science*, vol. 122, no. 16, pp. 2809-2819.
- Martin, C.C., Laforest, L., Akimenko, M. & Ekker, M. 1999, "A role for DNA methylation in gastrulation and somite patterning", *Developmental biology*, vol. 206, no. 2, pp. 189-205.
- Maruyama, E.O., Hori, T., Tanabe, H., Kitamura, H., Matsuda, R., Tone, S., Hozak, P., Habermann, F.A., von Hase, J. & Cremer, C. 2012, "The actin family member Arp6 and the histone variant H2A. Z are required for spatial positioning of chromatin in chicken cell nuclei", *J Cell Sci*, vol. 125, no. 16, pp. 3739-3743.
- Mathieu, O., Probst, A.V. & Paszkowski, J. 2005, "Distinct regulation of histone H3 methylation at lysines 27 and 9 by CpG methylation in Arabidopsis", *The EMBO journal*, vol. 24, no. 15, pp. 2783-2791.
- Matsuda, R., Hori, T., Kitamura, H., Takeuchi, K., Fukagawa, T. & Harata, M. 2010, "Identification and characterization of the two isoforms of the vertebrate H2A. Z histone variant", *Nucleic acids research*, vol. 38, no. 13, pp. 4263-4273.
- McGhee, J.D., Rau, D.C., Charney, E. & Felsenfeld, G. 1980, "Orientation of the nucleosome within the higher order structure of chromatin", *Cell*, vol. 22, no. 1, pp. 87-96.
- Mellone, B.G., Ball, L., Suka, N., Grunstein, M.R., Partridge, J.F. & Allshire, R.C. 2003, "Centromere silencing and function in fission yeast is governed by the amino terminus of histone H3", *Current Biology*, vol. 13, no. 20, pp. 1748-1757.
- Meppelink, A., Kabeche, L., Vromans, M.J., Compton, D.A. & Lens, S.M. 2015, "Shugoshin-1 balances Aurora B kinase activity via PP2A to promote chromosome bi-orientation", *Cell reports*, vol. 11, no. 4, pp. 508-515.
- Mhanni, A.A. & McGowan, R.A. 2004, "Global changes in genomic methylation levels during early development of the zebrafish embryo", *Development genes and evolution*, vol. 214, no. 8, pp. 412-417.
- Michaelis, C., Ciosk, R. & Nasmyth, K. 1997, "Cohesins: chromosomal proteins that prevent premature separation of sister chromatids", *Cell*, vol. 91, no. 1, pp. 35-45.

- Michal, S., Karim, M., Alain, C., Nikolaos, P., Emilien, N., Llères, D., François, G., Susana, P., Liliana, K. & Alexandre, D. 2016, "The cell proliferation antigen Ki-67 organises heterochromatin", *eLife*, vol. 5.
- Minc, E., Courvalin, J. & Buendia, B. 2000, "HP1 γ associates with euchromatin and heterochromatin in mammalian nuclei and chromosomes", *Cytogenetic and Genome Research*, vol. 90, no. 3-4, pp. 279-284.
- Minnebo, N., Görnemann, J., O'Connell, N., Van Dessel, N., Derua, R., Vermunt, M.W., Page, R., Beullens, M., Peti, W. & Van Eynde, A. 2012, "NIPP1 maintains EZH2 phosphorylation and promoter occupancy at proliferation-related target genes", *Nucleic acids research*, vol. 41, no. 2, pp. 842-854.
- Mishra, A. & Hawkins, R.D. 2017, "Three-dimensional genome architecture and emerging technologies: looping in disease", *Genome medicine*, vol. 9, no. 1, pp. 1-14.
- Mizuguchi, G., Shen, X., Landry, J., Wu, W., Sen, S. & Wu, C. 2004, "ATP-driven exchange of histone H2AZ variant catalyzed by SWR1 chromatin remodeling complex", *Science*, vol. 303, no. 5656, pp. 343-348.
- Moorhead, G.B., De Wever, V., Templeton, G. & Kerk, D. 2009, "Evolution of protein phosphatases in plants and animals", *Biochemical Journal*, vol. 417, no. 2, pp. 401-409.
- Morey, C., Da Silva, N.R., Perry, P. & Bickmore, W.A. 2007, "Nuclear reorganisation and chromatin decondensation are conserved, but distinct, mechanisms linked to Hox gene activation", *Development*, vol. 134, no. 5, pp. 909-919.
- Muchardt, C., Guillemé, M., Seeler, J.S., Trouche, D., Dejean, A. and Yaniv, M., 2002. "Coordinated methyl and RNA binding is required for heterochromatin localization of mammalian HP1 α ", *EMBO reports*, 3(10), pp.975-981.
- Mudbhary, R. & Sadler, K.C. 2011, "Epigenetics, development, and cancer: zebrafish make their mark", *Birth Defects Research Part C: Embryo Today: Reviews*, vol. 93, no. 2, pp. 194-203.
- Murphy, P.J., Wu, S.F., James, C.R., Wike, C.L. & Cairns, B.R. 2018, "Placeholder nucleosomes underlie germline-to-embryo DNA methylation reprogramming", *Cell*, vol. 172, no. 5, pp. 99-1006. e13.
- Musacchio, A. & Desai, A. 2017, "A molecular view of kinetochore assembly and function", *Biology*, vol. 6, no. 1, pp. 5.
- Nakayama, J., Rice, J.C., Strahl, B.D., Allis, C.D. & Grewal, S.I. 2001, "Role of histone H3 lysine 9 methylation in epigenetic control of heterochromatin assembly", *Science*, vol. 292, no. 5514, pp. 110-113.

- Narkaj, K., Stefanelli, G., Wahdan, M., Azam, A.B., Ramzan, F., Steininger Jr, Carl Frank David, Walters, B.J. & Zovkic, I.B. 2018, "Blocking H2A. Z incorporation via Tip60 inhibition promotes systems consolidation of fear memory in mice", *eNeuro*, vol. 5, no. 5.
- Nasa, I. and Kettenbach, A.N., 2018. "Coordination of protein kinase and phosphoprotein phosphatase activities in mitosis", *Frontiers in Cell and Developmental Biology*, 6, p.30.
- Németh, A., Conesa, A., Santoyo-Lopez, J., Medina, I., Montaner, D., Péterfia, B., Solovei, I., Cremer, T., Dopazo, J. & Längst, G. 2010, "Initial genomics of the human nucleolus", *PLoS genetics*, vol. 6, no. 3, pp. e1000889.
- Nguyen, V.Q., Ranjan, A., Stengel, F., Wei, D., Aebersold, R., Wu, C. & Leschziner, A.E. 2013, "Molecular architecture of the ATP-dependent chromatin-remodeling complex SWR1", *Cell*, vol. 154, no. 6, pp. 1220-1231.
- Nishibuchi, G. and Déjardin, J., 2017. "The molecular basis of the organization of repetitive DNA-containing constitutive heterochromatin in mammals", *Chromosome Research*, 25(1), pp.77-87.
- Nishibuchi, G., Machida, S., Osakabe, A., Murakoshi, H., Hiragami-Hamada, K., Nakagawa, R., Fischle, W., Nishimura, Y., Kurumizaka, H. & Tagami, H. 2014, "N-terminal phosphorylation of HP1 α increases its nucleosome-binding specificity", *Nucleic acids research*, vol. 42, no. 20, pp. 12498-12511.
- Nishibuchi, I., Suzuki, H., Kinomura, A., Sun, J., Liu, N., Horikoshi, Y., Shima, H., Kusakabe, M., Harata, M. & Fukagawa, T. 2014, "Reorganization of damaged chromatin by the exchange of histone variant H2A. Z-2", *International Journal of Radiation Oncology* Biology* Physics*, vol. 89, no. 4, pp. 736-744.
- Nishibuchi, G., Machida, S., Nakagawa, R., Yoshimura, Y., Hiragami-Hamada, K., Abe, Y., Kurumizaka, H., Tagami, H. and Nakayama, J.I., 2019. "Mitotic phosphorylation of HP1 α regulates its cell cycle-dependent chromatin binding", *The Journal of Biochemistry*, 165(5), pp.433-446.
- Nishiyama, T., Sykora, M.M., Huis, P.J., Mechtler, K. and Peters, J.M., 2013. Aurora B and Cdk1 mediate "Wapl activation and release of acetylated cohesin from chromosomes by phosphorylating Sororin", *Proceedings of the National Academy of Sciences*, 110(33), pp.13404-13409.
- Noma, K., Allis, C.D. & Grewal, S.I. 2001, "Transitions in distinct histone H3 methylation patterns at the heterochromatin domain boundaries", *Science*, vol. 293, no. 5532, pp. 1150-1155.
- Nonaka, N., Kitajima, T., Yokobayashi, S., Xiao, G., Yamamoto, M., Grewal, S.I. and Watanabe, Y., 2002. "Recruitment of cohesin to heterochromatic regions by Swi6/HP1 in fission yeast", *Nature cell biology*, 4(1), pp.89-93.

- Obri, A., Ouararhni, K., Papin, C., Diebold, M., Padmanabhan, K., Marek, M., Stoll, I., Roy, L., Reilly, P.T. & Mak, T.W. 2014, "ANP32E is a histone chaperone that removes H2A. Z from chromatin", *Nature*, vol. 505, no. 7485, pp. 648.
- O'Carroll, D., Erhardt, S., Pagani, M., Barton, S.C., Surani, M.A. & Jenuwein, T. 2001, "The polycomb-group GeneEzh2 is required for early mouse development", *Molecular and cellular biology*, vol. 21, no. 13, pp. 4330-4336.
- O'Connell, N., Nichols, S.R., Heroes, E., Beullens, M., Bollen, M., Peti, W. & Page, R. 2012, "The molecular basis for substrate specificity of the nuclear NIPP1: PP1 holoenzyme", *Structure*, vol. 20, no. 10, pp. 1746-1756.
- Olsen, J.V., Vermeulen, M., Santamaria, A., Kumar, C., Miller, M.L., Jensen, L.J., Gnad, F., Cox, J., Jensen, T.S. & Nigg, E.A. 2010, "Quantitative phosphoproteomics reveals widespread full phosphorylation site occupancy during mitosis", *Sci.Signal.*, vol. 3, no. 104, pp. ra3.
- Parada, L.A., McQueen, P.G. & Misteli, T. 2004, "Tissue-specific spatial organization of genomes", *Genome biology*, vol. 5, no. 7, pp. R44.
- Paro, R. & Hogness, D.S. 1991, "The Polycomb protein shares a homologous domain with a heterochromatin-associated protein of *Drosophila*", *Proceedings of the National Academy of Sciences*, vol. 88, no. 1, pp. 263-267.
- Pasini, D., Malatesta, M., Jung, H.R., Walfridsson, J., Willer, A., Olsson, L., Skotte, J., Wutz, A., Porse, B. & Jensen, O.N. 2010, "Characterization of an antagonistic switch between histone H3 lysine 27 methylation and acetylation in the transcriptional regulation of Polycomb group target genes", *Nucleic acids research*, vol. 38, no. 15, pp. 4958-4969.
- Peng, A., Lewellyn, A.L., Schiemann, W.P. & Maller, J.L. 2010, "Repo-man controls a protein phosphatase 1-dependent threshold for DNA damage checkpoint activation", *Current Biology*, vol. 20, no. 5, pp. 387-396.
- Peric-Hupkes, D., Meuleman, W., Pagie, L., Bruggeman, S.W., Solovei, I., Brugman, W., Gräf, S., Flicek, P., Kerkhoven, R.M. & van Lohuizen, M. 2010, "Molecular maps of the reorganization of genome-nuclear lamina interactions during differentiation", *Molecular cell*, vol. 38, no. 4, pp. 603-613.
- Peters, A.H., Kubicek, S., Mechtler, K., O'Sullivan, R.J., Derijck, A.A., Perez-Burgos, L., Kohlmaier, A., Opravil, S., Tachibana, M. & Shinkai, Y. 2003, "Partitioning and plasticity of repressive histone methylation states in mammalian chromatin", *Molecular cell*, vol. 12, no. 6, pp. 1577-1589.
- Peters, A.H., O'Carroll, D., Scherthan, H., Mechtler, K., Sauer, S., Schöfer, C., Weipoltshammer, K., Pagani, M., Lachner, M. & Kohlmaier, A. 2001, "Loss of the Suv39h histone methyltransferases impairs mammalian heterochromatin and genome stability", *Cell*, vol. 107, no. 3, pp. 323-337.

- Petter, M., Lee, C.C., Byrne, T.J., Boysen, K.E., Volz, J., Ralph, S.A., Cowman, A.F., Brown, G.V. & Duffy, M.F. 2011, "Expression of *P. falciparum* var genes involves exchange of the histone variant H2A. Z at the promoter", *PLoS pathogens*, vol. 7, no. 2, pp. e1001292.
- Poleshko, A., Mansfield, K.M., Burlingame, C.C., Andrade, M.D., Shah, N.R. & Katz, R.A. 2013, "The human protein PRR14 tethers heterochromatin to the nuclear lamina during interphase and mitotic exit", *Cell reports*, vol. 5, no. 2, pp. 292-301.
- Pontvianne, F., Blevins, T., Chandrasekhara, C., Mozgová, I., Hassel, C., Pontes, O.M., Tucker, S., Mokroš, P., Muchová, V. & Fajkus, J. 2013, "Subnuclear partitioning of rRNA genes between the nucleolus and nucleoplasm reflects alternative epiallelic states", *Genes & development*, vol. 27, no. 14, pp. 1545-1550.
- Probst, A.V., Dunleavy, E. & Almouzni, G. 2009, "Epigenetic inheritance during the cell cycle", *Nature reviews Molecular cell biology*, vol. 10, no. 3, pp. 192-206.
- Qian, J., Beullens, M., Huang, J., De Munter, S., Lesage, B. & Bollen, M. 2015, "Cdk1 orders mitotic events through coordination of a chromosome-associated phosphatase switch", *Nature communications*, vol. 6, pp. 10215.
- Qian, J., Beullens, M., Lesage, B. & Bollen, M. 2013, "Aurora B defines its own chromosomal targeting by opposing the recruitment of the phosphatase scaffold Repo-Man", *Current biology : CB*, vol. 23, no. 12, pp. 1136-1143.
- Qian, J., Lesage, B., Beullens, M., Van Eynde, A. & Bollen, M. 2011, "PP1/Repo-man dephosphorylates mitotic histone H3 at T3 and regulates chromosomal aurora B targeting", *Current biology : CB*, vol. 21, no. 9, pp. 766-773.
- Quinodoz, S.A., Ollikainen, N., Tabak, B., Palla, A., Schmidt, J.M., Detmar, E., Lai, M.M., Shishkin, A.A., Bhat, P., Takei, Y. and Trinh, V., 2018. "Higher-order inter-chromosomal hubs shape 3D genome organization in the nucleus", *Cell*, 174(3), pp.744-757.
- Quivy, J.P., Roche, D., Kirschner, D., Tagami, H., Nakatani, Y. and Almouzni, G., 2004. "A CAF-1 dependent pool of HP1 during heterochromatin duplication", *The EMBO journal*, 23(17), pp.3516-3526.
- Ragusa, M.J., Dancheck, B., Critton, D.A., Nairn, A.C., Page, R. & Peti, W. 2010, "Spinophilin directs protein phosphatase 1 specificity by blocking substrate binding sites", *Nature structural & molecular biology*, vol. 17, no. 4, pp. 459.
- Rai, K., Chidester, S., Zavala, C.V., Manos, E.J., James, S.R., Karpf, A.R., Jones, D.A. & Cairns, B.R. 2007, "Dnmt2 functions in the cytoplasm to promote liver, brain, and retina development in zebrafish", *Genes & development*, vol. 21, no. 3, pp. 261-266.
- Rai, K., Jafri, I.F., Chidester, S., James, S.R., Karpf, A.R., Cairns, B.R. & Jones, D.A. 2010, "Dnmt3 and G9a cooperate for tissue-specific development in zebrafish", *Journal of Biological Chemistry*, vol. 285, no. 6, pp. 4110-4121.

- Rai, K., Nadauld, L.D., Chidester, S., Manos, E.J., James, S.R., Karpf, A.R., Cairns, B.R. & Jones, D.A. 2006, "Zebra fish Dnmt1 and Suv39h1 regulate organ-specific terminal differentiation during development", *Molecular and cellular biology*, vol. 26, no. 19, pp. 7077-7085.
- Raisner, R.M., Hartley, P.D., Meneghini, M.D., Bao, M.Z., Liu, C.L., Schreiber, S.L., Rando, O.J. & Madhani, H.D. 2005, "Histone variant H2A. Z marks the 5' ends of both active and inactive genes in euchromatin", *Cell*, vol. 123, no. 2, pp. 233-248.
- Rangasamy, D. 2010, "Histone variant H2A. Z can serve as a new target for breast cancer therapy", *Current medicinal chemistry*, vol. 17, no. 28, pp. 3155-3161.
- Rangasamy, D., Berven, L., Ridgway, P. & Tremethick, D.J. 2003, "Pericentric heterochromatin becomes enriched with H2A. Z during early mammalian development", *The EMBO journal*, vol. 22, no. 7, pp. 1599-1607.
- Rangasamy, D., Greaves, I. & Tremethick, D.J. 2004, "RNA interference demonstrates a novel role for H2A. Z in chromosome segregation", *Nature structural & molecular biology*, vol. 11, no. 7, pp. 650.
- Ranjan, A., Mizuguchi, G., FitzGerald, P.C., Wei, D., Wang, F., Huang, Y., Luk, E., Woodcock, C.L. & Wu, C. 2013, "Nucleosome-free region dominates histone acetylation in targeting SWR1 to promoters for H2A. Z replacement", *Cell*, vol. 154, no. 6, pp. 1232-1245.
- Rao, S.S., Huntley, M.H., Durand, N.C., Stamenova, E.K., Bochkov, I.D., Robinson, J.T., Sanborn, A.L., Machol, I., Omer, A.D. & Lander, E.S. 2014, "A 3D map of the human genome at kilobase resolution reveals principles of chromatin looping", *Cell*, vol. 159, no. 7, pp. 1665-1680.
- Rao, S., Huang, S., Glenn St Hilaire, B., Engreitz, J.M., Perez, E.M., Kieffer-Kwon, K., Sanborn, A.L., Johnstone, S.E., Bochkov, I.D. & Huang, X. 2017, "Cohesin loss eliminates all loop domains, leading to links among superenhancers and downregulation of nearby genes", *bioRxiv.[Internet]*
- Razin, S.V. & Gavrillov, A.A. 2014, "Chromatin without the 30-nm fiber: constrained disorder instead of hierarchical folding", *Epigenetics*, vol. 9, no. 5, pp. 653-657.
- Rebelo, S., Santos, M., Martins, F., e Silva, Edgar F da Cruz & e Silva, Odete AB da Cruz 2015, "Protein phosphatase 1 is a key player in nuclear events", *Cellular signalling*, vol. 27, no. 12, pp. 2589-2598.
- Reddington, J.P., Perricone, S.M., Nestor, C.E., Reichmann, J., Youngson, N.A., Suzuki, M., Reinhardt, D., Dunican, D.S., Prendergast, J.G. & Mjoseng, H. 2013, "Redistribution of H3K27me3 upon DNA hypomethylation results in de-repression of Polycomb target genes", *Genome biology*, vol. 14, no. 3, pp. R25.
- Régnier, V., Vagnarelli, P., Fukagawa, T., Zerjal, T., Burns, E., Trouche, D., Earnshaw, W. & Brown, W. 2005, "CENP-A is required for accurate chromosome segregation and

- sustained kinetochore association of BubR1", *Molecular and cellular biology*, vol. 25, no. 10, pp. 3967-3981.
- Rispa, J., Baron, L., Beaulieu, J., Chevillard-Briet, M., Trouche, D. & Escaffit, F. 2019, "The H2A. Z histone variant integrates Wnt signaling in intestinal epithelial homeostasis", *Nature communications*, vol. 10, no. 1, pp. 1827.
- Rossi, A., Kontarakis, Z., Gerri, C., Nolte, H., Hölper, S., Krüger, M. & Stainier, D.Y. 2015, "Genetic compensation induced by deleterious mutations but not gene knockdowns", *Nature*, vol. 524, no. 7564, pp. 230.
- Rowley, M.J. & Corces, V.G. 2018, "Organizational principles of 3D genome architecture", *Nature Reviews Genetics*, vol. 19, no. 12, pp. 789-800.
- Ruhl, D.D., Jin, J., Cai, Y., Swanson, S., Florens, L., Washburn, M.P., Conaway, R.C., Conaway, J.W. & Chrivia, J.C. 2006, "Purification of a human SRCAP complex that remodels chromatin by incorporating the histone variant H2A. Z into nucleosomes", *Biochemistry*, vol. 45, no. 17, pp. 5671-5677.
- Ruppert, J.G., Samejima, K., Platani, M., Molina, O., Kimura, H., Jeyaprasath, A.A., Ohta, S. & Earnshaw, W.C. 2018, "HP1 α targets the chromosomal passenger complex for activation at heterochromatin before mitotic entry", *The EMBO journal*, vol. 37, no. 6.
- Ryan, D.P. & Tremethick, D.J. 2018, "The interplay between H2A. Z and H3K9 methylation in regulating HP1 α binding to linker histone-containing chromatin", *Nucleic acids research*, vol. 46, no. 18, pp. 9353-9366.
- Ryu, B., Kim, D.S., DeLuca, A.M. & Alani, R.M. 2007, "Comprehensive expression profiling of tumor cell lines identifies molecular signatures of melanoma progression", *PLoS one*, vol. 2, no. 7, pp. e594.
- Sanulli, S., Trnka, M.J., Dharmarajan, V., Tibble, R.W., Pascal, B.D., Burlingame, A.L., Griffin, P.R., Gross, J.D. and Narlikar, G.J., 2019. "HP1 reshapes nucleosome core to promote phase separation of heterochromatin", *Nature*, 575(7782), pp.390-394.
- Sarcinella, E., Zuzarte, P.C., Lau, P.N., Draker, R. & Cheung, P. 2007, "Monoubiquitylation of H2A. Z distinguishes its association with euchromatin or facultative heterochromatin", *Molecular and cellular biology*, vol. 27, no. 18, pp. 6457-6468.
- Sarraf, S.A. and Stancheva, I., 2004. "Methyl-CpG Binding Protein MBD1 Couples Histone H3 Methylation at Lysine 9 by SETDB1 to DNA Replication and Chromatin Assembly", *Mol Cell*.
- Sasaki, K., Shima, H., Kitagawa, Y., Irino, S., Sugimura, T. & Nagao, M. 1990, "Identification of members of the protein phosphatase 1 gene family in the rat and enhanced expression of protein phosphatase 1 α gene in rat hepatocellular carcinomas", *Japanese Journal of Cancer Research*, vol. 81, no. 12, pp. 1272-1280.

- Sawicka, A. & Seiser, C. 2012, "Histone H3 phosphorylation—a versatile chromatin modification for different occasions", *Biochimie*, vol. 94, no. 11, pp. 2193-2201.
- Schermelleh, L., Carlton, P.M., Haase, S., Shao, L., Winoto, L., Kner, P., Burke, B., Cardoso, M.C., Agard, D.A. & Gustafsson, M.G. 2008, "Subdiffraction multicolor imaging of the nuclear periphery with 3D structured illumination microscopy", *Science*, vol. 320, no. 5881, pp. 1332-1336.
- Scholzen, T., Endl, E., Wohlenberg, C., van der Sar, S., Cowell, I.G., Gerdes, J. & Singh, P.B. 2002, "The Ki-67 protein interacts with members of the heterochromatin protein 1 (HP1) family: a potential role in the regulation of higher-order chromatin structure", *The Journal of Pathology: A Journal of the Pathological Society of Great Britain and Ireland*, vol. 196, no. 2, pp. 135-144.
- Schotta, G., Lachner, M., Peters, A. & Jenuwein, T. 2004, "The indexing potential of histone lysine methylation", *Novartis Foundation Symposium* Chichester; New York; John Wiley; 1999, , pp. 22.
- Schwarzer, W., Abdennur, N., Goloborodko, A., Pekowska, A., Fudenberg, G., Loe-Mie, Y., Fonseca, N.A., Huber, W., Haering, C.H., Mirny, L. and Spitz, F., 2017. "Two independent modes of chromatin organization revealed by cohesin removal", *Nature*, 551(7678), pp.51-56.
- See, K., Lan, Y., Rhoades, J., Jain, R., Smith, C.L. & Epstein, J.A. 2019, "Lineage-specific reorganization of nuclear peripheral heterochromatin and H3K9me2 domains", *Development*, vol. 146, no. 3, pp. dev174078.
- Serrano, A., Rodríguez-Corsino, M. and Losada, A., 2009. "Heterochromatin protein 1 (HP1) proteins do not drive pericentromeric cohesin enrichment in human cells", *PLoS One*, 4(4).
- Shen, T., Ji, F., Wang, Y., Lei, X., Zhang, D. & Jiao, J. 2018, "Brain-specific deletion of histone variant H2A. z results in cortical neurogenesis defects and neurodevelopmental disorder", *Nucleic acids research*, vol. 46, no. 5, pp. 2290-2307.
- Shi, Y. 2009, "Serine/threonine phosphatases: mechanism through structure", *Cell*, vol. 139, no. 3, pp. 468-484.
- Shimada, A., Dohke, K., Sadaie, M., Shinmyozu, K., Nakayama, J., Urano, T. & Murakami, Y. 2009, "Phosphorylation of Swi6/HP1 regulates transcriptional gene silencing at heterochromatin", *Genes & development*, vol. 23, no. 1, pp. 18-23.
- Singh, R., Bassett, E., Chakravarti, A. & Parthun, M.R. 2018, "Replication-dependent histone isoforms: a new source of complexity in chromatin structure and function", *Nucleic acids research*, vol. 46, no. 17, pp. 8665-8678.
- Slupianek, A., Yerrum, S., Safadi, F.F. & Monroy, M.A. 2010, "The chromatin remodeling factor SRCAP modulates expression of prostate specific antigen and cellular

- proliferation in prostate cancer cells", *Journal of cellular physiology*, vol. 224, no. 2, pp. 369-375.
- Smith, T.H., Collins, T.M. & McGowan, R.A. 2011, "Expression of the dnmt3 genes in zebrafish development: similarity to Dnmt3a and Dnmt3b", *Development genes and evolution*, vol. 220, no. 11-12, pp. 347-353.
- Smothers, J.F. and Henikoff, S., 2001. "The hinge and chromo shadow domain impart distinct targeting of HP1-like proteins", *Molecular and cellular biology*, 21(7), pp.2555-2569.
- Sobecki, M., Mrouj, K., Camasses, A., Parisis, N., Nicolas, E., Lleres, D., Gerbe, F., Prieto, S., Krasinska, L. & David, A. 2016a, "The cell proliferation antigen Ki-67 organises heterochromatin", *Elife*, vol. 5, pp. e13722.
- Sobecki, M., Mrouj, K., Camasses, A., Parisis, N., Nicolas, E., Lleres, D., Gerbe, F., Prieto, S., Krasinska, L. & David, A. 2016b, "The cell proliferation antigen Ki-67 organises heterochromatin", *Elife*, vol. 5, pp. e13722.
- Solovei, I., Kreysing, M., Lanctôt, C., Kösem, S., Peichl, L., Cremer, T., Guck, J. & Joffe, B. 2009, "Nuclear architecture of rod photoreceptor cells adapts to vision in mammalian evolution", *Cell*, vol. 137, no. 2, pp. 356-368.
- Splinter, E., Heath, H., Kooren, J., Palstra, R., Klous, P., Grosveld, F., Galjart, N. & de Laat, W. 2006, "CTCF mediates long-range chromatin looping and local histone modification in the β -globin locus", *Genes & development*, vol. 20, no. 17, pp. 2349-2354.
- Stefanelli, G., Azam, A.B., Walters, B.J., Brimble, M.A., Gettens, C.P., Bouchard-Cannon, P., Cheng, H.M., Davidoff, A.M., Narkaj, K. & Day, J.J. 2018, "Learning and age-related changes in genome-wide H2A. Z binding in the mouse hippocampus", *Cell reports*, vol. 22, no. 5, pp. 1124-1131.
- Strom, A.R., Emelyanov, A.V., Mir, M., Fyodorov, D.V., Darzacq, X. & Karpen, G.H. 2017, "Phase separation drives heterochromatin domain formation", *Nature*, vol. 547, no. 7662, pp. 241.
- Subramanian, V., Mazumder, A., Surface, L.E., Butty, V.L., Fields, P.A., Alwan, A., Torrey, L., Thai, K.K., Levine, S.S., Bathe, M. and Boyer, L.A., 2013. "H2A. Z acidic patch couples chromatin dynamics to regulation of gene expression programs during ESC differentiation", *PLoS genetics*, 9(8).
- Sullivan, K.F., Hechenberger, M. & Masri, K. 1994, "Human CENP-A contains a histone H3 related histone fold domain that is required for targeting to the centromere.", *The Journal of cell biology*, vol. 127, no. 3, pp. 581-592.
- Swaminathan, J., Baxter, E.M. & Corces, V.G. 2005, "The role of histone H2Av variant replacement and histone H4 acetylation in the establishment of Drosophila heterochromatin", *Genes & development*, vol. 19, no. 1, pp. 65-76.

- Swift, H. 1959, "Studies on nuclear fine structure.", *Brookhaven symposia in biology*, pp. 134.
- Szabo, L., Morey, R., Palpant, N.J., Wang, P.L., Afari, N., Jiang, C., Parast, M.M., Murry, C.E., Laurent, L.C. & Salzman, J. 2015, "Statistically based splicing detection reveals neural enrichment and tissue-specific induction of circular RNA during human fetal development", *Genome biology*, vol. 16, no. 1, pp. 126.
- Tachibana, M., Sugimoto, K., Nozaki, M., Ueda, J., Ohta, T., Ohki, M., Fukuda, M., Takeda, N., Niida, H., Kato, H. and Shinkai, Y., 2002. "G9a histone methyltransferase plays a dominant role in euchromatic histone H3 lysine 9 methylation and is essential for early embryogenesis", *Genes & development*, 16(14), pp.1779-1791.
- Tadros, W. & Lipshitz, H.D. 2009, "The maternal-to-zygotic transition: a play in two acts", *Development*, vol. 136, no. 18, pp. 3033-3042.
- Takagi, M., Matsuoka, Y., Kurihara, T. & Yoneda, Y. 1999, "Chmadrin: a novel Ki-67 antigen-related perichromosomal protein possibly implicated in higher order chromatin structure", *Journal of cell science*, vol. 112, no. 15, pp. 2463-2472.
- Tanaka, T., Fuchs, J., Loidl, J. & Nasmyth, K. 2000, "Cohesin ensures bipolar attachment of microtubules to sister centromeres and resists their precocious separation", *Nature cell biology*, vol. 2, no. 8, pp. 492.
- Terrenoire, E., McDonald, F., Halsall, J.A., Page, P., Illingworth, R.S., Taylor, A.M.R., Davison, V., O'Neill, L.P. and Turner, B.M., 2010. "Immunostaining of modified histones defines high-level features of the human metaphase epigenome", *Genome biology*, 11(11), p.R110.
- Tie, F., Banerjee, R., Stratton, C.A., Prasad-Sinha, J., Stepanik, V., Zlobin, A., Diaz, M.O., Scacheri, P.C. & Harte, P.J. 2009, "CBP-mediated acetylation of histone H3 lysine 27 antagonizes Drosophila Polycomb silencing", *Development*, vol. 136, no. 18, pp. 3131-3141.
- Trinkle-Mulcahy, L., Andersen, J., Lam, Y.W., Moorhead, G., Mann, M. & Lamond, A.I. 2006, "Repo-Man recruits PP1 γ to chromatin and is essential for cell viability", *The Journal of cell biology*, vol. 172, no. 5, pp. 679-692.
- Uchida, F., Uzawa, K., Kasamatsu, A., Takatori, H., Sakamoto, Y., Ogawara, K., Shiiba, M., Bukawa, H. & Tanzawa, H. 2013, "Overexpression of CDCA2 in human squamous cell carcinoma: correlation with prevention of G1 phase arrest and apoptosis", *PLoS one*, vol. 8, no. 2, pp. e56381.
- Vagnarelli, P., Hudson, D.F., Ribeiro, S.A., Trinkle-Mulcahy, L., Spence, J.M., Lai, F., Farr, C.J., Lamond, A.I. & Earnshaw, W.C. 2006, "Condensin and Repo-Man-PP1 co-operate in the regulation of chromosome architecture during mitosis", *Nature cell biology*, vol. 8, no. 10, pp. 1133-1142.

- Vagnarelli, P., Ribeiro, S., Sennels, L., Sanchez-Pulido, L., de Lima Alves, F., Verheyen, T., Kelly, D.A., Ponting, C.P., Rappsilber, J. & Earnshaw, W.C. 2011, "Repo-Man coordinates chromosomal reorganization with nuclear envelope reassembly during mitotic exit", *Developmental cell*, vol. 21, no. 2, pp. 328-342.
- Vagnarelli, P. 2013, "Chromatin reorganization through mitosis" in *Advances in protein chemistry and structural biology* Elsevier, , pp. 179-224.
- Vagnarelli, P., Morrison, C., Dodson, H., Sonoda, E., Takeda, S. & Earnshaw, W.C. 2004, "Analysis of Scc1-deficient cells defines a key metaphase role of vertebrate cohesin in linking sister kinetochores", *EMBO reports*, vol. 5, no. 2, pp. 167-171.
- Vagnarelli, P., Ribeiro, S., Sennels, L., Sanchez-Pulido, L., de Lima Alves, F., Verheyen, T., Kelly, D.A., Ponting, C.P., Rappsilber, J. & Earnshaw, W.C. 2011, "Repo-Man coordinates chromosomal reorganization with nuclear envelope reassembly during mitotic exit", *Developmental cell*, vol. 21, no. 2, pp. 328-342.
- Valdés-Mora, F., Song, J.Z., Statham, A.L., Strbenac, D., Robinson, M.D., Nair, S.S., Patterson, K.I., Tremethick, D.J., Storzaker, C. & Clark, S.J. 2012, "Acetylation of H2A. Z is a key epigenetic modification associated with gene deregulation and epigenetic remodeling in cancer", *Genome research*, vol. 22, no. 2, pp. 307-321.
- van Daal, A. & Elgin, S.C. 1992, "A histone variant, H2AvD, is essential in *Drosophila melanogaster*.", *Molecular biology of the cell*, vol. 3, no. 6, pp. 593-602.
- Van Dessel, N., Beke, L., Görnemann, J., Minnebo, N., Beullens, M., Tanuma, N., Shima, H., Van Eynde, A. & Bollen, M. 2010, "The phosphatase interactor NIPP1 regulates the occupancy of the histone methyltransferase EZH2 at Polycomb targets", *Nucleic acids research*, vol. 38, no. 21, pp. 7500-7512.
- Van Hooser, A., Goodrich, D.W., Allis, C.D., Brinkley, B.R. & Mancini, M.A. 1998, "Histone H3 phosphorylation is required for the initiation, but not maintenance, of mammalian chromosome condensation", *Journal of cell science*, vol. 111, no. 23, pp. 3497-3506.
- van Koningsbruggen, S., Gierliński, M., Schofield, P., Martin, D., Barton, G.J., Ariyurek, Y., den Dunnen, J.T. & Lamond, A.I. 2010, "High-resolution whole-genome sequencing reveals that specific chromatin domains from most human chromosomes associate with nucleoli", *Molecular biology of the cell*, vol. 21, no. 21, pp. 3735-3748.
- Vardabasso, C., Gaspar-Maia, A., Hasson, D., Pünzeler, S., Valle-Garcia, D., Straub, T., Keilhauer, E.C., Strub, T., Dong, J. & Panda, T. 2015, "Histone variant H2A. Z. 2 mediates proliferation and drug sensitivity of malignant melanoma", *Molecular cell*, vol. 59, no. 1, pp. 75-88.
- Vass, S., Cotterill, S., Valdeolmillos, A.M., Barbero, J.L., Lin, E., Warren, W.D. & Heck, M.M. 2003, "Depletion of Drad21/Scc1 in *Drosophila* cells leads to instability of the cohesin complex and disruption of mitotic progression", *Current biology*, vol. 13, no. 3, pp. 208-218.

- Vian, L., Pękowska, A., Rao, S.S., Kieffer-Kwon, K.R., Jung, S., Baranello, L., Huang, S.C., El Khattabi, L., Dose, M., Pruetz, N. and Sanborn, A.L., 2018. The energetics and physiological impact of cohesin extrusion. *Cell*, 173(5), pp.1165-1178.
- Waizenegger, I.C., Hauf, S., Meinke, A. and Peters, J.M., 2000. "Two distinct pathways remove mammalian cohesin from chromosome arms in prophase and from centromeres in anaphase", *Cell*, 103(3), pp.399-410.
- Wakula, P., Beullens, M., Ceulemans, H., Stalmans, W. & Bollen, M. 2003, "Degeneracy and function of the ubiquitous RVXF motif that mediates binding to protein phosphatase-1", *Journal of Biological Chemistry*, vol. 278, no. 21, pp. 18817-18823.
- Wang, F., Dai, J., Daum, J.R., Niedzialkowska, E., Banerjee, B., Stukenberg, P.T., Gorbsky, G.J. & Higgins, J.M. 2010, "Histone H3 Thr-3 phosphorylation by Haspin positions Aurora B at centromeres in mitosis", *Science*, vol. 330, no. 6001, pp. 231-235.
- Wang, Y., Liu, S., Sun, L., Xu, N., Shan, S., Wu, F., Liang, X., Huang, Y., Luk, E. & Wu, C. 2019, "Structural insights into histone chaperone Chz1-mediated H2A. Z recognition and histone replacement", *PLoS biology*, vol. 17, no. 5, pp. e3000277.
- Wang, Z., Krasikov, T., Frey, M.R., Wang, J., Matera, A.G. & Marzluff, W.F. 1996, "Characterization of the mouse histone gene cluster on chromosome 13: 45 histone genes in three patches spread over 1Mb.", *Genome research*, vol. 6, no. 8, pp. 688-701.
- Warburton, P.E., Cooke, C.A., Bourassa, S., Vafa, O., Sullivan, B.A., Stetten, G., Gimelli, G., Warburton, D., Tyler-Smith, C. & Sullivan, K.F. 1997, "Immunolocalization of CENP-A suggests a distinct nucleosome structure at the inner kinetochore plate of active centromeres", *Current Biology*, vol. 7, no. 11, pp. 901-904.
- Watanabe, S., Mishima, Y., Shimizu, M., Suetake, I. & Takada, S. 2018, "Interactions of HP1 Bound to H3K9me3 Dinucleosome by Molecular Simulations and Biochemical Assays", *Biophysical journal*, vol. 114, no. 10, pp. 2336-2351.
- Watson, M.L. 1959, "Further observations on the nuclear envelope of the animal cell", *The Journal of cell biology*, vol. 6, no. 2, pp. 147-156.
- Weierich, C., Brero, A., Stein, S., von Hase, J., Cremer, C., Cremer, T. & Solovei, I. 2003, "Three-dimensional arrangements of centromeres and telomeres in nuclei of human and murine lymphocytes", *Chromosome research*, vol. 11, no. 5, pp. 485-502.
- West, M.H. & Bonner, W.M. 1980, "Histone 2A, a heteromorphous family of eight protein species", *Biochemistry*, vol. 19, no. 14, pp. 3238-3245.
- Westerfield, M. 2000, "A guide for the laboratory use of zebrafish (*Danio rerio*)", *The zebrafish book*, vol. 4.

- Whittle, C.M., McClinic, K.N., Ercan, S., Zhang, X., Green, R.D., Kelly, W.G. & Lieb, J.D. 2008, "The genomic distribution and function of histone variant HTZ-1 during *C. elegans* embryogenesis", *PLoS genetics*, vol. 4, no. 9, pp. e1000187.
- Wiese, M., Bannister, A.J., Basu, S., Boucher, W., Wohlfahrt, K., Christophorou, M.A., Nielsen, M.L., Klenerman, D., Laue, E.D. & Kouzarides, T. 2019, "Citruination of HP1 γ chromodomain affects association with chromatin", *Epigenetics & chromatin*, vol. 12, no. 1, pp. 21.
- Williams, M.M., Mathison, A.J., Christensen, T., Greipp, P.T., Knutson, D.L., Klee, E.W., Zimmermann, M.T., Iovanna, J., Lomberk, G.A. and Urrutia, R.A., 2019. "Aurora kinase B-phosphorylated HP1 α functions in chromosomal instability", *Cell Cycle*, 18(12), pp.1407-1421.
- Woodcock, C.L. & Ghosh, R.P. 2010, "Chromatin higher-order structure and dynamics", *Cold Spring Harbor perspectives in biology*, vol. 2, no. 5, pp. a000596.
- Wu, D., De Wever, V., Derua, R., Winkler, C., Beullens, M., Van Eynde, A. & Bollen, M. 2018, "A substrate-trapping strategy for protein phosphatase PP1 holoenzymes using hypoactive subunit fusions", *Journal of Biological Chemistry*, vol. 293, no. 39, pp. 15152-15162.
- Wu, W., Alami, S., Luk, E., Wu, C., Sen, S., Mizuguchi, G., Wei, D. & Wu, C. 2005, "Swc2 is a widely conserved H2AZ-binding module essential for ATP-dependent histone exchange", *Nature structural & molecular biology*, vol. 12, no. 12, pp. 1064.
- Wu, W., Wu, C., Ladurner, A., Mizuguchi, G., Wei, D., Xiao, H., Luk, E., Ranjan, A. & Wu, C. 2009, "N terminus of Swr1 binds to histone H2AZ and provides a platform for subunit assembly in the chromatin remodeling complex", *Journal of Biological Chemistry*, vol. 284, no. 10, pp. 6200-6207.
- Wutz, G., Várnai, C., Nagasaka, K., Cisneros, D.A., Stocsits, R.R., Tang, W., Schoenfelder, S., Jessberger, G., Muhar, M. & Hossain, M.J. 2017, "Topologically associating domains and chromatin loops depend on cohesin and are regulated by CTCF, WAPL, and PDS5 proteins", *The EMBO journal*, vol. 36, no. 24, pp. 3573-3599.
- Xu, Y., Ayrappetov, M.K., Xu, C., Gursoy-Yuzugullu, O., Hu, Y. & Price, B.D. 2012, "Histone H2A. Z controls a critical chromatin remodeling step required for DNA double-strand break repair", *Molecular cell*, vol. 48, no. 5, pp. 723-733.
- Xu, Z., Ogawa, H., Vagnarelli, P., Bergmann, J.H., Hudson, D.F., Ruchaud, S., Fukagawa, T., Earnshaw, W.C. & Samejima, K. 2009, "INCENP–aurora B interactions modulate kinase activity and chromosome passenger complex localization", *The Journal of cell biology*, vol. 187, no. 5, pp. 637-653.
- Yamagishi, Y., Honda, T., Tanno, Y. & Watanabe, Y. 2010, "Two histone marks establish the inner centromere and chromosome bi-orientation", *Science*, vol. 330, no. 6001, pp. 239-243.

- Yang, B., Tong, R., Liu, H., Wu, J., Chen, D., Xue, Z., Ding, C., Zhou, L., Xie, H. & Wu, J. 2018, "H2A. Z regulates tumorigenesis, metastasis and sensitivity to cisplatin in intrahepatic cholangiocarcinoma", *International journal of oncology*, vol. 52, no. 4, pp. 1235-1245.
- Yang, H.D., Kim, P., Eun, J.W., Shen, Q., Kim, H.S., Shin, W.C., Ahn, Y.M., Park, W.S., Lee, J.Y. & Nam, S.W. 2016, "Oncogenic potential of histone-variant H2A. Z. 1 and its regulatory role in cell cycle and epithelial-mesenchymal transition in liver cancer", *Oncotarget*, vol. 7, no. 10, pp. 11412.
- Yang, W., Meng, Y., Li, D. & Wen, Q. 2019, "Visual contrast modulates operant learning responses in larval zebrafish", *Frontiers in behavioral neuroscience*, vol. 13, pp. 4.
- Ye, Q., Callebaut, I., Pezhman, A., Courvalin, J. & Worman, H.J. 1997, "Domain-specific interactions of human HP1-type chromodomain proteins and inner nuclear membrane protein LBR", *Journal of Biological Chemistry*, vol. 272, no. 23, pp. 14983-14989.
- Ye, Q. & Worman, H.J. 1996, "Interaction between an integral protein of the nuclear envelope inner membrane and human chromodomain proteins homologous to *Drosophila* HP1", *Journal of Biological Chemistry*, vol. 271, no. 25, pp. 14653-14656.
- Yi, Q., Chen, Q., Liang, C., Yan, H., Zhang, Z., Xiang, X., Zhang, M., Qi, F., Zhou, L. & Wang, F. 2018, "HP1 links centromeric heterochromatin to centromere cohesion in mammals", *EMBO reports*, vol. 19, no. 4.
- Yi, Q., Chen, Q., Yan, H., Zhang, M., Liang, C., Xiang, X., Pan, X. & Wang, F. 2019, "Aurora B kinase activity-dependent and-independent functions of the chromosomal passenger complex in regulating sister chromatid cohesion", *Journal of Biological Chemistry*, vol. 294, no. 6, pp. 2021-2035.
- Yoshida, T., Shimada, K., Oma, Y., Kalck, V., Akimura, K., Taddei, A., Iwahashi, H., Kugou, K., Ohta, K. & Gasser, S.M. 2010, "Actin-related protein Arp6 influences H2A. Z-dependent and-independent gene expression and links ribosomal protein genes to nuclear pores", *PLoS genetics*, vol. 6, no. 4, pp. e1000910.
- Zemach, A., McDaniel, I.E., Silva, P. & Zilberman, D. 2010, "Genome-wide evolutionary analysis of eukaryotic DNA methylation", *Science*, vol. 328, no. 5980, pp. 916-919.
- Zhao, T., Heyduk, T. & Eisenberg, J.C. 2001, "Phosphorylation site mutations in heterochromatin protein 1 (HP1) reduce or eliminate silencing activity", *Journal of Biological Chemistry*, vol. 276, no. 12, pp. 9512-9518.
- Zhou, B., Margariti, A., Zeng, L. & Xu, Q. 2011, "Role of histone deacetylases in vascular cell homeostasis and arteriosclerosis", *Cardiovascular research*, vol. 90, no. 3, pp. 413-420.
- Zhou, Z., Feng, H., Hansen, D.F., Kato, H., Luk, E., Freedberg, D.I., Kay, L.E., Wu, C. & Bai, Y. 2008, "NMR structure of chaperone Chz1 complexed with histones H2A. Z-H2B", *Nature structural & molecular biology*, vol. 15, no. 8, pp. 868.

- Zilberman, D., Coleman-Derr, D., Ballinger, T. & Henikoff, S. 2008, "Histone H2A. Z and DNA methylation are mutually antagonistic chromatin marks", *Nature*, vol. 456, no. 7218, pp. 125.
- Zovkic, I.B., Paulukaitis, B.S., Day, J.J., Etikala, D.M. & Sweatt, J.D. 2014, "Histone H2A. Z subunit exchange controls consolidation of recent and remote memory", *Nature*, vol. 515, no. 7528, pp. 582.
- Zuin, J., Dixon, J.R., van der Reijden, Michael IJA, Ye, Z., Kolovos, P., Brouwer, R.W., van de Corput, Mariëtte PC, van de Werken, Harmen JG, Knoch, T.A. & van IJcken, W.F. 2014, "Cohesin and CTCF differentially affect chromatin architecture and gene expression in human cells", *Proceedings of the National Academy of Sciences*, vol. 111, no. 3, pp. 996-1001.